Dissertationes Forestales 303

Environmental controls of boreal forest soil CO_2 and CH_4 emissions and soil organic carbon accumulation

Boris Ťupek

Department of Forest Sciences
Faculty of Agriculture and Forestry
University of Helsinki

Academic dissertation

To be presented with the permission of the
Faculty of Agriculture and Forestry of the University of Helsinki,
for public examination
in the lecture hall 1041 (Viikinkaari 5, Biocenter 2)
on 30th September 2020, at 17 o'clock.

Title of dissertation: Environmental controls of boreal forest soil CO_2 and CH_4 emissions and soil organic carbon accumulation

Author: Boris Ťupek

Dissertationes Forestales 303

https://doi.org/10.14214/df.303
Use licence CC BY-NC-ND 4.0

Thesis Supervisors:
Professor Eero Nikinmaa
Professor Jukka Laine
Docent Kari Minkkinen
Department of Forest Sciences, University of Helsinki, Finland

Professor Timo Vesala
Department of Physics, University of Helsinki, Finland

Pre-examiners:
Professor Jari Liski
Finnish Meteorological Institute, Finland

Docent Narasinha Shurpali
Department of Environmental and Biological Sciences,
University of Eastern Finland, Finland

Opponent:
Professor Yiqi Luo
Center for Ecosystem Sciences and Society, Department of Biological Sciences,
Northern Arizona University, AZ, USA

ISSN 1795-7389 (online)
ISBN 978-951-651-696-0 (pdf)
ISSN 2323-9220 (print)
ISBN 978-951-651-697-7 (paperback)

Publishers:
Finnish Society of Forest Science
School of Forest Sciences of the University of Eastern Finland
Faculty of Agriculture and Forestry of the University of Helsinki

Editorial office:
Finnish Society of Forest Science
Viikinkaari 6, FI-00790 Helsinki, Finland
http://www.dissertationesforestales.fi

A Time for Everything (Solomon, c.450–180 BCE*)

3 There is a time for everything,
and a season for every activity under the heavens.

**Solomon, c.450–180 BCE, Ecclesiastes 3, Holy Bible, New International Version, 2011, Biblica Inc.*

Ťupek, B. (2020). Environmental controls of boreal forest soil CO_2 and CH_4 emissions and soil organic carbon accumulation. Dissertationes Forestales 303. 41 p. https://doi.org/10.14214/df.303

ABSTRACT

Process-based soil carbon models can simulate small short-term changes in soil organic carbon (SOC) by reconstructing the response of soil CO_2 and CH_4 emissions to simultaneously changing environmental factors. However, the models still lack a unifying theory on the effects of soil temperature, moisture, and nutrient status on the boreal landscape. Thus, even a small systematic error in modelled instantaneous soil CO_2 emissions and CH_4 emissions may increase bias in the predicted long-term SOC stock.

We studied the environmental factors that control CO_2 and CH_4 emissions in Finland in sites along a continuum of ecosystems (forest-mire ecotone) with increasing moisture and SOC (I and II); soil CO_2 emissions and SOC in four forest sites in Finland (III); and SOC sequestration at the national scale using 2020 forest sites from the Swedish national forest soil inventory (IV). The environmental controls of CO_2 and CH_4 emissions, and SOC were evaluated using non-linear regression and correlation analysis with empirical data and by soil C models (Yasso07, Q and CENTURY).In the forest-mire ecotone, the instantaneous variation in soil CO_2 emissions was mainly explained by soil temperature (rather than soil moisture), but the SOC stocks were correlated with long-term moisture. During extreme weather events, such as prolonged summer drought, soil CO_2 emissions from the upland mineral soil sites and CH_4 emissions from the mire sites were significantly reduced. The transition from upland forest to mire did not act as a hot spot for CO_2 and CH_4 emissions. The CO_2 emissions were comparable between forest/mire types but the CH_4 emissions changed from small sinks in forests to relatively large emissions in mires. However, the CH_4 emissions in mires did not offset their CO_2 sinks. In the Swedish data, upland forest SOC stocks clearly increased with higher moisture and nutrient status. The soil carbon models reconstructed SOC stocks well for mesotrophic soils but failed for soils of higher fertility and wetter soils with a peaty humus type. A comparison of measured and modelled SOC stocks and the seasonal CO_2 emissions from the soil showed that the accuracy of the estimates varied greatly depending on the mathematical design of the model's environmental modifiers of decomposition, and their calibration.

Inaccuracies in the modeling results indicated that soil moisture and nutrients are mathematically underrepresented (as drivers of long-term boreal forest soil C sequestration) in process-based models, resulting in a mismatch for both SOC stocks and seasonal CO_2 emissions. Redesigning these controls in the models to more explicitly account for microbial and enzyme dynamics as catalysts of decomposition would improve the reliability of soil carbon models to predict the effects of climate change on soil C.

Keywords: carbon dioxide, methane, hydrology, ecotone, climate change, peatland, process modeling, soil carbon models, temperature (T), water (W)

ACKNOWLEDGEMENTS

I am grateful to Dr. John Derome who was the first to hire me in Finland for a traineeship in Rovaniemi funded by Centrum for International Mobility of students (CIMO). On my return to Slovakia, Prof. Jaroslav Škvarenina, supervisor of my Slovak Ph.D. encouraged me to apply for another CIMO traineeship in Finland. This time in Joensuu for a CO_2, CH_4, and N_2O study in peatland buffers with Docent Jukka Alm.

Thanks to this experience I was accepted for a PhD program in Helsinki supervised by Prof. Jukka Laine, Prof. Eero Nikinmaa, and Docent Kari Minkkinen and funded by Nordic Centre for Studies of Ecosystem Carbon Exchange and its Interactions with the Climate System. I thank Jukka L. and Kari for the overarching theme of my Finnish Ph.D. "underlying processes behind CO_2 and CH_4 exchange" and for selecting the sites forming unique forest-mire ecotone. Prof. Hannu Ilvesniemi provided a soil moisture probe, Eero provided a data logger and weather sensors, and Kari a portable infrared CO_2 analyzer. Many thanks go to Dr. Terhi Riutta for helping with important details regarding greenhouse gas measurements in the field, gas chromatography in the lab, and for lending me her car multiple times to get between Lakkasuo and Hyytiälä station. Hyytiälä staff was friendly and helpful. I am grateful for their support during three seasons of field and laboratory work, and to Dr. Michal Gažovič and Dr. Tommy Chan and everyone who helped me to collect data.

When studying in Helsinki at the Department of Forest Sciences and Physics, the physicists inspired me to use Matlab. After Prof. Jukka Laine moved to Parkano, I appreciate Prof. Eero Nikinmaa for taking over as my main supervisor. Initially, our communication stumbled, as I had little knowledge about plant physiological process modeling, but thanks to that a new collaboration started with Prof. Jukka Pumpanen, Prof. Timo Vesala, Dr. Pasi Kolari, Docent Ilkka Korpela, Prof. Harri Vasander, and Prof. Mike Starr. I thank Ilkka and Harri for organizing airborne survey and lidar flights above the Vatiharju – Lakkasuo ecotone. Mike helped with planning measurements of soil water nutrients and with the scientific language of the first "CO_2 ecotone" thesis paper. I was happy about the revision but understood the limits of my writing ability. Furthermore, I've got stuck with the analysis of the "CO_2 moisture" paper. The moisture signal in CO_2 data was surprisingly weak. In a search for the reason, Prof. Pertti Hari thankfully sparked my interest in statistical methods. Inevitably my three and half years funding ended. Thanks to three months grant from the Finnish Society of Forest Science, and three months' salary from Timo for analysis of CH_4 and N_2O data, and a three months position on CarboEurope project with Dr. Marcus Lindner in European Forest Institute, I was paid a little longer. Without funding eventually, I returned to Slovakia for over a year.

However bad it seems, I am thankful for reconnection with family; mainly mother, father, brother, uncle, grandmother, cousins, friends, nature, and myself. I considered abandoning science and changing professions. Science prevailed by Prof. Ladislav Tužinský insisting on the completion of my Slovak Ph.D. With data from Docent Peter Fleischer and with a regression modeling I finalized and defended monograph on "O_3 in a mountainous forest". Also "CO_2 moisture" manuscript seemed to advance. Eero was impressed with the amount of work done and offered me a new chance to complete it. I returned to Finland and since then revised it three times, without success. However, thanks to published article on "European forest C modeling" with Marcus and a handful of Earth system modelers science held on to me.

I would like to thank Prof. Aleksi Lehtonen for rewarding and enjoyable research career at Finnish Forest Research Institute (METLA), later Natural Resources Institute Finland (LUKE), and to Prof. Raisa Mäkipää, Dr. Mikko Peltoniemi, and Prof. Kristiina Regina for working on their projects. Aleksi initiated the change from Matlab to R and importantly with Dr. Shoji Hashimoto and mobility funding of Academy of Finland use of process-based models. Challenges of studying the natural mechanisms with process-based models in combination with measured data far outweighed the satisfaction from the insights gained. Also, I thank my colleagues for their friendliness. I thank Dr. Abbot Oghenekaro for many good laughs and example of working hard on Ph.D.; Mikko and Hannele during times of METLA for making lunch fun by teaching me a bit of Finnish; friends from church for helping me to get grounded in life; and Dilara for joy.

I am grateful for doctoral program support from Prof. Jaana Bäck and Karen Sims-Huopaniemi from the graduate school in Atmospheric Sciences and Sustainable Use of Renewable Natural Resources. I appreciate funding for finalizing the dissertation from Helsinki University and LUKE.

I thank Dr. Tähti Pohjanmies for editing the Finnish abstract. I would like to thank my pre-examiners Prof. Jari Liski and Docent Narasinha Shurpali for their constructive comments. Finally, I can answer Prof. Harri Vasander and everyone asking, “when are you going to defend?” It is time.

To cut a long story short, I want to thank all mentioned here and also many other friends and colleagues who supported me and whom I could not list here for the lack of space, and last but not least God for forming me by saving grace.

LIST OF ORIGINAL ARTICLES

The doctoral thesis is based on the following publications, which are referred to in the text by their roman numerals.

I. **Ťupek B.**, Minkkinen K., Starr M., Kolari P., Chan T., Vesala T., Alm J., Laine J., Nikinmaa E. (2008). Forest floor versus ecosystem CO_2 exchange along boreal ecotone between upland forest and lowland mire. Tellus B 60(2): 153–166. https://doi.org/10.1111/j.1600-0889.2007.00328.x

II. **Ťupek B.**, Minkkinen K., Pumpanen J., Vesala T., Nikinmaa E. (2015). CH_4 and N_2O dynamics in the boreal forest–mire ecotone. Biogeosciences 12(2): 281–297. https://doi.org/10.5194/bg-12-281-2015

III. **Ťupek B.**, Launiainen S., Peltoniemi M., Sievänen R., Perttunen J., Kulmala L., Penttilä T., Lindroos A.J., Hashimoto S., Lehtonen A. (2019). Evaluating CENTURY and Yasso soil carbon models for CO2 emissions and organic carbon stocks of boreal forest soil with Bayesian multi-model inference. European Journal of Soil Science 70(4): 847–858. https://doi.org/10.1111/ejss.12805

IV. **Ťupek B**., Ortiz C. A., Hashimoto S., Stendahl J., Dahlgren J., Karltun E., Lehtonen A. (2016). Underestimation of boreal soil carbon stocks by mathematical soil carbon models linked to soil nutrient status. Biogeosciences 13(15): 4439–4459. https://doi.org/10.5194/bg-13-4439-2016

The articles are reprinted with the permission of their copyright holders.

Other selected closely related peer-review articles not included in the thesis summary:

Schneider J., **Ťupek B.,** Lukasheva M. et al. (2018). Methane Emissions from Paludified Boreal Soils in European Russia as Measured and Modelled. Ecosystems 21: 827–838. https://doi.org/10.1007/s10021-017-0188-y

Hashimoto S., Nanko K., **Ťupek B**., Lehtonen A. (2017). Data-mining analysis of factors affecting the global distribution of soil carbon in observational databases and Earth system models. Geoscientific Model Development 10(3): 1321–1337. https://doi.org/10.5194/gmd-10-1321-2017

Ťupek B., Zanchi G., Verkerk P. J., Churkina G., Viovy N., Hughes J. K., Lindner M. (2010). A comparison of alternative modelling approaches to evaluate the European forest carbon fluxes. Forest Ecology and Management 260(3): 241–251. https://doi.org/10.1016/j.foreco.2010.01.045

AUTHOR'S CONTRIBUTION

I & **II** The first author (author) contributed to the planning and establishment of the study, and by collecting data. TC contributed by data collection. JL, KM, TV, MS, and EN contributed to the planning and coordination of the studies. The author analyzed the data, interpreted the results, and wrote the papers. MS revised paper **I**. All authors contributed to papers by helpful comments.

III The author, AL, MP, and TP contributed to the planning and establishment of the study and carried out and supervised measurement campaigns. The author analyzed the data, run the CENTURY model, run Yasso model simulations on a monthly time step with help of RS, JP, and AL, interpreted the results with AL, SL, MP, LK, and RS, and wrote the paper. All authors contributed to the study with helpful comments.

IV The author contributed to the study by analyzing, and interpreting the data, and wrote the paper. The author had run Yasso and CENTURY model simulations. CAO run Q model. SH helped with running CENTURY. AL, the author, and SH coordinated the analysis. JS, JD, EK provided inventory data. All authors contributed to the paper with helpful comments.

TABLE OF CONTENTS

REVIEW OF THE ARTICLES

I. We studied the relations between the ecosystem component CO_2 fluxes and meteorological and environmental factors on nine sites along the forest-mire ecotone. The non-linear regression models were used to upscale instantaneous forest floor (FF) fluxes to the annual level with continuous records of temperature and light. The CO_2 fluxes of forest stand were based on an inventory-based forest growth model. The contribution of forest floor component fluxes to ecosystem fluxes significantly varied between sites. FF photosynthesis contributed from 4–90% to gross ecosystem photosynthetic production. FF respiration contributed from 70–98% to gross ecosystem respiration. The upscaled annual CO_2 fluxes correlated with site-specific factors. Tree stand biomass played a major role in controlling FF photosynthesis through intercepted light (correlation coefficient r = -0.96) and FF respiration through the stand foliar biomass (r = 0.77). The long-term moisture was not significantly correlated with soil respiration; however, it was significantly correlated with the thickness of an organic horizon.

II. We studied variable CH_4 and N_2O fluxes measured during wet, intermediate, and dry years in nine sites along the forest-mire ecotone. The statistical differences were evaluated by two-way analysis of variance. The relations between forest floor CH_4 and N_2O fluxes and soil temperature, moisture, and pH were evaluated by non-linear regression models and their residual sensitivity analysis. Small mineral soil forest FF CH_4 sink linearly increased from zero to over -100 ug $m^{-2}h^{-1}$ with increasing temperature and decreasing moisture. FF CH_4 exchange of forest-mire transitions was neutral and weakly correlated only to moisture. In contrast with small negative fluxes of mineral and organo-mineral soils, the histic soils in mires were large CH_4 sources. There, the modeled optimum net CH4 emissions reached 1200 ug $m^{-2}h^{-1}$ under conditions of -18 cm of water level depth and 14 ºC of topsoil temperature. All sites showed similar close to 0 ug $m^{-2}h^{-1}$ net N_2O FF exchange over intermediately moist and dry year. The net N_2O FF emission slightly increased to 50 ug $m^{-2}h^{-1}$ in late spring and early autumn, presumably due to a small increase of typically low N mineralization potential. For the landscape-level modeling, forest-mire transitions can be thus regarded as CH_4 and N_2O neutral and not as hot spots.

III. We evaluated soil CO_2 emissions and soil organic carbon (SOC) stocks of Yasso and CENTURY models against measurements on four forest sites in Finland. We aimed to evaluate seasonal dependencies of CO_2 fluxes and SOC stocks on environmental variables and compare the model outputs to empirical data. The results indicated that models with a default setting estimated well SOC stocks but underestimated CO_2 fluxes. Bayesian CO_2 data assimilation improved the level of the CO_2 estimates. Although the seasonal discrepancies prevailed. This highlighted the need for re-designing the modifiers to better account for seasonality or missing processes e.g. microbial growth. The calibrated CENTURY model using the environmental function with precipitation showed a better fit to the CO_2 data against the model with soil moisture. Also, the Yasso model outperformed the CENTURY. The better performing models had fewer parameters in the environmental functions and used precipitation instead of soil moisture. Thus, considering the CENTURY's effect of soil properties on decomposition and carbon sequestration could be an asset only if moisture function is simplified and soil moisture data is of high quality.

IV. In this study, we compared Swedish forest soil carbon inventory data with SOC sequestration estimated by process-based models of increasing complexity (Q, Yasso07, and CENTURY). The modes were primarily driven by plant litter input. The decomposition of litter on these models depends on temperature (Q), precipitation/moisture (Yasso07/CENTURY), and soil physicochemical properties such as clay content or topsoil N (CENTURY). Models accurately estimated SOC typically for mesotrophic soils but underestimated for fertile soils. CENTURY accounting for soil properties outperformed Yasso07 and Q models in clay soils but not in fertile soil with high topsoil N. We concluded that for accurate SOC stock modeling soil nutrient status should be re-evaluated in soil carbon models to account for the long-term C sequestration processes associated with microbial C transformation and C interactions with soil minerals.

1 INTRODUCTION

1.1 Boreal forest feedback to climate warming

Increasing atmospheric concentrations of greenhouse gas (GHG) e.g. carbon dioxide (CO_2), methane (CH_4), and nitrous oxide (N_2O) in the atmosphere with their higher radiative forcing and higher heat capacity than clean air cause climate warming (Santer et al. 2013, IPCC 2018, IPCC 2019a). CO_2 is the most abundant but least effective GHG. The radiative efficiency and global warming potential (GWP) of CH_4 is 21 times higher than for CO_2, and the GWP of N_2O is 310 times higher than for CO_2 (IPCC 2018).

Without mitigation globally increasing air temperature will also increase the frequency and severity of devastating extreme events such as droughts and fires (Turetsky et al. 2015, Holmberg et al. 2019, Walker et al. 2019). The northern latitude climate warming outpacing warming in other regions (Bintanja et al. 2011, Post et al. 2019). Climate warming is human-induced and natural contribution is minimal (Hegerl et al. 2011). The boreal forests taking up CO_2 from the atmosphere act as net C sinks (Goodale et al. 2002) with the photosynthesis counterbalancing the respiration and accumulating C mainly into the soil. It is not clear whether positive feedback of increased photosynthesis due to prolonging the vegetative season (Churkina et al. 2005) could counterbalance negative feedback of increased respiration due to warming the non-vegetative season (Piao et al. 2008, Vesala et al. 2010). However, the boreal forest soil C pool 400 Pg (10^{15} g) (Scharlemann et al., 2014) is temperature and moisture sensitive and under global warming, the soils could turn from a C sequestration to a loss (Crowther et al. 2016) thus triggering significant warming feedback.

In the boreal landscape, most GHG studies have focused on dominant forest and mire ecosystems whose C pools and fluxes significantly differ with water drainage (Weishampel et al., 2009). However, we also need to clarify greenhouse gas exchange in transitional zones which have been considered as potential biogeochemical hotspots in the landscape (McClain et al. 2003) due to their high water and nutrients dynamics (Howie and Meerveld 2011).

Locally CO_2 fluxes are controlled by moisture, whereas at regional and global scale temperature drives C sinks (Gong et al. 2013, Jung et al. 2017). Multiscale measurements such as chamber and eddy covariance techniques (Kolari et al. 2009, Aurela et al. 2007) are needed for the parametrization, evaluation, and further development of the models. Ecosystem and soil carbon models such as e.g. CENTURY (Parton et al. 1988), Biome-BGC (Thornton 1998), Yasso07 (Tuomi et al., 2011) among others are needed for reconstructing natural processes and their extrapolation in time and space and for evaluating feedback of climate change. As a result, Earth system models include drivers of scale-dependent processes. However, in modeling local and global feedback of climate warming on boreal forest C sink we still search for unifying functional representation of soil carbon change responses to drivers such as temperature and moisture (Todd Brown at al. 2013, Sierra et al. 2015) while accounting for soil nutrient status (Orwin et al. 2011, Fernández-Martínez et al. 2014, Hashimoto et al. 2017).

1.2 Forest-atmosphere C exchange

1.2.1 Forest and mire CO_2 and CH_4 fluxes

Soil heterotrophic respiration is the major ecosystem source of CO_2 emissions in a well-drained forest, while in mires soil CO_2 and net CH_4 emissions are equally important (Frolking et al. 2011, Oertel et al. 2016). Although net ecosystem CO_2 exchange (NEE) (a difference between fluxes of gross photosynthetic production (GPP) and total respiration (R), Figure 1) can be similar between forests and peatlands, the major C fluxes and pools are different. In a well-drained forest, net primary production (NPP, GPP minus growth and maintenance respiration (Ra)) results in relatively larger tree growth and C storage in the living biomass compared to the NPP of peatlands where tree growth is reduced in water-saturated soils due to limited oxygen and nutrient availability. As the living biomass regenerates, its litterfall (e.g. leaves, branches, and roots) is a source of organic matter for the soil decomposition processes (Rh), transformation, and accumulation of the soil organic matter by soil macro- and micro-biota (Cotrufo et al, 2013). The microbial activity and Rh vary spatially and seasonally with soil temperature and moisture, the amount and nutrient status of the organic substrate (Bond-Lamberty et al. 2004, Davison et al. 2012, Sierra 2012a,b, Pumpanen et al. 2015, Manzoni et al. 2017).

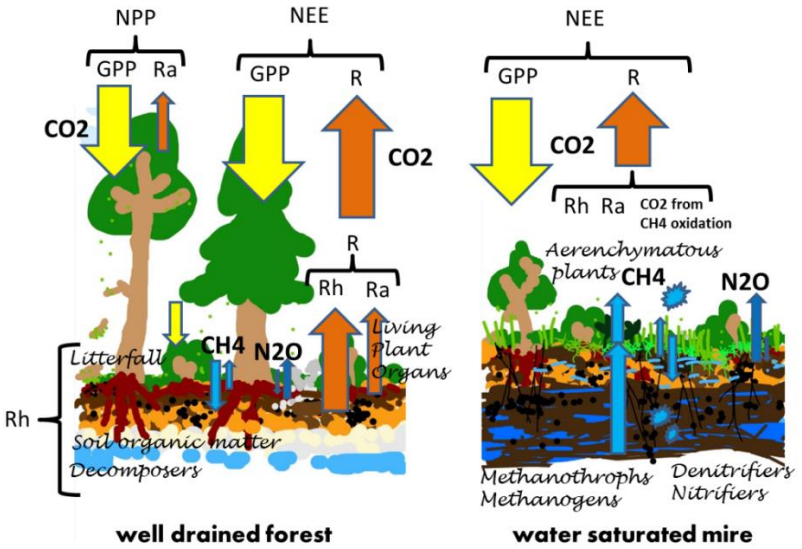

Figure 1. Schematic illustration indicating the main processes of component CO_2, CH_4, and N_2O gas exchange between the atmosphere and the forest or the mire ecosystem. In an atmospheric view, the forest – atmosphere CO_2 interactions are described from the perspective of the concentration change of the atmosphere. Component ecosystem fluxes that remove C from the atmosphere are shown by downward arrow (sinks, GPP, and CH_4 oxidation), and fluxes adding C to the atmosphere are shown by upward arrow (sources, R, Rh, and Ra, CH_4 emission).

Methane production and net emissions also vary spatially and temporally depending on the moisture, temperature, mosses, arenchymatous plants, and peatland nutrient status (Bubier et al. 1995, Riutta et al. 2007, Larmola et al. 2010, Yrjäla et al. 2011, Turetsky et al. 2014). Well-drained mineral soil forests and also boreal forestry –drained peatlands act as small net CH_4 sink (Moosavi et al. 1997, Ojanen et al. 2010, Marushchak et al. 2016) whereas mires are CH_4 sources (Riutta et al. 2007, Frolking et al. 2011, Gong et al. 2013, Marushchak et al. 2016, Raivonen et al, 2017). The CH_4 sink in mineral soils is primarily a result of oxidation whereas in mires the CH_4 is produced by methanogenic bacteria in anoxic conditions. In the presence of fresh organic input of deep roots in summer, methanogens dissimilate acetate (acetate pathway) while in winter CH_4 is produced by reduction of bicarbonate (hydrogen pathway) (Hines et al. 2008). Produced methane is then transported to the atmosphere by diffusion, ebullition, or by arenchymatous plants, or it is oxidized to CO_2 by methanotrophs while passing through the aerobic soil layer (Larmola et al. 2010, Raivonen et al, 2017).

1.2.2 Modeling soil C dynamics

Soil carbon dynamics can be modeled while incorporated into ecosystem models e.g. as in CENTURY (Parton et al., 1988), Forest-BGC (Running and Gower 1991), and TECO (Weng and Luo 2008). If the plant litter input is provided then soil carbon dynamics can be modeled by soil carbon models e.g. Yasso07 (Tuomi et al., 2009), ROMUL (Chertov et al., 2001), and RothC (Coleman & Jenkinson, 1996). Conventionally soil organic carbon (SOC) change in time is in mathematical terms expressed by first-order decay of C in soil pools (accounting for C input, decay rates, transfers and feedbacks between pools, and output) which is either inhibited or accelerated by environmental conditions.

For example, the Yasso07 (Tuomi et al., 2009; Tuomi et al., 2011) and CENTURY (Parton et al. 1988, Metherell et al. 1993, Del Grosso et al. 2001) models of the soil organic matter decomposition can be summarized by a set of differential equations as described by (Sierra et al., 2012) for the general dynamic model (Eq. 1)

$$\frac{dc(t)}{dt} = i(t) + \xi(t)A(t)c(t) \qquad \text{Eq. 1}$$

Where $\boldsymbol{c}(t)$ is a vector of n C pools at time t, the model structure $\mathbf{A}(t)$ is described by $n \times n$ matrix with decomposition rates for each pool in a diagonal and coefficients of transfers and feedbacks below and above the diagonal defining cross-pool C flows. The environmental modifier $\xi(t)$ is a scalar describing the environmental effect on decomposition rates and $\boldsymbol{i}(t)$ is a vector of carbon inputs to each pool.

The second-order decay models, apart from the principles of first-order models (mass balance, pools specific substrate dependence of decay, heterogeneity and transfers of organic matter between pools, and environmental effects), also account for nonlinear organic matter interactions (Manzoni & Porporato 2009, Sierra et al. 2015, Moyano et al. 2018). For example, the decay rate is proportional to microbial biomass whereas the production of substrate for decay is controlled by Michaelis–Menten reaction kinetics.

Although the models can have similar generic form, the individual model equations differ in the partitioning of the litter into the carbon pools, the number of pools and C flows, the environmental effect of air temperature, water stress and other variables e.g. bulk density (BD), sand and clay content of the soil. Accounting for some predictors explicitly e.g. measured BD may decrease the need for process based SOC modeling. As

measured SOC stock is derived from the C concentration in the soil profile and bulk density (BD) (Poeplau et al. 2017) thus both variables can be measured together. However, considering relatively easily available information on land fertility and land cover could spatially improve process based SOC predictions (Hashimoto et al. 2017).

1.2.3 Effects of T, W, and substrate on CO_2 and CH_4 emissions

The form of the empirically derived functions between CO_2 and CH_4 emissions and factors such as temperature and water largely depend on the collected data (e.g. Alm et al. 1999, Riutta et al. 2007, Ojanen et al. 2010). As a result, CO_2 empirical functions of temperature and moisture in biogeochemical models show high variation Sierra et al. (2012, 2015). Most temperature functions used in the models agree with Arhenius' type of increase of decomposition with increased temperature, however, some functions reduce decomposition at high temperatures. In Bayesian optimization of the Yasso07 model, Tuomi et al. (2008) also found that the Gaussian type temperature response fitted best to the respiration data. This could result from the confounded response of low soil moisture content under high-temperature constraining soil respiration. In the field conditions, soil water limits respiration either by limiting the solute transport or gas transport to microbes (Figure 2). The bell-shaped response of respiration thus results in two combined substrate responses of Oxygen and available solute on respiration if each follows Michaelis-Menten (MM) kinetics (Davidson et al. 2012).

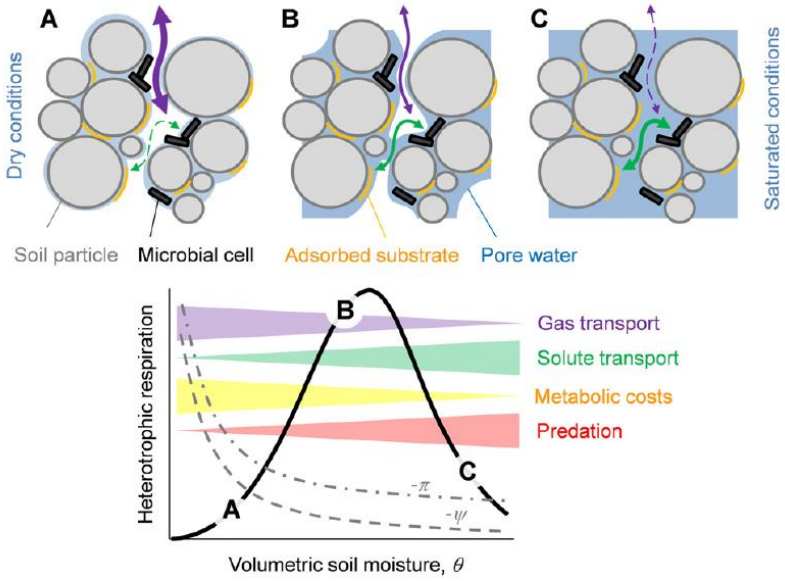

Figure 2. Soil moisture effects on microbial activity during dry conditions limiting solute transport (A), during optimal conditions for solute and gas transport (B), and during water-saturated conditions limiting the gas transport (C) (as presented by Moyano et al. 2013). The gray lines show the correlation between decreasing soil water potential ψ and microbial cell osmotic potential π.

In the soil incubation experiment, Sierra et al. (2017) found that under unconstrained substrate and moisture conditions, the temperature does not limit enzyme denaturation and follows Arrhenius temperature kinetics. In the same incubation experiment, Sierra et al. (2017) clarified that respiration, under unconstrained substrate and oxygen, saturates with increasing water content following MM kinetics. The MM saturation kinetics of respiration also applies to increasing Oxygen under an unconstrained substrate. The Michaelis-Menten type kinetics are characteristic for microbial enzyme models for soil CO_2 (Sierra et al. 2012, Davidson et al 2012, Moyano et al. 2013, Sierra et al. 2015, Manzoni et al. 2016, Abrahamoff et al. 2017, Moyano et al 2018) and CH_4 (Davidson et al 2014, Raivonen et al. 2017, Sihi et al. 2020). In microbial models, Arrhenius temperature kinetics are combined with water limitation through diffusivity of oxygen, and enzymatic transport in the soil pore space.

1.3 Aims of the study

The aims of this study were (1) to clarify in situ effects of environmental factors, namely temperature and water, on the boreal forest soil CO_2 and CH_4 emissions and SOC stocks (**I - III**), and (2) evaluate the impact of environmental factors on the mismatch between the measured soil CO_2 emissions and SOC stocks and the estimates of Yasso07 and CENTURY soil carbon models (**III - IV**). We evaluated these models due to them being listed among other models as potential tools for national greenhouse gas reporting to The United Nations Framework Convention on Climate Change (IPCC, 2019b) and their wide use (Yasso07 by several European countries, CENTURY by USA and Japan) (UNFCCC, 2019).

2 MATERIALS AND METHODS

2.1 Study sites

*2.1.1 Forest-mire ecotone (**I- II**)*

Nine forest/mire site types of Vatiharju-Lakkasuo ecotone form a gradient of soil moisture, nutrient conditions, and species distribution situated on the well-drained hill down the slope and wet depression in southern Finland (61º 47', 24º 19') (Figure 3). The ecotone extends from upland forests on mineral soil, through forest and mire transitions on gleyic soil, down to sparsely forested mires on histosoil. The soils form a catena of increased fertility from the xeric and saturated ends towards the midslope, and increased water saturation down the slope towards peatland. The site types were classified based on vegetation composition and production by the Finnish forest and mire classification systems (Cajander 1949; Laine et al. 2004). Sites range from four upland Scots pine (*Pinus sylvestris* L.) and Norway spruce (*Picea abies* L.) dominated forests (1) xeric, (2) subxeric, (3) mesic and (4) herb-rich forest types (CT - *Calluna*, VT - *Vitis Idea*, MT - *Myrtilus*, OMT - *Oxalis-Myrtillus*), through paludified forest - mire transitions (5 - 7) (OMT+ - *Oxalis-Myrtillus Paludified*, KgK – *Myrtillus Spruce Forest Paludified*, KR – *Spruce Pine Swamp*), to depression (8 - 9) with sparsely forested wet mire type (VSR1 and VSR2 - *Tall Sedge Pine Fen*). The forest/mire sites are situated along a 450 m transect

on a 3.3 % slope facing NE with a relative relief of 15 meters (Figure 3). More detailed stand, soil, and climate characteristics were reported in **I – II**.

*2.1.2 ICP - Level II forest sites (**III**)*

The four European intensive forest monitoring (ICP – Level II) forest sites included two Scots pine and two Norway spruce dominated forest sites situated in southern Finland (Figure 3). These four sites were part of a larger network of sites across Europe intensively monitored for litter-fall measurements, nutrient cycles, growth, defoliation, ground vegetation, biotic and abiotic damage, background air quality, and meteorological characteristics. We have chosen these sites because of available measurements of the soil and biomass carbon stocks, biomass growth, litter input to the soil, as well as meteorological variables needed for the evaluation of soil carbon models. We measured soil CO_2 emissions, heterotrophic respiration (Rh), to monitor seasonal SOC changes. The forest floor on each site was trenched on three locations (1 x 1 m) to exclude tree roots respiration from total CO_2 efflux. The ingrowth of tree roots was prevented. More detailed stand, soil, and climate characteristics were reported in **III**.

*2.1.3 Swedish forest soil inventory (**IV**)*

In study **IV**, we evaluated SOC stock estimates of soil carbon models using exceptionally large soil carbon data set collected by Swedish forest soil inventory (SFSI) (Stendahl et al. 2010). The 2020 SFSI sample plots corresponded to a subsample of larger Swedish forest inventory (SFI). The sites were aggregated by the closest distance to weather stations of the Swedish Meteorological and Hydrological Institute (SMHI) network (Figure 3). More detailed forest stand, soil, and climate characteristics were reported in **IV**. The samples in SFSI data contained in addition to soil C and N stocks numerous physicochemical characteristics.

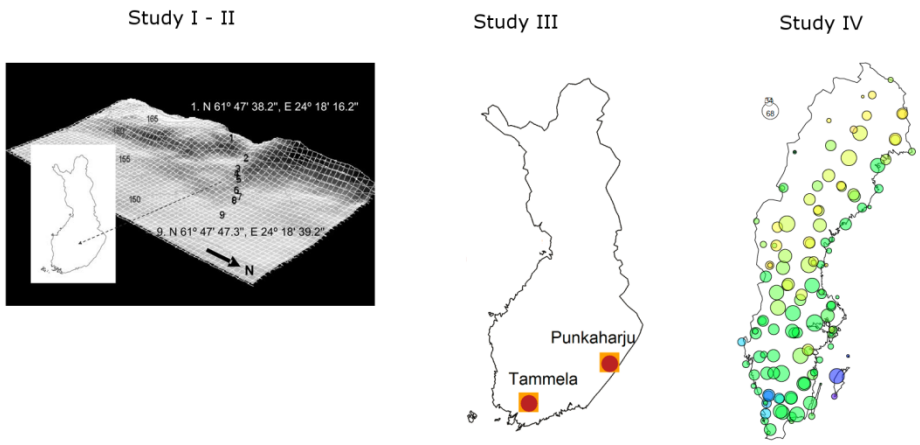

Figure 3. Geographical locations of the forest – mire ecotone sites (**I-II**) and ICPII forest sites (**III**) in Finland and aggregated number of sites of National Forest Inventory to the nearest weather station in Sweden (**IV**).

The high variability of physicochemical conditions in a large data set was ideal for model evaluations and identifying conditions where the models perform well or fail. Similar Finnish data is four times smaller and was used in another study by Lehtonen et al. (2016) for evaluating structural differences in Yasso07 and ROMUL soil carbon models.

2.2 Field data

*2.2.1 CO_2, CH_4, and weather (**I- III**)*

During 2004, 2005, and 2006 we simultaneously measured meteorological conditions and forest floor total CO_2 emissions ($gCO_2\ m^{-2}\ h^{-1}$) and forest floor net CH_4 fluxes ($\mu g\ m^{-2}\ h^{-1}$) on 9 sites with 3 plot replicates on each (**I - II**). The measurement campaigns were conducted in one or two days between 7 am and 6 pm weekly during the vegetative season of 2004 (July-November), 2005 (May-November), 2006 (May-September), and monthly during the non-vegetative season (December-April). The CO_2 emissions were measured by chamber technique with a portable infrared analyzer (EGM4, SRC-1 PP systems Inc.). The emissions were calculated from the CO_2 concentration increase in the non-transparent chamber measured every 4.8 s during 80 s intervals.

The net forest floor CH_4 fluxes were measured by static chamber technique and air sampling from the chamber into 5 syringes sampled every 5 min (**II**). The samples were subsequently analyzed in a laboratory with a gas chromatograph (Hewlett-Packard, USA) model number HP-5890A fitted with a flame ionization detector (FID). The net CH_4 fluxes were calculated from the concentration change in the non-transparent chamber.

Monitored meteorological conditions included soil temperatures at 5 cm depth (T_5, °C) measured with a thermometer, the depth of the water level (WT, cm) measured with contact meter, and the volumetric soil moisture at depths of 10cm (SWC_{10}, %, $m^3\ m^{-3}$) measured with a portable ML2 ThetaProbe (Delta-T Devices Ltd) (**I-III**).

In **III** the four ICPII stands we measured forest soil CO_2 emissions ($g\ CO_2\ m^{-2}\ h^{-1}$) on 12 trenched plots on each site (3 trenched 1 x 1 m squares per site, each sub-divided to 4 segments). Except for the trenching of the plots for measurements of CO_2 emissions the measurement setup in **III** was the same method as in **I-II**.

*2.2.2 Swedish Forest soil inventory (**IV**)*

Swedish forest soil inventory (SFSI) dataset which originated from a stratified national grid survey of vegetation and physicochemical properties of soils was identical to the one used in Stendahl et al. (2010).

2.3 Modeling instantaneous CO_2 and CH_4 fluxes (I-III)

*2.3.1 Empirical CO_2 models (**I, III**)*

We used models (i) to evaluate responses of environmental factors to respiration and (ii) to extrapolate R to monthly and annual levels. Nonlinear least squared regression analysis (NLS) was used at each site to fit empirical models of total forest floor respiration (R_{ff}, $g\ CO_2\ m^{-2}\ hour^{-1}$) to soil temperature at 5 cm depth (T_5, °C) (**I**) and (**III**) heterotrophic forest

soil respiration (R_h, g CO_2 m^{-2} $hour^{-1}$) to T_5 and volumetric soil water content at 10 cm depth (SWC_{10}, %). In study **I**, the R_{ff} NLS model used Loyd and Taylor (1994) exponential response to T_5 (Eq. 2):

$$R_{ffij} = R_{ffref} e^{\left(b\left(\frac{1}{56.02} - \frac{1}{T_5 + 46.02}\right)\right)} + \varepsilon_{ij} \quad \text{Eq. 2}$$

where i^{th} forest site and j^{th} observation, R_{ff} is forest floor respiration (g CO_2 m^{-2} h^{-1}), T_5 (°C) is predictor, R_{ffref}, and b are parameters, and ε_{ij} is the error for observation j in i^{th} forest type.

The R_h NLS model for heterotrophic soil respiration in **III** was a combined exponential Q_{10} based response to T_5 modified by a bell-shaped response to SWC_{10} accounting for the optimum soil water content (Davidson et al. 2012) (Eq. 3).

$$R_{hij} = R_{href} d^{(\mathrm{SWC_{opt}} - \mathrm{SWC_{10}})^2} Q_{10}^{\left(\frac{T_5 - 10}{10}\right)} + \varepsilon_{ij} \quad \text{Eq. 3}$$

Where i^{th} forest site and j^{th} observation R_h is soil respiration (g CO_2 m^{-2} h^{-1}), T_5 and SWC_{10} are predictors, and R_{href}, Q_{10}, SWC_{opt}, and d are parameters, and ε_{ij} is the error for observation j in i^{th} forest type.

*2.3.2 Empirical CH_4 models (**II**)*

The net CH_4 uptakes (µg m^{-2} h^{-1}) in mineral soil forest and small net CH_4 uptakes or emissions in the forest-mire transitions were fitted to T_5 and SWC_{10} by linear mixed-effects regression models with a random effect for forest types (Pinheiro et al. 2013).

The CH_4 fluxes for upland forests and transitions with SWC_{10} and T_5 as predictors were modeled as in following equations (Eq. 4 and Eq. 5):

$$yu_{ij} = \beta_{CT}\,SWC_{10} + \beta_{VT}\,SWC_{10} + \beta_{MT}\,SWC_{10} + \beta_{OMT}\,SWC_{10} + \beta_{CT}\,T_5 + \beta_{VT}\,T_5 + \beta_{MT}\,T_5 + \beta_{OMT}\,T_5 + b_{CT} + b_{VT} + b_{MT} + b_{OMT} + \varepsilon_{ij}, \quad \text{Eq. 4}$$

$$yt_{ij} = \beta_{OMT}SWC_{10} + \beta_{KgK}SWC_{10} + \beta_{KR}SWC_{10} + \beta_{OMT}T_5 + \beta_{KgK}T_5 + \beta_{KR}T_5 + b_{OMT+} + b_{KgK} + b_{KR} + \varepsilon_{ij}, \quad \text{Eq. 5}$$

where for i^{th} forest type and j^{th} observation of upland forests or transitions, yu_{ij}, and yt_{ij} is the CH_4 flux (µg m^{-2} h^{-1}), and β_{CT} through β_{KR} are the fixed effect coefficients. The predictors SWC_{10} and T_5 were fixed effect variables, b_{CT} … b_{KR} are intercepts for the random effect for i^{th} forest type, and ε_{ij} is the error for observation j in i^{th} forest type.

The response function used for net CH_4 emissions accounted for a possible optimum in WT and T_5 (Turetsky et al. 2014). Thus the net CH_4 emissions (µg m^{-2} h^{-1}) of mires were fitted by using the NLS model with a combined response to T_5 and water table depth (WT) (Eq. 6):

$$y_{ij} = a_0 e^{\left(-0.5\left(\frac{WT - WTopt}{WTtol}\right)^2\right)} e^{\left(-0.5\left(\frac{T5 - Topt}{Ttol}\right)^2\right)} + \varepsilon_{ij} \quad \text{Eq. 6}$$

where for i^{th} mire and the j^{th} observation yij is the CH_4 flux (µg m^{-2} h^{-1}), WT and T_5 are predictors, a_0, WT_{opt}, T_{opt}, WT_{tol}, and T_{tol} are fitted parameters, and ε_{ij} is the error

for observation j in i^{th} forest/mire type. The predictors and the errors were assumed to be multivariate normally distributed.

2.4 Boreal forest soil C and CO_2 modeling (III - IV)

The performance of two widely used biogeochemical models Yasso07 (Tuomi et al., 2009; Tuomi et al., 2011), and CENTURY (Parton et al. 1988, Metherell et al. 1993, Del Grosso et al. 2001) was evaluated against measurements of SOC stock and monthly extrapolated soil CO_2 emissions on four sites over two years (**III**) and SOC stocks of Swedish forest soil inventory sites (**IV**). The modeled SOC represented the equilibrium state between the litter input and decomposition for each site. The modeled CO_2 was calculated as the difference between monthly SOC change and the litter input (**III**). Modeled SOC strongly depends on the estimated litter input. In **III** and **IV**, the litter input was the same for both models and it was based on the method used in Liski et al. (2006).

Both soil C models use similar theoretical principles to divide litter input into the pools by chemistry e.g. percentage of cellulose and lignin (Tuomi et al., 2011, Adair et al. 2008) (Figure 4). Although the models structurally differ in mathematical representations of the principles of mass balance, pools specific substrate dependence of decay, heterogeneity, and transfers of organic matter between pools, and environmental effects described in more detail in following sections 2.4.1 and 2.4.2.

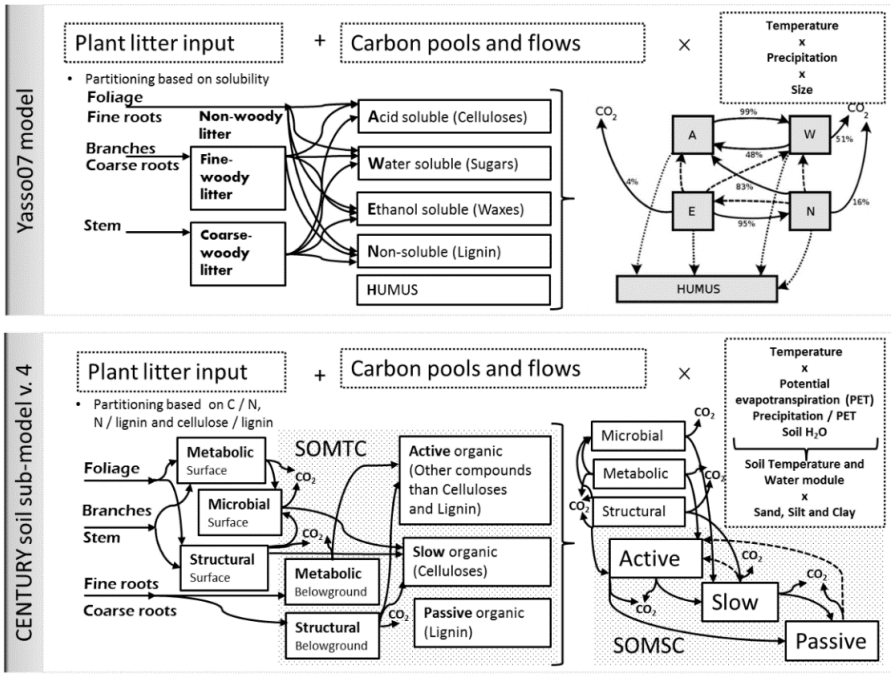

Figure 4. Comparison of the general form of C polls and flows and environmental modifiers between Yasso07 and CENTURY soil C models (based on Tuomi *et al.,* 2011; Parton et al. 1988) (**III**).

2.4.1 Yasso07 soil C model (**III-IV**)

In Yasso07 model (Tuomi et al., 2011) the C input is divided based on the solubility of organic material into five pools $c_A \ldots c_N$ from which three are fast (acid (c_A), water (c_W), ethanol (c_E)), one is slow (non-soluble (c_N)) and one is stable (humus (c_H)). The structural matrix **A** (5 × 5) consists of mass flow parameters $\alpha_A \ldots \alpha_H$ and decomposition coefficients $k_A \ldots k_H$ as matrix diagonal. The model can be expressed mathematically as a set of differential equations as in Eq. 7:

$$\frac{\mathrm{d}\boldsymbol{c}(t)}{\mathrm{d}t} = \begin{pmatrix} i_A \\ i_W \\ i_E \\ i_N \\ i_H \end{pmatrix} + \xi(t) \begin{pmatrix} -k_A s_L & \alpha_{A,W} k_W & \alpha_{A,E} k_E & \alpha_{A,N} k_N & 0 \\ \alpha_{W,A} k_A & -k_W s_L & \alpha_{W,E} k_E & \alpha_{W,N} k_N & 0 \\ \alpha_{E,A} k_A & \alpha_{E,W} k_W & -k_E s_L & \alpha_{E,N} k_N & 0 \\ \alpha_{N,A} k_A & \alpha_{N,W} k_W & \alpha_{N,E} k_E & -k_N s_L & 0 \\ \alpha_H k_A & \alpha_H k_W & \alpha_H k_E & \alpha_H k_N & -k_H \end{pmatrix} \begin{pmatrix} c_A \\ c_W \\ c_E \\ c_N \\ c_H \end{pmatrix} \quad \text{Eq. 7}$$

where, and ***i*** defines a vector of initial carbon pools $i_A \ldots i_H$, $\xi(t)$ is the scalar of the environmental rate modifier, $\alpha_{o,p}$ defines mass transfer coefficients from pool p to pool o and $k_A \ldots k_H$ maximum decomposition rate coefficients affected by the litter size function S_L delaying decomposition for large woody type litter (e.g. snags) (Eq. 8).

$$s_L = f(d_L) = (1 + \delta_1 + \delta_2)^r \quad \text{Eq. 8}$$

Where δ_1, δ_2, and r are parameters, and d_L (cm) is the diameter of the fine-woody and coarse-woody litter (e.g. 2 and 20), whereas d_L of non-woody litter is zero and not effecting decay rates. Empirical tests of this function showed that for typically managed forest litter (not including snags) the model can be run for all pools together reaching almost identical equilibrium with or without S_L modifier.

Although the model was calibrated for running on annual time steps (**IV**), it can also run on monthly time steps (**III**) if the litter input is provided on a monthly level. Then $\xi(t_m)$ (**III**) is formulated as a function of monthly air temperature (T_m) and 1/12 of annual precipitation (P_a/12) (Eq. 9).

$$\xi(t_m) = k_i e^{\left(\beta_1 T_m + \beta_2 T_m^{\,2}\right)} \left(1 - e^{\gamma \frac{P_a}{12}}\right) \quad \text{Eq. 9}$$

Where k_i is the maximum decomposition rate of the ith carbon pool, β_1, β_2, and γ are parameters of the environmental function. For running the model on the annual time step as in Tuomi et al. (2011) $\xi(t_a)$ function uses annual temperature (T_a) modified by approximation of temperature seasonality and annual precipitation (P_a) (**IV**).

2.4.2 CENTURY soil C model (**III-IV**)

In the CENTURY model (Metherell et al. 1993) the C input is divided between eight carbon pools $c_1 \ldots c_8$ (surface and soil structural, surface and soil metabolic, surface microbial, active, slow, and passive) (Figure 4). The structural matrix **A** (8 × 8) consists

of mass flow parameters $\alpha_1 \ldots \alpha_8$ and decomposition coefficients $k_1 \ldots k_8$ as matrix diagonal. The model can be expressed mathematically as a set of differential equations as in Eq. 10:

$$\frac{\mathrm{d}\boldsymbol{c}(t)}{\mathrm{d}t} = \boldsymbol{i}\begin{pmatrix} F_m \\ F_s \\ 0 \\ F_m \\ F_s \\ 0 \\ 0 \\ 0 \end{pmatrix} + \xi(t)\begin{pmatrix} -k_1 e^{-3L_s} & 0 & 0 & 0 & 0 & 0 & 0 & 0 \\ 0 & -k_2 & 0 & 0 & 0 & 0 & 0 & 0 \\ \alpha_{3,1}k_1 e^{-3L_s} & \alpha_{3,2}k_2 & -k_3 & 0 & 0 & 0 & 0 & 0 \\ 0 & 0 & 0 & -k_4 e^{-3L_s} & 0 & 0 & 0 & 0 \\ 0 & 0 & 0 & 0 & -k_5 & 0 & 0 & 0 \\ 0 & 0 & 0 & \alpha_{6,4}k_4 e^{-3L_s} & \alpha_{6,5}k_5 & -k_6 f(T_{SiC}) & \alpha_{6,7}k_7 & \alpha_{6,8}k_8 \\ \alpha_{7,1}k_1 e^{-3L_s} & 0 & \alpha_{7,3}k_3 & \alpha_{7,4}k_4 e^{-3L_s} & 0 & \alpha_{7,6}k_6 f(T_{SiC}) & -k_7 & 0 \\ 0 & 0 & 0 & 0 & 0 & \alpha_{8,6}k_6 f(T_C) & \alpha_{8,7}k_7 f(T_C) & -k_8 \end{pmatrix}\begin{pmatrix} c_1 \\ c_2 \\ c_3 \\ c_4 \\ c_5 \\ c_6 \\ c_7 \\ c_8 \end{pmatrix} \quad \text{Eq. 10}$$

Where $\boldsymbol{i}$ is the vector of plant C input partitioned between the above- and below-ground structural and metabolic pools with F_m and F_s fractions. The L_s is the lignin (structural) fraction. Maximum decomposition rates in the active, slow, and passive pool are also affected by functions of soil silt and clay contents $f(T_{SiC})$ or function of clay content $f(T_C)$.

The environmental rate modifier $\xi(t)$ is a function of monthly temperature $f(T)$ and water $f(W)$ as in Adair et al. (2008) (Eq. 11) (**III-IV**) and Kelly et al. (2000) and (Eq. 12) (**III**).

$$\xi = \frac{1}{1+w_1 e^{w_2 W}} t_1 \, e^{\frac{t_2}{t_3}\left(1-\left(\frac{T_{max}-T}{T_{max}-T_{opt}}\right)^{t_3}\right)\left(\frac{T_{max}-T}{T_{max}-T_{opt}}\right)^{t_2}} \quad \text{Eq. 11}$$

Where w_1, w_2, t_1, t_2, t_3, T_{max}, and T_{opt} are parameters, W is the ratio between precipitation and potential evapotranspiration, and T is mean monthly air temperature (°C).

$$\xi = \left(\frac{\frac{W}{1-\frac{bulkd}{partd}}-w_2}{w_1-w_2}\right)^{w_4\left(\frac{w_2-w_1}{w_1-w_3}\right)} \left(\frac{\frac{W}{1-\frac{bulkd}{partd}}-w_3}{w_1-w_3}\right)^{w_4} (t_1 + t_2 e^{t_3 T}) \quad \text{Eq. 12}$$

Where w_1, w_2, w_3, w_4, t_1, t_2, and t_3 are parameters, bulkd is bulk density, partd is particle density, W is volumetric soil water content (%), and T is mean monthly air temperature (°C).

3 RESULTS AND DISCUSSION

3.1 Controls of forest floor C fluxes in empirical models

3.1.1 CO_2 emissions (I)

The NLS analysis used to fit empirical models of total forest floor respiration (R_{ff}, g CO_2 m^{-2} $hour^{-1}$) to soil temperature at 5 cm depth (T_5, °C) showed a relatively high percentage of explained variance of measured data (R^2 in the range between 0.72 in VSR2 and 0.88 in VT) (Table 1) (**I**). The highly explained variance by temperature indicated that during the typical climatic conditions for the region the effect of soil moisture variation on forest floor

respiration was lower than that of temperature regardless of the high spatial variation of long-term moisture. This agreed with Webster et al. (2008) whose empirical model of measured soil respiration in a forest – mire transect in Canada related majority of the variance to temperature (48%) and only 9% to moisture.

The parameter of the basal respiration in **I** was comparable to the values of other studies in similar conditions (Riutta et al. 2007, Kolari et al. 2009, Pumpanen et al. 2015) but it was not a clear indicator of the spatial differences between forests and mires. Although the base respiration was higher for upland forest and transition compared to mires which could indicate either larger contribution of heterotrophic respiration from deeper soil layers but also a potentially larger contribution of autotrophic respiration of tree roots. Separation of the forest floor autotrophic and heterotrophic respiration components would be crucial for understanding the expected response of soil carbon to the warming climate (Bond-Lamberty et al. 2004, Wieder et al. 2013, Pumpanen et al. 2015). However, the activation energy of sites with the largest SOC such as swamp (KR) and mires (VSR) was significantly higher than in other forest sites with less SOC (CT…KgK). The higher activation energy of respiration in KR and VSR indicated that their SOC was lower quality, required larger enzyme pool to decompose, and it was thermally more stable than in CT…KgK (Allison et al. 2010, Sierra et al. 2012a).

Weak soil moisture effect on R_{ff} was seen also from the lack of significant correlation in Pearson correlation analysis. On the other hand, the strong ($r = 0.92$) correlation between the depth of the organic horizon and the annual mean soil moisture was highly significant (p-value = 0.01) (**I**). In conditions of warming climates, with more frequent droughts and water table drawn down, different changes to C stocks could be expected between peatlands and forested peatlands (Minkkinen et al. 1999, Lohila et al. 2011), nevertheless, the peatland's potential role as C sinks in the boreal landscape would be more pronounced (Leifeld and Menichetti 2018).

Table 1. Statistics (s) and parameters (p) of the non-linear regressions (Eq. 1) between the forest floor respiration (g CO_2 m^{-2} h^{-1}) and soil temperature at 5 cm depth (T5, °C) fitted for each forest/mire type including upland forests on mineral soils (CT, VT, MT, OMT), forest-mire transitions (OMT+, KgK, KR) and mire (VSR1, VSR2).

		Forest/mire types								
p	s	CT	VT	MT	OMT	OMT+	KgK	KR	VSR1	VSR2
	R^2	0.74	0.88	0.82	0.80	0.77	0.80	0.72	0.74	0.72
R_{ffref}	Mean	0.38	0.27	0.30	0.50	0.34	0.33	0.39	0.21	0.26
	SD	0.07	0.02	0.02	0.07	0.04	0.07	0.08	0.04	0.05
b, K	Mean	350	412	401	344	379	394	507	525	518
	SD	58	54	30	12	37	36	67	63	107

*3.1.2 CH_4 exchange (**II**)*

The mineral soils (in upland forests CT...OMT) and organo-mineral soils (in the forest – mire transitions) (OMT+…KR) showed small but significantly different net mean CH_4 oxidation between -26 and -58 (μg m^{-2} h^{-1}) (Table 2, parameters bi and "group bi") and occasionally small CH_4 emissions (<100 μg m^{-2} h^{-1}). The range of the mean CH_4 oxidation (Table 2) was relatively small in comparison with the order of magnitude larger differences in mean CH_4 emissions of organic soils in mires (VSR1, VSR2) (Table 3, parameter a0). The increasing SWC_{10} for both upland and transitional forests significantly correlated with reducing CH_4 oxidation up to around zero CH_4 exchange at maximum water content in transitions. The positive significant correlation between CH_4 oxidation and T_5 was observed only for uplands (Figure 5). In transitions, T_5 was not a significant ($p = 0.629$) predictor of CH_4 exchange (Table 2). Similar correlations for well-drained sites were found by Ullah et al. (2011) who extrapolated their CH_4 emissions with exponential relationship to the combined response of moisture and temperature.

In this study (**II**) we found that the CH_4 fluxes in undisturbed forest-mire transitions were near-zero, despite high SWC_{10} (SWC10 > 70 %) and close to surface annual average water level (WT -24 cm). Near-zero CH_4 fluxes agree with Ojanen et al. (2010) who for drained forested peatlands in Finland reported an exponential increase in CH_4 emissions with annual WT level increase from around -30 cm depth to the surface. Although the CH_4 exchange for their sites between -30 cm and -10 cm varied largely, between zero and 4 g CH_4 m^{-2} $year^{-1}$. The difference in WT depth of forest-mire transitions and lack of CH_4 emissions could be also attributed to the uncertainty of differences in nutrient status and differences in species composition (Turetsky et al. 2014).

Table 2. CH_4 flux (μg m^{-2} h^{-1}) model statistics (parameters, their standard errors and root mean square error) for the upland forest types (CT, VT … OMT (Eq. 4), and for the forest-mire transitions (OMT+, KgK, and KR (Eq. 5) fitted with volumetric soil moisture at 10 cm (%) and soil temperature at a depth of 5 cm (°C).

Eq. 4	bi	group bi	group bi SE	βi1	βi1 SE	βi2	βi2 SE	N	RMSE
CT	-39.3							137	35.2
VT	-26.2	-43.6	9.1	0.7[a]	0.3	-1.2	0.2	143	25.1
MT	-51.0							139	25.2
OMT	-58.0							144	32.1
Eq. 5									
OMT+	-49.9							139	22.3
KgK	-48.2	-50.2	7.5	0.6	0.1	-0.1[b]	0.2	146	17.9
KR	-52.6							149	31.5

$p < 0.001$ for all parameters, except [a] $p = 0.011$, [b] $p = 0.629$

βi1 - soil moisture at 10 cm, βi2 - soil temperature at 5 cm

Table 3. CH_4 flux (µg m^{-2} h^{-1}) model statistics (parameters, their standard errors and root mean square error) for the mires (VSR1, VSR2 (Eq. 6) fitted with water table depth from the surface (cm) and soil temperature at a depth of 5 cm (°C).

Eq. 3	a0	a0 SE	T_{opt}	T_{opt} SE	T_{tol}	T_{tol} SE	WT_{opt}	WT_{opt} SE	WT_{tol}	WT_{tol} SE	N	RMSE
mires	1207	127	13.9	1.4	6.4	1.3	18	1.9	16.6	2.1	324	656
VSR1	1570	155	13	0.8	5.8	0.8	18.6	1.6	15.5	1.7	162	424
VSR2	801.3	191	16.6[a]	6.8	8.7[b]	4.5	17.3[c]	5.3	20.7[d]	9.7	162	558

p values < 0.001, except [a] p = 0.016, [b] p = 0.053, [c] p = 0.002, [d] p = 0.035

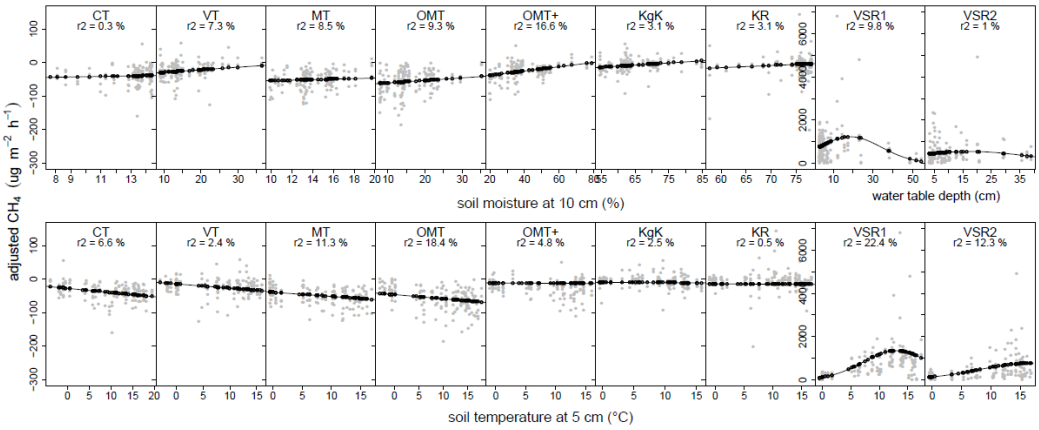

Figure 5. Residual figures of CH_4 fluxes (µg m^{-2} h^{-1}) of the NLS models and volumetric soil moisture at 10 cm (%) (CT…KR), water table depth (VSR1, VSR2), and soil temperature at a depth of 5 cm for nine forest/mire types. The CH_4 flux response for each factor is showed by modeled value for allowing only one factor at a time to vary while the other was at its mean. Black points show the model function and gray points show the corresponding residual for unexplained model variation. The r2 value is the percentage of explained variance. The sites are arranged from forests (left) to mires (right).

In comparison to few existing studies finding small CH4 emissions for forest –mire transects in Canada and Europe (Moosavi and Crill 1997, Ullah et al. 2011, Schneider et al. 2018), similarly in this study, the CH4 exchange of forest – mire transitions was near zero during wetter periods and a small sink during drier periods. In landscape biogeochemistry, forest-mire transitions have the potential to become small sources of CH4 if their water level increases closer to the surface, but their CH4 emissions are expected to be smaller than in mires.

The net CH4 emissions in mires showed asymmetric Gaussian response form to WT depth and T5. If the temperature was at its optimal 13.9 °C then CH4 emission peaked at

1207 µg m−2 h−1 at 18 cm WT depth (Table 3), decreased to 670 µg m−2 h−1 as WT rose to the surface and 115 µg m−2 h−1 with WT drawn down to its minimum (54 cm). The effect of T5 on CH4 emissions in mires also showed asymmetric Gaussian form with significant optimum for both mires fitted together (Table 3). However, in VSR2 the fitted function showed insignificant temperature optimum (Table 3, Figure 5).

Although gaussian functional WT response accounts for a wider range of conditions, depending on the measured data linear, exponential, and sigmoidal functions can sufficiently explain the observed variation (Kettunen et al. 2000, Alm et al. 2007, Ojanen et al. 2010, Ullah et al. 2011, Marushchak et al. 2016). The explained variances of the fitted Gaussian models in this study (II) were relatively low due to large temporal variation in water level variations and moisture (Figure 5) and due to processes unaccounted by empirical functions with T and WT. For example, besides T and WT in tall - sedge fens vegetation distribution is a major control of CH4 emissions by photosynthetic production of aerenchymal vegetation and supply of acetate for CH4 production and its direct transport to the atmosphere (Shurpali and Verma 1998, Hines 2007, Rinne et al. 2018).
The dynamics of CH4 production, consumption and transport mechanisms and their driving environmental variables such as vegetation development, photosynthesis, variation in water level, peat oxygenation, and temperature could be expressed more explicitly by process-based models e.g. HPM (Frolking at al. 2010, 2014), HIMMELI (Raivonen et al. 2017), or ORCHIDEE-PEAT (Qiu et al. 2019). Although the HPM and ORCHIDEE-PEAT models simulate primarily peat development than CH4 exchange, information on available soil C is key for simulating decomposition in Michaelis-Menten type gas exchange models (Davidson et al. 2014) such as HIMMELI. In HIMMELI, the anaerobic respiration (a product of vascular plants NPP and anaerobic peat decomposition) is a required input for O2 limited CH4 production while both aerobic respiration and CH4 oxidation follow substrate (O2 and CH4) dependent MM kinetics (Raivonen et al. 2017).

The models with moisture dependency expressed by dual substrate MM functions are mechanistically more reasonable but not fundamentally different from Gaussian moisture function fitted empirically. The performance between the two may be similar; however, if substrate C accessible to enzymes is dynamic then MM model performance improves (Davidson et al. 2014).

3.2 Controls of soil C stock change in process models

*3.2.1 T, W effects on soil heterotrophic respiration (**III**)*

The empirical environmental modifiers of decomposition in Yasso07 and CENTURY soil C models (Eq. 9, 11, and 12) show exponential or Gaussian dependence on air temperature, and sigmoidal or Gaussian dependence on water (precipitation or volumetric soil water content) (Figure 6) (**III**). Calibrating these functions with monthly R_h measurements (Figure 6) strongly improved the fit between the measured and modeled CO_2 values (Figure 7) demonstrating the need for their improvement towards more mechanistic representation.

For example, the environmental function of the Yasso07 model (Eq. 9) largely changed after calibration by reducing the inversion point of the Gaussian temperature modifier. The Yasso07 model's precipitation curve has not visibly changed after calibration. Although these environmental modifiers are not necessarily the best for all applications, the estimated CO_2 emissions of the Yasso07 model after calibration showed the best match with the

measurements in this study (Figure 7). For modeling, fine-scale spatial differences of SOC distributions and predicting response of SOC to warming, climate use of soil temperature instead of air temperature would be in the boreal region more feasible due to the lag between air and soil warming (Todd-Brown et al. 2013, Halim and Thomas 2018, Soong et al. 2020). The Gaussian air temperature function showed the best fit with calibrated data (Tuomi et al. 2008). This may not be the best if measurements of soil temperature would be used instead. Sierra et al. (2017) clarified that under the range of soil temperature in the boreal forests, the temperature response of decomposition is exponential due to no enzymatic constraints. However, the aerobic decomposition rate at a given temperature is limited due to dual substrate limitations (lack of O_2 is limiting microbial physiology under high moisture and physical constraints are limiting C solute transport to microbes during low moisture conditions) (Moyano et al. 2013, Manzoni et al. 2016). The study sites in **III** were well-drained mineral soil forests with a small number of measurements over the soil moisture optimum for which the model slightly overestimated CO_2 emissions. For higher soil moisture levels such as in forest – mire transitions, defining the modifier based on MM kinetics or Gaussian response would be more crucial as it would account for the reduction of respiration.

In Eq. 11 (CENTURY.A), the temperature response with default parameters showed steep increase just over 20 °C with an optimum over 30 °C but after the calibration the response was linear (Figure 6). The moisture effect of the same function remained similar after the calibration (Figure 6). As expected, the CENTURY.A model residuals after calibration showed a small mismatch with measurements (Figure 7).

Exponential relation with temperature and Gaussian relation with soil moisture in Eq. 12 (CENTURY.K) were like the NLS empirical Q_{10} temperature function and Gaussian moisture function of Eq. 3. The NLS functions were used for the extrapolation of hourly measurements to a monthly level. However, the CENTURY.K results remained similar after calibration and residuals have improved less compared to CENTURY.A (Figure 7) which could be an indication of the poor-quality soil water content measurements used. This points to the need for high-quality soil water data if those are to be used in the models.

Modeled soil respiration divergence with measurements after the calibration, the overestimation in spring, and underestimation in autumn highlights a need for reformulating the environmental modifiers. The modeled early increase of spring respiration could indicate the unaccounted lag between air and soil warming (Todd-Brown et al. 2013) whereas an early decline in autumn respiration could indicate unaccounted microbial pathway (Averill *et al*., 2014; Wieder *et al*., 2013, Luo *et al*., 2016).

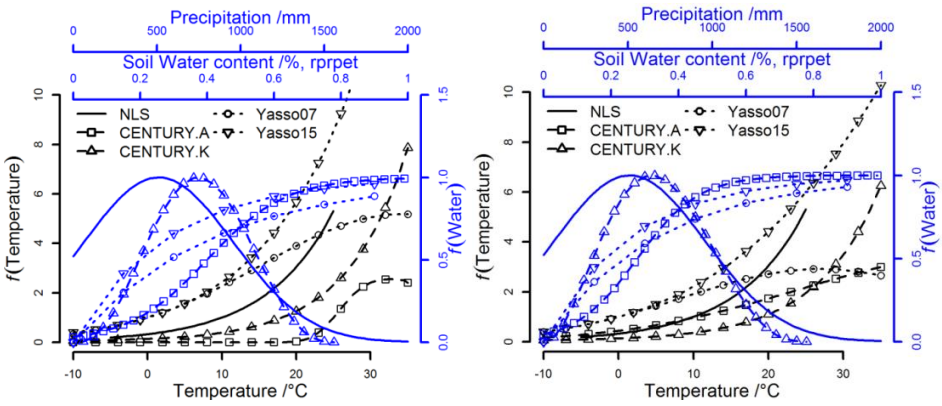

Figure 6. (Left) Default temperature and water functions of the Yasso and CENTURY models in comparison to the nonlinear model fit to the respiration measurements (Eq. 3). (Right) Calibrated functions with the respiration measurements (**III** Supplement).

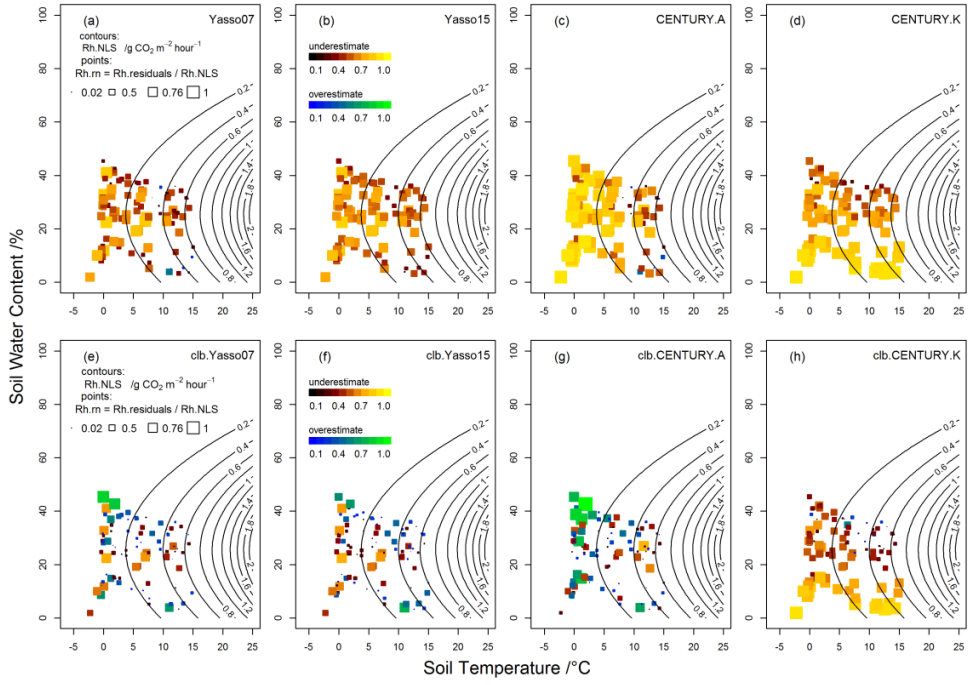

Figure 7 Point distributions of normalized model residuals (Rh.rn) of soil respiration (Rh, g CO_2 m^{-2} $hour^{-1}$) plotted in space of soil temperature and moisture. Contour lines, based on Rh measurements, show interpolated Rh.NLS values with Eq. 3. The Rh residuals were normalized (Rh.rn) with Rh.NLS values. The panels show model outputs with default parameters (a)…(d) and those with calibrated empirical models (e)…(h).

*3.2.2 Effect of soil W and nutrient status on SOC (**IV**)*

The well-drained mineral soils of Swedish forest soil inventory (SFSI) data were separated based on physicochemical soil properties into 10 groups by using the regression tree model (Figure 8). The main predictor for SOC levels was the cation exchange capacity of the BC horizon (CEC, $mmol_c\ kg^{-1}$) (**IV**) linked to the soil nutrient status. This supported conclusion on the importance of nutrient status on SOC accumulation based on ecosystem carbon use efficiency derived from forest CO_2 balance (Fernández-Martínez et al. 2014). The CEC levels had divided 2/3 of all SFSI SOCs to lower SOC stock groups (between 65 and 130 t C ha^{-1}) and 1/3 to larger groups (between 86 and 269 t C ha^{-1}) (Figure 8). Besides CEC, the sorted soil parent material (linked with higher clay content), the N deposition over 10 kg N $ha^{-1}\ y^{-1}$ and peat humus type were also influential controls for larger SOCs linked to site fertility (Figure 8).

The modeled Yasso07 and CENTURY SOCs matched the 2/3 of the lower level SOCs of sites with low and medium nutrient status, and underestimated 1/3 of SOCs of sites with higher fertility (Figure 9) (**IV**). The performance of both models was similar. Though, CENTURY, due to considering C association with soil minerals, outperformed Yasso07 for soils with higher clay content (group 5 in Figure 9). In the comparison of SOC from 11 ESM against observational databases, Todd-Brown et al. (2013) attributed modeled divergence from observations to uncertainty in input data, incorrect environmental response functions, and missing formulation of essential processes in seemingly uniform first-order decay models. Although the C/N ratio was identified as a key factor related to SOC accumulation in northern observational databases, the nutrient status is underrepresented in Earth system models (ESM) (Hashimoto et al. 2017).

Yasso07 and CENTURY models have also relatively similar structure (Figure 4) and use similar environmental functions (Figure 6). Although, the individual equations and parameters differ (see Eq. 7 and Eq. 9 for model structure, and Eq. 9 and Eq. 10 for environmental modifier). Yasso07 did not require soil properties and the variation in soil fertility was reflected in data through a difference in the quantity of litter input and chemistry between plant species and its components.

In contrast, CENTURY in addition to variation in litter input accounted for SOC association with soil clay content and for SOC increase with soil N content. However, the effect of the CENTURY's topsoil N function on SOC stock, when tested in **IV**, was negligible compared to the effect of litter input. Thus, in **IV** we had run only C sub-model of CENTURY. The CENTURY model also accounted for an optional reduction of decomposition using the approach of Reich et al. (2000) which was originally meant to be applied for poorly drained soils; thus, the approach could have been insufficient for simulating larger SOCs in relatively well-drained groups in **IV**.

a)

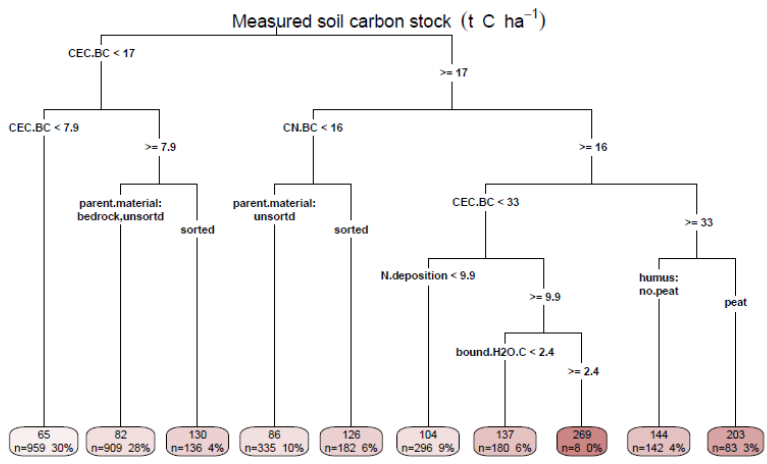

b)

	n=959	n=909	n=136	n=335	n=182	n=296	n=180	n=8	n=142	n=83
Carbon	low	medium	high	medium	high	medium	high	extra	high	extra
Moisture	dry–fresh	fresh	moist–fresh	fresh	moist–fresh	fresh	fresh	fresh	fresh	moist–fresh
Fertility	low	medium	medium	medium	high	low	high	high	medium	medium
Soil group	1	2	3	4	5	6	7	8	9	10

Figure 8. a) The regression tree for the SFDI SOC (t ha^{-1}) separated into 10 groups based on soil physicochemical properties and site environmental characteristics; the cation exchange capacity of BC horizon (CEC.BC, mmol$_c$ kg^{-1}), the C/N ratio (CN.BC), the nitrogen deposition (N.deposition, kg N ha^{-1} y^{-1}), the highly bound soil water of C horizon (bound.H2O.C, %), and soil class variables as type of sorted or unsorted soil parent material and humus type. The mean SOC and number and percentage of samples are shown for each group. b) The 10 physicochemical soil groups of the regression tree model are interpreted by increasing levels of carbon, soil moisture, and fertility from left to right.

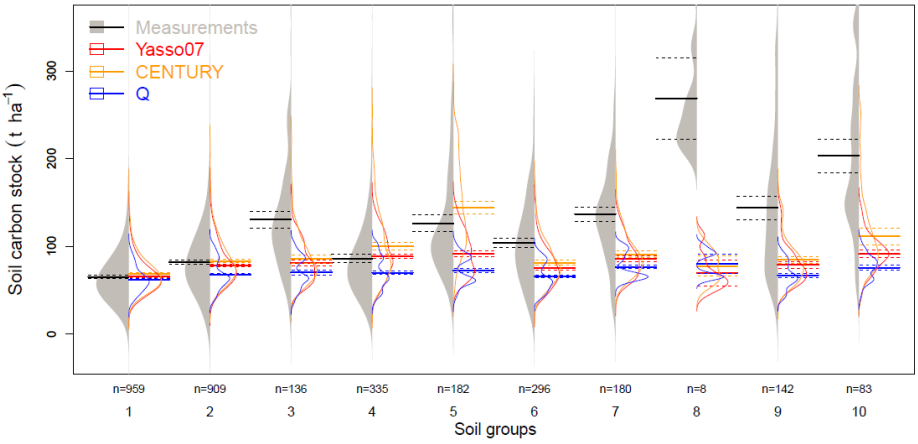

Figure 9. Measured (area) and modeled distributions (lines) of Yasso07, CENTURY, and Q models for 10 physicochemical groups of the soil carbon (t ha^{-1}). The thin lines are the density distributions. The thick lines are the group means and dashed lines are their confidence intervals. The n is number of samples. For a description of group levels of SOC stocks, moisture, and fertility see Figure 8.

In **IV**, we tested models against measured data with their default parameters. The default parameterization, as seen on the calibration of its environmental functions in **III**, contributed to data mismatch. The soil carbon models were parameterized globally for Yasso07 or regionally for CENTURY (coniferous forest) and do not require further calibrations. Nevertheless, the models could be calibrated for specific regions and datasets e.g. Nordic countries (Rantakari et al. 2012) where SOC responses to mean annual temperature, precipitation, and soil C/N ratio differ from the global trend (Hashimoto et al. 2017). However, in **IV** the Yasso07 model comparison against SFSI SOCs data showed larger underestimation with Nordic parameters from Rantakari et al. (2012) than with global parameters from Tuomi et al. (2011). Therefore, the SOCs underestimation for SFSI sites with higher moisture and fertility could also indicate the misconception in sensitivities to moisture (insufficient reduction of decomposition in wetter sites) and nutrient status (negligible increase with increasing soil N content).

Thus, the models could benefit from reformulating sensitivity to soil moisture and nutrient status. Moisture function could explicitly formulate MM substrate diffusion fluxes (O_2 and C substrate accessible to an enzyme) (Davidson et al. 2012) during soil drying. If the C substrate is modeled dynamically (e.g. with pool-specific MM kinetics), models could account for both drying and wet up events (Oikawa et al. 2014, Davidson et al. 2014, Sihi et al. 2018). In a study by Goll et al. (2017), Yasso environmental modifier affecting the decomposition rate of C_A, C_W, C_E, and C_N pools was found to be downregulated by N depending on the soil supply and demand by microbes and plants. Resulting SOC accumulation was smaller for soils with limited N. The structure of the N sub-model in CENTURY is the same as for C (Metherell et al. 1993, Del Grosso et al. 2001) and like that of Goll et al. (2017). Coupled CENTURY C-N sub-models were run e.g. in modeling SOC sequestration of European arable soils (Lugato et al. 2014). Mechanisms of increased SOC accumulation with higher soil nutrient status related with reduced C uptake and increasing microbial carbon use efficiency with available N (Manzoni et al. 2016) were integrated already in microbial enzyme MM models (Allison et al. 2010, Wieder et al. 2014, Abramoff et al. 2017) and combined microbial MM and first-order decay model (Moyano et al. 2018).

In **III** and **IV**, the forest soils were relatively well-drained, as Yasso07 and CENTURY models are meant for application on mineral soils. Improved representations of model functions would be especially important for extending the application of modeling studies from mineral soils to organic soils. Although mineral soils are most common, the less represented organic soils could be more crucial for climate change related dynamics of boreal zone soil carbon storage (Turetsky et al. 2015, Leifeld and Menichetti 2018). As indicated by studies in the gradient of soil moisture and nutrient status (**I** and **II**), the forest – mire transitions on organo-mineral forest soil and peatlands, with the largest soil C storage, have the largest potential for acting as soil C sink in the landscape or the vulnerability to become C sources.

4 CONCLUSIONS

In **I-IV**, the main controls of boreal forest soil organic carbon (SOC) accumulation and CO_2 and CH_4 emissions were demonstrated and discussed in the order of importance; soil temperature and water (**I-III**), and nutrient status (**IV**). The main emphasis was to evaluate the empirical representation of the controls in the data, and their mathematical formulation in the semi-empirical process-based models (Yasso07 and CENTURY) concerning current knowledge of the processes and the model development.

Spatially, soil temperature (and not the soil moisture) explained the most instantaneous variation of soil CO_2 emissions, although the long-term moisture strongly correlated with SOC socks (**I**). However, during extreme weather events such as prolonged summer drought, mainly soil CO_2 emissions in mineral soil forests and CH_4 emissions in mires were significantly reduced (**II**). Similar temperature and moisture sensitivities of forest-mire transitions to upland forests indicated that transitions do not act as hot spots of CO_2 and CH_4 emissions in the boreal landscape (**I -II**). Both parametrization and formulation between the representation of temperature and moisture functions in Yasso07 and CENTURY affected the fit between the measured and modeled seasonal soil CO_2 emissions (**III**). Similarly, at the country level, the forest SOC stocks in Sweden increased with higher moisture and nutrient status (**IV**). Yasso07 and CENTURY reconstructed SOCs well for mesotrophic soils but failed for soils with higher fertility and wetter soils (**IV**).

The main conclusion is that the empirically based representation of soil temperature, water, and productivity controls in Yasso07 and CENTURY models affected the mismatch between measured and modeled seasonal CO_2 emissions and long-term SOC sequestration. These models are currently applicable on mineral soils, however, due to a large C storage in organo-mineral and organic soils in boreal landscape, we also need models for forest-mire transitions and peatlands. Thus, further model development could be more explicit about a supply of the C-N to microbes, microbial C-N uptake related to nutrient status and enzyme kinetics. Including microbial and enzyme kinetics in the models would account for climate – plant – soil – microbial C-N interactions more mechanistically. As a result, more mechanistic and spatially applicable models would improve the estimates of boreal forest soil C feedback to changing climates.

REFERENCES

Abramoff, R.Z., Davidson, E.A., Finzi, A.C., 2017. A parsimonious modular approach to building a mechanistic belowground carbon and nitrogen model. Journal of Geophysical Research: Biogeosciences 122, 2418–2434. https://doi.org/10.1002/2017JG003796

Adair, E.C., Parton, W.J., Del Grosso, S.J., Silver, W.L., Harmon, M.E., Hall, S.A., Burke, I.C. and Hart, S.C., 2008. Simple three-pool model accurately describes patterns of long-term litter decomposition in diverse climates. *Global Change Biology*, 14, 2636-2660. https://doi.org/10.1111/j.1365-2486.2008.01674.x

Allison, S.D., Wallenstein, M.D. and Bradford, M.A., 2010. Soil-carbon response to warming dependent on microbial physiology. *Nature Geoscience*, 3, 336-340. https://doi.org/10.1038/ngeo846

Alm, J., Saarnio, S., Nykänen, H., Silvola, J. & Martikainen, P. J. 1999. Winter CO2, CH4 and N2O fluxes on some natural and drained boreal peatlands. *Biogeochemistry*, 44, 163-186. https://doi.org/10.1023/A:1006074606204

Alm, J., Shurpali, N. J., Tuittila, E. S., Laurila, T., Maljanen, M., Saarnio, S. & Minkkinen, K. 2007. Methods for determining emission factors for the use of peat and peatlands - flux measurements and modelling. *Boreal Environment Research* 12, 85-100.

Aurela, M., Riutta, T., Laurila, T., Tuovinen, J.P., Vesala, T., Tuittila, E.S., Rinne, J., Haapanala, S. and Laine, J., 2007. CO2 exchange of a sedge fen in southern Finland-The impact of a drought period. *Tellus B: Chemical and Physical Meteorology*, *59*, 826-837. https://doi.org/10.1111/j.1600-0889.2007.00309.x

Averill, C., Turner, B.L. and Finzi, A.C., 2014. Mycorrhiza-mediated competition between plants and decomposers drives soil carbon storage. *Nature*, *505*, 543-545. https://doi.org/10.1038/nature12901

Bintanja, R., Graversen, R.G. and Hazeleger, W., 2011. Arctic winter warming amplified by the thermal inversion and consequent low infrared cooling to space. *Nature Geoscience*, *4*, 758-761. https://doi.org/10.1038/ngeo1285

Bond-Lamberty, B., Wang, C. and Gower, S.T., 2004. A global relationship between the heterotrophic and autotrophic components of soil respiration?. *Global Change Biology*, *10*, 1756-1766. https://doi.org/10.1111/j.1365-2486.2004.00816.x

Bubier, J.L., 1995. The relationship of vegetation to methane emission and hydrochemical gradients in northern peatlands. *Journal of Ecology*, pp.403-420. https://doi.org/2261594

Cajander, A.K., 1949. Forest types and their significance. *Acta For Fenn*, *56*, pp.1-72.

Chertov, O.G., Komarov, A.S., Nadporozhskaya, M., Bykhovets, S.S., Zudin, S.L., 2001. ROMUL — a model of forest soil organic matter dynamics as a substantial tool for forest ecosystem modeling. Ecological Modelling 138, 289–308. https://doi.org/10.1016/S0304-3800(00)00409-9

Churkina, G., Schimel, D., Braswell, B.H. and Xiao, X., 2005. Spatial analysis of growing season length control over net ecosystem exchange. *Global Change Biology*, *11*(10), pp.1777-1787. https://doi.org/10.1111/j.1365-2486.2005.001012.x

Coleman, K., Jenkinson, D.S., 1996. RothC-26.3 - A Model for the turnover of carbon in soil, in: Powlson, D.S., Smith, P., Smith, J.U. (Eds.), Evaluation of Soil Organic Matter Models, NATO ASI Series. Springer, Berlin, Heidelberg, pp. 237–246. https://doi.org/10.1007/978-3-642-61094-3_17

Cotrufo, M.F., Wallenstein, M.D., Boot, C.M., Denef, K. and Paul, E., 2013. The Microbial Efficiency-Matrix Stabilization (MEMS) framework integrates plant litter decomposition with soil organic matter stabilization: do labile plant inputs form stable soil organic matter?. *Global Change Biology*, 19, 988-995. https://doi.org/10.1111/gcb.12113

Crowther, T.W., Todd-Brown, K., Rowe, C., Wieder, W.R., Carey, J.C., Machmuller, M.B., Snoek, B., Fang, S., Zhou, G. & Allison, S.D. 2016. Quantifying global soil carbon losses in response to warming. *Nature*, 540, 104–8. https://doi.org/10.1038/nature20150

Davidson, E.A., Samanta, S., Caramori, S.S. and Savage, K., 2012. The Dual Arrhenius and Michaelis–Menten kinetics model for decomposition of soil organic matter at hourly to seasonal time scales. *Global Change Biology*, 18, 371-384. https://doi.org/10.1111/j.1365-2486.2011.02546.x

Davidson, E.A., Savage, K.E. and Finzi, A.C., 2014. A big-microsite framework for soil carbon modeling. *Global change biology*, *20*, 3610-3620. https://doi.org/10.1111/gcb.12718

Del Grosso, S.J., Parton, W.J., Mosier, A.R., Hartman, M.D., Brenner, J., Ojima, D.S. and Schimel, D.S., 2001. Simulated interaction of carbon dynamics and nitrogen trace gas fluxes using the DAYCENT model. *Modeling carbon and nitrogen dynamics for soil management*, pp.303-332. https://doi.org/DOI:10.1201/9781420032635.ch8

Fernández-Martínez, M., Vicca, S., Janssens, I.A. & Campioli, M. 2014. Nutrient availability as the key regulator of global forest carbon balance. *Nature Climate Change*, 4, 471–6. https://doi.org/10.1038/nclimate2177

Frolking, S., Roulet, N.T., Tuittila, E.S., Bubier, J.L., Quillet, A., Talbot, J. and Richard, P.J.H., 2010. A new model of Holocene peatland net primary production, decomposition, water balance, and peat accumulation. *Earth System Dynamics*, 1, 1-21, https://doi.org/10.5194/esd-1-1-2010

Frolking, S., Talbot, J., Jones, M.C., Treat, C.C., Kauffman, J.B., Tuittila, E.S. and Roulet, N., 2011. Peatlands in the Earth's 21st century climate system. *Environmental Reviews*, 19, pp.371-396. https://doi.org/10.1139/a11-014

Frolking, S., Talbot, J. and Subin, Z.M., 2014. Exploring the relationship between peatland net carbon balance and apparent carbon accumulation rate at century to millennial time scales. *The Holocene*, *24*, 1167-1173. https://doi.org/10.1177/0959683614538078

Goll, D. S., Winkler, A. J., Raddatz, T., Dong, N., Prentice, I. C., Ciais, P., and Brovkin, V., 2017. Carbon–nitrogen interactions in idealized simulations with JSBACH (version 3.10), *Geosci. Model Dev.*, 10, 2009–2030, https://doi.org/10.5194/gmd-10-2009-2017

Goodale, C.L., Apps, M.J., Birdsey, R.A., Field, C.B., Heath, L.S., Houghton, R.A., Jenkins, J.C., Kohlmaier, G.H., Kurz, W., Liu, S. and Nabuurs, G.J., 2002. Forest carbon sinks in the Northern Hemisphere. *Ecological applications*, *12*, 891-899. https://doi.org/10.1890/1051-0761(2002)012[0891:FCSITN]2.0.CO;2

Gong, J., Kellomäki, S., Wang, K., Zhang, C., Shurpali, N. and Martikainen, P.J., 2013. Modeling CO2 and CH4 flux changes in pristine peatlands of Finland under changing climate conditions. *Ecological modelling*, *263*, 64-80. https://doi.org/10.1016/j.ecolmodel.2013.04.018

Halim, M.A. and Thomas, S.C., 2018. A proxy-year analysis shows reduced soil temperatures with climate warming in boreal forest. *Scientific reports*, *8*, 1-9. https://doi.org/10.1038/s41598-018-35213-w

Hashimoto, S., Nanko, K., Ťupek, B., and Lehtonen, A. 2017. Data-mining analysis of the global distribution of soil carbon in observational databases and Earth system models, Geosci. Model Dev., 10, 1321–1337. https://doi.org/10.5194/gmd-10-1321-2017

Hegerl, G., Luterbacher, J., González-Rouco, F., Tett, S.F., Crowley, T. and Xoplaki, E., 2011. Influence of human and natural forcing on European seasonal temperatures. *Nature Geoscience*, *4*, 99-103. https://doi.org/10.1038/ngeo1057

Hines, M.E., Duddleston, K.N., Rooney-Varga, J.N., Fields, D. and Chanton, J.P., 2008. Uncoupling of acetate degradation from methane formation in Alaskan wetlands: connections to vegetation distribution. *Global Biogeochemical Cycles*, *22*. https://doi.org/10.1029/2006GB002903

Holmberg, M., Aalto, T., Akujärvi, A., Arslan, A.N., Bergström, I., Böttcher, K., Lahtinen, I., Mäkelä, A., Markkanen, T., Minunno, F. and Peltoniemi, M., 2019. Ecosystem services related to carbon cycling–modelling present and future impacts in boreal forests. *Frontiers in plant science*, *10*, 343. https://doi.org/10.3389/fpls.2019.00343

Howie, S.A. and Tromp-van Meerveld, I., 2011. The essential role of the lagg in raised bog function and restoration: a review. *Wetlands*, *31*, 613-622. https://doi.org/10.1007/s13157-011-0168-5

ICPII European intensive forest monitoring network (ICP – level II). www.metla.fi/metinfo/forest-condition/programmes/intensive-monitoring.htm

IPCC 2018. Intergovernmental Panel on Climate Change (IPCC) The Fifth Assessment Report (AR5): Mitigation of Climate Change https://www.ipcc.ch/report/ar5/syr/

IPCC 2019a. Climate Change and Land: an IPCC special report on climate change, desertification, land degradation, sustainable land management, food security, and greenhouse gas fluxes in terrestrial ecosystems [P.R. Shukla, J. Skea, E. Calvo Buendia, V. Masson-Delmotte, H.-O. Pörtner, D. C. Roberts, P. Zhai, R. Slade, S. Connors, R. van Diemen, M. Ferrat, E. Haughey, S. Luz, S. Neogi, M. Pathak, J. Petzold, J. Portugal Pereira, P. Vyas, E. Huntley, K. Kissick, M. Belkacemi, J. Malley, (eds.)]. Retrieved June 18, 2020, from https://www.ipcc.ch/srccl/

IPCC 2019b. Generic Methodologies Applicable to Multiple Land-Use Categories: 2019 Refinement to the 2006 IPCC Guidelines for National Greenhouse Gas Inventories, p. 63, https://www.ipcc-nggip.iges.or.jp/public/2019rf/pdf/4_Volume4/19R_V4_Ch02_Generic%20Methods.pdf

Kelly, R. H., Parton, W. J., Hartman, M. D., Stretch, L. K., Ojima, D. S., and Schimel, D. S. 2000. Intra-annual and interannual variability of ecosystem processes in shortgrass steppe, *Journal of Geophysical Research*, 105, 20093–20100. https://doi.org/10.1029/2000JD900259

Kettunen, A., Kaitala, V., Alm, J., Silvola, J., Nykanen, H. and Martikainen, P.J., 2000. Predicting variations in methane emissions from boreal peatlands through regression models. *Boreal Environment Research*, *5*, 115-132.

Kolari, P., Kulmala, L., Pumpanen, J., Launiainen, S., Ilvesniemi, H., Han, P. & Nikinmaa, E. 2009. CO2 exchange and component CO2 fluxes of a boreal Scots pine forest. *Boreal Environment Research*, 14, 761–783.

Laine, J., Komulainen, V.M., Laiho, R., Minkkinen, K., Rasinmäki, A., Sallantaus, T., Sarkkola, S., Silvan, N., Tolonen, K., Tuittila, E.S. and Vasander, H., 2004. Lakkasuo: a guide to mire ecosystem. Helsinki University

Larmola, T., Tuittila, E.S., Tiirola, M., Nykänen, H., Martikainen, P.J., Yrjälä, K., Tuomivirta, T. and Fritze, H., 2010. The role of Sphagnum mosses in the methane cycling of a boreal mire. *Ecology*, 91, 2356-2365. https://doi.org/10.1890/09-1343.1

Lehtonen, A., Linkosalo, T., Peltoniemi, M., Sievänen, R., Mäkipää, R., Tamminen, P., Salemaa, M., Nieminen, T., Ťupek, B., Heikkinen, J., & Komarov, A. 2016. Forest soil carbon stock estimates in a nationwide inventory: Evaluating performance of the ROMULv and Yasso07 models in Finland. Geoscientific Model Development, 9, 4169–4183. https://doi.org/10.5194/gmd-9-4169-2016

Leifeld, J. and Menichetti, L., 2018. The underappreciated potential of peatlands in global climate change mitigation strategies. *Nature communications*, 9, 1-7. https://doi.org/10.1038/s41467-018-03406-6

Liski, J., Lehtonen, A., Palosuo, T., Peltoniemi, M., Eggers, T., Muukkonen, P. and Mäkipää, R., 2006. Carbon accumulation in Finland's forests 1922–2004–an estimate obtained by combination of forest inventory data with modelling of biomass, litter and soil. *Annals of Forest Science*, 63, 687-697. https://doi.org/10.1051/forest:2006049

Lohila, A., Minkkinen, K., Aurela, M., Tuovinen, J.-P., Penttilä, T., Ojanen, P., and Laurila, T., 2011. Greenhouse gas flux measurements in a forestry-drained peatland indicate a large carbon sink, *Biogeosciences*, 8, 3203–3218, https://doi.org/10.5194/bg-8-3203-2011

Lugato, E., Bampa, F., Panagos, P., Montanarella, L. and Jones, A., 2014. Potential carbon sequestration of European arable soils estimated by modelling a comprehensive set of management practices. *Global change biology*, *20*, 3557-3567. https://doi.org/10.1111/gcb.12551

Luo, Y., Ahlström, A., Allison, S.D., Batjes, N.H., Brovkin, V., Carvalhais, N., Chappell, A., Ciais, P., Davidson, E.A., Finzi, A. and Georgiou, K., 2016. Toward more realistic projections of soil carbon dynamics by Earth system models. *Global Biogeochemical Cycles*, *30*, 40-56. https://doi.org/10.1002/2015GB005239

Manzoni, S., Moyano, F., Kätterer, T. and Schimel, J., 2016. Modeling coupled enzymatic and solute transport controls on decomposition in drying soils. *Soil Biology and Biochemistry*, *95*, 275-287. https://doi.org/10.1016/j.soilbio.2016.01.006

Manzoni, S. and Porporato, A., 2009. Soil carbon and nitrogen mineralization: theory and models across scales. *Soil Biology and Biochemistry*, *41*, 1355-1379. https://doi.org/10.1016/j.soilbio.2009.02.031

Manzoni, S., Čapek, P., Mooshammer, M., Lindahl, B.D., Richter, A. and Šantrůčková, H., 2017. Optimal metabolic regulation along resource stoichiometry gradients. *Ecology letters*, *20*,1182-1191. https://doi.org/10.1111/ele.12815

Marushchak, M.E., Friborg, T., Biasi, C., Herbst, M., Johansson, T., Kiepe, I., Liimatainen, M., Lind, S.E., Martikainen, P.J., Virtanen, T. and Søgaard, H., and Shurpali, N., J., 2016. Methane dynamics in the subarctic tundra: combining stable isotope analyses, plot-and ecosystem-scale flux measurements. *Biogeosciences*, *13*, 597. https://doi.org/10.5194/bg-13-597-2016

McClain, M.E., Boyer, E.W., Dent, C.L., Gergel, S.E., Grimm, N.B., Groffman, P.M., Hart, S.C., Harvey, J.W., Johnston, C.A., Mayorga, E. and McDowell, W.H., 2003. Biogeochemical hot spots and hot moments at the interface of terrestrial and aquatic ecosystems. *Ecosystems*, 6, 301-312. https://doi.org/10.1007/s10021-003-0161-9

Metherell, A., Harding, L., Cole, C.V. and Parton, W.J., 1993. CENTURY Soil organic matter model environment: Technical documentation. Agroecosystem version 4.0. https://www2.nrel.colostate.edu/projects/century/MANUAL/html_manual/man96.html

Minkkinen, K., Vasander, H., Jauhiainen, S., Karsisto, M. and Laine, J., 1999. Post-drainage changes in vegetation composition and carbon balance in Lakkasuo mire, Central Finland. *Plant and Soil*, *207*, 107-120. https://doi.org/10.1023/A:1004466330076

Moosavi, S.C. and Crill, P.M., 1997. Controls on CH4 and CO2 emissions along two moisture gradients in the Canadian boreal zone. *Journal of Geophysical Research: Atmospheres*, 102(D24), 29261-29277. https://doi.org/10.1029/96JD03873

Moyano, F.E., Manzoni, S. and Chenu, C., 2013. Responses of soil heterotrophic respiration to moisture availability: An exploration of processes and models. *Soil Biology and Biochemistry*, *59*, 72-85. https://doi.org/10.1016/j.soilbio.2013.01.002

Moyano, F.E., Vasilyeva, N. and Menichetti, L., 2018. Diffusion limitations and Michaelis–Menten kinetics as drivers of combined temperature and moisture effects on carbon fluxes of mineral soils. *Biogeosciences*, *15*, 5031-5045. https://doi.org/10.5194/bg-15-5031-2018

Oertel, C., Matschullat, J., Zurba, K., Zimmermann, F. and Erasmi, S., 2016. Greenhouse gas emissions from soils—A review. *Geochemistry*, *76*, 327-352. https://doi.org/10.1016/j.chemer.2016.04.002

Ojanen, P., Minkkinen, K., Alm, J. and Penttilä, T., 2010. Soil–atmosphere CO2, CH4 and N2O fluxes in boreal forestry-drained peatlands. *Forest Ecology and Management*, 260, 411-421. https://doi.org/10.1016/j.foreco.2010.04.036

Orwin, K.H., Kirschbaum, M.U., St John, M.G. and Dickie, I.A., 2011. Organic nutrient uptake by mycorrhizal fungi enhances ecosystem carbon storage: a model-based assessment. *Ecology Letters*, *14*, 493-502. https://doi.org/10.1111/j.1461-0248.2011.01611.x

Parton, W.J., Stewart, J.W. and Cole, C.V., 1988. Dynamics of C, N, P and S in grassland soils: a model. *Biogeochemistry*, *5*, 109-131. https://doi.org/10.1007/BF02180320

Piao, S., Ciais, P., Friedlingstein, P., Peylin, P., Reichstein, M., Luyssaert, S., Margolis, H., Fang, J., Barr, A., Chen, A. and Grelle, A., 2008. Net carbon dioxide losses of northern ecosystems in response to autumn warming. *Nature*, *451*, 49-52. https://doi.org/10.1038/nature06444

Poeplau, C., Vos, C. and Axel, D., 2017. Soil organic carbon stocks are systematically overestimated by misuse of the parameters bulk density and rock fragment content. *Soil*, 3, 61-66. https://doi.org/10.5194/soil-3-61-2017

Post, E., Alley, R.B., Christensen, T.R., Macias-Fauria, M., Forbes, B.C., Gooseff, M.N., Iler, A., Kerby, J.T., Laidre, K.L., Mann, M.E., Olofsson, J., Stroeve, J.C., Ulmer, F., Virginia, R.A., Wang, M., 2019. The polar regions in a 2°C warmer world. *Science Advances* 5, eaaw9883. https://doi.org/10.1126/sciadv.aaw9883

Pumpanen, J., Kulmala, L., Linden, A., Kolari, P., Nikinmaa, E. and Hari, P., 2015. Seasonal dynamics of autotrophic respiration in boreal forest soil estimated by continuous chamber measurements. Boreal Environment Research, 20(5).

Qiu, C., Zhu, D., Ciais, P., Guenet, B., Peng, S., Krinner, G., Tootchi, A., Ducharne, A., and Hastie, A., 2019. Modelling northern peatland area and carbon dynamics since the Holocene with the ORCHIDEE-PEAT land surface model (SVN r5488), *Geosci. Model Dev.*, 12, 2961–2982, https://doi.org/10.5194/gmd-12-2961-2019

Raivonen, M., Smolander, S., Backman, L., Susiluoto, J., Aalto, T., Markkanen, T., Mäkelä, J., Rinne, J., Peltola, O., Aurela, M., Lohila, A., Tomasic, M., Li, X., Larmola, T., Juutinen, S., Tuittila, E.-S., Heimann, M., Sevanto, S., Kleinen, T., Brovkin, V., and Vesala, T., 2017. HIMMELI v1.0: HelsinkI Model of MEthane buiLd-up and emIssion for peatlands, *Geosci. Model Dev.*, 10, 4665–4691, https://doi.org/10.5194/gmd-10-4665-2017.

Rantakari, M., Lehtonen, A., Linkosalo, T., Tuomi, M., Tamminen, P., Heikkinen, J., Liski, J., Mäkipää, R., Ilvesniemi, H. and Sievänen, R., 2012. The Yasso07 soil carbon model–Testing against repeated soil carbon inventory. *Forest Ecology and Management*, *286*, pp.137-147. https://doi.org/10.1016/j.foreco.2012.08.041

Riutta, T., Laine, J., Aurela, M., Rinne, J., Vesala, T., Laurila, T., Haapanala, S., Pihlatie, M. and Tuittila, E.S., 2007. Spatial variation in plant community functions regulates carbon gas dynamics in a boreal fen ecosystem. *Tellus B: Chemical and Physical Meteorology*, 59, 838-852. https://doi.org/10.1111/j.1600-0889.2007.00302.x

Rinne, J., Tuittila, E.S., Peltola, O., Li, X., Raivonen, M., Alekseychik, P., Haapanala, S., Pihlatie, M., Aurela, M., Mammarella, I. and Vesala, T., 2018. Temporal variation of ecosystem scale methane emission from a boreal fen in relation to temperature, water

table position, and carbon dioxide fluxes. *Global Biogeochemical Cycles*, *32*, 1087-1106. https://doi.org/10.1029/2017GB005747

Running, S.W., Gower, S.T., 1991. FOREST-BGC, A general model of forest ecosystem processes for regional applications. II. Dynamic carbon allocation and nitrogen budgets. Tree Physiol 9, 147–160. https://doi.org/10.1093/treephys/9.1-2.147

Saarnio, S., Morero, M., Shurpali, N.J., Tuittila, E.S., Mäkilä, M. and Alm, J., 2007. Annual CO_2 and CH_4 fluxes of pristine boreal mires as a background for the lifecycle analyses of peat energy. *Boreal Environmental research* 12, 101-113.

Santer, B.D., Painter, J.F., Mears, C.A., Doutriaux, C., Caldwell, P., Arblaster, J.M., Cameron-Smith, P.J., Gillett, N.P., Gleckler, P.J., Lanzante, J. and Perlwitz, J., 2013. Identifying human influences on atmospheric temperature. *Proceedings of the National Academy of Sciences*, *110*, 26-33. https://doi.org/10.1073/pnas.1210514109

Scharlemann, J.P., Tanner, E.V., Hiederer, R. and Kapos, V., 2014. Global soil carbon: understanding and managing the largest terrestrial carbon pool. *Carbon Management*, *5*, 81–91. https://doi.org/10.4155/cmt.13.77

Schneider, J., Ťupek, B., Lukasheva, M., Gudyrev, V., Miglovets, M. and Jungkunst, H.F., 2018. Methane emissions from paludified boreal soils in European Russia as measured and modelled. *Ecosystems*, *21*, 827-838. https://doi.org/10.1007/s10021-017-0188-y

Soong, J.L., Phillips, C.L., Ledna, C., Koven, C.D. and Torn, M.S., 2020. CMIP5 models predict rapid and deep soil warming over the 21st century. *Journal of Geophysical Research: Biogeosciences*, *125*, https://doi.org/10.1029/2019JG005266

Shurpali, N.J. and Verma, S.B., 1998. Micrometeorological measurements of methane flux in a Minnesota peatland during two growing seasons. *Biogeochemistry*, *40*, 1-15. https://doi.org/10.1023/A:1005875307146

Sierra, C.A., Harmon, M.E. and Perakis, S.S., 2011. Decomposition of heterogeneous organic matter and its long-term stabilization in soils. *Ecological Monographs*, 81, 619-634. https://doi.org/10.1890/11-0811.1

Sierra, C.A., 2012a. Temperature sensitivity of organic matter decomposition in the Arrhenius equation: some theoretical considerations. *Biogeochemistry*, 108, 1-15. https://doi.org/10.1007/s10533-011-9596-9

Sierra, C.A., Müller, M. and Trumbore, S.E., 2012b. Models of soil organic matter decomposition: the SoilR package, version 1.0. *Geoscientific Model Development*, *5*, 1045-1060. https://doi.org/10.5194/gmd-5-1045-2012

Sierra, C.A., Trumbore, S.E., Davidson, E.A., Vicca, S. & Janssens, I. 2015. Sensitivity of decomposition rates of soil organic matter with respect to simultaneous changes in temperature and moisture. *Journal of Advances in Modeling Earth Systems*, 7, 335–56. https://doi.org/10.1002/2014MS000358

Sierra, C., Malghani, S. and Loescher, H.W., 2017. Interactions among temperature, moisture, and oxygen concentrations in controlling decomposition rates in a boreal forest soil. *Biogeosciences*, *14*, 703-710. https://doi.org/10.5194/bg-14-703-2017

Sihi, D., Davidson, E.A., Chen, M., Savage, K.E., Richardson, A.D., Keenan, T.F. and Hollinger, D.Y., 2018. Merging a mechanistic enzymatic model of soil heterotrophic respiration into an ecosystem model in two AmeriFlux sites of northeastern USA. *Agricultural and Forest Meteorology*, 252, 155-166. https://doi.org/10.1016/j.agrformet.2018.01.026

Sihi, D., Davidson, E.A., Savage, K.E. and Liang, D., 2020. Simultaneous numerical representation of soil microsite production and consumption of carbon dioxide, methane,

and nitrous oxide using probability distribution functions. *Global Change Biology*, 26, 200-218. https://doi.org/10.1111/gcb.14855

Stendahl, J., Johansson, M., Eriksson, E., Nilsson, Å. and Langvall, O., 2010. Soil organic carbon in Swedish spruce and pine forests–differences in stock levels and regional patterns, *Silva Fenn*., 44, 5-21. https://www.silvafennica.fi/pdf/article159.pdf

Thornton, P. E. 1998. Regional Ecosystem Simulation: Combining Surface- and SatelliteBased Observations to Study Linkages between Terrestrial Energy and Mass Budgets. College of Forestry. Missoula, MT, The University of Montana. Doctor of Philosophy: 288. https://scholarworks.umt.edu/etd/10519/

Todd-Brown, K.E., Hopkins, F.M., Kivlin, S.N., Talbot, J.M. and Allison, S.D., 2012. A framework for representing microbial decomposition in coupled climate models. *Biogeochemistry*, *109*(1-3), 19-33. https://doi.org/10.1007/s10533-011-9635-6

Todd-Brown, K., Randerson, J.T., Post, W.M., Hoffman, F.M., Tarnocai, C., Schuur, E.A.G. and Allison, S.D. 2013. Causes of variation in soil carbon simulations from CMIP5 Earth system models and comparison with observations. *Biogeosciences*, 10, 1717–36. https://doi.org/10.5194/bg-10-1717-2013

Tuomi, M., Vanhala, P., Karhu, K., Fritze, H. and Liski, J., 2008. Heterotrophic soil respiration—comparison of different models describing its temperature dependence. *Ecological Modelling*, *211*(1-2), 182-190. https://doi.org/10.1016/j.ecolmodel.2007.09.003

Tuomi, M., Thum, T., Järvinen, H., Fronzek, S., Berg, B., Harmon, M., Trofymow, J.A., Sevanto, S. and Liski, J. 2009. Leaf litter decomposition—Estimates of global variability based on Yasso07 model. *Ecological Modelling*, 220, 3362–71. https://doi.org/10.1016/j.ecolmodel.2009.05.016

Tuomi, M., Laiho, R., Repo, A. and Liski, J. 2011. Wood decomposition model for boreal forests. *Ecological Modelling*, 222, 709–718. https://doi.org/10.1016/j.ecolmodel.2010.10.025

Turetsky, M.R., Kotowska, A., Bubier, J., Dise, N.B., Crill, P., Hornibrook, E.R., Minkkinen, K., Moore, T.R., Myers-Smith, I.H., Nykänen, H. and Olefeldt, D., 2014. A synthesis of methane emissions from 71 northern, temperate, and subtropical wetlands. *Global change biology*, 20(7), 2183-2197. https://doi.org/10.1111/gcb.12580

Turetsky, M.R., Benscoter, B., Page, S., Rein, G., Van Der Werf, G.R. and Watts, A., 2015. Global vulnerability of peatlands to fire and carbon loss. *Nature Geoscience*, 8(1), 11-14. https://doi.org/10.1038/ngeo2325

Yrjälä, K., Tuomivirta, T., Juottonen, H., Putkinen, A., Lappi, K., Tuittila, E.S., Penttilä, T., Minkkinen, K., Laine, J., Peltoniemi, K. and Fritze, H., 2011. CH4 production and oxidation processes in a boreal fen ecosystem after long-term water table drawdown. *Global change biology*, 17(3), 1311-1320. https://doi.org/10.1111/j.1365-2486.2010.02290.x

Ullah, S. and Moore, T.R., 2011. Biogeochemical controls on methane, nitrous oxide, and carbon dioxide fluxes from deciduous forest soils in eastern Canada. *Journal of Geophysical Research: Biogeosciences*, *116*(G3). https://doi.org/10.1029/2010JG001525

UNFCCC 2019. The National Inventory Submissions 2019. Retrieved June 18, 2020, from https://unfccc.int/process-and-meetings/transparency-and-reporting/reporting-and-review-under-the-convention/greenhouse-gas-inventories-annex-i-parties/national-inventory-submissions-2019

Van Gestel, N., Shi, Z., Van Groenigen, K.J., Osenberg, C.W., Andresen, L.C., Dukes, J.S., Hovenden, M.J., Luo, Y., Michelsen, A., Pendall, E.and Reich, P.B., 2018. Predicting soil carbon loss with warming. *Nature*, 554, 7693. https://doi.org/10.1038/nature25745

Vesala, T., Launiainen, S., Kolari, P., Pumpanen, J., Sevanto, S., Hari, P., Nikinmaa, E., Kaski, P., Mannila, H., Ukkonen, E. and Piao, S.L., 2010. Autumn temperature and carbon balance of a boreal Scots pine forest in Southern Finland. *Biogeosciences, 7*(1). https://doi.org/10.5194/bg-7-163-2010

Weng, E., Luo, Y., 2008. Soil hydrological properties regulate grassland ecosystem responses to multifactor global change: A modeling analysis. Journal of Geophysical Research: Biogeosciences 113. https://doi.org/10.1029/2007JG000539

Webster, K.L., Creed, I.F., Bourbonniere, R.A. and Beall, F.D., 2008. Controls on the heterogeneity of soil respiration in a tolerant hardwood forest. *Journal of Geophysical Research: Biogeosciences*, 113(G3). https://doi.org/10.1029/2008JG000706

Weishampel, P., Kolka, R. and King, J.Y., 2009. Carbon pools and productivity in a 1-km2 heterogeneous forest and peatland mosaic in Minnesota, USA. *Forest Ecology and Management*, *257*(2), 747-754. https://doi.org/10.1016/j.foreco.2008.10.008

Wieder, W. R., Bonan, G. B., and Allison, S. D., 2013. Global soil carbon projections are improved by modelling microbial processes. *Nature Climate Change*, **3**, 909–912. https://doi.org/10.1038/nclimate1951

Wieder, W.R., Grandy, A.S., Kallenbach, C.M. and Bonan, G.B., 2014. Integrating microbial physiology and physio-chemical principles in soils with the MIcrobial-MIneral Carbon Stabilization (MIMICS) model. *Biogeosciences*, 11(14), 3899-3917. https://doi.org/10.5194/bg-11-3899-2014

I

Tellus (2008), 60B, 153–166
Printed in Singapore. All rights reserved

© 2007 The Authors
Journal compilation © 2007 Blackwell Munksgaard

TELLUS

Forest floor versus ecosystem CO_2 exchange along boreal ecotone between upland forest and lowland mire

By BORIS ŤUPEK[1]*, KARI MINKKINEN[1], PASI KOLARI[1], MIKE STARR[1], TOMMY CHAN[2], JUKKA ALM[3], TIMO VESALA[4], JUKKA LAINE[5] and EERO NIKINMAA[1], [1]*Dept. Forest Ecology, P.O. Box 27, 00014 Univ. of Helsinki, Finland;* [2]*University of Toronto, 27 King's College Circle, Toronto, ON M5S 1A1, Canada;* [3]*Finnish Forest Research Institute, P.O. Box 68, 80101 Joensuu, Finland;* [4]*Dept. of Physical Sciences, P.O. Box 64, 00014 Univ. of Helsinki, Finland;* [5]*Finnish Forest Research Institute, Kaironiementie 54, 39700 Parkano, Finland*

(Manuscript received 30 December 2006; in final form 20 September 2007)

ABSTRACT

We determined the landscape variation of forest floor (FF) CO_2 uptake (photosynthesis, P), FF CO_2 emission (respiration, R) in relation to net ecosystem CO_2 exchange (NEE) and environmental factors along a forest-mire ecotone in Finland. The 450 m long ecotone extended from xeric, upland pine dominated habitats, through spruce and transitional spruce-pine-birch forest, to sedge peatlands downslope. The CO_2 fluxes were measured at nine stations during 2005 using chamber and IR techniques. Instantaneous P and R measurements for each station were interpolated by fitting their response to continuous records of light (mean $R^2 = 0.66$) and temperature (mean $R^2 = 0.77$) recorded nearby to give annual estimates. Stand biomass increment was used to estimate the annual CO_2 exchange contribution of the trees. Annual *P* values from -307 to -1632 $gCO_2m^{-2}yr^{-1}$ were inversely correlated with FF light ($r = -0.96$), FF above-ground biomass ($r = -0.92$) and canopy openness ($r = -0.95$). Annual R values from 1263 to 2813 $gCO_2\ m^{-2}\ yr^{-1}$ were correlated with tree stand foliar biomass ($r = 0.77$). Estimated NEE values varied from 546 to -1679 gCO_2m^{-2}/yr^{-1}, with *P* contributing from -307 to -1632 $gCO_2m^{-2}yr^{-1}$ (4–90%) to gross ecosystem photosynthetic production, and R from 1263 to 2813 $gCO_2m^{-2}yr^{-1}$ (70–98%) to gross ecosystem respiration (GR).

1. Introduction

The boreal landscape has been highly eroded by glaciations and typically has low relative relief, shallow upland mineral soils and peatlands in lower depressions (Granö et al., 1952). Soil development is related to relief and a sequence of soil types (catena) are shown along slopes. Similarly, the forest and ground vegetation shows a transition downslope. Upslope, xeric pine dominated forests on iron podsols give way to wetter spruce habitats with gleyic soils, then to mixed pine–spruce–birch forest with peaty (histic) soils, and eventually to water saturated peat (histosols) with sparse tree cover. The estimated area of forested mire margins (area >20 ha, peat thickness <30 cm) in Finland is 3.1Mill.ha, and there are 5.1Mill.ha of forested peatlands (area > 20 ha and peat thickness >30 cm) (Lappalainen and Hänninen, 1993).

The transition zone between upland and peatland may be very dynamic in terms of fluctuating environmental conditions and to show high species richness. Large differences in greenhouse gas (GHG) fluxes in transition zones may also be expected to occur. Although small in area, it may play an important role in regional GHG dynamics. For example, the lower flooded littoral zone of shore-lake margin has been shown to act as a sink for atmospheric CO_2 while the upper littoral to act as a net source of CO_2 (Larmola et al., 2003). Most GHG studies have ignored transition zones, preferring to concentrate on typical upland (Pumpanen et al., 2003; Kolari et al., 2004) or typical peatland conditions (Alm et al., 1997; Nykänen et al., 2003).

The net ecosystem production (NEP) of upland forests is approximately the difference between the net primary production (NPP) of trees and forest floor (FF) vegetation and heterotrophic respiration (Liski et al., 2006). Kolari et al. (2006) found that CO_2 uptake of the FF vegetation in an upland Scots pine forest contributed 13% to the ecosystem annual gross photosynthetic production (GPP). In peatlands, the growth of trees is limited by water table depth (Pepin et al., 2002), and carbon accumulation is mostly that of ground vegetation (Turunen et al., 2002). The net flux of CO_2 from a particular ecosystem depends on the balance between the uptake of atmospheric CO_2 by vegetation (photosynthesis) on the one hand, and the autotrophic and

*Corresponding author.
e-mail: boris.tupek@helsinki.fi
DOI: 10.1111/j.1600-0889.2007.00328.x

heterotrophic emissions of CO_2 to the atmosphere (respiration) on the other. The carbon balance of forests is mainly controlled by temperature (Valentini et al., 2000), with soil moisture only becoming important under very dry or very moist conditions (Minkkinen and Laine, 1998; Pumpanen et al., 2003; Tuittila et al., 2004; Weimin et al., 2006). Soil respiration is mainly dependent on the recent photosynthesis of living biomass (Högberg et al., 2001; Janssens et al., 2001), and on moisture conditions if they inhibit primary production.

The aim of our study was to determine annual FF and whole ecosystem carbon balance at nine sites along an upland forest–peatland toposequence in the boreal zone. We hypothesized that the annual carbon balance of the FF would vary spatially in relation to a number of environmental factors, nutrient status, and water table depth. The greatest spatial variation was expected to be found in the forest-mire transitional zone.

2. Materials and methods

2.1. Study ecotone

A forest-mire ecotone forming a continuum of plant communities, soil moisture and nutrient conditions was identified near to the Hyytiälä Forestry Station in Central Finland (61°47′, 24°18′). The forest-mire ecotone was 450 m long with a relative relief of 15 m and a slope 3.3% facing North East (Fig. 1). The forest types ranged from Scots pine forest through more fertile pine–spruce forest and spruce dominated type to paludified mixed spruce forest, and finally to a tall-sedge pine fens (Table 1). The ecotone is 6 km apart to the station for continuous measurements of forest-atmosphere relations (SMEAR II) recorded since 1996 (http://www.honeybee.helsinki.fi/smear) (Vesala et al., 1998; Mäkelä et al., 2006). Ecotone and SMEARII data of environmental factors like the light above canopy, soil moisture and temperature are strongly correlated.

2.2. Field measurements and sampling

Nine stations were established, four situated in upland forest, two in forest-mire transition and mire margin and three in forested peatlands (Fig. 1, Table 1). At each sampling stations three steel collars (31.5 cm in diameter, 5 cm deep) were installed 1–3 m apart, and into the moss layer, just above the roots of ground vegetation (Fig. 2).

A closed flow-trough chamber was fitted to the collar to measure CO_2 efflux repeatedly. The measurements were taken once a week during the growing season 2005 (May–November), and once in a month in winter. On each occasion the measurements were made between 8 am and 5 pm and the order in which each station was measured was random. Measurements were made with a portable infrared CO_2 analyser (EGM4, SRC-1 PP systems Inc.) fitted to modified closed soil respiration chambers (transparent and non-transparent, volume 21.2 L) (Fig. 3). The CO_2 flux was calculated automatically as the slope of a linear fit to 25 concentration readings at 4.8 second intervals within a 120 second measuring period. Twenty-five CO_2 concentrations were recorded for each gas exchange measurement and subsequently used for evaluation of linearity and data quality. We first measured the net forest floor exchange CO_2 flux (NFFE) with the transparent chamber, and total FF respiration (R) immediately after with the non-transparent chamber. Photosynthesis (P, negative sign), carbon fixation of the ground vegetation was subsequently calculated as the difference between NFFE and R.

Simultaneously with the CO_2 flux measurements, soil temperatures at 5, 15 and 30 cm depth were also measured using permanently installed thermocouples. Soil temperature at 5 cm

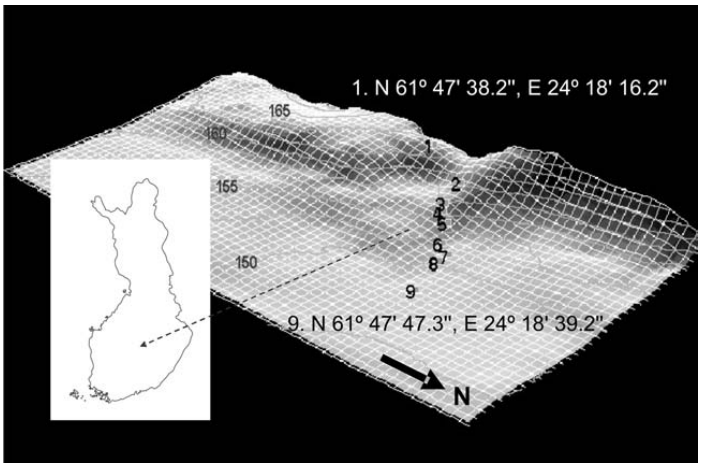

Fig. 1. Spatial distribution of nine studied forest types on Northern slope of glacial esker 'Vatiharju' in central Finland. The map of Finland and digital elevation model with contour lines and site numbers; (Upland forest types: 1 CT – *Calluna,* 2 VT – *Vitis Idea,* 3 MT – *Myrtilus,* 4 OMT – *Oxalis-Myrtillus;* Forest – mire transition and mire margin types: 5 OMT+ – *Oxalis-Myrtillus Paludified, 6* KgK – *Myrtillus Spruce Forest Paludified*; Open mire types: 7 KR – *Spruce Pine Swamp, 8 and 9* VSR – *Tall Sedge Pine Fen*); coordinates in Finnish Geographical Coordinate System. The catena of 450 meters represents moisture and fertility gradient based on classification, English names and acronyms of Cajander (1949), and Laine et al. (2004).

Table 1. Study site characterisctics

Characteristic	Station								
	1	2	3	4	5	6	7	8	9
Site type[a]	CT	VT	MT	OMT	OMT+	KgK	KR	VSR1	VSR2
Elevation, m a.s.l.	164	160	157	156	154	152	151	150	149
Slope position	Crest	Upper Slope	Middle Slope	Middle Slope	Lower Slope	Lower Slope	Toe	Toe	Level
Slope, °	2.3	3	3.5	4	3.5	2.9	1	1	0.3
Aspect, °	27	103	70	50	30	18	70	85	62
Soil type[b]	Haplic podzol	Haplic podzol	Haplic podzol	Haplic podzol	Histic podzol	Gleyic histic podzol	Hemic histosol	Hemic histosol	Hemic histosol
Humus layer or peat thickness, m	0.07	0.08	0.07	0.12	0.15	0.32	0.78	1	1.2
Stocking density, stems ha^{-1}	600	2050	925	650	400*	1825	1300	900	275
Basal area, m^{-2} ha^{-1}	33.6	38.9	41.6	51.0	14.4	41.2	15.4	8.4	1.7
Canopy openness,%	37	26	18	20	21	22	24	50	80
Stand biomass[c], kg m^{-2}	20.7	23.6	32.5	46.0	11.2	26.8	7.5	3.1	0.5
Pine,% (age, yr)	96 (100)	75 (100)	0	0	0	32 (130)	75 (130)	95 (110)	100 (100)
Spruce,% (age, yr)	4 (30)	25 (30)	95 (90)	99 (80)	68 (70)	41 (120)	14 (60)	1	0
Birch,% (age, yr)	0	0	5 (95)	1	32 (85)	27 (120)	11 (100)	4 (60)	0
Ground vegetation biomass[d], g m^{-2}	181	130	165	52	135	190	162	360	550
Soil temperature at 5 cm [°C]	5.7	5.2	5.3	4.9	5.2	5.6	5.1	5.7	5.1
Water table depth [cm]	881	217	69	65	33	19	19	7	8

[a]CT: Calluna vulgaris type; VT: Vaccinium vitis-idaea type; MT: Vaccinium myrtillus type; OMT: Oxalis acetosella-Vaccinium myrtillus type; OMT+ : Oxalis acetosella-Vaccinium myrtillus, paludified type; KgK: Myrtillus Spruce Forest, Paludified; KR: Spruce Pine Swamp; VSR: Tall Sedge Pine Fen (Cajander 1949; Laine et al., 2004).
[b]IUSS Working Group WRB (2006), [c]above- and below-ground biomass, *exceptionally low because of windblown trees, [d]above-ground biomass only.

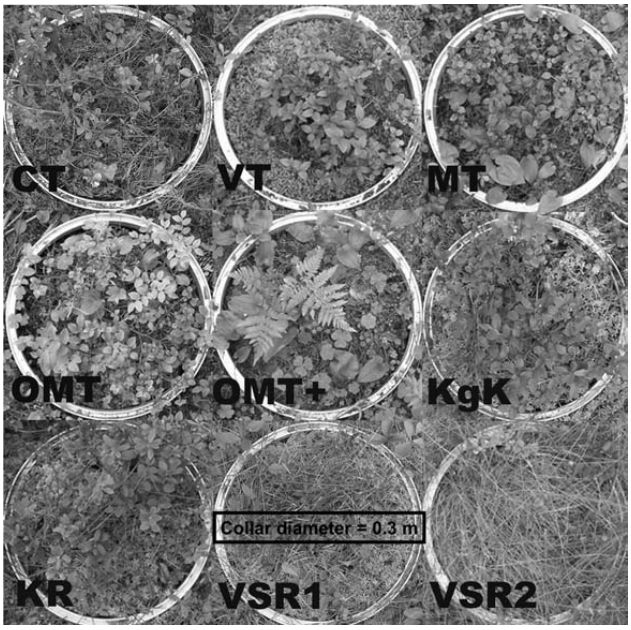

Fig. 2. Forest floor species comparison along the catena (one study plot per site) of nine studied forest types. For forest type acronyms, see Table 1.

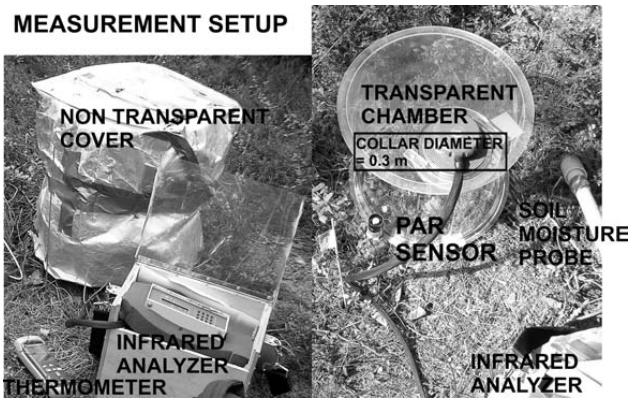

Fig. 3. Closed chamber setup to measure total respiration (R) (left), and net CO_2 exchange of forest floor (NFFE) [g m^{-2} h^{-1}] (right). Fluxes were obtained directly during the measurement intervals, and at the end from IR analyser. Location of sensors is demonstrated by annotations.

depth (T_5) was also recorded continuously at 3 hours intervals during the period from 1 January to 31 May, and at 1 hour intervals during 1 June to 12 October with permanently installed sensors (DS1920 Temperature iButton® – Maxim/Dallas Semiconductor). Missing soil temperature data at the end of season (13 October to 31 December) for all stations were filled with soil temperature records from nearby micro-meteorological stations (upland forest SMEARII and lowland mire Lakkasuo).

Photosynthetically active radiation (PAR) reaching the FF was recorded with portable Delta-T PAR sensor and delta data logger. We placed the PAR sensor in a spot considered the most representative of light conditions nearby the chamber. Volumetric soil moisture at 10 cm depth (SM10) was measured with portable Delta-T ThetaProbe (calibrated for each soil type) inserted into diagonally installed polyvinylchloride perforated tubes. To make annual estimates, SM10 measurements at the study stations were calibrated with continuous hourly records of soil moisture recorded at the SMEARII station. Water table depth (WT) was measured weekly during the vegetative period from vertically installed perforated plastic tubes. To give the annual estimates, the WT measurements at the study sites were calibrated with continuous hourly seasonal records of WT recorded at a ground water well located 100 m away in the open peatland Lakkasuo.

The ground vegetation at each collar was photographed with digital camera nine times during growing season 2005. The images were analysed for proportional development of leaf (photosynthesizing) area and non-leaf (not photosynthesizing) area using geographic information software (ArcInfo9). The tree stand canopy for each station was photographed once using a 'fish eye' lens, and canopy openness estimated using Gap Light Analyser (GLA) software (Frazer et al., 1999). Above-ground FF biomass was determined in July 2004 for each station by harvesting three 0.07 m^2 sample plots located near to the measuring collars, oven drying and weighing. Total above- and below-ground biomasses of trees were estimated from June 2005 measurements of breast height diameter (dbh), height, and canopy lengths and applying Marklund's allometric biomass functions (Marklund, 1988). The mean age of the trees was estimated by counting the annual internodes from photographs of tree stands.

A digital elevation model (Fig. 1) was reconstructed with map elevation points in ArcInfo9. The study stations were positioned with global positioning system to determine the position, elevation, slope and aspect of each station.

3. Integration of CO_2 exchange measurements

FF CO_2 uptake (P, ground vegetation photosynthesis, a negative sign) was calculated as a difference between net forest floor CO_2 exchange (NFFE) and FF CO_2 emission (R, autotrophic and heterotrophic respiration, a positive sign) (eq. 1). Positive values of NFFE indicate a net CO_2 emission to the atmosphere (i.e. FF is a source) and negative values of NFFE indicate a net uptake of CO_2 (i.e. FF is a sink).

$$\mathrm{P} = \mathrm{NFFE} - \mathrm{R} \tag{1}$$

The half an hour values of P and R derived from measurements for each collar were subsequently used for non-linear regressions to interpolate P, R and NFFE values during whole year. The simulated values were then summed to give the annual value for each collar.

3.1. Photosynthesis model

For each of 27 sample plots, the measurements of P were fitted to those of *PAR* using Michaelis–Menten function and proportional leaf area development *LA* (eq. 2).

$$\mathrm{P} = \left(\frac{P_{\max} PAR}{PAR + b}\right) LA, \tag{2}$$

where *PAR* is the mean photosynthetically active radiation [μmol $m^{-2}s^{-1}$] reaching the FF; $P_{\max}$ is maximum potential photosynthesis [g CO_2 $m^{-2}h^{-1}$] limited by light saturation; b is the PAR level, when photosynthesis is half the maximum value. Equation was fitted for each sample plot in each station (20 measuring occasions, 27 collars in nine stations). Parameters $P_{\max}$ and b for each studied sample plot are in Table 2. Each forest floor P being 30 min (half an hour) averages. Tree stand average PAR levels were estimated using a stand photosynthesis model (Mäkelä et al., 2006) the stand characteristics (Mäkelä et al., 2006; Mäkelä, 1997), and continuous above-canopy PAR measurements recorded 6km distant at the SMEARII environmental monitoring station.

We modelled LA [%] during growing season 18 April to 21 November 2005 by fitting ArcInfo9 measurements to lognormal function, with faster increase in early summer and gradual decline in autumn (Wilson et al., 2006) (eq. 3).

$$LAi = LA_{\max} \exp\left(-0.5\left(\frac{\ln\left(\frac{day}{x_{\max}}\right)}{b}\right)^2\right) \tag{3}$$

Where, $\mathrm{LA_i}$ is leaf area projection for i^{th} sample plot, $LA_{\max}$ is maximal leaf area projection and $x_{\max}$ is the day of year when it occurs, *day* is Day of year, and b is the parameter. Length of growing season starts 18 April and ends 21 November 2005. It is determined by snowmelt in spring and permanent snow cover in winter measured at SMEARII located 6 km NW. The start of the growing season was taken to be the moment when the daily average temperature of the soil humus layer was permanently above 0 °C.

3.2. Respiration model

Total respiration [g CO_2 $m^{-2}h^{-1}$] was modelled for each collar by fitting measurements of respiration fluxes to soil temperatures at 5 cm depth using the exponential function reported by Lloyd and Taylor (1994) (eq. 4).

$$R = R_T \exp\left(b\left(\frac{1}{56.02} - \frac{1}{T_5 + 46.02}\right)\right) \tag{4}$$

Where T_5 is the soil temperature in 5 cm [°C], and R_T is respiration level at site reference temperature [g CO_2 $m^{-2}h^{-1}$], b[K] activation energy divided by gas constant (parameters for individual sample plots are in Table 2). The reference temperature T_{ref} is 283.15 °K, T_{o} is 227.13 °K, and the given constants (56.02 and 46.02) are result of using T_5 in °C. Respiration over the year was calculated by continuously integrating measured temperatures at 5 cm at the stations.

3.3. Calculation of Net ecosystem CO_2 exchange

Annual Net ecosystem CO_2 exchange (NEE) [g CO_2 m^{-2} yr^{-1}] was calculated by summing simulated values of R and P(P, negative values for CO_2 uptake), gross increment of tree stand biomass converted to stand net photosynthetic production (NPPt, negative values for CO_2 uptake) and estimated respiration of tree roots (Rtr) (eq. 5).

$$\mathrm{NEE} = \mathrm{NPPt} - \mathrm{Rtr} + \mathrm{R} + \mathrm{P} \tag{5}$$

Table 2. Forest floor photosynthesis and respiration (eq. 2 and 4), non-linear regression model R^2, parameters and their estimation errors (± standard deviation SD, and standard error SE) for each of the nine study stations (CT, VT, MT, OMT, OMT+, KgK, KR, VSR1, VSR2, see Table 1 for forest-type acronyms)

CO_2 exchange component and model parameter	Statistic	Station (and site type)								
		1(CT)	2(VT)	3(MT)	4(OMT)	5(OMT+)	6(KgK)	7(KR)	8(VSR1)	9(VSR2)
Photosynthesis, obs/pred	R^2	0.603	0.646	0.629	0.608	0.586	0.474	0.726	0.855	0.85
P_{max}, g CO_2 m^{-2} h^{-1}	Mean	−0.012	−0.015	−0.009	−0.007	−0.007	−0.005	−0.011	−0.027	−0.043
	SD	±0.002	±0.008	±0.004	±0.006	±0.002	±0.002	±0.001	±0.004	±0.010
	SE	0.003	0.008	0.003	0.002	0.003	0.003	0.003	0.004	0.009
b, mmol m^{-2} s^{-1}	Mean	0.076	0.157	0.080	0.049	0.084	0.042	0.105	0.290	0.487
	SD	±0.006	±0.118	±0.047	±0.083	±0.007	±0.034	±0.020	±0.084	±0.205
	SE	0.049	0.131	0.05	0.033	0.068	0.048	0.058	0.091	0.195
Respiration, obs/pred	R^2	0.743	0.883	0.821	0.804	0.768	0.803	0.717	0.742	0.719
R_T, g CO_2 m^{-2} h^{-1}	Mean	0.380	0.269	0.299	0.498	0.339	0.334	0.391	0.205	0.259
	SD	±0.068	±0.024	±0.016	±0.069	±0.036	±0.069	±0.083	±0.041	±0.053
	SE	0.028	0.012	0.014	0.025	0.017	0.022	0.028	0.02	0.034
b, K	Mean	349.6	411.6	401.2	344.4	378.6	393.6	506.7	525.1	517.6
	SD	±58.0	±54.1	±30.1	±12.3	±36.7	±36.4	±67.0	±62.7	±106.6
	SE	51.4	41.6	49	47.6	56.9	55.4	86.9	89.6	87.4

Positive values of NEE indicate a net CO_2 emission to the atmosphere (i.e. ecosystem is a source) and negative values of NEE indicate a net uptake of CO_2 (i.e. ecosystem is a sink).

Gross biomass increment of stand [g m^{-2} yr^{-1}] was calculated with measurements of tree dbh, height, mean estimated age of each species and site type using the SIMO simulator (Tokola et al., 2006). Dry biomass was converted to carbon (factor 0.519 for spruce and pine and 0.505 for birch; Karjalainen and Kellomäki, 1996) and to CO_2 mass equivalents NPPt [g CO_2 m^{-2} yr^{-1}]. For the respiration of tree roots we used the ratio of Rtr to autotrophic respiration (Ra) according to Ryan et al., (1997). Ra values were calculated from previously estimated NPPt and from carbon use efficiency (CUE) for spruce, pine and birch corresponding to NSA-OBS, NSA-OJP, and NSA-OA stands found for boreal forests by Ryan et al. (1997).

4. Results

4.1. Variation among forest type environmental conditions

The annual PAR level reaching the FF ranged between 9 and 143 umol$m^{-2}s^{-1}$ and were correlated with the biomass characteristics (e.g. Pearson correlation with canopy openness $r = 0.92$ and forest stand biomass $r = -0.84$) (Table 3). Annual PAR under four forest canopies is less than 20% (densest, spruce dominated forest type, OMT just 6%) of maximum incoming light in open mire VSR2 (Fig. 4). Gradient of incoming light on the FF has declining tendency from both ends of the catena towards OMT, towards the more fertile mineral soils and highest amount of tree biomass. Transitional forest OMT+, situated close to upland site OMT, has exceptionally high-annual light level (45% of maximum VSR2), because nearly half of trees were windblown.

The annual average of soil temperature at 5 cm ranged between 4.94 and 5.72 °C. Weekly trends of soil temperatures for all sites are in Fig. 4. Wet peatland sites tend to show a delay in warmed up and cooling in early autumn compared to upland forest sites. Maximum difference in soil temperature among study sites was 2.2 °C during the snow and soil melting period in April. The differences in June, July T5 were rather stable around 1 °C, until beginning of August when the soil temperature difference was declined and stabilized at 0.5 °C in the middle of October until December.

The annual average soil moisture content at 10 cm depth was similar (around 15%) just for the upland mineral soil stations (CT, VT, MT, OMT), but increased considerably further downslope for forest-mire transition types (OMT+ 42%, KgK 69%) Drier forest-mire margin (OMT+) fluctuates between field capacity (surface layer 65%) in wet early and late summer to drier conditions (15%) during summer drought (Fig. 4). Wetter forest-mire margin (KgK) had moisture conditions closer to those of peatlands down the slope (KR, VSR1, VSR2), than to ones of upland minerals soils (CT, VT, MT, OMT). The annual soil moisture contents were negatively correlated with elevation of forest types ($r = -0.86$) (Table 3). Increasing wetness of soils have shown also good correlation with increasing depth of organic horizons ($r = 0.92$) (Table 3).

The annual WT depth varied greatly between the stations, ranging from 881 cm (highest upland Scots pine forest on sandy podzol) to 7 cm (lowland tall-sedge pine fen on histosol). Transitional forest-mire sites showed the highest seasonal fluctuation of WT depths, with annual level of 20 cm and a summer minimum as low as 70 cm (Fig. 4).

4.2. Reliability of estimated forest floor CO_2 exchanges

The measurements of FF CO_2 fluxes of forest-mire transition were similar to those of the upland sites, but the CO_2 uptakes of peatlands were generally higher than others (Fig. 5).

The models we used to predict half an hour average FF respiration and photosynthesis values explained around 77% of variance in the corresponding measurements of CO_2 emissions, and around 58% of variance in the CO_2 uptake measurements (Figure 6). The greatest source of error was in modelling the FF light and light response curves. Also difference in time compatibility could be erroneous, when comparing modelled half an hour average to observed data of 120-second interval (especially forest floor PAR). The greatest variation in the annual average net ecosystem CO_2 fluxes was associated with the forest-mire transition stations (Table 4).

4.3. Variation in forest floor CO_2 uptakes (P, negative sign)

There is clear difference in the annual CO_2 uptake between nine stations (Table 4, Figs. 7 and 8). Annual levels of FF CO_2 uptake were strongly correlated to annual levels of PAR reaching the FF ($r = -0.96$) and FF above-ground biomass ($r = -0.92$) (Table 3). Higher annual PAR levels reaching the ground vegetation promoted higher CO_2 uptake by FF vegetation. FF above-ground biomass was correlated to intercepted PAR ($r = 0.9$), and forest floor PAR was correlated to canopy openness ($r = 0.92$). The *P* values of the nine stations were not significantly correlated to soil temperature at 5 cm depth or to WT depth. The FF photosynthesis contributed from -307 to -1632 g CO_2 m^{-2} yr^{-1} (4–90%) to total forest photosynthetic production (Table 4, Fig. 8).

4.4. Variation in forest floor CO_2 emissions (R)

The annual FF CO_2 emissions showed higher values of the upland forest and forest-mire transitions, and lower values of peatlands (Table 4, Figs. 7 and 8). FF respiration rates were not significantly correlated to soil temperature, soil moisture content or WT depth, but only to the tree stand leaf mass ($r = 0.77$). Despite the dryness of the pine dominated CT site (deepest WT) with relatively open canopy (forest floor PAR 45% of

Table 3. Pearson Correlations Sig. 2-tailed between annual forest floor CO_2 fluxes, and environmental factors along the forest-mire ecotone for nine forest types

	NFFE	R	P	STANDM	CANOP	LEAFM	GVAM	OH	SM	PAR	ELEV	SLOPE
NFFE	1.000											
R	0.825(**)	1.000										
	0.006											
P	0.856(**)	0.419	1.000									
	0.003	0.262										
STANDM	0.860(**)	0.654	0.811(**)	1.000								
	0.003	0.056	0.008									
CANOP	−0.815(**)	−0.379	−0.951(**)	−0.658	1.000							
	0.007	0.315	0.000	0.054								
LEAFM	0.904(**)	0.766(*)	0.768(*)	0.831(**)	−0.669(*)	1.000						
	0.001	0.016	0.016	0.006	0.049							
GVAM	−0.902(**)	−0.559	−0.925(**)	−0.724(*)	0.952(**)	−0.710(*)	1.000					
	0.001	0.118	0.000	0.027	0.000	0.032						
OH	−0.809(**)	−0.486	−0.862(**)	−0.774(*)	0.794(*)	−0.759(*)	0.850(**)	1.000				
	0.008	0.184	0.003	0.014	0.011	0.018	0.004					
SM	−0.742(*)	−0.526	−0.724(*)	−0.765(*)	0.660	−0.599	0.779(*)	0.922(**)	1.000			
	0.022	0.146	0.027	0.016	0.053	0.088	0.013	0.000				
PAR	−0.865(**)	−0.484	−0.956(**)	−0.838(**)	0.920(**)	−0.708(*)	0.904(**)	0.792(*)	0.726(*)	1.000		
	0.003	0.186	0.000	0.005	0.000	0.033	0.001	0.011	0.027			
ELEV	0.498	0.372	0.447	0.503	−0.406	0.378	−0.553	−0.794(*)	−0.864(**)	−0.444	1.000	
	0.172	0.324	0.228	0.168	0.279	0.316	0.122	0.011	0.003	0.231		
SLOPE	0.820(**)	0.476	0.903(**)	0.845(**)	−0.792(*)	0.842(**)	−.818(**)	−0.916(**)	−0.800(**)	−0.791(*)	0.532	1.000
	0.007	0.195	0.001	0.004	0.011	0.004	0.007	0.001	0.010	0.011	0.141	

**.Correlation is significant at the 0.01 level (2-tailed); *. Correlation is significant at the 0.05 level (2-tailed); NFFE: net forest floor CO2 exchange; R: forest floor respiration; P: forest floor photosynthesis; STANDM: stand biomass; CANOP : canopy openness; LEAFM: stand leaf mass; GVAM: aboveground ground vegetation biomass; OH: depth of organic horizon; SM: soil moisture at 10 cm; PAR: photosynthetically active radiation; ELEV: elevation.

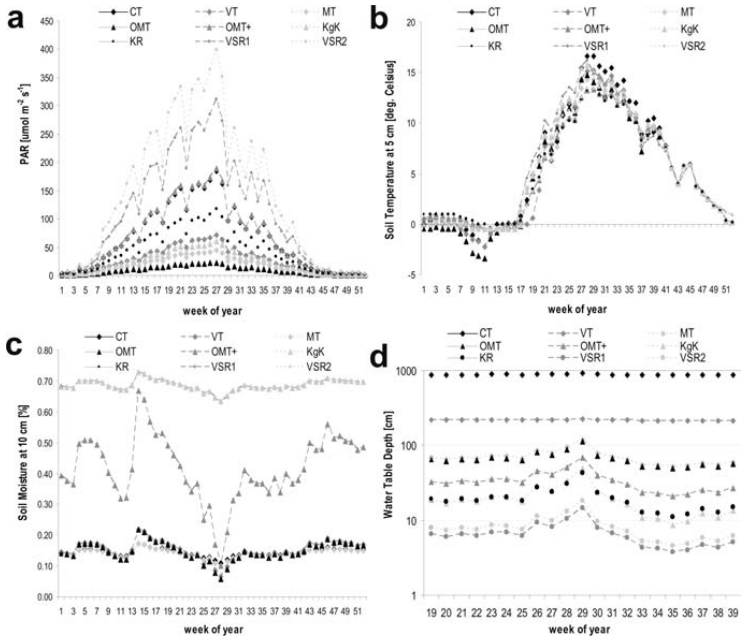

Fig. 4. Time series of weekly environmental characteristics found along the catena during year 2005); (a) integrated forest floor photosynthetically active radiation (PAR) [umol m^{-2} s^{-1}]; (b) measured soil temperature at 5 cm depth [°C]; (c) integrated volumetric soil moisture at 10 cm depth [%] for upland and transitional forest (VSR peatland sites were at 10 cm mostly saturated); (d) integrated water table depth shown in logarithmic scale; For forest type acronyms, see Table 1.

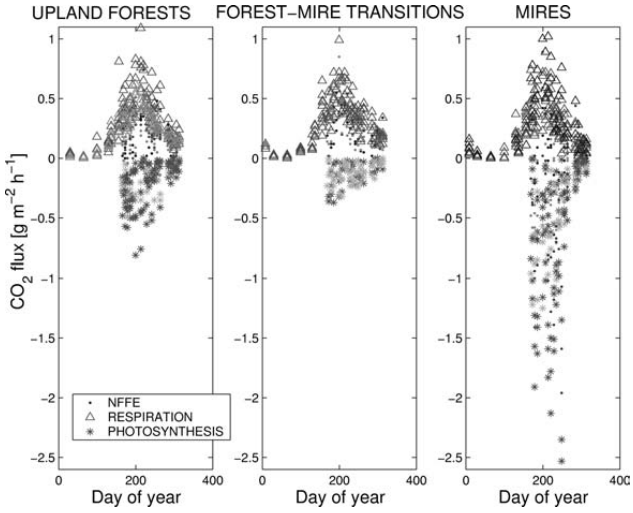

Fig. 5. Forest floor instantaneous (120 seconds) measurements of CO_2 fluxes [g m^{-2} h^{-1}] during year 2005. NFFE and Respiration was measured, Photosynthesis (minus sign for CO_2 uptake) was calculated, as a difference between NFFE and Respiration. Fluxes are grouped to upland forests types (CT, VT, MT, OMT); forest mire transitions (OMT+, KgK); and mire types (KR, two VSR sites). For forest type acronyms, see Table 1.

maximum PAR of VSR2), the annual mean respiration rate of 2401 ± 469 g m^{-2} h^{-1} (Table 4) was 85% of the OMT station, which had the highest emissions. Increasing R/GR ratio from transitions (e.g. OMT+ 78%) towards peatlands (e.g. VSR2 98%) reflects the diminishing role of tree stand and increasing part of the forest soil with ground plants (Table 4, Fig. 8).

4.5. *Variation in net forest floor CO_2 exchanges (NFFE)*

With the exception of the two tall-sedge pine fens, the annual net FF CO_2 exchange was clearly positive (Fig. 8, Table 4). The NFFE of the tall-sedge pine fens were nearly zero (VSR1) or negative (VSR2), indicating the FF was a net sink for CO_2.

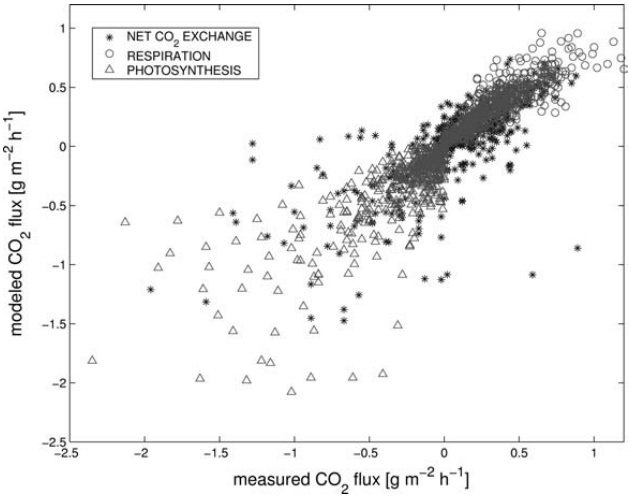

Fig. 6. Evaluation of fit between measured instantaneous CO_2 fluxes [g m^{-2} h^{-1}]; (120 second intervals) and modelled half an hour CO_2 average fluxes [g m^{-2} h^{-1}]; for nine studied forest types. For forest type acronyms, see Table 1, and for regression statistics see Table 2.

However, the balance between CO_2 uptake and efflux varied during the year at all stations. The FF acted as a sink during early spring and late summer at some sites, and in midsummer (with exception of the open mire sites) all the sites acted as net CO_2 sources (Fig. 7). The forest canopy was found to be the main factor controlling FF photosynthesis, respiration and also net forest floor CO_2 exchange (NFFE correlation with canopy openness $r = -0.82$)(Table 3). One of the main features of the ecotone is the marked opening of tree canopy between upper forested-mire margin and lower mire types (Fig. 8, Table 4). The NFFE values are thus seen change from small net emission from FF at the edge of closed forest canopy (KR) to net uptake of CO_2 in open mires with sparse trees (VSR1, VSR2).

4.6. *Variation in net forest ecosystem CO_2 exchanges (NEE)*

After adding the net tree stand exchange to NFFE the resulting NEE values indicated that seven of the stations (VT, MT, OMT, OMT+, KgK, VSR1, VSR2) were behaving overall as CO_2 sinks (-19 ± 732 to -1679 ± 1091 g CO_2 m^{-2} yr^{-1}) and two of the stations (Callunna type Scots pine forest and Spruce pine swamp type forest-mire margin) were sources of CO_2 (respectively, 546 ± 860 and 261 ± 667) (Fig. 8, Table 4). However, there was great within-station variability. Also great estimation errors suggest wide range of NEE values for each ecosystem. Some forest types (VT, MT, OMT, OMT+) were clearly sinks, while CT, KgK, KR and VSR types could be either sinks or sources. Forest floor P fluxes contributed to whole forest GPP from -307 to -1632 g CO_2 m^{-2} yr^{-1} (4–90%) and the R contributed to whole forest gross respiration (GR) from 1263 to 2813 g CO_2 m^{-2} yr^{-1} (70–98%) (Fig. 8, Table 4).The NEE along the forest-mire ecotone was correlated to the amount of spruce ($r = -0.84$) and pine ($r = 0.72$) biomass.

5. Discussion

Net carbon uptake of ecosystems results from large but opposing fluxes of photosynthesis and respiration. In relation to ecosystem carbon uptake and emissions, the net flow may only be a small proportion of them (Lindroth et al., 1998; Markkanen et al., 2001). Studying FF carbon uptake and emissions by indirect chamber measurements helps to understand net ecosystem exchange determined from direct methods (eddy covariance techniques). The annual net FF CO2 exchange values found in our study are in good agreement with the findings reported for similar and nearby ecosystems studied with chamber and eddy covariance measurements. Our NFFE value of -256 ± 208 g CO_2 m^{-2} yr^{-1} for the Tall Sedge Pine Fen, VSR2, with sparse trees compares with the mean value of -430 g CO_2 m^{-2} yr^{-1} for period 1 May to 30 September during 2001–2004 reported by Riutta et al., (2007). Pumpanen et al. (2004) report a R value of 1900 g CO_2 m^{-2} yr^{-1}, and Kolari et al. (2006) report an NFFE value 1756 g CO_2 m^{-2} yr^{-1} for the period 20 April to 20 November 2003 for upland an Vitis Idea, VT, Scots pine–Norway spruce forest. These values are comparable to our value of 1124 ± 116 g CO_2 m^{-2} yr^{-1} for upland VT forest station. Also the NEE value from our VT forest of 100 yr (-806 ± 448 g CO_2 m^{-2} yr^{-1}) corresponds well to the value of -1184 g CO_2 m^{-2} yr^{-1} for a VT Scots pine–Norway spruce forest of 75 yr reported by Kolari et al. (2004).

Several studies have shown that ecosystem respiration is dominated by the CO_2 efflux from soil (Valentini et al., 2000; Janssens et al., 2001; Kolari et al., 2004). However, the soil carbon efflux seems to follow a different seasonal pattern from that of total

Table 4. Annual mean values (± standard deviation) of forest floor respiration efflux (R), forest floor vegetation photosynthetic uptake (P), net forest floor exchange (NFFE), net primary production of trees (NPPt), autotrophic respiration of trees (Ra), respiration of tree roots (Rtr) ±25% deviation, ecosystem gross photosynthetic production (GPP), ecosystem gross respiration (GR), net ecosystem exchange (NEE) ±sum of all deviations, all in $gCO_2\ m^{-2}\ yr^{-1}$. Minus sign for CO_2 uptake. Ratios of R/GR and P/GPP in%. (See Table 1 for forest type acronyms). * Carbon use efficiency (CUE) (Spruce 0.292, Pine 0.338, Birch 0.461), and Rtr/Ra ratio (Spruce 0.625, Pine 0.698, Birch 0.65) values are according to Ryan et al., (1997)

CO_2 exchange Component	Station (and site type)								
	1(CT)	2(VT)	3(MT)	4(OMT)	5(OMT+)	6(KgK)	7(KR)	8(VSR1)	9(VSR2)
R	2401	1549	1653	2813	1852	2010	1951	1263	1605
	±469	±126	±109	±403	±230	±420	±448	±268	±315
P	−858	−425	−384	−307	−548	−371	−796	−1168	−1632
	±247	±44	±27	±83	±88	±72	±90	±113	±109
NFFE	1543	1124	1269	2507	1304	1639	1155	95	−256
	±361	±116	±102	±321	±233	±483	±382	±277	±208
NPPt	−420	−812	−1216	−1761	−865	−697	−376	−154	−49
Ra = NPPt/CUE* -NPPt	825	1597	2392	3464	1701	1372	740	303	97
Rtr from Rtr/Ra ratio*	578	1118	1674	2425	1191	960	518	212	68
	±145	±280	±419	±607	±298	±241	±130	±54	±17
GPP = NPPt - Ra + P	−2102	−2834	−3992	−5532	−3114	−2440	−1912	−1625	−1778
GR = R + Ra - Rtr	2648	2028	2370	3853	2362	2421	2173	1354	1634
NEE = NPPt - Rtr + R + P	546	−806	−1621	−1679	−752	−19	261	−271	−373
	±860	±448	±554	±1091	±616	±732	±667	±433	±440
R/GR	91%	76%	70%	73%	78%	83%	90%	93%	98%
P/GPP	41%	15%	10%	6%	18%	15%	42%	72%	92%

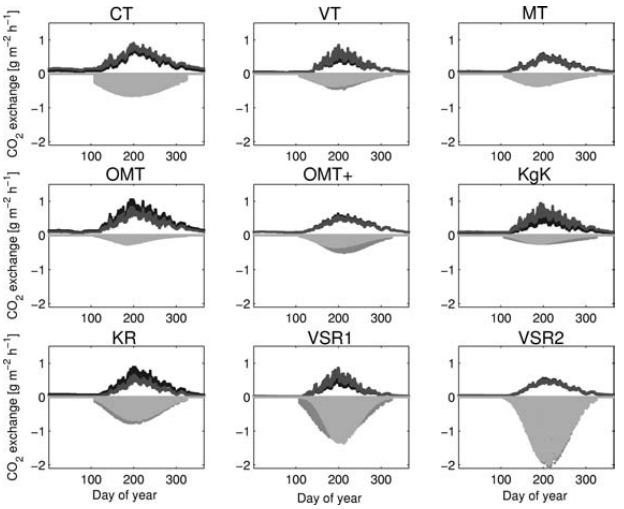

Fig. 7. Integrated 30 min forest floor CO_2 emissions to atmosphere (respiration R), and CO_2 uptakes from atmosphere (photosynthesis P, minus sign) [g m^{-2} h^{-1}]; for individual study plots of nine forests (CT, VT, MT, OMT, OMT+, KgK, KR and two VSR sites; for forest type acronyms, see Table 1). *high density of points in figure overlap into areas

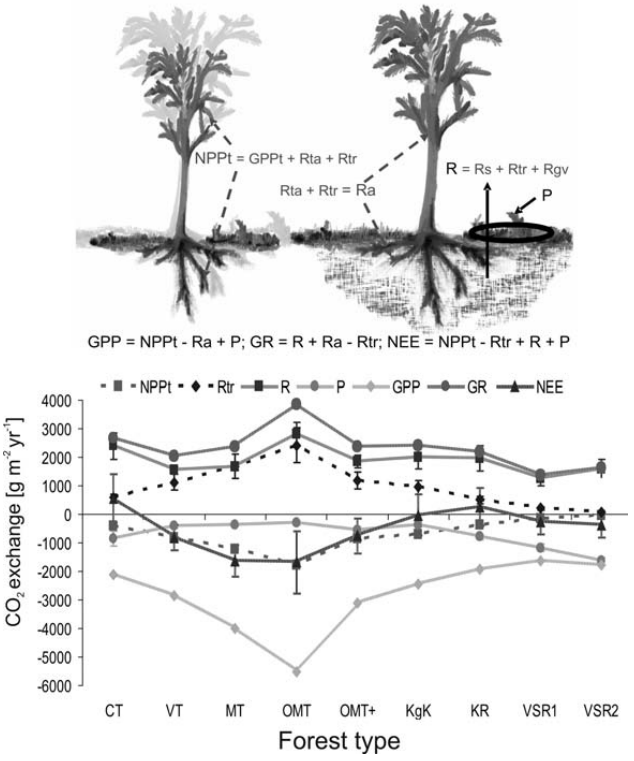

Fig. 8. Schematic of CO_2 exchange [g m^{-2} yr^{-1}] components and relationship to the studied forest-mire ecotone; annual net ecosystem CO_2 exchange (NEE) of nine different forest types; CO_2 emissions to atmosphere – gross respiration of ecosystem (GR), trees (Ra) including parts above-ground (Rta) and tree roots (Rtr), forest floor (R) including forest soil autotrophic (ground vegetation (Rgv) and Rtr and heterotrophic part (Rs); CO_2 uptake from atmosphere – gross photosynthesis of ecosystem (GPP, negative values), forest floor plants (P, negative values) and net photosynthetic production of trees (NPPt, negative values) including tree gross photosynthetic production (GPPt, negative values), Rta and Rtr. The Rtr value is a proportion of Ra and calculated from NPPt and carbon use efficiency (CUE) according to Ryan et al. (1997) after adapting to similar ecosystem and climate conditions (for Ra equation, CUE values and Rtr/Ra ratios, see Table 4). Error bars for R and P values represent standard deviation of three forest type plots, for Rtr values 25% of estimate, and for NEE values the sum of all (no error estimation for NPPt values). For forest type acronyms, see Table 1.

ecosystem respiration. Davidson et al. (2006) found a distinct seasonal pattern in the ratio between soil respiration and total ecosystem respiration, with a clear minimum in spring. Kolari et al. (2006) found that 13% of the annual GPP in an upland pine dominated forest was fixed by ground vegetation. FF photosynhtesis values observed in our study contributed from 6% to 41% to GPP for upland mineral forests, from 15% to 18% for forest-mire transitions, and 42% to 92% for peatlands with

sparse trees. In sparsely forested peatlands, the proportion of carbon uptake by ground vegetation is so high that the role of the trees is usually neglected (Alm et al., 1997; Nykänen et al., 2003). However, the total carbon stores of forested peatlands will increase if WT level would be lowered and forest growth increased (Laine and Minkkinen, 1996).

The largest differences in FF respiration between the forest types due to soil temperature mainly occur during spring (Aurela et al., 2004). Also during summer large differences in R-values between upland and peatland forest types can occur. For example, during hot periods when high FF respiration rates occur in peatlands with lowered WT levels (Alm et al., 1999). However, in our study the annual soil temperature differences between the forest types did not correspond to their differences in annual respiration. The FF CO_2 effluxes did, however, correlate with stand foliar biomass. Janssens et al. (2001) and Högberg et al. (2001) claimed that most soil CO_2 emissions come from rather recently photosynthesized assimilates. Thus, instead of differences in annual temperature, it is the differences in tree photosynthesis and tree root respiration that mainly governs FF and total ecosystem respiration of treed sites. For the upland sites, the highest standing stock and foliage biomass was associated with the Spruce dominated *Oxalis-Myrtillus*, OMT, station, which also had the highest annual respiration value. The second highest soil CO_2 efflux value was associated with least fertile pine dominated *Calluna*, CT, station but which had the highest upland FF photosynthesis. It is possible that the upland respiration values reflected variation in fine root biomass along the mesic gradient, and that high FF respiration corresponds to high fine root biomass of trees and FF plants. The ratio of tree fine root biomass to foliage biomass tends to increases from fertile to less fertile conditions (Vanninen and Mäkelä, 1999), and pine tends to have more roots per leaf area than spruce (Chen et al., 2004). The pine dominated CT station had almost four times more above-ground FF biomass than the spruce dominated OMT station. The above-ground FF biomass was most strongly correlated to FF photosynthesis, and therefore P also increased enhanced R.

The net FF CO_2 exchange in the forest-mire transition zone was at similar level to that of the upland forests. The NFFE of the less stocked transition (*Oxalis-Myrtillus Paludified*, OMT+ and *Myrtillus Spruce Forest Paludified*, KgK) sites indicated that the importance of the respiration of the peat was contributing more to R than the respiration of the tree fine root biomass, while P was still limited by the tree canopy light reduction. The NFFE values of peatlands with only sparse trees showed a balanced C budget. However, the net CO_2 exchange at the FF is only a part of the net ecosystem exchange. When the CO_2 exchange of the above-ground part of the tree stands was included, most of our forested sites acted as carbon sinks, as reported in other studies (Valentini et al., 2000; Kolari et al., 2004; Liski et al., 2006). However, the least forested peatland site the *Tall Sedge Pine Fen*, VSR, remained a net CO_2 sink, and the forest-mire transition and *Spruce Pine Swamp*, KR, sites were balanced.

6. Conclusions

FF CO_2 uptake was most strongly related to the above-ground biomass of the FF, and solar radiation received, which are both strongly determined by the tree canopy. FF CO_2 emission therefore correlated to the tree stand foliar biomass. Whole net ecosystem CO_2 exchange was related to the amount of spruce and pine biomass. The proportion of FF CO_2 exchange in ecosystem CO_2 exchange generally increased as the tree stand became sparser. The net ecosystem exchange of the forest-mire transition zone was balanced because FF light, soil moisture and temperature conditions are so dynamic in this zone, it can fluctuate between being a carbon sink or source. Therefore, for landscape level CO_2 exchange assessment, the dynamics of forest-mire transitional zone, although narrow, is particularly important and in need of further study.

7. Acknowledgments

We thank Nordic Centre for Studies of Ecosystem Carbon Exchange and its Interactions with the Climate System (NECC), Nordic Centre of Excellence (NCoE), REBECCA by Helsinki University Environmental Research Centre (HERC), European Carbon Balance project (CarboEurope), Centre for International Mobility (CIMO) and all colleagues who helped to realize this study. Special thanks to Sakari Sarkkola for tree age estimation, and to Antti Mäkinen and Jussi Rasinmäki for tree biomass simulation.

References

Alm, J., Talanov, A., Saarnio, S., Silvola, J., Ikkonen, E. and co-authors. 1997. Reconstruction of the carbon balance for microsites in a boreal oligotrophic pine fen, Finland. *Oecologia* **110**, 423–431.

Alm, J., Schulman, L., Walden, J., Nykänen, H., Martikainen, P. J. and co-authors. 1999. Carbon balance of a boreal bog during a year with an exceptionally dry summer. *Ecology* **80**, 161–174.

Aurela, M., Laurila, T. and Tuovinen, J. P. 2004. The timing of snow melt controls the annual CO2 balance in a subarctic fen. *Geophysical Research Letters* **31**, 31:L16119. doi: 632 10.1029/2004GL020315.

Cajander, A. K. 1949. Forest types and their significance. *Acta Forestalia Fennica* **56**, 1–69.

Chen, W., Zhang, Q., Cihlar, J., Bauhus, J. and Price, D. T. 2004. Estimating fine-root biomass and production of boreal and cool temperate forests using aboveground measurements: A new approach. *Plant Soil* **265**, 31–46.

Davidson, E. A., Richardson, A. D., Savage, K. E. and Hollinger, D. Y. 2006. A distinct seasonal pattern of the ratio of soil respiration to total ecosystem respiration in a spruce-dominated forest. *Global Change Biol.* **12**(2), 230–239.

Frazer, G. W., Canham, C. D. and Lertzman, K. P. 1999. Gap Light Analyzer (GLA), Version 2.0: Imaging software to extract canopy structure and gap light transmission indices from true-colour fisheye photographs, users manual and program documentation. Copyright © 1999: Simon Fraser University, Burnaby, British Columbia and

the Institute of Ecosystem Studies, Millbrook, New York. Available at: http://www.rem.sfu.ca/forestry/downloads/gap_light_analyzer.htm

Granö, J. G., Jurva, R., Keränen, J., Kujala, V., Laitakari, A. and co-authors. 1952. Suomi, a general handbook on the geography of Finland. *Fennia* **72**, 74–99.

Högberg, P., Nordgren, A., Buchmann, N., Taylor, A. F. S., Ekblad, A. and co-authors. 2001. Large-scale forest girdling shows that current photosynthesis drives soil respiration. *Nature* **411**, 789–792.

IUSS Working Group WRB. 2006. World reference base for soil resources 2006. *World Soil Resources Reports* No. 103. FAO, Rome.

Janssens, I. A., Lankreijer, H., Matteucci, G., Kowalski, A. S., Buchmann, N. and co-authors. 2001. Productivity overshadows temperature in determining soil and ecosystem respiration across European forests. *Global Change Biology* **7**(3), 269–278. doi: 10.1046/j.1365–2486.2001.00412.x

Karjalainen, T. and Kellomäki, S. 1996. Greenhouse gas inventory for land use changes and forestry in Finland based on international guidelines. *Mitigation A d a p .Strategies Global Clim.* **1**, 51–71.

Koslari, P., Pumpanen, J., Rannik, U., Ilvesniemi, H., Hari, P. and co-authors. 2004. Carbon balance of different aged Scots pine forests in Southern Finland. *Global Change Biol.* **10**(7), 1106–1119.

Kolari, P., Pumpanen, J., Kulmala, L., Ilvesniemi, H., Nikinmaa, E. and co-authors. 2006. Forest floor vegetation plays an important role in photosynthetic production of boreal forests. *Forest Ecol Manage.* **221**, 241–248.

Laine, J. and Minkkinen, K. 1996. Effect of forest drainage on the carbon balance of a mire: A case study. *Scand J Forest Res.* **11**, 307–312.

Laine, J., Komulainen, V.-M., Laiho, R., Minkkinen, K., Rasinmäki, A. and co-authors. 2004. *Lakkasuo, a guide to mire ecosystems*. Helsingin Yliopiston Metsäekologian Laitoksen Julkaisuja, **31**. Helsinki, Finland. 123 p.

Lappalainen, E. and Hänninen, P. 1993. Suomen turvevarat. Geological survey of Finland. *Rep invest.* **117**, 118 p.

Larmola, T., Alm, J., Juutinen, S., Martikainen, P. J. and Silvola, J. 2003. Ecosystem CO2 exchange and plant biomass in the littoral zone of a boreal lake. *Freshw. Biol.* **48**, 1295–1310.

Lindroth, A., Grelle, A. and Moren, A.-S. 1998. Long-term measurements of boreal forest carbon balance reveal large temperature sensitivity. *Global Change Biol.* **4**, 443–45.

Liski, J., Lehtonen, A., Palosuo, T., Peltoniemi, M., Eggers, T. and co-authors. 2006. Carbon accumulation in Finland's forests 1922–2004 – an estimate obtained by combination of forest inventory data with modelling of biomass, litter and soil. *Ann. Forest Sci.* **63**, 687–697.

Markkanen, T., Rannik, Ü., Keronen, P., Suni, T. and Vesala, T. 2001. Eddy covariance fluxes over boreal Scots pine forest. *Boreal Env. Res.* **6**, 65–78.

Marklund, L. G. 1988. Biomassafunktioner för tall, gran och björk i Sverige. Sveriges Lantbruksuniversitet. *Rapporter-Skog* **45**, 1–73.

Mäkelä, A. 1997. A carbon balance model of growth and self-pruning in trees based on structural relationships. *Forest Science* **43**, 7–24.

Mäkelä, A., Kolari, P., Karimäki, J., Nikinmaa, E., Perämäki, M. and co-authors. 2006. Modelling five years of weather-driven variation of GPP in a boreal forest. *Agr. Forest Meteorol.* **139**, 382–398.

Nykänen, H., Heikkinen, J. E. P., Pirinen, L., Tiilikainen, K. and Martikainen, P. J. 2003. Annual CO2 exchange and CH4 fluxes on a subarctic palsa mire during climatically different years. *Global Biogeochemical Cycles* **17**, 1018. doi:10.1029/2002GB001861

Pepin, S., Plamondon, A. P. and Britel, A. 2002. Water relations of black spruce trees on a peatland during wet and dry years. *Wetlands* **22**, 225–233.

Pumpanen, J., Ilvesniemi, H. and Hari, P. 2003. A process-based model for predicting soil carbon dioxide efflux and concentration. *Soil Sci. Soc. Am. J.* **67**, 402–413.

Pumpanen, J., Westman, C. J. and Ilvesniemi, H. 2004. Soil CO2 efflux from a podzolic forest soil before and after forest clear-cutting and site praparation. *Boreal Environ Res.* **9**, 199–212.

Ryan, M. G., Lavigne, M. B. and Gower, S. T. 1997. Annual carbon cost of autotrophic respiration in boreal forest ecosystems in relation to species and climate. *J Geophysical Res.* BOREAS Special Issue, **102**(D24), 28871–28884.

Riutta, T., Laine, J. and Tuittila, E.-S. Sensitivity of CO2 exchange of fen ecosystem components to water level variation. *Ecosystems*, **40**, 718–733. doi: 10.1007/s10021–007-9046–7.

Tokola, T., Kangas, A., Kalliovirta, J., Mäkinen, A. and Rasinmäki, J. 2006. SIMO – SIMulointi ja Optimointi uuteen metsäsuunnitteluun. *Metsätieteen aikakauskirja* **1**, 60–65. (in Finnish).

Tuittila, E. S., Vasander, H. and Laine, J. 2004. Sensitivity of C sequestration in reintroduced Sphagnum to water-level variation in a cutaway peatland. *Restoration Ecol.* **12**, 483–493.

Turunen, J., Tomppo, E., Tolonen, K. and Reinikainen, A. 2002. Estimating carbon accumulation rates of undrained mires in Finland – application to boreal and subarctic regions. *Holocene* **12**, 69–80.

Valentini, R., Matteucci, G., Dolman, A. J., Schulze, E.-D., Rebmann, C. and co-authors. 2000. Respiration as the main determinant of carbon balance in European forests. *Nature* **404**, 861–865.

Vanninen, P. and Mäkelä, A. 1999. Fine root biomass of Scots pine stands differing in age and soil fertility in southern Finland. *Tree Physiol.* **19**, 823–830.

Vesala, T., Haataja, J., Aalto, P., Altimir, N., Buzorius, G. and co-authors. 1998. Long-term field measurements of atmospheresurface interactions in boreal forest combining forest ecology, micrometeorology, aerosol physics and atmospheric chemistry. *Trends in Heat, Mass, Momentum Transfer* **4**, 17–35.

Weimin, J., Chen, J. M., Black, A. T., Barr, A. G., Mccaughey, H. and co-authors. 2006. Hydrological effects on carbon cycles of Canada's forests and wetlands. *TellusB* **58**, 16–30.

Wilson, D., Alm, J., Riutta, T., Laine, J., Byrne, K. A. and co-authors. 2006. A high resolution green area index for modelling the seasonal dynamics of CO2 exchange in peatland. *Plant Ecology* DOI 10.1007/s11258–006-9189–1.

II

Biogeosciences, 12, 281–297, 2015
www.biogeosciences.net/12/281/2015/
doi:10.5194/bg-12-281-2015
© Author(s) 2015. CC Attribution 3.0 License.

Biogeosciences Open Access

CH_4 and N_2O dynamics in the boreal forest–mire ecotone

B. Ťupek[1], K. Minkkinen[1], J. Pumpanen[1], T. Vesala[2], and E. Nikinmaa[1]

[1]Department of Forest Sciences, P.O. Box 27, 00014 University of Helsinki, Finland
[2]Department of Physics, P.O. Box 48, 00014 University of Helsinki, Finland

Correspondence to: B. Ťupek (boris.tupek@helsinki.fi)

Received: 28 April 2014 – Published in Biogeosciences Discuss.: 4 June 2014
Revised: 13 November 2014 – Accepted: 3 December 2014 – Published: 16 January 2015

Abstract. In spite of advances in greenhouse gas research, the spatiotemporal CH_4 and N_2O dynamics of boreal landscapes remain challenging, e.g., we need clarification of whether forest–mire transitions are occasional hotspots of landscape CH_4 and N_2O emissions during exceptionally high and low ground water level events.

In our study, we tested the differences and drivers of CH_4 and N_2O dynamics of forest/mire types in field conditions along the soil moisture gradient of the forest–mire ecotone. Soils changed from Podzols to Histosols and ground water rose downslope from a depth of 10 m in upland sites to 0.1 m in mires. Yearly meteorological conditions changed from being exceptionally wet to typical and exceptionally dry for the local climate. The median fluxes measured with a static chamber technique varied from -51 to 586 $\mu g\,m^{-2}\,h^{-1}$ for CH_4 and from 0 to 6 $\mu g\,m^{-2}\,h^{-1}$ for N_2O between forest and mire types throughout the entire wet–dry period.

In spite of the highly dynamic soil water fluctuations in carbon rich soils in forest–mire transitions, there were no large peak emissions in CH_4 and N_2O fluxes and the flux rates changed minimally between years. Methane uptake was significantly lower in poorly drained transitions than in the well-drained uplands. Water-saturated mires showed large CH_4 emissions, which were reduced entirely during the exceptional summer drought period. Near-zero N_2O fluxes did not differ significantly between the forest and mire types probably due to their low nitrification potential. When upscaling boreal landscapes, pristine forest–mire transitions should be regarded as CH_4 sinks and minor N_2O sources instead of CH_4 and N_2O emission hotspots.

1 Introduction

Soil fertility, soil water content, and soil carbon storage of boreal forests varies between well-drained mineral soils mainly found in uplands and poorly drained organic soils mainly found in peatlands (Seibert et al., 2007; Weishampel et al., 2009). The CH_4 and N_2O fluxes from mineral and organic soils are impacted by varying soil moisture conditions (Solondz et al., 2008; Pihlatie et al., 2004). Typical mineral soil forests are small sinks of CH_4 and small sources or sinks of N_2O (Moosavi and Crill, 1997; Pihlatie et al., 2007). Sparsely forested peatlands are typically large or small sources of CH_4 and small sources or sinks of N_2O (Martikainen et al., 1995; Nykänen et al., 1995; D'Angelo and Reddy, 1998). Field CH_4 and N_2O studies of natural boreal forest–mire ecotones are rare (e.g., Ullah et al., 2009; Ullah and Moore, 2011) in comparison to those of typical forests or mires. However, the area of forest–mire transitions is relatively large, e.g., in Finland, forested mires with an organic horizon < 30 cm cover 1.5 million hectare or approximately 7 % of the total forest area (Finnish statistical yearbook of forestry, 2013), and at the present time it is not clear whether the terrestrial–aquatic interfaces, such as the forest–mire transition, represents a biogeochemical hotspot of CH_4 and N_2O emissions (McClain et al., 2003).

The lagg transitional zone in the forest–mire ecotone receives nutrients from the adjacent mineral soil runoff, and is thus more minerotrophic, biologically diverse, and productive than open mires or bogs (Howie and Meerveld, 2011). Furthermore, ecotones between forests and mires are ecological switches (Agnew et al., 1993), where the vegetation of forests and mires coincide and soils frequently undergo fluctuations in water level position and chemistry (Hartshorn et al., 2003; Howie and Meerveld, 2011), and where the CH_4

and N_2O dynamics of forest–mire transitions may be expected to differ generally and on a year-to-year basis from those of typical forests and mires.

The CH_4 uptake of forest soils is a result of CH_4 oxidizing aerobic methanotrophs sensitive to water saturation, soil porosity, moisture, temperature, pH, and ammonium (Moosavi and Crill, 1997; Saari et al., 2004; Jaatinen et al., 2004). Unsaturated upland forest soils oxidize CH_4 at higher rates than more water-saturated, acidic, and ammonium rich forested peat soils (Saari et al., 2004). In contrast to the CH_4 sinks of upland forest soils, and drained peatlands, natural mires emit CH_4 to the atmosphere (Bubier et al., 1995; Nykänen et al., 1998; Kettunen et al., 1999). CH_4 production in peat soil is a result of methanogenic and methanotrophic active bacteria, whose activity depends on anoxic and oxic conditions below and above the water level, temperature, and availability of carbon substrate (Kettunen et al., 1999). Increasing soil wetness increases anoxic conditions necessary for increased methanogenesis (Juottonen et al., 2005), and as a result CH_4 emissions increase (Saarnio et al., 1997; Ojanen et al., 2010; Yrjälä et al., 2011). Methane production potential in peat soils generally increases positively with pH (Juottonen et al., 2005; Ye et al., 2012), whereas CH_4 oxidation of forested peatlands has a narrow pH optimum around 5.5 (Saari et al., 2004). Increased pH levels, e.g., through the inflow of less acidic mineral soil water, typically containing greater calcium and bicarbonate concentrations than peat water (Howie and Meerveld, 2011), could increase CH_4 emissions from transitions.

N_2O emissions in well-drained boreal forest soils are controlled by soil moisture, pH, available nitrate, ammonium, oxygen, and carbon concentrations (Regina et al., 1996; Ullah et al., 2008). N_2O production is limited by the amount of nitrogen and is subject to denitrification and nitrification processes (Ambus et al., 2006). In well-drained soils NO_3 limitation, anoxic microsites, and larger soil porosity may also promote N_2O consumption (Frasier et al., 2010). N_2O consumption of soils correlates with dehydrogenase activity, which is affected by oxidation-reduction status and possibly controlled by soil moisture (Wlodarczyk et al., 2005). The N_2O consumption by soils is attributed to respiratory reduction (Conrad, 1996) caused by denitrifiers and nitrifiers (Rosenkranz et al., 2006). N_2O emissions increase during drier periods through increased ammonification and nitrification (Regina et al., 1996; Nykänen et al., 1995; Von Arnold et al., 2005). In water-saturated minerotrophic peatlands nitrification supplies nitrate (Wrage et al., 2001) for denitrification, which is the main but small N_2O source (Wray et al., 2007; Frasier et al., 2010). In nutrient rich mires, N_2O emissions increase during drier periods through increased ammonification and nitrification (Regina et al., 1996; Nykänen et al., 1995; Von Arnold et al., 2005). Nitrification and the supply of nitrate for denitrification increases with higher pH (Regina et al., 1996). However, if nitrate is available, low pH increases N_2O emissions (Weslien et al., 2009). Therefore, if nitrate were present during water level drawdown, the forest–mire transitions could become sources of N_2O.

Our aims were (1) to test whether forest floor CH_4 and N_2O fluxes of the forest–mire transition differ from the typical upland forests and lowland mires of natural boreal landscapes and (2) how meteorologically different years, i.e., exceptionally wet (2004), typical (2005), and exceptionally dry (2006), affect the fluxes.

We addressed the question of whether increasing wetness in forest–mire transitions promotes CH_4 production, and whether dry conditions reduce CH_4 production and increase N_2O emissions. We hypothesized that forest/mire types exhibit distinct levels of CH_4 and N_2O fluxes due to the changing soil structure from Podzols to Histosols and due to increasing soil water content from xeric to saturated. We expected that the occasionally saturated organo-mineral soils of forest–mire transitions are variable sources of CH_4 and N_2O fluxes. In order to evaluate the underlying factors behind CH_4 and N_2O forest floor fluxes, we measured the fluxes and environmental variables, such as soil temperature, soil moisture, water table depth, and soil water pH, in nine sites along the forest–mire ecotone during exceptionally different meteorological conditions. In order to detect statistically significant differences between CH_4 and N_2O fluxes of nine sites we used two-way analysis of variance, and for better understanding of flux responses to environmental factors we used linear and nonlinear regression models, and residual sensitivity analysis.

2 Material and methods

2.1 Study site characteristics

The Vatiharju–Lakkasuo ecotone of nine forest and mire study sites forms a gradient in vegetation communities, soil moisture and nutrient conditions in central Finland (61°47′, 24°19′) (Ťupek et al., 2008). Forest/mire types were classified using the Finnish classification systems (Cajander, 1949; Laine et al., 2004) based on soil fertility reflected by the composition and abundance of forest floor vegetation, and by the site location on the slope. The ecotone study sites are situated along a 450 m transect on a hillslope with a relative relief of 15 m and a 3.3 % slope facing NE (Fig. 1a). The fertility of the forest/mire sites increase from the poorly fertile sites at the xeric and saturated edges of the ecotone towards the most fertile *Oxalis-Myrtillus* type forest (OMT) in the middle of the hillslope (Fig. 1b).

Dominant vegetation composition changes with increasing soil moisture down the slope. Xeric Scots pine forest (CT – *Calluna* type) on the summit of glacial sandy esker gives way to subxeric Scots pine Norway spruce forest (VT – *Vaccinium vitis-idaea* type) on the shoulder, and mesic and herb rich Norway spruce dominated types on the back slope and footslope (MT – *Vaccinium myrtillus*

Table 1. Site soil water solution pH and soil properties.

	CT		VT		MT		OMT		OMT+		KgK		KR		VSR1		VSR2	
	mean	SE	mean	SE	mean	SE	mean	SE	mean	SE	mean	SE	mean	SE	mean	SE	mean	SE
pH 10 cm	5.57	0.36	5.14	0.42	5.24	0.08	4.68	0.39	4.58	0.30	4.46	0.14	4.37	0.22	5.06	0.39	4.80	0.44
pH 30 cm	6.20	0.06	6.18	0.02	5.91	0.13	5.30	0.11	5.53	0.04	4.91	0.10	4.55	0.08	5.32	0.15	4.79	0.19
Bulk density 0–10 cm	0.37	0.09	0.28	0.04	0.48	0.03	0.27	0.09	0.31	0.13	0.33	0.05	0.24	0.02	0.40	0.12	0.40	0.12
Bulk density 10–30 cm									0.92	0.07	0.31	0.12	0.85	0.03	0.90	0.07	0.90	0.07
Tot C (%) 0–10 cm	43.17		24.22		49.63		47.09		45.36		48.68		50.30		45.76		48.20	
Tot C (%) 10–30 cm									21.76		53.31		48.33		47.70		49.97	
Tot N (%) 0–10 cm	1.02		0.61		1.18		1.59		2.19		1.47		1.12		1.29		0.96	
Tot N (%) 10–30 cm									0.96		1.95		1.45		1.87		1.81	
C / N 0–10 cm	42.32		39.70		42.06		29.62		20.71		33.12		44.91		35.47		50.21	
C / N 10–30 cm									22.67		27.34		33.33		25.51		27.61	

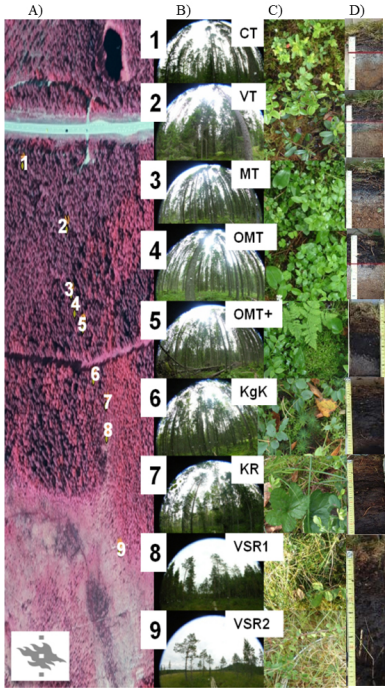

Figure 1. (a) Airborne infrared photograph shows a 450 m long boreal forest–mire ecotone located on the NE slope of the glacial Vatiharju–Lakkasuo esker in Finland (61°47′, 24°19′). **(b)** The fish-eye photographs show tree stands of xeric (1), subxeric (2), mesic (3), herb rich (4), paludified (5–7), and saturated (8–9) forest/mire types. **(c)** Photographs show ground vegetation and **(d)** soil profiles of nine forest/mire types. Upland forests: 1 CT – *Calluna*, 2 VT – *Vaccinium vitis-idaea*, 3 MT – *Vaccinium myrtillus*, 4 OMT – *Oxalis-Myrtillus*; forest–mire transition types: 5 OMT+ – *Oxalis-Myrtillus* paludified, 6 KgK – *Myrtillus* spruce forest paludified, 7 KR – spruce pine swamp; sparsely forested wet mire types: 8 VSR1 and 9 VSR2 – tall sedge pine fen.

type, OMT – *Oxalis-Myrtillus* type). The toe slope contains forest–mire transitions of paludified mixed spruce–pine–birch forests (OMT+ – *Oxalis-Myrtillus* paludified, KgK – *Myrtillus* spruce forest paludified). There is a permanently wet mixed spruce–pine–birch swamp (KR – spruce pine swamp) at the mire edge of the forest–mire transitions. On the level of the hillslope there are birch–pine fen mires with open tree canopies (VSR1 and VSR2 – tall sedge pine fen) (Fig. 1b). The forest floor vegetation is composed of site-specific mosses and vascular plants (Fig. 1c).

Soils are formed by well-drained Haplic Podzols on the hillslope, intermediately drained Histic and Gleyic-Histic Podzols in the forest–mire transitions on the toe of the slope, and permanently wet Hemic Histosols downslope (Fig. 1d).

We measured pH during summer campaign 2005 from soil water data collected on all sites by suction cup lysimeters. Three lysimeters were installed in 10 cm and one in 30 cm depth below the soil surface in each site. Detailed description of the lysimeters and sampling procedure can be found in Starr (1985). The pH was measured on the day of water sampling in the laboratory by pH meter equipped with a glass electrode. The mean acidity level of the sites of forest–mire ecotone was gradually increasing from pH 5.6 in uplands (CT) to 4.4 in transitions (KR), whereas mires were less acid than transitions with pH 5.1 and 4.8 (VSR1 and VSR2, respectively) (Table 1). Collected soil water from 30 cm depth showed generally higher pH than soil water pH at 10 cm depth. Three soil cores for each plot were taken in July 2006 from the top soil (0–10 cm) in upland forests and from the two profile depths (0–10, 10–30 cm) in forest–mire transitions and in peatlands. The volume of samples was measured before the oven drying at 70 °C to determine the bulk density. The bulk density of the upper organic layer ranged from 0.24 g cm^{-3} (KR) to 0.48 g cm^{-3} (MT) and was approximately half of the bulk density of the organic layer from 10 to 30 cm depth (mean of transitions and mires 0.77 g cm^{-3}) (Table 1). The C / N ratio was determined once for each plot from the soil organic matter analyzed by dry combustion with Leco CNS-1000 (Leco Corp., USA). The C / N ratio was wider in the 0–10 cm profile (mean 37) than in the 10–30 cm profile (mean 27). The highest N content as well as the lowest C / N ratio along the ecotone was found in forest–mire

transitions OMT+ and KgK (Table 1). A more detailed forest/mire type characterization is given by Ťupek et al. (2008).

2.2 Micrometeorological conditions

The micrometeorological measurements along the Vatiharju–Lakkasuo forest–mire ecotone were taken weekly during the summers of 2004 (July–November), 2005 (May–November), 2006 (May–September), and monthly during the winters (December–April). The forest floor soil temperatures (°C) at depths of 5, 15, and 30 cm (T_5, T_{15}, and T_{30}) were measured using a portable thermometer connected to thermocouples installed permanently in the soil. The volumetric soil moisture (%) at depths of 5, 10, and 30 cm (soil water content – SWC_5, SWC_{10}, and SWC_{30}) was measured by a portable ThetaProbe (Delta-T Devices Ltd.) in diagonally installed perforated PVC tubes, to ensure the same compactness of the soil. The depth of water table was measured inside PVC tubes (∅ 30 mm) installed at each site. Precipitation was measured by an automated bucket system at a station for monitoring forest – atmosphere relations, SMEARII (Hari and Kulmala, 2005), located 6 km north – west from the forest–mire ecotone. Missing soil temperature and moisture data of ecotone were gap filled by linear regression between continuous measurements of soil temperature and moisture at SMEARII.

2.3 CH_4 and N_2O fluxes

The field gas sampling was conducted weekly in the 2004 and 2005 seasons, bi-weekly during the 2006 season, and monthly during the winters. The gas sampling was done within 3-days interval of the micrometeorological measurements. If there was packed snow on the ground, the gas samples would be taken from the top and bottom layers; and the CH_4 ($\mu g\,m^{-2}\,h^{-1}$) and N_2O ($\mu g\,m^{-2}\,h^{-1}$) fluxes were calculated by the snowpack diffusion method using each gas concentration difference, snow depth, porosity and temperature, and gas diffusion coefficients as in Sommerfeld et al. (1993). Otherwise, if there was no snowpack, the samples would be taken from three opaque, vented, closed, static chambers (∅ 315 mm, *h* 295 mm) placed air tightly on preinstalled collars. On each measuring occasion a sample of ambient gas and four 15 ml samples from each of the three chambers were drawn in syringes at intervals of 5, 10, 15, and 20 min from chamber closure, totaling 13 samples for each site. Chamber temperature was monitored during the sampling. After the sampling event, the gas samples were stored in coolers at +4 °C and analyzed within 36 h in a laboratory with a gas chromatograph. The gas chromatograph (Hewlett-Packard, USA) model number HP-5890A was fitted with a flame ionization detector (FID) for CH_4 and an electron capture detector (ECD) for N_2O detection. The gas chromatograph was also equipped with a moisture trap. Prior to analysis of field samples and after each set of 13 samples a reference gas sample of known CH_4 and N_2O concentration was analyzed. The CH_4 ($\mu g\,m^{-2}\,h^{-1}$) and N_2O ($\mu g\,m^{-2}\,h^{-1}$) fluxes were calculated from the slope of linear regression between the set of four gas concentrations and sampling time, time elapsed after the chamber closure, and by applying temperature correction. For the flux calculation we used a MATLAB (The Mathworks Inc.) script developed at the Dept. of Physics, University of Helsinki.

The method quantification limit (MQL) of the gas chromatograph was based on 100 subsequently analyzed samples of reference gas of known CH_4 and N_2O concentrations (mean ± two SD: 1.837 ± 0.055 and 0.295 ± 0.023 ppm, respectively) and reference gas samples analyzed before the set of field samples for each site. The MQL was a gas-specific standard deviation of the random fluxes derived from 1000 random sets of four CH_4 or N_2O concentrations of reference gas samples (22 $\mu g\,m^{-2}\,h^{-1}$ for CH_4 and 18 $\mu g\,m^{-2}\,h^{-1}$ for N_2O). In order to minimize the random error related to gas sampling in the field, fluxes were verified using the ambient field air sample analyzed before each sequence of chamber samples adopting similar criteria as used in Alm et al. (2007). Due to gas sampling disturbances in the field and poor gas chromatograph accuracy 17 % of CH_4 and 49 % of N_2O fluxes were discarded.

2.4 Statistical analysis

Two-way analysis of variance (ANOVA) was used to test whether CH_4 and N_2O fluxes of forest/mire types have common means in wet, typical, and dry years. Post hoc Tukey HSD (honest significant difference) tests were used to test the pairwise differences between the forest and mire types and years changing from wet to dry. For CH_4 fluxes we ran ANOVA tests twice, first on the whole data set including nine forest/mire types and then on a subset of data including upland forests and forest–mire transitions, and excluding mires. For testing significant differences between the two groups of data we performed Welch's two sample *t* test, e.g., between the N_2O fluxes from the snow on the ground season (January–April in 2006) and the N_2O fluxes from the snowless seasons (May–November in 2005 and May–September in 2006).

In addition to ANOVA, we tested the dependence between the measured CH_4 ($\mu g\,m^{-2}\,h^{-1}$) and the gap filled half-hourly environmental variables in separate models for: (a) the upland forests on mineral soils (CT, VT, MT, OMT), and (b) forest–mire transitions on organo-mineral soils and (OMT+, KgK, and KR) (c) mires (VSR1, VSR2).

CH_4 fluxes ($\mu g\,m^{-2}\,h^{-1}$) of uplands and transitions were fitted by two linear mixed-effects regression models with a random effect for forest types (Pinheiro et al., 2013). For both groups of forest types, we evaluated the effect of all our environmental variables on CH_4 together and their combinations iteratively by selecting the model combination of variables that were significant.

The CH_4 fluxes for upland forests and transitions included soil moisture at 10 cm (%) (SWC_{10}) and soil temperature at 5 cm (°C) (T_5) as predictors in separate models (Eqs. 1 and 2):

$$yu_{ij} = \beta_{CT}SWC_{10} + \beta_{VT}SWC_{10} + \beta_{MT}SWC_{10} + \beta_{OMT}SWC_{10} + \beta_{CT}T_5 + \beta_{VT}T_5 + \beta_{MT}T_5 + \beta_{OMT}T_5 + b_{CT} + b_{VT} + b_{MT} + b_{OMT} + \varepsilon_{ij}, \quad (1)$$

$$yt_{ij} = \beta_{OMT+}SWC_{10} + \beta_{KgK}SWC_{10} + \beta_{KR}SWC_{10} + \beta_{OMT+}T_5 + \beta_{KgK}T_5 + \beta_{KR}T_5 + b_{OMT+} + b_{KgK} + b_{KR} + \varepsilon_{ij}, \quad (2)$$

where yu_{ij} and yt_{ij} are the CH_4 flux ($\mu g\,m^{-2}\,h^{-1}$) for upland forests or transitions and for a particular ith forest type and the jth observation, β_{CT} through β_{KR} are the fixed effect coefficients for a particular ith forest type (CT, VT, MT, OMT Eq. 1, or OMT+, KgK, and KR Eq. 2), SWC_{10}, and T_5 are the fixed effect variables (predictors) for observation j in forest type i where each forest type's predictor is assumed to be multivariate normally distributed, b_{CT} through b_{KR} are intercepts for the random effect for a particular ith forest type, and ε_{ij} is the error for case j in forest type i where each forest type's error is assumed to be multivariate normally distributed (Table 2).

The CH_4 fluxes ($\mu g\,m^{-2}\,h^{-1}$) of mires were fitted by using a multiplicative nonlinear regression model with a combined response to water table depth and soil temperature at 5 cm Eq. (1):

$$y_{ij} = a_0 e^{\left(-0.5\left(\frac{WT-WTopt}{WTtol}\right)^2\right)} e^{\left(-0.5\left(\frac{T5-Topt}{Ttol}\right)^2\right)} + \varepsilon_{ij}, \quad (3)$$

where y_{ij} is the CH_4 flux ($\mu g\,m^{-2}\,h^{-1}$) for the ith mire (VSR1,VSR2) and for the jth case, WT (cm) is water table depth, $T5$ (°C) is soil temperature at 5 cm, and a_0, WTopt, WTtol, Topt, and Ttol are parameters (Table 3).

The N_2O fluxes ($\mu g\,m^{-2}\,h^{-1}$) of all forest/mire types were fitted by using one multiplicative nonlinear regression model with a combined response to soil moisture and soil temperature at 5 cm Eq. (4):

$$z_{ij} = a_0 SWC_5 e^{\left(-0.5\left(\frac{T5-Topt}{Ttol}\right)^2\right)} + \varepsilon_{ij}, \quad (4)$$

where z_{ij} is the N_2O flux ($\mu g\,m^{-2}\,h^{-1}$) for the ith mire (VSR1,VSR2) and for the jth case, SWC_5 (%) is soil moisture at 5 cm, and T5 (°C) is soil temperature at 5 cm, and a_0, Topt, and Ttol are parameters (Table 4).

To illustrate the sensitivity of CH_4 and N_2O flux response to environmental factors we performed a residual analysis by simulating a value for each data point with only one factor allowed to vary and the other set to its mean level. To examine correlations between CH_4 and N_2O fluxes and pH, and soil properties we preformed the Pearson's correlation tests. The statistical analyses were performed in MATLAB R2012a (The Mathworks Inc.) and in R (R Core Team 2013) software environments.

3 Results

3.1 Micrometeorological conditions

The largest differences between years 2004, 2005, and 2006 were seen in changing summer precipitation patterns (measured nearby the SMEARII station). The average June–August monthly precipitation was reduced from 94 to 44 mm from a wet 2004 to a dry 2006, while ambient temperature increased from 14 to 17 °C. In the coldest summer (2004) the average precipitation in June and July was over 117 mm, and dropped to 47 mm in August. In the typically warm summer of 2005 the monthly precipitation gradually increased up to 123 mm in August, and dropped to 58 mm in September. However, in the warmest summer (2006) the monthly precipitation never reached more than 48 mm. In July 2006, two rainless weeks induced a drought. By drought we mean that the soil water content in the upper soil layer (in mineral soils) was so low that mosses wilted and dried (all along the ecotone). The drought conditions lessened in mid-August and ended in September with increasing rains towards autumn. Late autumn was exceptionally warm and snowless.

Monthly median soil temperatures at 5 cm (T_5) ranged from around 5 °C in May, culminated to around 15–16 °C in July and August, and subsided again to around 5 °C in October. The non-vegetative season T_5 minimum was close to 0 °C. The warmest T_5 was in upland forest CT and the coldest was in upper forest–mire transition OMT+. Soil temperature slightly increased from forest–mire transitions towards mires. In spite of the ambient air temperature difference throughout all the months in the 3 years, we detected differences mainly during early and late season in 2004, 2005, and 2006 T_5 (Fig. 2a).

The median water table (WT) showed the obvious rise from 10 m at the summit of the hill, to around 1 m in the mid-slope, between 0.5 and 0.1 m at the toe slope, and close to 0.01 m on the level (Fig. 2b). The seasonal WT rise in 2005 was observed between the July and August medians. During the drought of 2006, the WT values dropped less than 0.1 m for the uppermost forest sites, but dropped heavily by ~ 1 m in the forest–mire transitions, and more than 0.5 m in the lowermost peatland sites.

Volumetric SWC in 10 cm depth ranged from a dry value of around 10 % in the mineral soils to a water-saturated value of around 80 % in swamp and mires (Fig. 2c). The largest drought reduction of SWC was in August 2006 on the well-drained sandy Podzols at the summit of the hill, and also on the poorly drained Histic Podzols on the toe slope.

3.2 CH_4 fluxes

The median fluxes from the forest floor varied from -51 to 586 $\mu g\,m^{-2}\,h^{-1}$ for CH_4 among individual sites during the entire period (Fig. 3a). The small negative CH_4 fluxes associated with prevailing oxidation were mostly observed

Table 2. Parameter estimates and their standard errors for trend coefficients of CH_4 fluxes ($\mu g\,m^{-2}\,h^{-1}$) of the upland forest types (CT, VT, MT, and OMT, Eq. 1), and for the forest–mire transitions (OMT+, KgK, and KR, Eq. 2). Both equations are functions of volumetric soil moisture at 10 cm (%) and soil temperature at a depth of 5 cm (°C).

Eq. (1)	bi	Group bi	Group bi SE	$\beta i1$	$\beta i1$ SE	$\beta i2$	$\beta i2$ SE	N	RMSE
CT	−39.345	−43.632	9.102	0.762[a]	0.299	−1.249	0.223	137	35.2
VT	−26.213							143	25.1
MT	−50.984							139	25.2
OMT	−57.985							144	32.1
Eq. (2)									
OMT+	−49.898	−50.248	7.507	0.638	0.105	−0.109[b]	0.226	139	22.3
KgK	−48.216							146	17.9
KR	−52.630							149	31.5
Eq. (2) soil temperature excluded from fitting									
OMT+	−51.799	−52.466	6.341	0.660	0.099			139	22.3
KgK	−50.404							146	17.9
KR	−55.196							149	31.5

$p < 0.001$ for all parameters, except [a] $p = 0.011$, [b] $p = 0.629$. $\beta i1$ – soil moisture at 10 cm, $\beta i2$ – soil temperature at 5 cm.

Table 3. Parameter estimates and their standard errors for trend coefficients of CH_4 fluxes ($\mu g\,m^{-2}\,h^{-1}$) of the mires (VSR1, VSR2, Eq. 3). Equation (3) is a function of water table depth (cm) and soil temperature at a depth of 5 cm (°C).

Eq. (3)	$a0$	$a0$ SE	T_{opt}	T_{opt} SE	T_{tol}	T_{tol} SE	WT_{opt}	WT_{opt} SE	WT_{tol}	WT_{tol} SE	N	RMSE
mires	1207.1	126.7	13.9	1.4	6.4	1.3	−18.0	2.2	16.6	2.8	324	656
VSR1	1570.3	155.1	13.0	0.8	5.8	0.8	−18.6	1.6	15.5	1.7	162	424
VSR2	801.3	190.8	16.6[a]	6.8	8.7[b]	4.5	−17.3[c]	5.3	20.7[d]	9.7	162	558

p values < 0.001, except [a] $p = 0.016$, [b] $p = 0.053$, [c] $p = 0.002$, [d] $p = 0.035$.

in uplands and in transitions, while mires typically showed large positive CH_4 fluxes associated with prevailing production. The CH_4 flux dynamics changed exponentially with increasing levels of the ground water table from small uptake to large emissions (Figs. 2, 3). The median CH_4 fluxes of uplands (CT, VT, MT, OMT), transitions (OMT+, KgK, KR), and mires (VSR1, VSR2) varied from −38, −48, and 392 $\mu g\,m^{-2}\,h^{-1}$, respectively (Fig. 3b). Momentary CH_4 fluxes of uplands and transitions ranged from −342 to 143 $\mu g\,m^{-2}\,h^{-1}$, whereas in mires the fluxes ranged from −12 to 6808 $\mu g\,m^{-2}\,h^{-1}$ (Fig. 3b). The median CH_4 fluxes for one upland (VT) and all the transitions (OMT+, KgK, KR) were found inside the range of the gas chromatograph detection limits ($MQL_{CH_4} = 22\,\mu g\,m^{-2}\,h^{-1}$). In forest–mire transitions the ground water level in August 2005 increased towards the surface and approached the levels typically found in mires (Fig. 2b), but the soil water saturation in transitions was not followed by CH_4 emissions such as those found in mires.

ANOVA showed that forest floor CH_4 fluxes differed significantly for the nine forest/mire types of the ecotone F(8, 1252) = 108, $p < 0.001$ and for the wet, typical, and dry years F(2, 1252) = 10, $p < 0.001$. There was a significant interaction between CH_4 fluxes of forest/mire types and wet, typical, and dry years F(16, 1252) = 5, $p < 0.001$. The post hoc Tukey comparison of the nine forest/mire types indicated that the mires had significantly higher CH_4 fluxes than the forests. Differences in means (M) and 95 % confidence limits (CI) ranged from minimum VSR2–KgK ($M = 481$, 95 % CI [352, 610]) to maximum VSR1–OMT ($M = 793$, 95 % CI [668, 918]) at $p < 0.001$. Also the CH_4 fluxes of the mires were significantly different from each other VSR2–VSR1 ($M = -260$, 95 % CI [−384, -137]), $p < 0.001$. Differences between the years were significant at p < 0.001 for dry–typical ($M = -96$, 95 % CI [−149, −43]) when CH_4 fluxes of mires were highly reduced. The comparison of mean CH_4 fluxes of typical–wet ($M = 51$, 95 % CI [−6, 108]), $p = 0.089$, and dry–wet years did not show a significant difference ($M = -45$, 95 % CI [−111, 20]), $p = 0.237$.

Differences between the forest types (transitions, uplands) were not significant when analyzed together with the CH_4 fluxes of mires, but became significantly different F(6, 976) = 71, $p < 0.001$, when ANOVA was run without mires. Though unlike the nine forest/mire type data set, for the

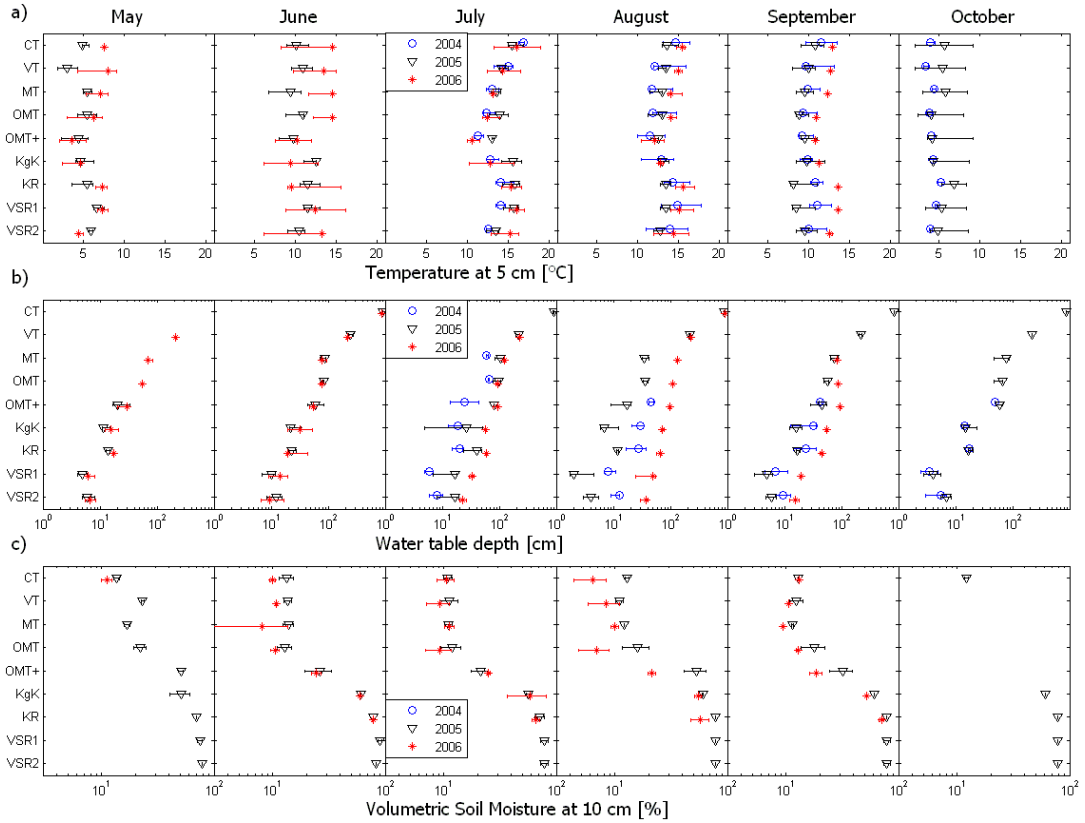

Figure 2. The panels **(a–c)** show the monthly medians of environmental variables: **(a)** soil temperature at a depth of 5 cm, **(b)** ground water level, and **(c)** volumetric soil moisture at 10 cm depth observed along the forest–mire ecotone during wet (2004), intermediate (2005), and dry years (2006). The top–down arrangement of sites mimics the locations on the slope (see Fig. 1). The error bars represent the 25th and 75th percentiles.

Table 4. Parameter estimates and their standard errors for forest floor N_2O fluxes ($\mu g\,m^{-2}\,h^{-1}$) of all forest/mire types (CT–VSR2) in one group Eq. (4). Eq. (4) is function of volumetric soil moisture at 5 cm (%) and soil temperature at a depth of 5 cm (°C).

Eq. (4)	$a0$	$a0$ SE	T_{opt}	T_{opt} SE	T_{tol}	T_{tol} SE	N	RMSE
forests/mires	4.034	0.635	11.268	0.183	1.414	0.181	400	36.2

$p < 0.001$ for all parameters.

group of uplands with transitions there was no difference between wet, typical, and dry years $F(2, 976) = 1$, $p = 0.292$, or their interactions $F(12, 976) = 1$, $p = 0.135$. The mean CH_4 uptake of the upland forests ($-42.9\,\mu g\,m^{-2}\,h^{-1}$) was for the whole period significantly larger than the mean CH_4 uptake of the forest–mire transitions ($-12.8\,\mu g\,m^{-2}\,h^{-1}$) according to Welch's two sample t test $t(994) = 15.56$, $p < 0.001$. The post hoc Tukey comparison of the differences in the mean CH_4 fluxes for 21 pairs of seven upland and transitional forest types was significant for 17 pairs at $p < 0.001$ and ranged from OMT–VT ($M = -35$, 95 % CI [−45, −25]) to KR–OMT ($M = 51$, 95 % CI [41, 61]). The post hoc Tukey comparisons showed non-significant p values for 4 of the 21 pairs of CH_4 fluxes of transitional and upland forest types (MT–CT 0.056, OMT+–VT 0.965, OMT–MT 0.431, and KR–KgK 0.999).

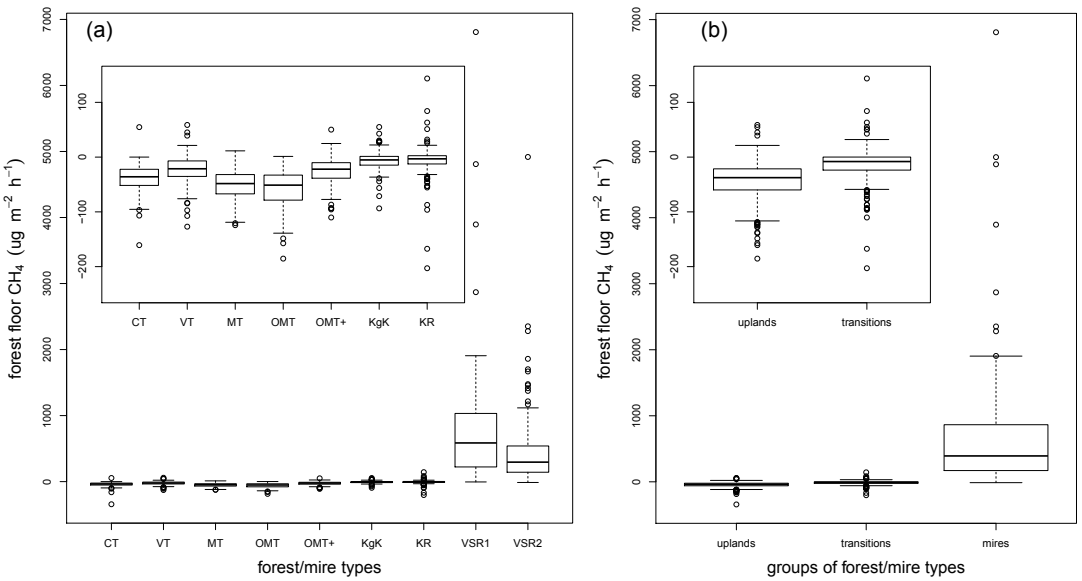

Figure 3. The box plots of forest floor CH_4 fluxes ($\mu g\,m^{-2}\,h^{-1}$) for each forest/mire type (a), and (b) for uplands (CT, VT, MT, OMT), transitions (OMT+, KgK, KR), and mires (VSR1, VSR2) during the whole period. The left–right arrangement of sites mimics the locations on the slope (see Fig. 1).

3.3 Factors controlling CH_4 fluxes

The mean level of CH_4 fluxes of upland and transitional forests differed (Table 2, parameter group bi), though the sensitivity response to environmental factors was similar (Fig. 4). The largest part of the CH_4 fluxes remained unexplained with our models, as the proportion of explained variance was relatively low for uplands (10 %) and transitions (15 %) and slightly higher for mires (22 %). The modeled CH_4 flux response for the upland and transitional forest sites to soil moisture at 10 cm was nearly flat, although the soil moisture parameter was significant ($p = 0.011$, Table 2). In the transitional *Oxalis-Myrtillus* paludified forest type OMT+, where the soil moisture at 10 cm ranged from 20 % (in the uplands) to over 70 % (in the mires), the modeled CH_4 flux response between dry and water-saturated soil differed by $50\,\mu g\,m^{-2}\,h^{-1}$. A stronger gradient than that in the soil moisture was detected by modeling stronger temperature responses of CH_4 fluxes for the uplands and the nearly flat response for the transitions (Fig. 4). The model parameter to soil temperature at 5 cm in the uplands was highly significant at $p < 0.001$, in contrast to transitions where the temperature parameter was insignificant $p = 0.629$ (Table 2). In the mires the observed range of water level during wet, typical, and dry years spanned from the surface to a depth of 54 cm and showed a sigmoidal response with lower CH_4 fluxes towards the extreme ends. The optimum water level for CH_4 emissions was 18 cm below the surface with 16.6 cm tolerance which is deviation of water level up to 60 % of CH_4 flux maximum (Fig. 4; $p < 0.001$, WT_{opt} and WT_{tol} in Table 3). Optimum near-surface peat temperature for the CH_4 emissions was found at 13.9 °C with 6.4 °C tolerance (Fig. 4; $p < 0.001$, T_{opt} and T_{tol} in Table 3).

3.4 N_2O fluxes

During the typical and dry years the momentary forest floor N_2O fluxes of forest/mire types ranged from −107 to $248\,\mu g\,m^{-2}\,h^{-1}$. The median N_2O fluxes were similar for the forest/mire types and ranged only from 0 to $6\,\mu g\,m^2\,h^{-1}$ (Fig. 5). The median N_2O fluxes of all forest/mire types were found inside the range of the method quantification limits ($MQL_{N_2O} = 18\,\mu g\,m^{-2}\,h^{-1}$). The N_2O fluxes of the snow on the ground period were significantly lower than the N_2O fluxes of the snowless period according to Welch's two sample t test $t(297) = 5.094$, $p < 0.001$. Forest floor N_2O fluxes did not differ significantly for the nine forest/mire types of the ecotone for the snowless periods $F(8, 284) = 0.708$, $p = 0.684$. Though, the momentary N_2O fluxes were significantly different in typical and dry snowless seasons $F(1, 284) = 6.157$, $p < 0.014$. N_2O fluxes were lower during dry snowless seasons and a small increase was observed only in one forest–mire transition (KR – spruce pine swamp) and in one mire (VSR2 – tall sedge pine fen) (Fig. 6).

In general N_2O fluxes were low and did not show clear spatial differences in relation to increasing soil moisture from

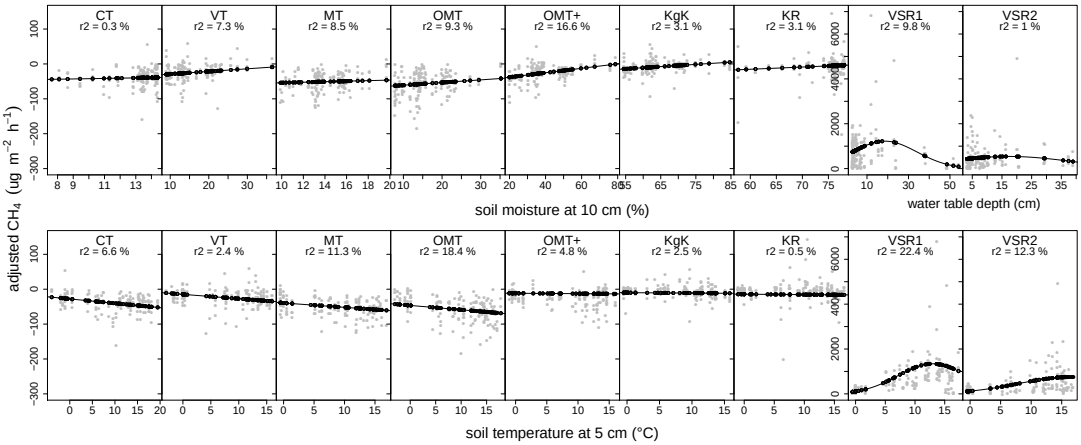

Figure 4. Comparison of sensitivity of forest floor CH_4 fluxes ($\mu g\,m^{-2}\,h^{-1}$) to environmental factors for nine forest/mire types. Modeled in the upper panels is CH_4 flux response to soil moisture at 10 cm (uplands and transitions) or to water table depth (cm) (mires) for uplands (CT, VT, MT, OMT) Eq. (1), for transitions (OMT+, KgK, KR) Eq. (2), and for mires (VSR1, VSR2) Eq. (3). Water table depth is indicated as negative when it is above the soil surface. In the lower panels, CH_4 flux response (Eqs. 1–3) is modeled to soil temperature at 5 cm of the same forest/mires types and during the same period as in the upper panel. The CH_4 flux response for each individual environmental factor is illustrated so that the simulated value for each data point was recalculated by allowing only one factor at a time to vary while the other was set to its mean level. To the adjusted CH_4 flux responses (black points) the corresponding residual of each data point was added in order to describe the unexplained model variation (gray points). The r^2 (%) is the proportion of explained variance. The left–right arrangement of sites mimics the locations on the slope (see Fig. 1).

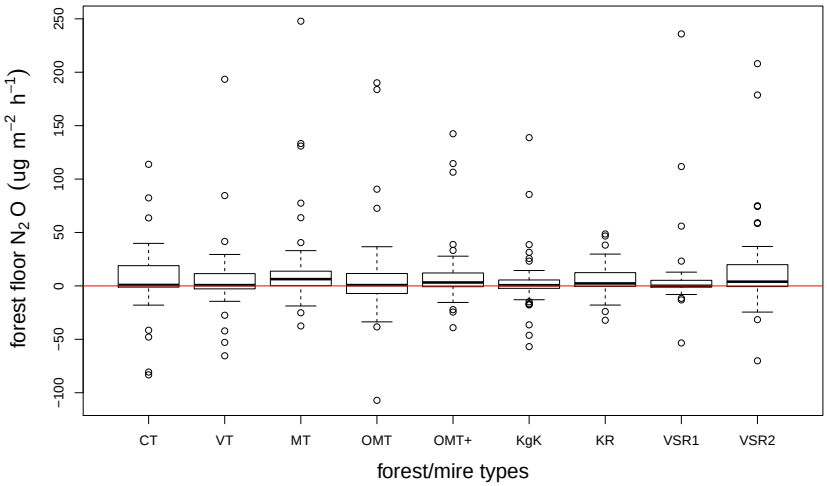

Figure 5. The box plot of forest floor N_2O fluxes ($\mu g\,m^{-2}\,h^{-1}$) for each forest/mire type (uplands – CT, VT, MT, OMT; transitions – OMT+, KgK, KR; and mires – VSR1, VSR2) during the period including typical and dry years. The left–right arrangement of sites mimics the locations on the slope (see Fig. 1).

xeric uplands to water-saturated mires, but the N_2O fluxes were lower in the dry than in the typical year. The post hoc Tukey tests of means and 95 % confidence limits of N_2O fluxes for all pairs (except one) showed insignificant forest/mire type pairwise differences during the whole period and also during the snowless periods of wet or dry years (Fig. 6). The significant N_2O flux difference for VSR2–OMT

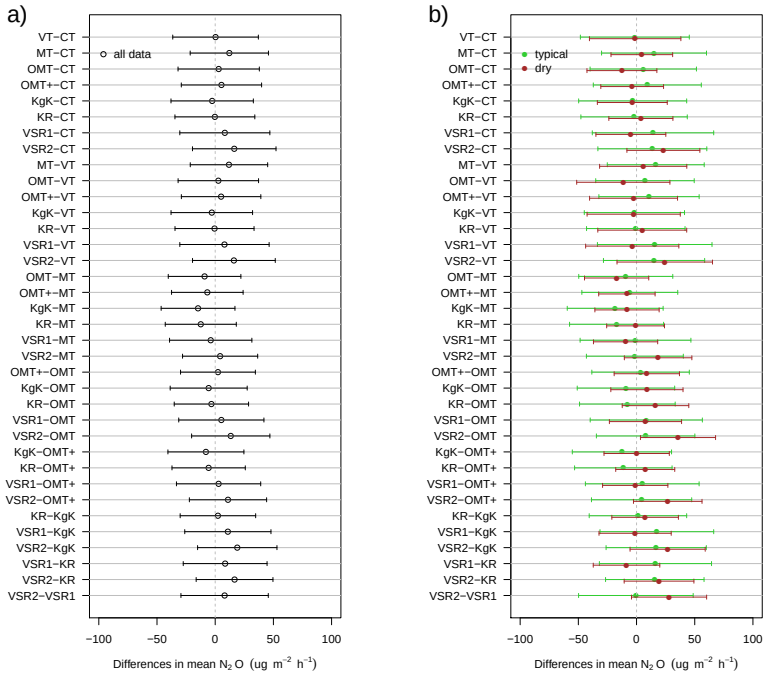

Figure 6. The post hoc Tukey differences (error bars for 95 % confidence intervals) of mean N_2O ($\mu g\,m^{-2}\,h^{-1}$) fluxes from the forest floor for the pairwise comparisons of forest/mire types (uplands – CT, VT, MT, OMT; transitions – OMT+, KgK, KR; and mires – VSR1, VSR2): **(a)** the N_2O flux differences over the whole period for a typical and dry year, **(b)** the N_2O flux differences only for snowless seasons and separately for typical and dry years.

in a dry year ($M = 35$, 95 % CI [3, 68], $p = 0.02$) was caused by a small decrease in OMT and increase in VSR2 fluxes.

3.5 Factors controlling N_2O fluxes

The sensitivity response of fluxes was weak in relation to soil moisture at 5 cm and had a somewhat clearer and significant relation with soil temperature at 5 cm ($p < 0.001$, Table 4, Fig. 7). The modeled Gaussian type response showed optimum N_2O production at 11.3 (°C) soil temperature at a depth of 5 cm with a very narrow temperature range increasing from 7 °C and subsiding at 14 °C.

3.6 Effects of pH and soil properties on CH_4 and N_2O flux

The site-specific momentary CH_4 and N_2O fluxes did not show significant correlation with varying soil water pH (except for one correlation coefficient $r = -0.45$, $p = 0.02$ on MT for N_2O and pH at 10 cm). Neither was any correlation found between pH and momentary CH_4 on the ecotone level. However, when mires were excluded, Pearson correlation between momentary CH_4 fluxes and soil water pH was significant ($r = -0.32$, $p < 0.001$). Mean values of summer 2005 CH_4 of upland forests and forest–mire transition were negatively correlated with mean pH ($CH_4 = 129.35–33.36 \times$ pH, $r^2 = 0.49$; Fig. 8a). The ecotone N_2O fluxes were significantly correlated with pH ($r = 0.174$, $p = 0.004$). The mean N_2O values of sites increased with mean pH ($N_2O = -117.07 + 27.33 \times$ pH, $r^2 = 0.32$; Fig. 8b). However, the post hoc Tukey differences of mean N_2O fluxes from the forest floor for the pairwise comparisons of forest/mire types were not significant for 31 pairs and mean N_2O flux differences were significant only for 5 pairs (KgK–CT, VSR1–KgK, VSR1–KR, VSR1–MT, VSR1–OMT, Fig. 9). We did not find significant correlation between site-specific mean CH_4 and N_2O flux and bulk density and/or C / N ratio.

4 Discussion

4.1 CH_4 dynamics

The forest/mire types significantly differed in forest floor CH_4 fluxes and between wet, typical, and dry years. As expected, the largest difference was found between emissions of mires and the small uptake of other forest types. However, CH_4 uptake also showed significant differences between the

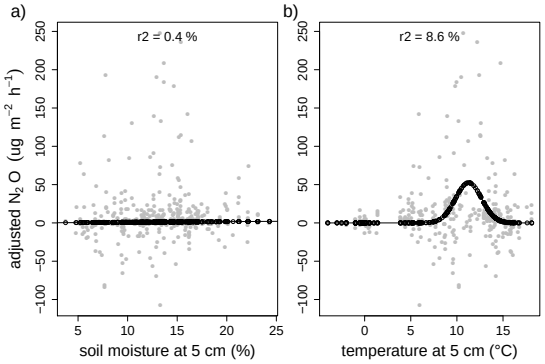

Figure 7. Sensitivity of forest floor N_2O fluxes ($\mu g\,m^{-2}\,h^{-1}$) of forest/mire types together with environmental factors: **(a)** N_2O flux response to soil moisture at 5 cm, and **(b)** N_2O flux response to soil temperature at 5 cm during the period including wet, typical, and dry years. The N_2O flux response form to each individual environmental factor is illustrated so that the simulated value by Eq. (4) for each data point was recalculated by allowing only one factor at a time to vary, while the other was set to its mean level. To the adjusted N_2O flux responses (black points) the corresponding residual of each data point was added in order to describe the unexplained model variation (gray points). The r^2 (%) is the proportion of explained variance.

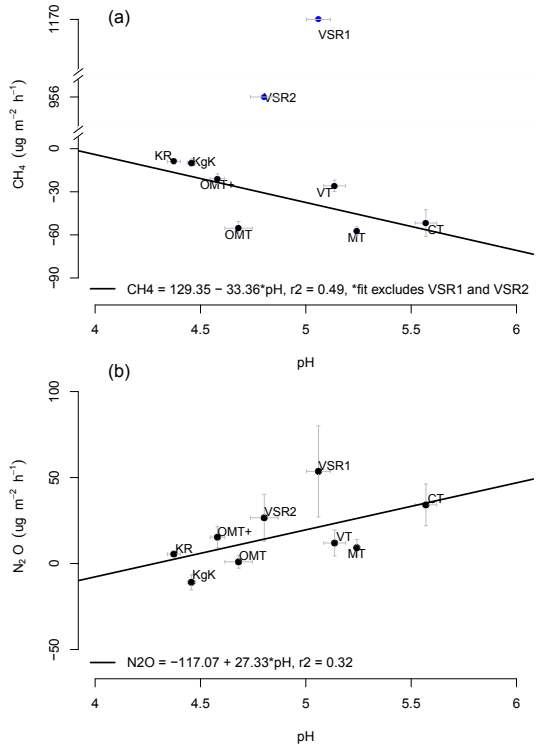

Figure 8. Scatterplot between site-specific mean pH and mean flux ($\mu g m^{-2}\,h^{-1}$) of **(a)** CH_4 or **(b)** N_2O of summer with intermediate moisture over the period of soil water sampling campaign (July–September 2005). Error bars show standard error. The CH_4 error bars for VSR1 and VSR2 are not shown.

forest types on mineral soil (uplands) and organo-mineral soil (transitions). Our study demonstrated that the CH_4 flux response to soil moisture changes with the relatively small mesoscale levels of a forest–mire ecotone (450 m long transect) (Fig. 4). The CH_4 flux sensitivity to soil moisture showed a positive linear response to CH_4 oxidation for the drier soils of transitions and uplands. Alternatively, CH_4 emission in mires showed a Gaussian form response to water level depth with a reduction of the optimum under saturated or dry peat conditions (Fig. 4). We have complemented the few studies on forest–mire gradients (e.g., Moosavi and Crill, 1997; Ullah et al., 2009; Ullah and Moore, 2011) and have lowered the likelihood of forest–mire transitions being biogeochemical hotspots of CH_4 emissions during short-term water level fluctuations.

The lack of an increase in CH_4 emissions during increased ground water levels in the transitions in our study could be attributed more to the relatively slow response of CH_4 producing bacteria than to the effectiveness of CH_4 oxidation which was reduced by a reduction in the aerated soil layer. Mäkiranta et al. (2009) showed that in forested peatlands the highest abundance of respiratory microbes could be found in the zone around the average water level. It is also known that the depth of maximum CH_4 production and oxidation is strongly related to 30-day average water level depth with time lag differences between the drier and wetter microsites (Kettunen et al., 1999). The duration of exceptionally increased high water levels was probably too short for CH_4 producing bacteria to relocate and/or adapt to water-saturated conditions. The methane production potential of mire varies in relation to methanogen communities, substrate availability, pH, and temperature (Juottonen et al., 2005, Juottonen et al., 2008). Unlike open mires, in drier conditions (similar to our forest–mire margin) decreases in the methanogen community are associated with low CH_4 production potential and with low emissions (Yrjälä et al., 2011). In the forest–mire margin, a relatively small population of methanotrophic microbes coupled with *Sphagnum* mosses and low CH_4 oxidation potential, related to low CH_4 concentrations in moss layer, could indicate low production potential (Larmola et al., 2010). It is known that water level depth is a major control of CH_4 oxidation, and that *Sphagnum* species originally not oxidising CH_4 need from several days to a month to activate methanotrophs through a water phase (Larmola et al., 2010; Putkinen et al., 2012).

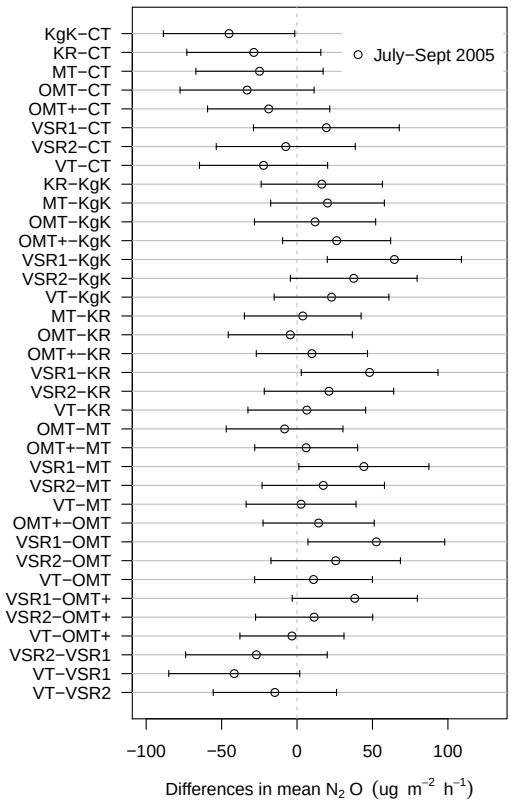

Figure 9. The post hoc Tukey differences (error bars for 95 % confidence intervals) of mean N_2O ($\mu g m^{-2} h^{-1}$) fluxes from the forest floor for the pairwise comparisons of forest/mire types (uplands – CT, VT, MT, OMT; transitions – OMT+, KgK, KR; and mires – VSR1, VSR2) over the period of the soil water sampling campaign (July–September 2005).

Temporally water-saturated soil layers of pristine forest–mire transitions had low CH_4 emissions possibly due to low pH, imposing physiological restrictions on soil microbial communities. Methanogenic activity in water-saturated organic soils can be reduced by high acidity (e.g., Ye et al., 2012). Activity of methanotrophic microbes is also pH dependent with optimum above 5 (Danilova and Dedysh, 2013; Saari et al., 2004). Our forest–mire transitions had mean pH below 5 and demonstrated lower net CH_4 uptake rates in comparison to upland forests on mineral soils (Fig. 8), which is in line with Saari et al. (2004). In spite of positive pH and CH_4 correlation found for the group of transitions and uplands together, the net CH_4 sink of upland well-drained mineral soil sites was primarily determined by high oxygen content. Small momentary CH_4 emissions (Supplement Fig. S3a) observed in forest–mire transitions also indicated potential for occasionally higher production than oxidation.

Beside differences in microsite soil water saturation, pH, and microbial communities, also plant communities (e.g., Saarnio et al., 1997; Strom et al., 2003; Riutta et al., 2007; Dorodnikov et al., 2011) play an important role in explaining net CH_4 emissions. In the forest–mire margin sites (KR and KgK) vascular plants (Fig. 1c) contributed to net forest floor CH_4 emissions (Fig. S3), if methane production occasionally increased. It is known that transport of recently photosynthesized carbon downwards to plant roots feeds microbial methane production (Alm et al., 1997; Strom et al., 2003; Dorodnikov et al., 2011). Aerenchyma of vascular plants transports most of produced CH_4 from peat to the atmosphere without oxidation in the acrotelm, and increases net CH_4 emissions (Hornibrook et al., 2009, Dorodnikov et al., 2011). A smaller amount of produced methane that is transported by pore water diffusion is efficiently oxidized by methanotrophs in the aerobic layer of peat and *Sphagnum* mosses (Hornibrook et al., 2009; Larmola et al., 2010).

Small CH_4 emissions as observed in relatively dry Scots pine dominated forests (VT – *Vaccinium vitis-idaea* type) (Fig. 3) with sandy Podzols soil and ground water depths around 2 m, have been occasionally found in mineral soil forests in other studies. The occasional mineral soil CH_4 effluxes suggested that plants' deepest roots transport CH_4 via the transpiration stream (Megonigal and Guenther 2008). Ullah et al., (2009) found that Spruce forest soils produced CH_4 only during the spring thaw season but later under drier summer conditions soils switched to CH_4 consumption. In our study the rare occurrence of small CH_4 emissions from forest soils differed between forest types and cannot only be attributed to increased soil moisture levels of microsites or transport from deep ground water sources. Small CH_4 emissions could be also partly attributed to the random noise in measurements. However, all the data showed a significant reduction of CH_4 uptake with increasing soil moisture at 10 cm, this may be associated with oxidation processes.

The form of dependence of CH_4 flux on soil moisture is better known from soil incubation studies (Pihlatie et al., 2004; Ullah et al., 2007) than from field studies, as field soil moisture ranges may be narrow (e.g., Nakamo et al., 2004). In order to describe the sensitivity of CH_4 uptake to moisture in the field we need a large amount of data covering a wide range of soil conditions (e.g., Hashimoto et al., 2011). In our study soil moisture varied between xeric and saturated conditions both spatially along the ecotone and temporally between years. Temporal soil water saturation in transitional forest–mire sites rather reduced CH_4 oxidations than promoted such CH_4 emissions as found in nearby permanently saturated mires. Beside the sensitivity of CH_4 fluxes to moisture we also observed sensitivity to soil temperature (Fig. 4) possibly also reflecting the role of soil physiochemical properties and/or the activity of methanogens. The linearly increasing CH_4 oxidation rates with temperature in up-

land forest types could reflect the importance of soil physiochemical properties, whereas the Gaussian form may also reflect a biological driven response in mires.

In our upland forests the role of soil physiochemical and microbiological drivers may have contributed to the fact that the temperature and moisture explained just 10 % of the variation. Although our mean CH_4 data did not show significant correlations with bulk density, the porous organic horizon is known to enable larger diffusion and CH_4 oxidation (Nakamo et al., 2004; Ullah and Moore 2011). It was difficult to assess the differences in sensitivity of CH_4 oxidation because of poor MQL and low fluxes of CH_4 oxidation. The absolute levels of the temperature effect on CH_4 fluxes in forest–mire transitions caused part of the signal to be mixed with variable sources of sampling errors and gas chromatograph precision errors. Though, in transitions both soil physiochemical and microbiological drivers may be important for CH_4 oxidations, as our forest–mire transitions showed a significant relation to soil moisture but not to temperature. The weak response of CH_4 oxidation to temperature was in contrast to the strong response to moisture and bulk density found in forests growing on mineral soils (Hashimoto et al., 2011). However, Nakamo et al. (2004) reported a clear relation with temperature but not with moisture for boreal birch forest (similar to our KR – spruce pine swamp).

In mires, the form of CH_4 sensitivity to temperature and water table depth may be also determined by differences in pH, and the composition of microbial and plant functional communities (Bubier et al., 1995; Jaatinen et al., 2004; Juottonen et al., 2005, 2008; Larmola et al., 2010; Riutta et al., 2007; Saarnio et al., 1997; Saari et al., 2004; Yrjälä et al., 2011). The CH_4 emissions in VSR1 were larger than in VSR2 (Fig. 4). Differences in pH could favor methanogen activity in less acid fen (Jouttonen et al., 2005; Yrjälä et al., 2011; Ye et al., 2012). Different coverage of vascular aerenchymous plants and *Sphagnum* mosses between VSR1 and VSR2 could affect site-specific CH_4 production and oxidation potentials. For example in VSR1 the water level was closer to the surface, and the lawn microsites had abundance of *Menyanthes* species (Fig. 1c), which are known to mediate higher CH_4 transport (Bubier et al., 1995; Macdonald et al., 1998), whereas in VSR2 *Menyanthes* species was absent. Shallower form of CH_4 sensitivity to water table in a hummock type fen VSR2 than in lawn type of fen VSR1 could resulted from differences in plant mediated CH_4 emissions (e.g., Riutta et al., 2007; Hornibrook et al., 2009; Dorodnikov et al., 2011) or CH_4 oxidation potential between *Sphagnum* species (Larmola et al., 2010). For example in the study by Saarnio et al. (1997) the CH_4 flux response to water level would be exponential if it accounted only for emissions from hummock and *Carex* lawn microsites, but the response was Gaussian for flark, hummock, *Eriophorum* lawn and *Carex* lawn microsites taken together.

4.2 N_2O dynamics

The momentary N_2O fluxes in the range from -107 to 248 ($\mu g\,m^{-2}\,h^{-1}$) and median emissions close to 0 ($\mu g\,m^{-2}\,h^{-1}$) for forest/mire types (Fig. 5) were in the proximity of values for soils in similar climates (Von Arnold et al., 2005a, b, Pihlatie et al., 2007; Matson et al., 2009; Ullah et al., 2009; Ojanen et al., 2010). Forest floor N_2O fluxes did not differ significantly for the nine forest/mire types of the ecotone $p = 0.637$ for the whole period from May 2005 to September 2006, probably due to the low nitrification potential of boreal forests in natural conditions (Regina et al., 1996). In contrast to our results, Ullah and Moore (2009, 2011) found that soil drainage and dominant tree species strongly control net nitrification rates, and that N_2O emissions from poorly drained soils can be three times larger than those from well-drained soils due to slower denitrification than nitrification activity. Statistically significant differences were also found between drained and undrained forests growing on organic soils and between evergreens and deciduous plants (Von Arnold et al., 2005a, b).

Soil incubation studies under various moisture and temperature regimes (Pihlatie et al., 2004; Szukics et al., 2010) imply that our higher forest floor N_2O emissions during typical summer 2005 than during dry summer 2006 (Supplement Fig. 3b) were probably induced by stimulated N turnover through the soil wetting and drying cycle under favorable temperature. During conditions with intermediate moisture (July–September 2005) we also observed mean N_2O flux of dry pine forest significantly larger than that of paludified spruce forest (larger CT than KgK), whereas mean N_2O flux of water-saturated mire was larger than four sites (VSR1–KgK, VSR1–KR, VSR1–MT, VSR1–OMT) (Figs. 8, 9). Therefore, during fluctuating soil moisture, we could expect increased N_2O fluxes of a normally xeric (CT) and water-saturated (VSR1) site due to stimulated nitrification (CT in rewetting phase, and VSR1 in drying phase). During July–September 2005, CT and VSR1 sites were also least acid along the ecotone which could favor nitrification and consequently N_2O emissions through denitrification (Regina et al., 1996; Ste-Marie and Pareé, 1999; Paavolainen et al., 2000). These studies reported that the increase of pH by rewetting could initiate nitrification. In contrast to less acid CT and VSR1, the more acid forest–mire transitions with the widest range of water level fluctuations ranked into a group of sites with lower N_2O fluxes. Highly acid conditions prevent development of nitrifiers, substrate affinity, and nitrification, even if ammonium is available (Ste-Marie and Pareé, 1999; Paavolainen et al., 2000). The fact that net nitrification of acid sensitive nitrifiers positively increases with forest floor pH, whereas acidification reduces it, suggests that nitrifiers in our sites were acid sensitive and not acid tolerant. The lack of nitrate renders denitrification potential to be negligible. Although, if nitrate were present, low pH would enhance N_2O emissions due to inhibiting di-nitrogenoxide reductase

and increasing N_2O / N_2 ratio of denitrification (e.g., Weslien et al., 2009).

In pristine mires nitrification positively depended on pH and negatively on water level (Regina et al., 1996) in supply of nitrate for denitrification, as the main source of N_2O emissions (Regina et al., 1996; Nykänen et al., 1995; Wray et al., 2007). Thus, during drying–rewetting periods as in July–September 2005, our sites could initiate short-term significant differences, but for the whole measurement period the lack of a statistically significant difference in N_2O fluxes was probably due to low nitrification potential. Generally, low pH and high C / N ratios of our forest floors suggest conditions of low nitrification potential. Thus, the lack of a statistically significant difference in N_2O fluxes was probably due to low nitrification potential. Other reasons could be the low field sampling frequency and relatively high noise in the data (MQL compared to low fluxes). Measuring three microsites per site could lead to missing some peak N_2O emission events due to a large microscale spatial variation (Von Arnold et al., 2005a). With our weekly or bi-weekly sampling frequency we could not identify larger microsite specific peak events possibly occurring after N was mobilized from, e.g., fast decomposition of deciduous foliage during the drought related early peak in litterfall or during sudden soil freeze–thaw cycles (Pihlatie et al., 2007). However, during the active growing season these events might be rare in typical boreal conditions where plants are adapted to a rapid uptake of limited rates of soil N mineralization (Hikosaka, 2003; Korhonen et al., 2013; Lupi et al., 2013).

Several studies (Martikainen et al., 1995; Regina et al., 1996) reported that peatlands in a pristine state showed small N_2O emissions, but when drained, nitrification rates were enhanced depending on nutrient status (a large increase for rich sites and no increase for poor sites). The limited increase in N_2O emissions during the summer drought in our mires may be therefore attributed to low nutrient levels, a low supply of nitrate and/or low nitrification potential. Relatively low fertility may also be expected to limit the N_2O emissions during the dry season of our forests and forest–mire transitions as the N_2O emissions are also known to correlate with site fertility, e.g., expressed as C / N ratio (Klemedtsson et al., 2005; Ojanen et al., 2010; Hashimoto et al., 2011).

The N_2O fluxes of forest/mire types fitted by nonlinear regression models showed positive linear response to soil moisture at a depth of 5 cm and significant Gaussian type response to temperature at depths of 5 cm (Table 4, Fig. 7). However, the residuals of the moisture and temperature model were large (Fig. 7) and r^2 was only 10 %. Luo et al. (2012) demonstrated for temperate forests that N_2O emissions depended nonlinearly on the soil moisture and positively on soil temperature. In our study, the weak linear response of soil moisture to N_2O fluxes could be an artifact of fitting several N_2O processes of different sensitivity to different forest/mire types. For example in well-drained uplands the N_2O fluxes may be mainly due to processes of ammonification and nitrification, while in mires nitrification in the drier surface layer may be coupled with denitrification in deeper water-saturated layers (Ambus et al., 2006; Regina et al., 1996). The soil moisture and temperature from deeper layers did not significantly explain the N_2O fluxes (results not shown). An active depth of 5 cm corresponding to the top of the organic layer is in agreement with Pihlatie et al. (2007) who demonstrated that N turnover in poor boreal forest soil takes place in the litter layer and that N_2O emissions originate mainly from the top soil. The N_2O production in our study increased with rising soil temperature of the humus layer from 7 °C typically found after the soil thawed during spring warming and in autumn during soil cooling. These could be the periods when the nitrification potential increased; in spring probably due to mobilization of nitrogen during freeze–thaw cycles and in autumn probably due to mobilization of nitrogen from the quickly decomposing foliar litterfall (Pihlatie et al., 2007, 2010; Luo et al., 2012).

5 Conclusions

The CH_4 fluxes of forest–mire ecotone were significantly different not only between sources or sink type forests but also between sinks (upland and transitional types) and between sources (mires). The forest–mire transitions showed CH_4 oxidation rather than emission with very small sensitivity to wet and dry events. The N_2O fluxes of forest mire types were generally low. Despite small N_2O peaks in spring and autumn, the N_2O fluxes showed low sensitivity to soil moisture probably due to poor soil nitrogen content and the low nitrification potential of the forest/mire types in pristine conditions. In spite of the potential of pristine forest–mire transitions to represent biogeochemical hotspots in the landscape, the CH_4 and N_2O flux levels in the transitions changed minimally during extremely large range of weather conditions. Our pristine forest–mire transitions did not act as biogeochemical hotspots for CH_4 and N_2O emissions. Therefore, when making attempts to upscale boreal landscape carbon and nitrogen cycles, the organo-mineral soils of pristine forest–mire transitions should be regarded as CH_4 sinks and minor N_2O sources rather than having the peak emissions on the landscape level.

The Supplement related to this article is available online at doi:10.5194/bg-12-281-2015-supplement.

Acknowledgements. This work was supported by Academy of Finland projects ICOS 271878, ICOS-Finland 281255 and ICOS-ERIC 281250; EU projects; NordForsk, through the Nordic Centre of Excellence (project DEFROST); the Finnish Centre of Excellence in Physics, Chemistry, Biology and Meteorology of

Atmospheric Composition and Climate Change (FCoE); and the Academy of Finland Center of Excellence program (project number 1118615). We also thank Jukka Laine, Jukka Alm, Mike Starr and Frank Berninger for valuable discussions; Mike Starr for providing suction cup lysimeters; Hannu Ilvesniemi for the soil moisture probe; Mari Pihlatie for providing us with the flux calculation script; Ilkka Korpela for providing the aerial image, courtesy of Finnish National Land Survey 2004; and Donald Smart for English language revision. We appreciate the useful comments of the editor Donatella Zona and three anonymous reviewers who improved the manuscript.

Edited by: D. Zona

References

Agnew, A. D. Q., Wilson, J. B., and Sykes, M. T.: A vegetation switch as the cause of a forest/mire ecotone in New Zealand, J. Veget. Sci., 4, 273–278, 1993.

Alm, J., Talanov, A., Saarnio, S., Silvola, J., Ilkkonen, E., Aaltonen, H., Nykänen, H., and Martikainen, P. J.: Reconstruction of carbon balance for microsites in a boreal oligotrophic pine fen, Finland, Oecologia, 110, 423–431, 1997.

Alm, J., Shurpali, N. J., Tuittila, E.-S., Laurila, T., Maljanen, M., Saarnio, S., and Minkkinen, K.: Methods for determining emission factors for the use of peat and peatlands – flux measurements and modelling, Boreal Env. Res., 12, 85–100, 2007.

Ambus, P., Zechmeister-Boltenstern, S., and Butterbach-Bahl, K.: Sources of nitrous oxide emitted from European forest soils, Biogeosciences, 3, 135–145, doi:10.5194/bg-3-135-2006, 2006.

Bubier, J., Moore, T., and Juggins, S.: Predicting methane emissions from bryophyte distribution in northern Canadian peatlands, Ecology, 76, 677–693, 1995.

Cajander, A. K.: Forest types and their significance, Acta Forestalia Fennica, 56, 1–69, 1949.

D'Angelo, E. and Reddy, K.: Regulators of heterotrophic microbial potentials in wetland soils, Soil Biol. Biochem., 31, 815–830, 1999.

Danilova, O. V. and Dedysh, S. N.: Abundance and diversity of methanotrophic *Gammaproteobacteria* in northern wetlands, Microbiology, 83, 67–76, 2014.

Dorodnikov, M., Knorr, K.-H., Kuzyakov, Y., and Wilmking, M.: Plant-mediated CH4 transport and contribution of photosynthates to methanogenesis at a boreal mire: a ^{14}C pulse-labeling study, Biogeosciences, 8, 2365–2375, 2011, http://www.biogeosciences.net/8/2365/2011/.

Frasier, R., Ullah, S., and Moore, T. R.: Nitrous oxide consumption potentials of well-drained forest soils in southern Quebec, Canada, Geomicrobiol. J., 27, 53–60, 2010.

Finnish statistical yearbook of forestry 2013. Finnish Forest Research Institute, Metsäntutkimuslaitos, Finland, http://www.metla.fi/julkaisut/metsatilastollinenvsk/index-en.htm, 2014.

Hari, P. and Kulmala, M.: Station for Measuring Ecosystem–Atmosphere Relations (SMEAR II), Boreal Env. Res., 10, 315–322, 2005.

Hartshorn, A. S., Southard, R. J., and Bledsoe, C. S.: Structure and function of peatland-forest ecotones in southeastern Alaska, Soil Sci. Soc. Am. J., 67, 1572–1581, 2003.

Hashimoto, S., Morishita, T., Sakata, T., Ishizuka, S., Kaneko, S., and Takahashi, M.: Simple models for soil CO_2, CH_4, and N_2O fluxes calibrated using a Bayesian approach and multi-site data, Ecol. Modell., 222, 1283–1292, 2011.

Hikosaka K.: A model of dynamics of leaves and nitrogen in a plant canopy: an integration of canopy photosynthesis, leaf life span, and nitrogen use efficiency, The American Naturalist , 162, 149–164, 2003.

Hornibrook, E. R. C., Bowes, H. L., Culbert, A., and Gallego-Sala, A. V.: Methanotrophy potential versus methane supply by pore water diffusion in peatlands, Biogeosciences, 6, 1491–1504, doi:10.5194/bg-6-1491-2009, 2009.

Howie, S. A. and Tromp-van Meerveld, I.: The essential role of the lagg in raised bog function and restoration: a review, Wetlands, 31, 613–622, 2011.

Huttunen, J., Nykänen, H., Martikainen, P., and Nieminen, M.: Fluxes of nitrous oxide and methane from drained peatlands following forest clear-felling in Southern Finland, Plant Soil, 255, 457–462, 2003.

Jaatinen, K., Knief, C., Dunfield, P. F., Yrjälä, K., and Fritze, H.: Methanotrophic bacteria in boreal forest soil after fire, FEMS Microbiol. Ecol., 50, 195–202, 2004.

Juottonen, H., Galand, P. E., Tuittila, E., Laine, J., Fritze, H., and Yrjälä, K.: Methanogen communities and bacteria along an ecohydrological gradient in a northern raised bog complex, Environ. Microbiol., 7, 1547–1557, 2005.

Juottonen, H., Tuittila, E., Juutinen, S., Fritze, H., and Yrjälä, K.: Seasonality of rDNA- and rRNA-derived archaeal communities and methanogenic potential in a boreal mire, The ISME J., 2, 1157–1168, 2008.

Kettunen, A., Kaitala, V., Lehtinen, A., Lohila, A., Alm, J., Silvola, J. and Martikainen, P. J.: Methane production and oxidation potentials in relation to water table fluctuations in two boreal mires, Soil Biol. Biochem., 31, 1741–1749, 1999.

Klemedtsson, L., Von Arnold, K., Weslien, P., and Gundersen, P.: Soil CN ratio as a scalar parameter to predict nitrous oxide emissions, Global Change Biol., 11, 1142–1147, 2005.

Korhonen, J. F. J., Pihlatie, M., Pumpanen, J., Aaltonen, H., Hari, P., Levula, J., Kieloaho, A.-J., Nikinmaa, E., Vesala, T., and Ilvesniemi, H.: Nitrogen balance of a boreal Scots pine forest, Biogeosciences, 10, 1083–1095, doi:10.5194/bg-10-1083-2013, 2013.

Laine, J., Komulainen, V.-M., Laiho, R., Minkkinen, K., Rasinmäki, A., Sallantaus, T., Sarkkola, S., Silvan, N., Tolonen, K., Tuittila, E-S., Vasander, H., and Päivänen, J.: Lakkasuo, a guide to mire ecosystems, University of Helsinki Department of Forest Ecology Publications 31, Helsinki, Finland, 123 pp., 2004.

Larmola, T., Tuittila, E.-S., Tiirola, M., Nykäne, H., Martikainen, J.P., Yrjälä, K., Tuomivirta, T., and Fritze, H.: The role of *Sphagnum* mosses in the methane cycling of a boreal mire, Ecology, 91, 2356–2365, 2010.

Luo, G. J., Brüggemann, N., Wolf, B., Gasche, R., Grote, R., and Butterbach-Bahl, K.: Decadal variability of soil CO_2, NO, N_2O, and CH_4 fluxes at the Höglwald Forest, Germany, Biogeosciences, 9, 1741–1763, doi:10.5194/bg-9-1741-2012, 2012.

Lupi, C., Morin, H., Deslauriers, A., Rossi, S., Houle, D.: Role of soil nitrogen for the conifers of the boreal forest: a critical review, International Journal of Plant and Soil Science, 2, 155-189, 2012.

Macdonald, J. A., Fowler, D., Hargreaves, K. J., Skiba, U., Leith, I. D., and Murray, M. B.: Methane emission rates from a north-

ern wetland; response to temperature, water table and transport, Atmos. Environ., 32, 3219–3227, 1998.

Mäkiranta, P., Laiho, R., Fritze, H., Hytönen, J., Laine, J., and Minkkinen, K.: Indirect regulation of heterotrophic peat soil respiration by water level via microbial community structure and temperature sensitivity, Soil Biol. Biochem., 41, 695–703, 2009.

Martikainen, P. J., Nykanen, H., Crill, P., and Silvola, J.: Effect of a lowered water table on nitrous oxide fluxes from northern peatlands, Nature, 366, 51–53, 1993.

Martikainen, P. J., Nykänen, H., Alm, J., and Silvola, J.: Change in fluxes of carbon dioxide, methane and nitrous oxide due to forest drainage of mire sites of different trophy, Plant Soil, 168/169, 571–577, 1995.

Matson, A., Pennock, D., and Bedard-Haughn A.: Methane and nitrous oxide emissions from mature forest stands in the boreal forest, Saskatchewan, Canada, For. Ecol. Manage., 258, 1073–1083, 2009.

McClain, M. E., Boyer, E. W.,Dent, C. L., Gergel, S. E., Grimm, N. B., Groffman, P. M., Hart, S. C., Harvey, J. W., Johnston, C. A., Mayorga, E., McDowell, W. H., and Pinay, G.: Biogeochemical hot spots and hot moments at the interface of terrestrial and aquatic ecosystems, Ecosystems 6, 301–312, 2003.

Megonigal, J. P and Guenther, A. B.: Methane emissions from upland forest soils and vegetation, Tree Physiol., 28, 491–498, 2008.

Moosavi, S. C. and Crill, P. M.: Controls on CH_4 and CO_2 emissions along two moisture gradients in the canadian boreal zone, J.Geophys.Res., 102, 29261–29277, 1997.

Nakano, T., Tnoue, G., and Fukuda, M.: Methane consumption and soil respiration by a birch forest soil in West Siberia, Tellus B, 56, 223–229, 2004.

Nykänen, H., Alm, J., Lang, K., Silvola, J., and Martikainen, P.: Emissions of CH_4, N_2O and CO_2 from a virgin fen and a fen drained for grassland in Finland, J. Biogeogr., 22, 351–357, 1995.

Nykänen, H., Alm, J., Silvola, J., Tolonen, K., and Martikainen, P. J.: Methane fluxes on boreal peatlands of different fertility and the effect of long-term experimental lowering of the water table on flux rates, Global Biogeochem. Cy., 12, 53–69, 1998.

Ojanen, P., Minkkinen, K., and Alm, J.: Soil–atmosphere CO_2, CH_4 and N_2O fluxes in boreal forestry-drained peatlands, Forest Ecol. Manage., 260, 411–421, 2010.

Paavolainen, L., Fox, M., and Smolander, A.: Nitrification and denitrification in forest soil subjected to sprinkling infiltration, Soil Biol. Biochem., 32, 669–678, 2000.

Pihlatie, M., Syväsalo, E., Simojoki, A., Esala, M., and Regina, K.: Contribution of nitrification and denitrification to N_2O production in peat, clay and loamy sand soils under different soil moisture conditions, Nutr. Cy. Agroecosyst., 70, 135–141, 2004.

Pihlatie, M., Pumpanen, J., Rinne, J., Ilvesniemi, H., Simojoki, A., Hari, P., and Vesala, T.: Gas concentration driven fluxes of nitrous oxide and carbon dioxide in boreal forest soil, Tellus B, 59, 458–469, 2007.

Pihlatie, M. K., Kiese, R., Brüggemann, N., Butterbach-Bahl, K., Kieloaho, A.-J., Laurila, T., Lohila, A., Mammarella, I., Minkkinen, K., Penttilä, T., Schönborn, J., and Vesala, T.: Greenhouse gas fluxes in a drained peatland forest during spring frost-thaw event, Biogeosciences, 7, 1715–1727, doi:10.5194/bg-7-1715-2010, 2010.

Pinheiro, J., Bates, D., DebRoy, S., Sarkar, D., and the R Development Core Team: nlme: Linear and Nonlinear Mixed Effects Models, R package version, 3.1, 113, http://cran.r-project.org/web/packages/nlme/nlme.pdf, 2013.

Putkinen, A., Larmola, T., Tuomivirta, T., Siljanen, H.M.P., Bodrossy, L., Tuittila, E.-S., and Fritze, H.: Water dispersal of methanotrophic bacteria maintains functional methane oxidation in Sphagnum mosses, Front. Microbio., 3, 15, doi:10.3389/fmicb.2012.00015, 2012.

R Core Team, R: A language and environment for statistical computing, R Foundation for Statistical Computing, Vienna, Austria, http://www.R-project.org/, 2013.

Regina, K., Nykänen, H., Silvola, J., and Martikainen, P.: Fluxes of nitrous oxide from boreal peatlands as affected by peatland type, water table level and nitrification capacity, Biogeochemistry, 35, 401–418, 1996.

Riutta, T., Laine, J., Aurela, M., Rinne, J., Vesala, T., Laurila, T., Haapanala, S., Pihlatie, M., and Tuittila, E.: Spatial variation in plant community functions regulates carbon gas dynamics in a boreal fen ecosystem, Tellus B, 59, 838–852, 2007.

Rosenkranz, P., Brűggemann, N., Papen, H., Xu, Z., Seufert, G., and Butterbach-Bahl, K.: N_2O, NO and CH_4 exchange and microbial N turnover over a Mediterranean pine forest soil, Biogeosciences, 3, 121–133, doi:10.5194/bg-3-121-2006, 2006.

Saari, A., Rinnan, R., and Martikainen, P. J.: Methane oxidation in boreal forest soils: Kinetics and sensitivity to pH and ammonium, Soil Biology and Biochemistry, 36, 1037–1046, 2004.

Saarnio, S., Alm, J., Silvola, J., Lohila, A., Nykanen, H., and Martikainen, P.: Seasonal variation in CH_4 emissions and production and oxidation potentials at microsites on an oligotrophic pine fen, Oecologia, 110, 414–422, 1997.

Seibert, J., Stendahl, J., and Sørensen, R.: Topographical influences on soil properties in boreal forests, Geoderma, 141, 139–148, 2007.

Solondz, D. S., Petrone, R. M., and Devito, K. J.: Forest floor carbon dioxide fluxes within an upland-peatland complex in the Western Boreal Plain, Canada, Ecohydrology, 1, 361–376, 2008.

Sommerfeld, R. A., Mosier, A. R., and Musselman, R. C.: CO_2, CH_4 and N_2O flux through a Wyoming snowpack and implications for global budgets, Nature, 361, 140–142, 1993.

Starr, M. R.: Variation in the quality of tension lysimeter soil water samples from a Finnish forest soil. Soil Sci., 140, 453–461, 1985.

Ste-Marie, C. and Pareé, D.: Soil, pH and N availability effects on net nitrification in the forest floors of a range of boreal forest stands, Soil Biol. Biochem., 31, 1579–1589, 1999.

Strom, L., Ekberg, A., Mastepanov, M., and Christensen, T. R.: The effect of vascular plants on carbon turnover and methane emissions from a tundra wetland, Global Change Biol., 9, 1185–1192, doi:10.1046/j.1365-2486.2003.00655.x., 2003.

Szukics, U., Abell, G.C., Hödl, V., Mitter, B., Sessitsch, A., Hackl, E., and Zechmeister-Boltenstern, S.: Nitrifiers and denitrifiers respond rapidly to changed moisture and increasing temperature in a pristine forest soil, FEMS Microbiol. Ecol., 72, 395–406, 2010.

Ťupek, B., Minkkinen, K., Kolari, P., Starr, M., Chan, T., Alm, J., Vesala, T., Laine, J., and Nikinmaa, E.: Forest floor versus ecosystem CO_2 exchange along boreal ecotone between upland forest and lowland mire, Tellus B, 60, 153–166, 2008.

Ullah, S. and Moore, T. R.: Soil drainage and vegetation controls of nitrogen transformation rates in forest soils, southern Quebec, J. Geophys. Res., 114, 01014, doi:10.1029/2008JG000824, 2009.

Ullah, S. and Moore, T. R.: Biogeochemical controls on methane, nitrous oxide, and carbon dioxide fluxes from deciduous forest soils in eastern Canada, J. Geophys. Res., Biogeosciences, 116, G03010, doi:10.1029/2010JG001525, 2011.

Ullah, S., Frasier, R., King, L., Picotte-Anderson, N., and Moore, T. R.: Potential fluxes of N_2O and CH_4 from three forests type soils in eastern Canada, Soil Biol. Biochem., 40, 986–994, 2008.

Ullah, S., Frasier, R., Pelletier, L., and Moore, T. R.: Greenhouse gas fluxes from boreal forest soils during the snow-free period in Quebec, Canada, Canadian Journal of Forest Research-Revue Canadienne De Recherche Forestiere, 39, 666-680, 2009.

Von Arnold, K., Ivarsson, M., Öqvist, M., Majdi, H., Björk, R.G., Weslien P., and Klemedtsson, L.: Can distribution of trees explain variation in nitrous oxide fluxes?, Scand. J. Forest. Res., 20, 481–489, 2005a.

Von Arnold, K., Weslien, P., Nilsson, M., Svensson, B., and Klemedtsson, L.: Fluxes of CO_2, CH_4 and N_2O from drained coniferous forests on organic soils, Forest Ecol. Manage., 210, 239–254, 2005b.

Weishampel, P., Kolka, R., and King, J. Y.: Carbon pools and productivity in a 1 km^2 heterogeneous forest and peatland mosaic in Minnesota, USA, Forest Ecol. Manage., 257, 747–754, 2009.

Weslien, P., Kasimir Klemedtsson, Å., Börjesson, G., and Klemedtsson, L.: Strong pH influence on N_2O and CH_4 fluxes from forested organic soils, Europ. J. Soil Sci., 60, 311–320, 2009.

Włodarczyk, T., Szarlip, P., and Brzezińska, M.: Nitrous oxide consumption and dehydrogenase activity in Calcaric Regosols, Polish J. Soil Sci., 2, 97–110, 2005.

Wrage, N., Velthof, G. L., van Beusichem, M. L., and Oenema, O.: Role of nitrifier denitrification in the production of nitrous oxide, Soil Biol. Biochem., 33, 1723–1732, 2001.

Wray, H. E. and Bayley, S. E.: Denitrification rates in marsh fringes and fens in two boreal peatlands in Alberta, Canada, Wetlands, 27, 1036–1045, 2007.

Ye, R. Z., Jin, Q. S., Bohannan, B., Keller, J. K., McAllister, S. A., and Bridgham, S. D.: pH controls over anaerobic carbon mineralization, the efficiency of methane production, and methanogenic pathways in peatlands across an ombrotrophic-minerotrophic gradient, Soil Biol. Biochem., 54, 36–47, 2012.

Yrjälä, K., Tuomivirta, T., Juottonen, H., Putkinen, A., Lappi, K., Tuittila, E., Penttilä, T., Minkkinen, K., Laine, J., Peltoniemi, K., and Fritze, H.: CH_4 production and oxidation processes in a boreal fen ecosystem after long-term water table drawdown, Glob. Change Biol., 17, 1311–1320, 2011.

III

Received: 19 February 2018 | Revised: 22 January 2019 | Accepted: 5 February 2019

DOI: 10.1111/ejss.12805

SPECIAL ISSUE

European Journal of Soil Science WILEY

Evaluating CENTURY and Yasso soil carbon models for CO_2 emissions and organic carbon stocks of boreal forest soil with Bayesian multi-model inference

Boris Ťupek[1,2] | Samuli Launiainen[1] | Mikko Peltoniemi[1] | Risto Sievänen[1] | Jari Perttunen[1] | Liisa Kulmala[2] | Timo Penttilä[1] | Antti-Jussi Lindroos[1] | Shoji Hashimoto[3] | Aleksi Lehtonen[1]

[1]Bioeconomy and environment, Natural Resources Institute Finland, Helsinki, Finland

[2]Department of Forest Sciences, University of Helsinki, Helsinki, Finland

[3]Department of Forest Soils, Forestry and Forest Products Research Institute, Tsukuba, Japan

Correspondence
Boris Ťupek, Bioeconomy and environment, Natural Resources Institute Finland, Latokartanonkaari 9, FI - 00790 Helsinki, Finland.
Email: boris.tupek@luke.fi
Aleksi Lehtonen.
Email: aleksi.lehtonen@luke.fi

Funding information
Academy of Finland, Grant/Award Number: Climoss /296116; FutMon programme, Grant/Award Number: LIFE07 ENV/DE/000218; Climforisk, Grant/Award Number: LIFE09 ENV/FI/000571; Finnish Ministry of the Environment and the Ministry of Agriculture and Forestry, Grant/Award Number: Developing methods for GHG-inventory

We can curb climate change by improved management decisions for the most important terrestrial carbon pool, soil organic carbon stock (SOC). However, we need to be confident we can obtain the correct representation of the simultanous effect of the input of plant litter, soil temperature and water (which could be altered by climate or management) on the decomposition of soil organic matter. In this research, we used regression and Bayesian statistics for testing process-based models (Yasso07, Yasso15 and CENTURY) with soil heterotrophic respiration (Rh) and SOC, measured at four sites in Finland during 2015 and 2016. We extracted climate modifiers for calibration with Rh. The Rh values of Yasso07, Yasso15 and CENTURY models estimated with default parameterization correlated with measured monthly heterotrophic respiration. Despite a significant correlation, models on average underestimated measured soil respiration by 43%. After the Bayesian calibration, the fitted climate modifier of the Yasso07 model outperformed the Yasso15 and CENTURY models. The Yasso07 model had smaller residual mean square errors and temperature and water functions with fewer, thus more efficient, parameters than the other models. After calibration, there was a small overestimate of Rh by the models that used monotonic moisture functions and a small generic underestimate in autumn. The mismatch between measured and modelled Rh indicates that the Yasso and CENTURY models should be improved by adjusting climate modifiers of decomposition or by accounting for missing controls in, for example, microbial growth.

Highlights

- We tested soil carbon models against monthly soil Rh fluxes and amounts of SOC stock.
- The models accurately reproduced most of the seasonal Rh trends and amounts of SOC.
- Under autumn temperature and moisture, Rh was mismatched before and even after the parameterization.
- The seasonality of the temperature and water functions should be adjusted in models.

 © 2019 British Society of Soil Science

1 | INTRODUCTION

Forest soil has been a carbon sink over millennia because of its slightly larger ecosystem CO_2 sequestration than decomposition. However, the positive offset of the carbon balance might be unlikely in future climates (Crowther et al., 2016), especially in the northern latitudes where the soil carbon stocks are largest and climate change is most rapid (Delworth et al., 2016). Accurate predictions are needed to adopt the most appropriate strategies for preserving soil carbon stocks (Smith, 2005). However, an accurate and precise estimate of SOC and its change is still a major challenge.

A warmer climate could promote soil carbon sources instead of sinks (Crowther et al., 2016; Kirschbaum, 2000; Lal, 2009). Prolonged droughts could alter photosynthetic uptake or modify the soil respiration response to temperature (Davidson & Janssens, 2006; Gaumont-Guay et al., 2006). Neither soil carbon data nor soil carbon models show consensus on the response of decomposition to temperature and moisture extremes (Sierra et al., 2015; Van Gestel et al., 2018).

The Yasso07 (Tuomi et al., 2009) and CENTURY (Parton et al., 1994) are two state of the art soil carbon models widely applied for simulating changes in SOC and soil CO_2 emissions. For example, these models have a similar form but differ in various conceptual ways (e.g. pools, processes and interactions) representing organic matter decomposition and its dependence on environmental conditions (temperature and moisture and other variables) (Figure 1). However, prediction of the magnitude and spatial

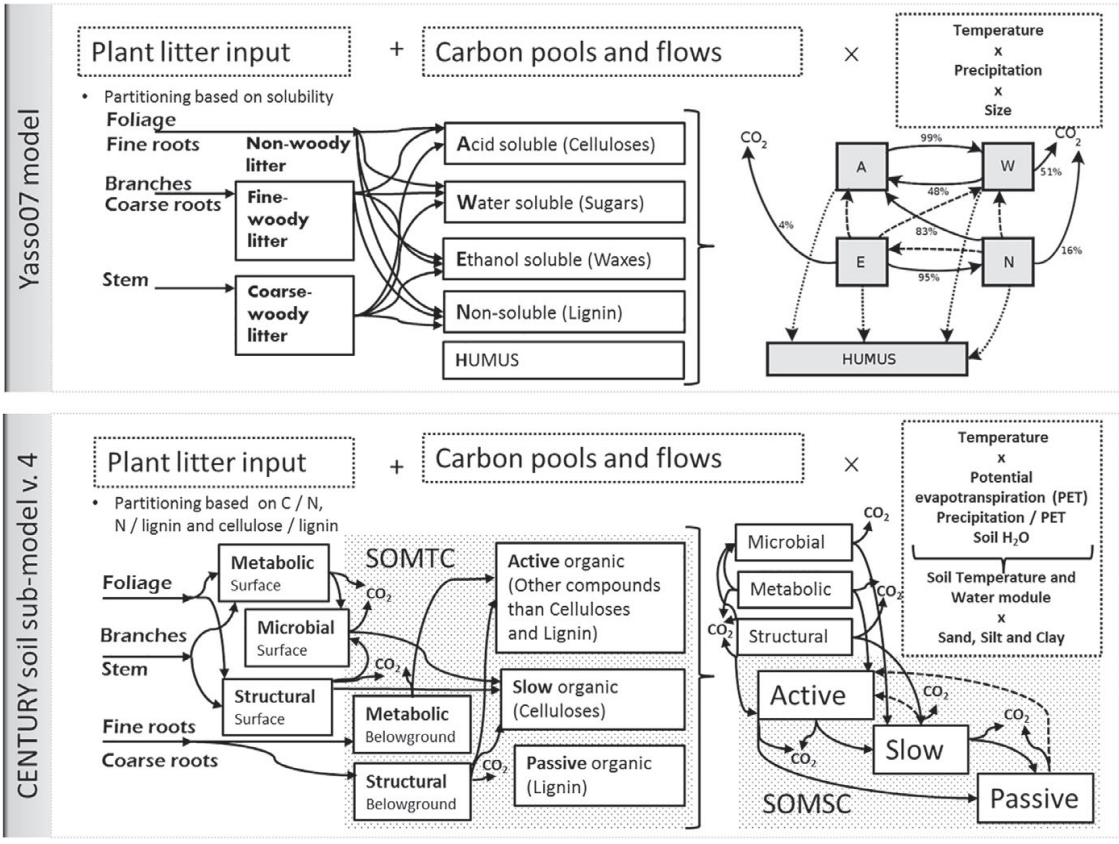

FIGURE 1 Conceptual representations of soil organic matter decomposition of the Yasso07 and Century models described in a general way as carbon (plant litter) entering the n number of time-dependent carbon pools and cross-pool flows controlled by a state of environmental conditions. The models differ in terms of their structure (pools and flows) and environmental dependence. The active pool of CENTURY in Yasso07 is represented by three pools (A, W and E) and rates of decomposition in Yasso07 are controlled by temperature and precipitation, but not explicitly by soil properties such as soil moisture and texture as in CENTURY. More detailed mathematical representations of the models are given in the Supporting Information File S1

variation of SOC is far from perfect (Hashimoto et al., 2017; Lehtonen et al., 2016; Todd-Brown et al., 2013; Ťupek et al., 2016). Model uncertainties hinder conclusions on both changes of SOC and CO_2 emissions (Lehtonen & Heikkinen, 2015). The imbalance between observed and modelled soil carbon stocks can be caused by incorrectly represented or missing biotic and abiotic factors of long-term soil carbon accumulation (Schmidt et al., 2011; Todd-Brown et al., 2013).

The Yasso07 model (Tuomi et al., 2009) was developed mainly to quantify changes in carbon stock of mineral soils. The model predicts changes in carbon stock and heterotrophic soil respiration from the balance between decomposing soil organic matter and litter input. Yasso07 was calibrated with almost 10,000 items of litter bag data from Europe, North and South America, and relatively few soil C stocks from Finnish forests (Tuomi et al., 2009). The model has been widely used for reporting SOC change in Finland to the United Nation Framework Convention on Climate Change (UNFCCC) and is also used together with Earth system models (Thum et al., 2011). Compared to Yasso07, Yasso15 (Järvenpää et al., 2015) has more detailed dependence of decomposition on temperature and has been calibrated against a larger dataset. CENTURY (Parton et al., 1994) is one of the most widely used soil carbon models of the Earth system models and is also used by Canada, Japan and the USA for soil carbon reporting to the UNFCCC. CENTURY was initially developed for grassland systems by Parton et al. (1994) and modified later to be applied also to boreal forests (e.g., Nalder & Wein, 2006). Unlike the Yasso models that do not need soil data, the CENTURY soil submodel v.4 requires soil input data (sand, silt and clay content, and bulk density) and by default operates at weekly rather than annual time-steps.

The Yasso07 and CENTURY models are used for national greenhouse gas reporting; however, neither has been tested with soil respiration and SOC data simultaneously. Furthermore, the models are mostly used with default calibrations. We aimed to test the performance of the soil carbon models Yasso07, Yasso15 and CENTURY for soil organic carbon stocks and heterotrophic respiration with and without calibration at four sites in Finland. We aimed to test the models with default parameters and to evaluate whether the expected mismatch between data and models is caused by parametrization or by the mathematical formulation of temperature and moisture functions. To test our hypothesis, we ran the models with the same litter fall data and separated the effects of functional forms from model parametrization of dependence on temperature and moisture with Bayesian inference.

2 | MATERIAL AND METHODS

2.1 | Study sites

Two Scots pine (*Pinus sylvestris* L.)-dominated and two Norway spruce (*Picea abies* L.)-dominated forest sites (Table 1) in the southern boreal zone of Finland (Figure S1a in Supporting Information File S1) were selected for this study. The sites are part of intensive monitoring of forest ecosystems (Level II) of the International Co-operative Programme on Assessment and Monitoring of Air Pollution Effects on Forests (ICP) (www.metla.fi/metinfo/forest-condition/programmes/intensive-monitoring.htm; Merilä et al., 2014). In October 2014, we trenched three square plots (1 m × 1 m) at each site to be able to subtract the autotrophic respiration of the tree roots from total forest floor CO_2 efflux to obtain soil heterotrophic respiration (Rh). The plots were divided further into four sub-squares (Figure S1b). The ingrowth of tree roots was prevented. On eight plots around the trench, we measured reference soil respiration, which included autotrophic and heterotrophic respiration (Figure S1b). At each forest site, we established three groups of trenched and control plots, yielding in total 12 trenched and 24 control plots. Respiration from the trenched plot (Rh) was used for comparison with the soil carbon models and total respiration from the control plots was used as a reference only.

2.2 | Soil respiration measurements and ancillary data

Forest floor respiration was measured once a week during the growing season (April–October) in 2015 and 2016, both on trenched and control plots (Figure S1). We used a portable infrared CO_2 analyser (EGM4, SRC-1 PP systems Inc., Amesbury, MA) connected to a closed-path ventilated non-transparent chamber (volume = 14.1 L; diameter = 30 cm). The measurements were made between 08.00 and 17.00, and the order in which the plots were measured at each station was random. The CO_2 concentration was measured every 4.8 s during 120 s of chamber closure and CO_2 fluxes (Figure S2) were calculated from the raw data (Jurasinski et al., 2014). During the flux measurements, we also measured the soil temperature (T) and moisture (SWC) with a portable thermometer and portable ThetaProbe (Delta-T Devices Ltd) at 5-, 10-, 15- and 20-cm depths. Soil temperature and moisture were also measured continuously by permanently installed sensors (iButton® temperature loggers from Maxim Integrated (San Jose, CA, USA); soil moisture sensors from Delta-T devices and Soil Scout Oy (Helsinki, Finland) (Figure S2).

TABLE 1 The characteristics of four ICP-level II sites used in this study (data from Merilä et al. (2014); Ťupek et al. (2015); Finnish Meteorological Institute)

Site name	Tammela pine	Tammela spruce	Punkaharju pine	Punkaharju spruce
Latitude /°	60.62	60.65	61.77	61.81
Longitude /°	23.84	23.81	29.33	29.32
Soil type [a]	Albic Arenosol	Haplic Arenosol	Rustic Podzol	Haplic Regosol
Sand content /%	98	59	97	68
Silt content /%	2	40	2	31
Clay content /%	0	1	1	1
Bulk density /g cm^{-3}	1.4	1.0	1.5	1.2
Humus C/N	32	30	35	31
Soil C/N	26	20	37	19
Total SOC up to 0.5 m /t C ha^{-1}	83.2	84	45	88.7
Stems /ha^{-1}	619	663	741	370
Stem volume /m^3 ha^{-1}	306	360	362	435
Basal area /m^2 ha^{-1}	29	33	32	34
Height /m	22	22	24	28
Diameter at 1.3 m /cm	25	26	24	35
Age /year	70	70	90	80
Annual temperature /°C	4.38	4.32	3.62	3.62
Annual precipitation /mm	627	625	593	594

[a]According to IUSS Working group WRB (2006) as cited in Merilä et al. (2014). SOC: soil organic carbon.

2.3 | Nonlinear least squared regression analysis

We used nonlinear least squared regression analysis (NLS) models for (a) evaluating responses of the instantaneous measurements of soil respiration (R, g CO_2 m^{-2} hr^{-1}) to environmental factors (T_5 and SWC_{10}), (b) the flux gap filling and (c) upscaling R to the monthly level (g CO_2 m^{-2} $month^{-1}$). The immediate R values were fitted to the corresponding T_5 and SWC_{10} (Figure S2 in File S1) separately for each site and treatment. We used a Q_{10}-based temperature response curve (Equation 1) modified by a response to soil water content (Davidson et al., 2012) (Equation 2):

$$R_{ij} = R_{\text{ref}} Q_{10}^{\left(\frac{T_5 - 10}{10}\right)}, \quad (1)$$

$$R_{ij} = R_{\text{ref}} d^{\left(\text{SWC}_{\text{opt}} - \text{SWC}_{10}\right)^2} Q_{10}^{\left(\frac{T_5 - 10}{10}\right)}, \quad (2)$$

where R is soil respiration, T_5 is soil temperature at 5-cm depth (°C) and SWC_{10} is volumetric soil moisture at 10-cm depth (%, m^3 m^{-3}). The R_{ref}, Q_{10}, SWC_{opt} and d are calibrated parameters for the i^{th} forest site and j^{th} treatment. The R_{ref} is the reference R (g CO_2 m^{-2} hr^{-1}) at 10°C, Q_{10} the relative increase in R per 10°C change in temperature and SWC_{opt} the optimum soil water content for respiration. The goodness of fit statistics and the parameter values are in Supporting Information, Table S1. To obtain monthly R (g CO_2 m^{-2} $month^{-1}$) we first estimated the continuous hourly R from continuous site-specific T_5 and SWC_{10} with Equation (2) (Figure S2). The monthly standard error of forest floor CO_2 fluxes was estimated as the standard deviation of model residuals divided by the square root of the number of CO_2 measurements and multiplied by the number of hours in a month.

2.4 | Soil carbon stock and CO_2 efflux modelling

We used Yasso07, Yasso15 and CENTURY to estimate initial SOC (January 1, 2014), monthly and annual SOC change and heterotrophic soil CO_2 respiration in 2014–2016. The initial SOC values were set to match the estimated equilibrium state between the litter input and decomposition for each site. The Yasso07 and Yasso15 models had a 3000-year spin up period, whereas for CENTURY it took 5000 years to reach equilibrium.

2.5 | Short model descriptions

Yasso07 is a reasonably simple soil carbon model (Tuomi et al., 2009) where soil C is divided into five pools based on plant litter chemistry (Figure 1). The rates of decomposition and C flows are affected by temperature and precipitation. The central assumptions of Yasso07 have been challenged in the Yasso15 model (Järvenpää et al., 2015), which (a) assumes different temperature and precipitation sensitivity between pools and (b) is calibrated against global SOC measurements. To allow inter-comparison between Yasso07, Yasso15 and CENTURY, we used the CENTURY soil sub-model only (Parton et al., 1994). In CENTURY, the soil carbon flows between structural, metabolic, active, slow and passive C pools with different turnover rates (Figure 1). Temperature and moisture modify the rates of decomposition. The rates of decomposition of the slow and passive pools also rely on lignin to N and C to N ratios. In the active pool, the rate of decomposition is modified by soil texture.

The models differ in their representation of soil temperature and moisture responses. CENTURY runs on air temperature and soil moisture (Kelly et al., 2000) or precipitation (Adair et al., 2008). The Yasso models run just on air temperature and precipitation (Järvenpää et al., 2015; Tuomi et al., 2009). The CENTURY model, unlike the Yasso models, has a sub-routine that computes soil temperature and water balance. The environmental modifier of the CENTURY model was altered in different applications. In CENTURY (Kelly et al., 2000) soil water function has an optimum, but temperature increases exponentially. In CENTURY (Adair et al., 2008) the temperature function has an optimum, whereas water function only saturates. Furthermore, in Adair et al. (2008) precipitation is relative to evapotranspiration but the ratio is limited to one, with the result that more precipitation than evapotranspiration does not reduce decomposition. Both Yasso models use the same equations for temperature and precipitation functions. Temperature dependence is exponential in both models, but in Yasso07 (Tuomi et al., 2009) it reaches an optimum and declines, unlike in Yasso15 (Järvenpää et al., 2015). Precipitation functions in the Yasso models are similar to CENTURY in Adair et al. (2008), in that they reach saturation although they do not account for potential evapotranspiration. More detail on the mathematical representation of the models is given in the Supporting Information, File S1.

2.6 | Model inputs

The Yasso07, Yasso15 and CENTURY models require air temperature, precipitation and litter as either monthly or annual input data. We used the same input for litterfall for all three soil carbon models (Figure S3). The daily weather data originated from the Finnish Meteorological Institute (www.fmi.fi). The litter input originated from the litterfall measurements for needles and branches (Ťupek et al., 2015; Liisa Ukonmaanaho, unpublished data), whereas stem, root and stump litter were modelled with data from Merilä et al. (2014) following Lehtonen et al. (2016). The spruce and pine needles were distributed in time (Figure S3). The annual litterfall of other components was equally distributed throughout the year (Figure S3). After trenching, we regarded fine and coarse tree roots as litterfall (Figure S3). The site-specific soil data required by CENTURY were available from Merilä et al. (2014).

2.7 | Model simulations

The Yasso07 and Yasso15 models are designed for simulations in annual time-steps. It is also possible to apply the model with a monthly time-step because of monthly timespans of litter-bag mass-loss measurements and calibration with global data, which account for considerable variation in climate. We ran the Yasso07 model using global parameters from Tuomi et al. (2009) and the Yasso15 model with parameters from Järvenpää et al. (2015) in annual and monthly time-steps. Running Yasso07 and Yasso15 in monthly time-steps (1/12 of yearly) required a transformation of monthly input data to representative 'annual' numbers. Monthly litter input and precipitation were multiplied by 12. The mean monthly air temperature was used directly without annual approximation. According to our tests of the feasibility of running the Yasso models in monthly time-steps, the predicted SOC and annual CO_2 respiration were not sensitive to the model time-step used.

We ran CENTURY using general parameters from the parameter file 'tree.100,' parameters of the site 'AND H_J_ANDREWS' for conifers and site 'CWT Coweeta' for deciduous trees (the file was available online at http://www.nrel.colostate.edu/projects/century/century-description.php from the model source code). The model accounted for topsoil N and plant litter C:N ratio, despite N being held constant during the simulations. The sensitivity of SOC stock to topsoil N and plant C:N ratio was weak compared to the sensitivity to litter input (Ťupek et al., 2016). We ran CENTURY simulations using two alternative temperature and moisture response functions for the rate of decomposition: Kelly et al. (2000) and Adair et al. (2008) (Table S2), later referred to as CENTURY.K and CENTURY.A, respectively. CENTURY estimated SOC and soil CO_2 emissions for the top 20 cm; thus to account for the deep soil carbon we increased the estimates by 40% following Jobbágy & Jackson (2000).

2.8 | Comparison of model outputs and measurements

To support the visual comparison of seasonal trends, we evaluated the performance of the models in predicting the annual and monthly soil heterotrophic respiration by linear regression statistics (slope, root mean square error and coefficient of determination) and Pearson correlation coefficient. The distributions of CO_2 values were near normal because of the seasonal character of the data. We assumed that monthly CO_2 values from separate sites were independent. In the comparison of annual SOC, we assumed uncertainty around the measured mean ± 12.8% (Häkkinen et al., 2011).

2.9 | Bayesian inference

To clarify whether the mismatch between the models' outputs and measurements originated from the formulation of temperature and moisture dependencies or their default parametrization, we constructed the empirical formulation of model matching (Equation 2). Each empirical model formulation consisted of the original temperature $f(T)$ and moisture $f(W)$ dependencies multiplied by the 'lumped' parameter of reference respiration R_{ref} (Equation 3):

$$\text{Empirical Model}_i = R_{ref} f(T) f(W), \quad (3)$$

where i represents the Yasso07, Yasso15, CENTURY.A and CENTURY.K models. The original temperature and moisture functions and their default parameters are in Tables S2 and S3. The prior values of R_{ref} were medians of monthly respiration (Table S3) estimated by each model in default settings for the model structure describing rates of decomposition for each pool, but with no climatic effect on rates of decomposition (Equation (S1) in File S1). In other words, for the R_{ref} simulations, the $\mathbf{A}(t)$ matrix describing carbon transfers and feedbacks between pools was set to default values, but the climatic effect on rates of decomposition $\xi(t)$ was equal to one. Prior and posterior change in the R_{ref} parameter accounted for changes in parametrization of the model structure separately from environmental functions.

For parametrization of the empirical models, we used measured soil respiration data, the general purpose Markov chain Monte Carlo (MCMC) sampler and Bayesian multimodel inference (Hartig et al., 2018). The median posterior parameters were used for simulations of the calibrated empirical models. The calibrated parameters of empirical models were intended only to estimate the best fit between Rh data and could not be applied to running full versions of the models. In empirical models the lumped parameter represented the base rate of carbon decomposition, which corresponds to respiration unaffected by environmental conditions in the original models. However, the calibrated lumped parameter does not apply to model runs with the original model's structure. We have not opted for calibrated equilibrium estimates of SOC, which would require full model calibrations. We compared the annual and seasonal trends of respiration simulated by calibrated empirical models with the same statistics for the models with default parameters. In addition, we also compared the models based on the deviance information criterion (DIC), which accounts for degrees of freedom by trying to estimate the effective number of parameters from MCMC outputs and is similar to Akaike's information criterion (AIC) (Spiegelhalter et al., 2002). We used R software for all data analyses (R core team, 2017).

3 | RESULTS

The predicted heterotrophic respiration (Rh) by Yasso07, Yasso15 and CENTURY identified the seasonal course of the observed Rh fluxes and environmental conditions (Figure 2, and Figures S2 and S3). As expected, the calibrated empirical models improved the absolute Rh values compared to the models with default parametrization. However, both default and calibrated empirical models showed a mismatch for Rh in both the summer and autumn.

3.1 | Models with default parametrization

The annual and monthly Rh values were, for models with default parameters, typically underestimated at all sites (Figures 2 and 3). The mean predicted annual Rh was on average 1.0 kg CO_2 m^{-2} $year^{-1}$; 44% only of the mean measured annual Rh (2.3 kg CO_2 m^{-2} $year^{-1}$) (Figure 3). The modelled monthly Rh accorded with the smallest but underestimated mean and the largest values.

The monthly predictions were correlated with the measured Rh (mean $r = 0.79$, $p < 0.001$). However, during the summer months the models failed to correlate significantly with the soil respiration measurements (Figure S2, Table S4). On average, the models underestimated observed summer Rh by 38% (Figure 3). Underestimation by the models with default settings clearly increased with temperature (Figure 4). The Yasso models showed a better fit to measurements and smaller residual error than the CENTURY models (Table S4). CENTURY simulations that used air temperature and precipitation as controlling factors (CENTURY.A) outperformed those that used air temperature and soil moisture (CENTURY.K) (Figures 2–4, and Table S4).

The equilibrium state forest SOCs estimated in the range from 7.0 to 11.6 kg C m^{-2} compared well to the measurements of Merilä et al. (2014), except for those at the Punkaharju pine site (Figure 2). At that site, all the models

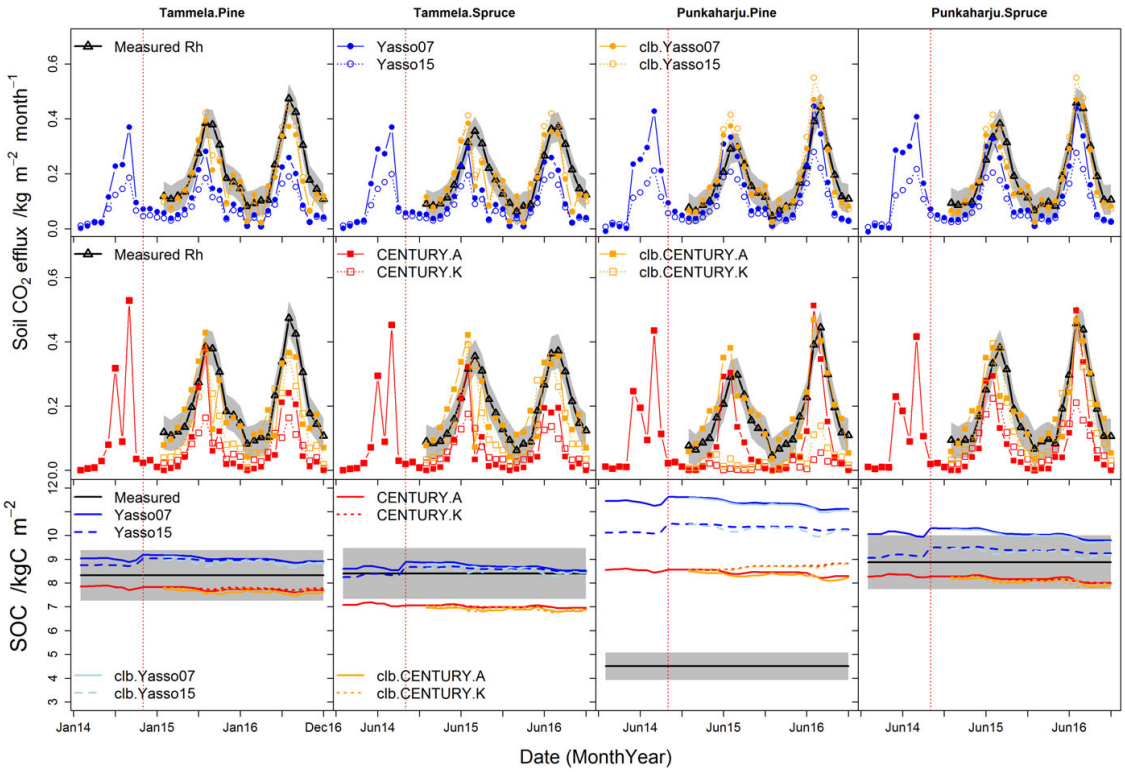

FIGURE 2 Simulated and measured monthly heterotrophic respiration (Rh, kg m^{-2} $month^{-1}$) for trenched plots from 2014 to 2016. Orange lines show Rh of calibrated empirical models. The lower panel shows simulated monthly soil organic carbon stocks, the effect of calibrated Rh on soil organic carbon (SOC) and the measured amount of SOC by Merilä et al. (2014). The grey shaded areas represent the uncertainty bounds of Rh and SOC stock measurements. The red dotted vertical line (October 2014) indicates the trenching date

estimated larger SOC stock (from 8.5 to 11.6 kg C m^{-2}) than that observed 4.5 kg C m^{-2}. The SOC stock of the Yasso models was within the error bounds of observations at three sites and that from CENTURY was in accord with the observations at two sites. The Yasso models showed more abrupt changes in SOC than CENTURY after trenching and the subsequent increase of the litter input from tree roots (Figure 2 and Figure S3). The small increase in CENTURY SOC at pine and not spruce sites before the trenching (Figure 2) was related to the different phenology of the foliar litterfall (pine maximum in the autumn and spruce maximum in the spring) (Figure S3).

3.2 | Calibrated empirical models

Mean posterior base respirations were twice as large for Yasso and four times larger for the CENTURY model (Table S3). The annual and monthly Rh of calibrated empirical models agreed well with measurements (Figures 2 and 3). However, autumn Rh was still underestimated by 26% on average (Figure 3, Table S4). Calibrated CENTURY.K Rh was especially underestimated at the Punkaharju pine site (Figure 3), the site with smaller amounts of soil water than the average for the others (Figure S2). The Rh residuals of calibrated empirical models did not show a clear relation with temperature (Figure 4). In relation to SWC, the calibrated empirical models slightly overestimated Rh values outside the moisture optimum (Figure 4). The Rh correlation statistics of calibrated empirical models favoured Yasso over CENTURY (Table S4). Model comparison by DIC also favoured the Yasso07 and Yasso15 models (−299 and −297, respectively) over CENTURY.A (−248) and CENTURY.K (338).

The empirical models comprising temperature and moisture functions and reference respiration showed almost identical Rh estimates to the soil carbon models with default parameters (Figure S4). The Rh estimates of empirical models in the climate space had a similar distribution to Rh for the NLS model based on observations (Figure S4). The models differed in their estimated Rh values and in their forms (e.g. whether they had or had not accounted for the reduction with moisture saturation). As expected, the

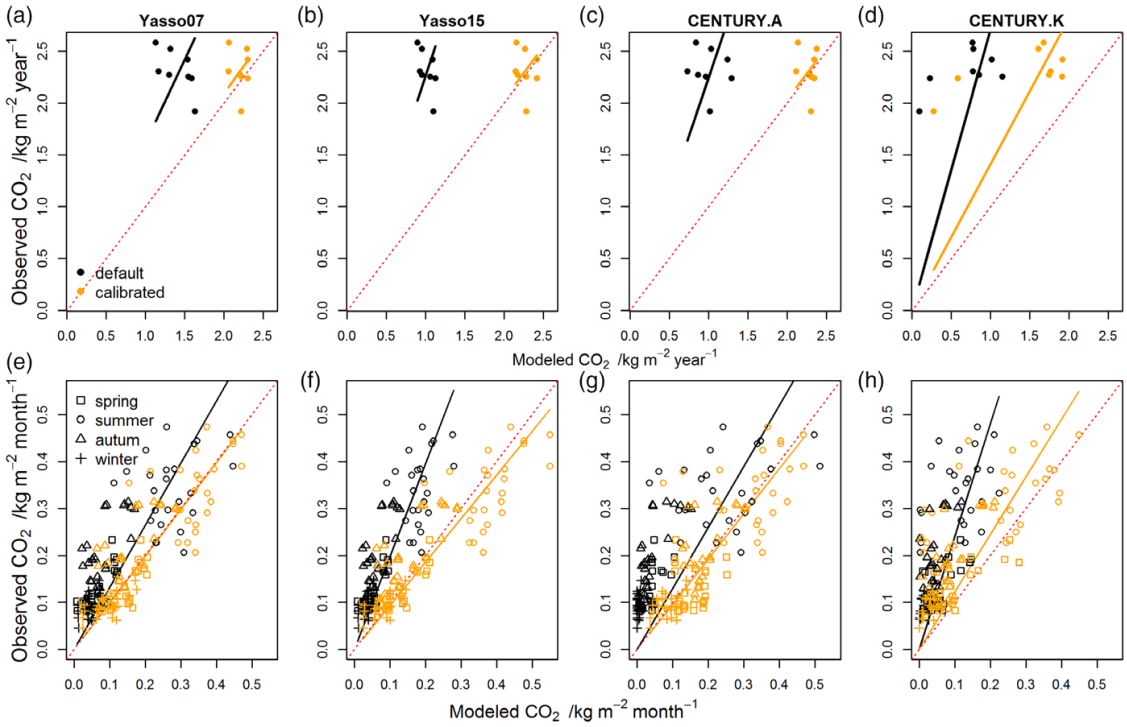

FIGURE 3 One-to-one plots between measured and modelled heterotrophic soil respiration (Rh, (a–d) kg CO_2 m^{-2} $year^{-1}$ and (e–h) kg m^{-2} $month^{-1}$). Orange points and trend lines correspond to calibrated empirical models. The annual and seasonal correlation statistics are in Table S2 in Supporting Information

recalibrated empirical models matched the distributions of the measured Rh data and of the NLS models (Figure S5). However, depending on a specific model's use of temperature and water functions, the Rh predictions showed little agreement outside the climate space of measured data (for air temperature over 20°C and for SWC over 45%) (Figure S5).

4 | DISCUSSION

We need to test process-based models with observations to increase our confidence in projected soil CO_2 emissions (Powlson, 1996). In this study, we evaluated measured SOC and heterotrophic respiration against estimates by the Yasso07, Yasso15 and CENTURY soil carbon models at monthly and annual intervals. The weak correlations between the measured and modelled CO_2 fluxes of Yasso07, Yasso15 and CENTURY soil carbon models (Figures 2 and 3) with their default parameters indicated a reduced ability to map the development of Rh according to the seasonal trends (weather and vegetation).

The models with default settings correlated with monthly Rh observations for the part of the year with lower temperatures, but there was no significant correlation for the summer months when soil moisture is likely to play its most important role. At the annual level, the models underestimated observed heterotrophic respiration by 43% on average. The diffence in Rh could be partly a result of parametric and structural uncertainty or errors in measured data (e.g. contributions of autotrophic respiration). In our study, forest floor vegetation was undisturbed; however, it contributed only slightly to the forest soil CO_2 observations (Kolari et al., 2009) and trenching excluded the main proportion of autotrophic respiration from the tree roots.

Bayesian calibration reduced the parameter uncertainty of all the models and greatly improved the fit for annual and monthly intervals (slopes close to 1). Temperature and water functions for Yasso and CENTURY models, as well as type and quality of input data, proved to be essential for the best fit. Regardless of whether temperature functions had or had not included the optimum and further decline of respiration, the calibrated empirical models slightly underestimated the observed data, mainly in autumn by 26% on average for all the models. This mismatch was probably related to water

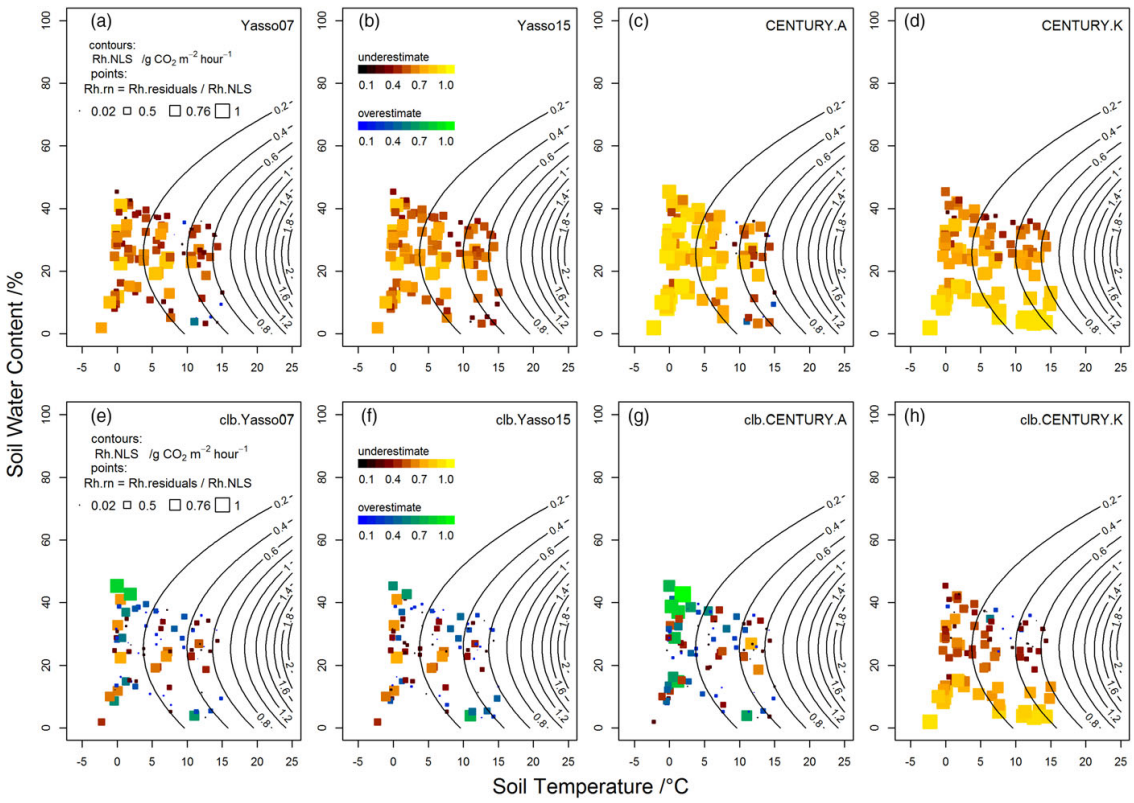

FIGURE 4 Normalized residuals (Rh.rn) between measured and modelled heterotrophic soil respiration (Rh, g CO_2 m^{-2} hr^{-1}) plotted in a climate space for soil carbon models. Contour lines show interpolated Rh.NLS (nonlinear least squares regression) values based on Equation (2) derived from Rh measurements. Note that Rh.residuals were normalized (Rh.rn) with Rh.NLS values. The Rh in panels (a–d) were modelled with default parameters and in panels (e–h) with calibrated empirical models

functions that did not acount for the reduction in Rh with large moisture content (unlike the moisture function fitted to measurements). In calibrated models the large change of prior and posterior parameters for base respiration suggested a strong influence of the model structure on the fit between measured and modelled soil respiration. However, the model structure represented the absolute difference in respiration rather than the difference in seasonal trend, which was reflected by the environmental functions.

Bayesian multi-model comparison by DIC identified Yasso models to be more plausible than CENTURY, probably because of fewer but more efficient parameters and smaller residual errors. Model ranking might have been different if SWC for CENTURY.K was generated with a water balance module. The CENTURY.K model using measured SWC data could have been biased at the Tammela pine forest because of exceptionally small SWC measurements compared to such data at the other sites.

Although the CENTURY.K model (Kelly et al., 2000) has double the number of parameters, it has temperature and water functions that are most similar to those used for interpolation of measurements (Davidson et al., 2012). When comparing CENTURY.K and CENTURY.A climate modifiers (DEFAC, a product of temperature and moisture modifiers) of Kelly et al. (2000) and Adair et al. (2008), CENTURY.K was more prone to reducing respiration under dry conditions. As a result, the climate modifier based on measured soil data overly limited potential decompositon and modelled Rh.

Differences in residuals and correlations between monthly predictions and observations, notably for spring and autumn respiration for the models, could be associated with differences in functional model formulation and or missing processes (Todd-Brown et al., 2013). Recent studies suggest that microbes represent a missing pathway in modelling soil carbon sequestration (Averill et al., 2014; Luo et al., 2016; Wieder et al., 2013). Increased root carbon

allocation associated with increased carbon exudates and root turnover favours microbial and fungal development (Kaiser et al., 2010). In late summer microbial activity could increase with reallocation of carbon storage to roots after the allocation of new photosynthetic carbon to foliage and stem growth ceases (Kuptz et al., 2011). We assumed that adding representation of seasonality, for example modifying the temperature response of decomposition by accounting for the time lag of temperature-related Rh diffusion from the deep soil, could improve estimates of late summer respiration. On the other hand, we suggest that the autumn mismatch between the calibrated empirical models and observations could also indicate changes in microbial growth efficiency (MGE) because of newly shed foliar litterfall. The MGE dependence on decomposition and SOC accumulation is missing in first-order substrate-decomposing models such as CENTURY or Yasso, but could be decisive for soil carbon loss in a warming climate (Wieder et al., 2013).

Differences between the estimated soil carbon stocks for the equilibrium state forest and the SOC measurements of Merilä et al. (2014) might originate not only from uncertainty in the models but also from the uncertainty in measurements. The Punkaharju pine forests are less productive than spruce forests and small SOC values might still have reflected extensive slash and burn cultivation in the 19th century. The similarity between modelled and measured SOC on spruce sites, and the more considerable difference in pine sites, might also result from differences in plant litter production, which is a predominant factor for the models. The essential role of plant nutrient status in SOC accumulation (Fernández-Martínez et al., 2014), but its underrepresentation in soil C models (Ťupek et al., 2016), could partly explain the difference in measured SOC. The pine forest sites differed in the C/N ratio of the mineral soil, and the soil in the Tammela Pine forest was more moist and fertile than that in the Punkaharju pine forest.

Although CENTURY accounted for site-specific differences in both litterfall and soil characteristics, CENTURY SOC showed little variation between the sites, which was comparable to the Yasso models that do not use specific soil information. These spatially unchanging amounts of SOC were consistent with testing of the CENTURY model with data from a Swedish forest soil inventory, where its SOC differed only for soils with large clay content (Ťupek et al., 2016).

Monthly SOC followed the seasonal patterns of litter input, temperature and precipitation in all models; however, the SOC values from individual models differed. On an annual timescale, Yasso07 stored slightly more carbon in the soil thanYasso15. Such a difference between the pools and fluxes could have resulted from more CO_2 emissions from the pool with a slower rate of turnover (Kuzyakov, 2011). The difference in SOC and heterotrophic respiration between the two CENTURY versions was caused by the temperature response formulation because the model structure remained the same otherwise. The exponential temperature function used by Kelly et al. (2000) resulted in smaller summer CO_2 emissions and larger SOC than that of the Gaussian function of Adair et al. (2008). Although CENTURY has been found to be sensitive to litter input from the fine roots (McCormack et al., 2015), its SOC did not increase abruptly after trenching. The difference in CENTURY SOC development after trenching was a result of more gradual litter transfer between the carbon pools than for the Yasso07 and Yasso15 models.

5 | CONCLUSIONS

Our research has shown that soil carbon models developed for changes in SOC estimates with their default parametrization could not reliably predict the seasonal and long-term pattern of heterotrophic respiration. Despite the correlation between the observed soil heterotrophic respiration (Rh) and the monthly Yasso and CENTURY Rh estimates, the predicted Rh accounted for only half of the measured annual respiration. A better fit between measured and modelled soil respiration was obtained by Bayesian parametrization of the empirical models (model's empirical climate modifiers of the reference respiration). Based on a smaller underestimate and smaller deviance information criterion, the Yasso-based climate modifier was more plausible than CENTURY at the forest sites considered in this study.

We found that similar differences between the models that run with default parameters persisted after calibration of the functions of the environmental rate modifiers. The Yasso models with simpler functions for environmental modifiers fitted respiration data better than the CENTURY model with more parameters in the modifiers. The change of prior and posterior parameters for base respiration also suggested that the model structure had a strong influence on the fit between measured and modelled soil respiration. For more detailed comparison of the model structure rather than the environmental modifiers, however, more base respiration data from low temperature conditions and calibration with full versions of the models would be necessary.

We demonstrated that soil CO_2 emissions estimated based on changes in SOC from the Yasso and CENTURY models in default settings might be underestimated in greenhouse gas reporting. In addition, we clarified how estimates of soil respiration differ between these models depending on the type and parameterization of the temperature and moisture functions used. The data mismatch after calibration indicated that further improvement in the representation of environmental functions and accounting for missing

processes (e. g. deep soil respiration, microbial controls) in the models is needed for accurate predictions of CO2 emissions under changing temperature and precipitation regimes of future climates.

ACKNOWLEDGEMENTS

This work was part of the project "Developing methods for GHG-inventory" funded by the Finnish Ministry of the Environment and the Ministry of Agriculture and Forestry. We acknowledge the following projects for support: Climforisk (LIFE09 ENV/FI/000571), FutMon programme (LIFE07 ENV/DE/000218), Finnish UN-ECE ICP Forests Level II monitoring program, particularly Liisa Ukonmaanaho for providing branch litter data, and Climoss (Academy of Finland no 296116). We thank our field team for collecting valuable data, Donald Smart for English language editing, and the reviewers and editors for valuable comments. We have no conflict of interest to declare.

ORCID

Boris Ťupek https://orcid.org/0000-0003-3466-0237
Aleksi Lehtonen https://orcid.org/0000-0003-1388-0388

REFERENCES

Adair, E. C., Parton, W. J., Del Grosso, S. J., Silver, W. L., Harmon, M. E., Hall, S. A., … Hart, S. C. (2008). Simple three-pool model accurately describes patterns of long-term litter decomposition in diverse climates. *Global Change Biology*, *14*, 2636–2660.

Averill, C., Turner, B. L., & Finzi, A. C. (2014). Mycorrhiza-mediated competition between plants and decomposers drives soil carbon storage. *Nature*, *505*, 543–545.

Crowther, T. W., Todd-Brown, K., Rowe, C., Wieder, W. R., Carey, J. C., Machmuller, M. B., … Allison, S. D. (2016). Quantifying global soil carbon losses in response to warming. *Nature*, *540*, 104–108.

Davidson, E. A., & Janssens, I. A. (2006). Temperature sensitivity of soil carbon decomposition and feedbacks to climate change. *Nature*, *440*, 165–173.

Davidson, E. A., Samanta, S., Caramori, S. S., & Savage, K. (2012). The Dual Arrhenius and Michaelis–Menten kinetics model for decomposition of soil organic matter at hourly to seasonal time scales. *Global Change Biology*, *18*, 371–384.

Delworth, T. L., Zeng, F., Vecchi, G. A., Yang, X., Zhang, L., & Zhang, R. (2016). The North Atlantic Oscillation as a driver of rapid climate change in the Northern Hemisphere. *Nature Geoscience*, *9*, 509–512.

Fernández-Martínez, M., Vicca, S., Janssens, I. A., & Campioli, M. (2014). Nutrient availability as the key regulator of global forest carbon balance. *Nature Climate Change*, *4*, 471–476.

Gaumont-Guay, D., Black, T. A., Griffis, T. J., Barr, A. G., Jassal, R. S., & Nesic, Z. (2006). Interpreting the dependence of soil respiration on soil temperature and water content in a boreal aspen stand. *Agricultural and Forest Meteorology*, *140*, 220–235.

Häkkinen, M., Heikkinen, J., & Mäkipää, R. (2011). Soil carbon stock increases in the organic layer of boreal middle-aged stands. *Biogeosciences*, *8*, 1279–1289.

Hartig, F., Minunno, F., & Paul, S. (2018). *BayesianTools: General-Purpose MCMC and SMC Samplers and Tools for Bayesian Statistics.* R package version 0.1.6. Retrieved from https://cran.r-project.org/web/packages/BayesianTools/BayesianTools.pdf

Hashimoto, S., Nanko, K., Ťupek, B., & Lehtonen, A. (2017). Data-mining analysis of the global distribution of soil carbon in observational databases and Earth system models. *Geoscientific Model Development*, *10*, 1321–1337.

Järvenpää, M., Repo, A., Akujärvi, A., Kaasalainen, M., & Liski, J. (2015). *Bayesian calibration of Yasso15 soil carbon model using global-scale litter decomposition and carbon stock measurements.* Oral presentation at the 5th Nordic–Baltic Biometric Conference, Reykjavik, June 8–10 2015. Retrieved from http://math.tut.fi/inversegroup/material/jarvenpaa2015bayesian.pdf

Jobbágy, E. G., & Jackson, R. B. (2000). The vertical distribution of soil organic carbon and its relation to climate and vegetation. *Ecological Applications*, *10*, 423–436.

Jurasinski, G., Koebsch, F., Guenther, A., & Beetz, S. (2014). *R Package "flux". Flux Rate Calculation from Dynamic Closed Chamber Measurement.* Retrieved from https://cran.r-project.org/web/packages/flux/flux.pdf

Kaiser, C., Koranda, M., Kitzler, B., Fuchslueger, L., Schnecker, J., Schweiger, P., … Richter, A. (2010). Belowground carbon allocation by trees drives seasonal patterns of extracellular enzyme activities by altering microbial community composition in a beech forest soil. *New Phytologist*, *187*, 843–858.

Kelly, R. H., Parton, W. J., Hartman, M. D., Stretch, L. K., Ojima, D. S., & Schimel, D. S. (2000). Intra-annual and interannual variability of ecosystem processes in shortgrass steppe. *Journal of Geophysical Research*, *105*, 20093–20100.

Kirschbaum, M. U. (2000). Will changes in soil organic carbon act as a positive or negative feedback on global warming? *Biogeochemistry*, *48*, 21–51.

Kolari, P., Kulmala, L., Pumpanen, J., Launiainen, S., Ilvesniemi, H., Han, P., & Nikinmaa, E. (2009). CO_2 exchange and component CO_2 fluxes of a boreal Scots pine forest. *Boreal Environment Research*, *14*, 761–783.

Kuptz, D., Fleischmann, F., Matyssek, R., & Grams, T. E. (2011). Seasonal patterns of carbon allocation to respiratory pools in 60-yr-old deciduous (*Fagus sylvatica*) and evergreen (*Picea abies*) trees assessed via whole-tree stable carbon isotope labeling. *New Phytologist*, *191*, 160–172.

Kuzyakov, Y. (2011). How to link soil C pools with CO_2 fluxes? *Biogeosciences*, *8*, 1523–1537.

Lal, R. (2009). Challenges and opportunities in soil organic matter research. *European Journal of Soil Science*, *60*, 158–169.

Lehtonen, A., & Heikkinen, J. (2015). Uncertainty of upland soil carbon sink estimate for Finland. *Canadian Journal of Forest Research*, *46*, 310–322.

Lehtonen, A., Linkosalo, T., Peltoniemi, M., Sievänen, R., Mäkipää, R., Tamminen, P., … Heikkinen, J. (2016). Forest soil carbon stock estimates in a nationwide inventory: Evaluating performance of the ROMULv and Yasso07 models in Finland. *Geoscientific Model Development*, *9*, 4169–4183.

Luo, Y., Ahlström, A., Allison, S. D., Batjes, N. H., Brovkin, V., Carvalhais, N., … Finzi, A. (2016). Toward more realistic projections of soil carbon dynamics by Earth system models. *Global Biogeochemical Cycles*, *30*, 40–56.

McCormack, M. L., Crisfield, E., Raczka, B., Schnekenburger, F., Eissenstat, D. M., & Smithwick, E. A. (2015). Sensitivity of four ecological models to adjustments in fine root turnover rate. *Ecological Modelling*, *297*, 107–117.

Merilä, P., Mustajärvi, K., Helmisaari, H., Hilli, S., Lindroos, A.-J., Nieminen, T. M., … Ukonmaanaho, L. (2014). Above-and belowground N stocks in coniferous boreal forests in Finland: Implications for sustainability of more intensive biomass utilization. *Forest Ecology and Management*, *311*, 17–28.

Nalder, I. A., & Wein, R. W. (2006). A model for the investigation of long-term carbon dynamics in boreal forests of western Canada: I. Model development and validation. *Ecological Modelling*, *192*, 37–66.

Parton, W. J., Schimel, D. S., Ojima, D. S., & Cole, C. V. (1994). A general model for soil organic matter dynamics: Sensitivity to litter chemistry, texture and management. In R. B. Bryant & R. W. Arnold (Eds.), *Quantitative modeling of soil forming processes* (pp. 147–167. SSSA Special Publication 39). Madison, WI: ASA, CSSA, and SSA.

Powlson, D. S. (1996). Why evaluate soil organic matter models? In D. S. Powlson, P. Smith, & J. U. Smith (Eds.), *Evaluation of soil organic matter models* (pp. 3–11). Berlin, Heidelberg, Germany: Springer–Verlag.

R Core Team. (2017). *R: A language and environment for statistical computing*. Vienna, Austria: R Foundation for Statistical Computing. Retrieved from https://www.R-project.org/

Schmidt, M. W. I., Torn, M. S., Abiven, S., Dittmar, T., Guggenberger, G., Janssens, I. A., … Trumbore, S. E. (2011). Persistence of soil organic matter as an ecosystem property. *Nature*, *478*, 49–56.

Sierra, C. A., Trumbore, S. E., Davidson, E. A., Vicca, S., & Janssens, I. (2015). Sensitivity of decomposition rates of soil organic matter with respect to simultaneous changes in temperature and moisture. *Journal of Advances in Modeling Earth Systems*, *7*, 335–356.

Smith, P. (2005). An overview of the permanence of soil organic carbon stocks: Influence of direct human-induced, indirect and natural effects. *European Journal of Soil Science*, *56*, 673–680.

Spiegelhalter, D. J., Best, N. G., Carlin, B. P., & van der Linde, A. (2002). Bayesian measures of model complexity and fit. *Journal of the Royal Statistical Society: Series B*, *64*, 583–639.

Thum, T., Räisänen, P., Sevanto, S., Tuomi, M., Reick, C., Vesala, T., … Altimir, N. (2011). Soil carbon model alternatives for ECHAM5/JSBACH climate model: Evaluation and impacts on global carbon cycle estimates. *Journal of Geophysical Research: Biogeosciences*, *116*, G02028. https://doi.org/10.1029/2010JG001612

Todd-Brown, K., Randerson, J. T., Post, W. M., Hoffman, F. M., Tarnocai, C., Schuur, E. A. G., & Allison, S. D. (2013). Causes of variation in soil carbon simulations from CMIP5 Earth system models and comparison with observations. *Biogeosciences*, *10*, 1717–1736.

Tuomi, M., Thum, T., Järvinen, H., Fronzek, S., Berg, B., Harmon, M., … Liski, J. (2009). Leaf litter decomposition—Estimates of global variability based on Yasso07 model. *Ecological Modelling*, *220*, 3362–3371.

Ťupek, B., Mäkipää, R., Heikkinen, J., Peltoniemi, M., Ukonmaanaho, L., Hokkanen, T., … Lehtonen, A. (2015). Foliar turnover rates in Finland–comparing estimates from needle-cohort and litterfall-biomass methods. *Boreal Environment Research*, *20*, 283–304.

Ťupek, B., Ortiz, C. A., Hashimoto, S., Stendahl, J., Dahlgren, J., Karltun, E., & Lehtonen, A. (2016). Underestimation of boreal soil carbon stocks by mathematical soil carbon models linked to soil nutrient status. *Biogeosciences*, *13*, 4439–4459.

Van Gestel, N., Shi, Z., Van Groenigen, K. J., Osenberg, C. W., Andresen, L. C., Dukes, J. S., … Reich, P. B. (2018). Predicting soil carbon loss with warming. *Nature*, *554*, E4–E5. https://doi.org/10.1038/nature25745

Wieder, W. R., Bonan, G. B., & Allison, S. D. (2013). Global soil carbon projections are improved by modelling microbial processes. *Nature Climate Change*, *3*, 909–912.

SUPPORTING INFORMATION

Additional supporting information may be found online in the Supporting Information section at the end of this article.

How to cite this article: Ťupek B, Launiainen S, Peltoniemi M, et al. Evaluating CENTURY and Yasso soil carbon models for CO_2 emissions and organic carbon stocks of boreal forest soil with Bayesian multi-model inference. *Eur J Soil Sci*. 2019; 1–12. https://doi.org/10.1111/ejss.12805

IV

Biogeosciences, 13, 4439–4459, 2016
www.biogeosciences.net/13/4439/2016/
doi:10.5194/bg-13-4439-2016
© Author(s) 2016. CC Attribution 3.0 License.

Biogeosciences Open Access EGU

Underestimation of boreal soil carbon stocks by mathematical soil carbon models linked to soil nutrient status

Boris Ťupek[1], Carina A. Ortiz[2], Shoji Hashimoto[3], Johan Stendahl[2], Jonas Dahlgren[4], Erik Karltun[2], and Aleksi Lehtonen[1]

[1]Natural Resources Institute Finland, P.O. Box 18, 01301 Vantaa, Finland
[2]Swedish University of Agricultural Sciences, P.O. Box 7014, 75007 Uppsala, Sweden
[3]Forestry and Forest Products Research Institute, Tsukuba, Ibaraki 305-8687, Japan
[4]Swedish University of Agricultural Sciences, Skogsmarksgränd, 90183 Umeå, Sweden

Correspondence to: Boris Ťupek (boris.tupek@luke.fi), Aleksi Lehtonen (aleksi.lehtonen@luke.fi)

Received: 21 December 2015 – Published in Biogeosciences Discuss.: 18 January 2016
Revised: 6 July 2016 – Accepted: 7 July 2016 – Published: 10 August 2016

Abstract. Inaccurate estimate of the largest terrestrial carbon pool, soil organic carbon (SOC) stock, is the major source of uncertainty in simulating feedback of climate warming on ecosystem–atmosphere carbon dioxide exchange by process-based ecosystem and soil carbon models. Although the models need to simplify complex environmental processes of soil carbon sequestration, in a large mosaic of environments a missing key driver could lead to a modeling bias in predictions of SOC stock change.

We aimed to evaluate SOC stock estimates of process-based models (Yasso07, Q, and CENTURY soil sub-model v4) against a massive Swedish forest soil inventory data set (3230 samples) organized by a recursive partitioning method into distinct soil groups with underlying SOC stock development linked to physicochemical conditions.

For two-thirds of measurements all models predicted accurate SOC stock levels regardless of the detail of input data, e.g., whether they ignored or included soil properties. However, in fertile sites with high N deposition, high cation exchange capacity, or moderately increased soil water content, Yasso07 and Q models underestimated SOC stocks. In comparison to Yasso07 and Q, accounting for the site-specific soil characteristics (e. g. clay content and topsoil mineral N) by CENTURY improved SOC stock estimates for sites with high clay content, but not for sites with high N deposition.

Our analysis suggested that the soils with poorly predicted SOC stocks, as characterized by the high nutrient status and well-sorted parent material, indeed have had other predominant drivers of SOC stabilization lacking in the models, presumably the mycorrhizal organic uptake and organo-mineral stabilization processes. Our results imply that the role of soil nutrient status as regulator of organic matter mineralization has to be re-evaluated, since correct SOC stocks are decisive for predicting future SOC change and soil CO_2 efflux.

1 Introduction

In spite of the historical net carbon sink of boreal soils, 500 Pg of carbon since the last ice age (Rapalee et al., 1998; DeLuca and Boisvenue, 2012; Scharlemann et al., 2014), boreal soils could become a net source of carbon dioxide to the atmosphere as a result of long-term climate warming (Kirschbaum, 2000; Amundson, 2001). They have the potential to release larger quantities of carbon than all anthropogenic carbon emissions combined (337 Pg; Boden et al., 2010). In order to preserve the soil carbon pool and to utilize the soil carbon sequestration potential to mitigate anthropogenic CO_2 emissions, mitigation strategies of climate forcing aim to improve soil organic matter management (Schlesinger, 1999; Smith, 2005; Wiesmeier et al., 2014).

Supporting soil management decisions requires an accurate quantification of spatially variable soil organic carbon (SOC) stock and SOC stock changes (Scharlemann et al., 2014). The initial level of SOC stock is essential in order to estimate SOC stock changes (Palosuo et al., 2012; Todd-Brown et al., 2014), especially when estimating carbon emissions due to land-use change, e.g., afforestation of grass-

lands (Berthrong et al., 2009). Process-oriented soil carbon models like CENTURY, Roth-C, Biome-BCG, ORCHIDEE, JSBACH, ROMUL, Yasso07, and Q are important tools for predicting SOC stock change, but there are also risks for poor predictions (Todd-Brown et al., 2013; DeLuca and Boisvenue, 2012). The models need further validation and improvement as they show poor spatial agreement on fine scale and moderate agreement on regional scale against SOC stock data (Todd-Brown et al., 2013; Ortiz et al., 2013). Despite the potentially quantitative importance of CO_2 emissions the expected change will be small in relation to the SOC stock. Therefore, the uncertainty of measurements and/or model estimates could prevent conclusions on SOC stock changes (Palosuo et al., 2012; Ortiz et al., 2013; Lehtonen and Heikkinen, 2015) especially for the soils with the largest SOC stocks, which are the most sensitive to carbon loss. Beside large uncertainties, the poor agreement between the modeled and measured SOC stocks (Todd-Brown et al., 2013) could also indicate missing biotic or abiotic drivers of long-term carbon storage (Schmidt et al., 2011; Averill et al., 2014).

For example, ignoring the essential role of soil nutrient availability in ecosystem carbon use efficiency (Fernández-Martínez et al., 2014) could lead to missing important controls of plant litter production and soil organic matter stabilization mechanisms. Soil nutrient status is linked to the mobility of nutrients in the water solution (Husson et al., 2013), production, quality and microbial decomposition of plant litter (Orwin et al., 2011), and formation of the soil organic matter (SOM). The SOM affects soil nutrient status by recycling of macronutrients (Husson et al., 2013), and water retention and water availability (Rawls et al., 2003).

In spite of state of the art soil carbon modeling based on the amount and quality of plant litter "recalcitrance", affected by climate and/or soil properties as in the Yasso07, Q, and CENTURY models, these types of process-based models do not include mechanisms for SOM stabilization by (a) the organic nutrient uptake by mycorrhizal fungi; (b) humic organic carbon interactions with silt-clay minerals; and (c) the inaccessibility of deep soil carbon and carbon in soil aggregates to soil biota (Orwin et al., 211; Sollins et al., 1996; Torn et al., 1997; Six et al., 2002; Fan et al., 2008; Dungait et al., 2012; Clemente et al., 2011). Although the models do not contain aforementioned mechanisms and controls for changes in SOM stabilization processes, they have been parameterized using a wide variety of data sets and can treat soil biotic, physicochemical, and environmental changes implicitly. The Yasso07 model (Tuomi et al., 2009, 2011) is an advanced forest soil carbon model and it is used for Kyoto protocol reporting of changes in soil carbon amounts for the United Nations Framework Convention on Climate Change (UNFCCC) by European countries, e.g., Austria, Finland, Norway, and Switzerland. The Q model (Ågren et al., 2007) is a mechanistic litter decomposition model developed in Sweden and used, e.g., to compare results produced with Swedish national inventory data (Stendahl et al., 2010; Ortiz et al., 2011) and also with other models at national or global scales (Ortiz et al., 2013; Yurova et al., 2010). The CENTURY model (Parton et al., 1987, 1994; Adair et al., 2008) is one of the most widely applied models and it is used for soil carbon reporting to the UNFCCC by Canada, Japan, and USA. Although individual parameters and functions vary, mathematical models such as Yasso07, Q, and CENTURY have similar structures. For example, these models are driven by the decomposition rates of litter input and SOM. Decomposing litter and SOM is divided into pools based on litter quality, and its transfer from one pool to another is, apart from model functions and parameters, affected by temperature (Q), and/or water (Yasso07), and/or soil texture and structure (CENTURY). The Q model does not include explicit moisture functions, whereas precipitation affects decomposition for the Yasso07 and CENTURY models (Tuomi et al., 2009; Adair et al., 2008). On the other hand, the models do not explicitly or by default include mechanisms that reduce decomposition by excessive precipitation/moisture (Falloon et al., 2011).

We hypothesized that (1) soil carbon estimates of the Yasso07, Q, and CENTURY models would deviate for soils where SOC stabilization processes not implicitly accounted by the models are predominant, (2) the Yasso07 and Q models ignoring soil properties would fail on the nutrient-rich sites of the southwestern coast of Sweden and on occasionally paludified clay and silt soils, and (3) the CENTURY model outperforms the Yasso07 and Q models due to fact that it includes soil properties as input variables.

We grouped Swedish forest soil inventory data into homogenous groups with specific soil physicochemical conditions using a regression tree and recursive partitioning modeling methods. After that we ran the models until they reached an equilibrium with a litter input that was derived from the Swedish forest inventory. Thereafter, we compared the model estimates against data by groups that were obtained from the regression tree model. In discussion we address the reasons why the models deviate and indicate directions of further improvements.

2 Material and methods

2.1 Measurements

We analyzed data from the Swedish forest soil inventory (SFSI), which is a stratified national grid survey of vegetation and physicochemical properties of soils (SLU, 2011; Olsson et al., 2009). The soil data distinguished between the organic, B (0–5 cm of B horizon), BC (45–55 cm below ground surface), and C (55–65 cm from the top of the mineral soil) horizons (Olsson et al., 2009). All analysis was done using R software for statistical computing and graphics (R Core Team, 2014). The soil data were identical to a data set used in Stendahl et al. (2010). We restricted our sample plots

Table 1. Description of the Swedish Forest Soil Inventory (SFSI) data reduction of soil sorting of parent material and humus types; SFSI conversion estimate of soil classes of soil moisture to numerical representation of soil water content; and SFSI conversion estimate of classes to numerical representation of soil texture (sand, silt, and clay content for sediments by Lindén (2002) and for tills by Albert Atterberg's distribution of the different grain size fractions).

Sorting parent material		Humus type		Moisture		
SFSI	Reduced	SFSI	Reduced	SFSI	SFSI	Numeric
Bedrock	Bedrock	Moder	No-peat		Water	Long-term
Poorly sorted sediments	Unsorted	Mor 1	No-peat		level (m)	moisture %
Tills	Unsorted	Mor 2	No-peat	Dry	< 2	10
Well-sorted sediments	Sorted	Mull	No-peat	Fresh	1–2	20
		Mull-Moder	Peat	Fresh-moist	< 1	30
		Peat	Peat	Moist	< 0.5	50
		Peat-Mor	Peat			
Texture						
SFSI	Numeric Sediments			Tills		
	Sand %	Silt %	Clay %	Sand %	Silt %	Clay %
Bedrock	0	0	0	0	0	0
Boulder	0	0	0	0	0	0
Gravel	10	0	0	10	0	0
Coarse sand	40	5	0	40	5	0
Sand	80	10	0	45	10	0
Fine sand	70	25	5	55	15	0
Coarse silt	50	40	10	65	20	5
Fine silt	10	75	15	55	35	10
Clay	0	65	35	0	85	15
Peat	0	0	0	0	0	0

to minerogenic soils since the Q, Yasso07, and CENTURY models were not developed for use on peat soils, and only to plots for forest land use with Swedish forest inventory data (SFI). We also excluded samples with total SOC stock below 2.8 and above 470.5 ($tC\,ha^{-1}$), i.e., samples with SOC stock below 0.01 and above 99.9 percentile. Measurement data originated from 1993 to 2002, which constitute a full inventory, and from 2020 sample plots located around Sweden, and in total it included 3230 samples. For each sample plot the weather (years 1961–2011) and N deposition (years 1999–2001) data were retrieved from the nearest stations of Swedish Meteorological and Hydrological Institute (SMHI) network (Fig. 1). The plots, which were linked by the closest distance to the given weather station had the same weather and N deposition data, and the number of soil samples per station ranged between 10 and 70. The mean total SOC stock of samples corresponding to weather stations ranged from 40 to 200 ($tC\,ha^{-1}$), and the SOC stock level decreased from southern to northern Sweden (Fig. 1).

Each sample plot contained categorical data from the field survey on the sorting of soil parent material, humus type, soil texture, and soil moisture. In our analysis we reduced categorical classes by basing them on the sorting of soil parent material and humus type (Table 1). We determined numeric values for silt, clay, and sand content from soil texture categories by Albert Atterberg's distribution of the different grain size fractions in tills and distributions for sediments by Lindén (2002) (Table 1). We also determined numeric values of volumetric soil water content (SWC) from categorical field data classified according to the depth of the ground water level (WL; Table 1).

As is typical for soil carbon inventories, the variation of data was large (Table 2). For example, the mean total SOC stock of all samples was 93 ($tC\,ha^{-1}$) while 1st and 99th percentiles were 17 and 309 (Table 2). The mean SOC stock was 33.3 and 66.8 ($tC\,ha^{-1}$) for the humus horizon and the mineral soil. The mean values of cation exchange capacity (CEC) (23.9 $mmol_c\,kg^{-1}$), the base saturation (36.4 %), and the C / N ratio (16.5) indicated conditions of medium fertility, although the soils were mostly acidic (mean pH was 5.2). The mean prevailing soil water content (22.3) was typical for the well-drained forest soils. The mean annual temperatures ranged from below 0 to above 8 °C, and annual precipitation varied between 392 and 1154 mm (Table 2). Total SOC stock for all the samples generally increased for peat and peat like humus forms, for well-sorted sediments, for soils with high fraction of silt and clay and with increasing soil moisture (Fig. S1 in the Supplement).

Table 2. Descriptive characteristics (mean, confidence interval, 1st, 50th, and 99th percentile) of selected variables ($n = 3230$ samples). The values of the bulk density, cation exchange capacity, base saturation, C / N ratio, and pH are shown only for BC soil horizon (fixed 45–50 cm depth below the ground surface) due to the strong correlation to the total soil carbon stock. The soil was cut off at 1 m. The site productivity index (H100, m) is an approximation of the site fertility expressed as the height of trees at 100 years of age. Stand and understory biomass, and litter input are modeled values for approximated equilibrium conditions based on observations.

	Mean	CI	1st percentile	50th percentile	99th percentile
Total soil carbon stock ($tC\,ha^{-1}$)	93.24	1.95	17.02	79.68	308.68
Humus carbon stock ($tC\,ha^{-1}$)	33.29	1.17	3.89	22.82	176.66
Mineral soil carbon stock ($tC\,ha^{-1}$)	66.82	1.7	6.92	54.81	273.91
Depth of humus (cm)	10.52	0.27	1	8	36
Depth of soil (cm)	93.37	0.6	18	99	99
Stoniness (%)	39.91	0.54	3.96	42.37	65.05
Bulk density of BC ($g\,dm^{-3}$)	1267.1	5.5	790.55	1294.9	1522.13
Cation exchange capacity of BC ($mmol_c\,kg^{-1}$)	23.94	1.28	1.53	12.33	203.25
Base saturation of BC (%)	36.44	1.02	4.33	25.73	100
C / N ratio of BC	16.5	0.35	3.33	14.98	62.45
pH of BC	5.17	0.02	4.36	5.08	7.26
Silt content (%)	19.98	0.57	0	15	85
Clay content (%)	3.16	0.25	0	0	35
Sand content (%)	51.25	0.63	0	55	80
Long-term soil moisture (%)	22.36	0.2	10	20	30
Mean air temperature (°C)	4.63	0.09	−0.44	5.34	8.47
Total precipitation (mm)	697.87	7.13	392.54	637.11	1154.55
Nitrogen deposition ($kgN\,ha^{-1}\,y^{-1}$)	7.17	0.14	2.35	6.56	17.67
Productivity class (H100, m)	23.61	0.21	12	23	36
Total stand biomass ($tC\,ha^{-1}$)	56.02	1.39	1.34	51.14	156.52
Total understory biomass ($tC\,ha^{-1}$)	2.69	0.05	0.96	2.37	6.02
Total litterfall input ($tC\,ha^{-1}$)	3.17	0.03	1.65	3.07	5.28

2.1.1 Biomass and litterfall estimates

For the biomass and litterfall estimation we adopted a standard method of national greenhouse gas inventories for estimating soil carbon stock changes (Statistics Finland, 2013). In order to model SOC stocks of forest in equilibrium (not SOC stocks changes), we modified the method by estimating the long-term litterfall of forest in equilibrium. Forest stand biomass was estimated by allometric biomass functions for stem with bark, branch, foliage, stump, coarse roots and fine roots applied to basic tree dimensions (breast height diameter, total height of tree, number of trees) of SFI stands (Marklund, 1988; Pettersson and Ståhl, 2006; Repola, 2008; Lehtonen et al., 2016a). In order to simulate "equilibrium" soil carbon stock, we estimated long-term mean forest biomass, referred to as "equilibrium forest" below.

We adopted an observed fraction of photosynthetically active absorbed radiation (f_{APAR}; Fig. A1 in Appendix A) as a relative indicator of a site's capacity to produce biomass (minimum is 0, maximum is 1) by accounting for the forest stand structure, ranging from the absent stand $f_{\mathrm{APAR}} = 0$ to the closed canopy stand $f_{\mathrm{APAR}} = 1$, through its major role on limiting of the potential gross primary production (Peltoniemi et al., 2015). The f_{APAR} was calculated based on SFI measurements of basic tree dimensions as in Härkönen et al. (2010) and for the main tree species (pine, spruce, deciduous) it was well correlated with the stand basal area (Appendix A).

The equilibrium forest f_{APAR} values were assumed to be in a range between the median and the maximum fraction of the observed state forest f_{APAR} for a given species, latitudinal degree, and site productivity index (Appendix A). We selected equilibrium f_{APAR} as the 70th percentile (f_{APAR70}) out of a range from the 50th to 95th, because the modeled soil carbon distributions with a litter input from the f_{APAR70} biomass agreed best with the measured soil carbon distributions (Fig. S2). The f_{APAR70} was the estimated 70th percentile of the observed fraction of absorbed radiation specific for a given species, latitudinal degree, and site productivity index H100 (height of trees at 100 years of age; m; Fig. B1 in Appendix B). The site index H100, that can be translated to a specific productivity ($m^3\,ha^{-1}\,yr^{-1}$), was for Swedish forest inventory plots determined based on height development curves and observed site properties by using the methodology of Hagglund and Lundmark (1977) (Swedish Statistical Yearbook of Forestry, 2014). Instead of modeling of equilibrium biomasses for every tree stand component separately for the species, latitude, and site productivity index, we simplified the biomass modeling first by estimating only equilib-

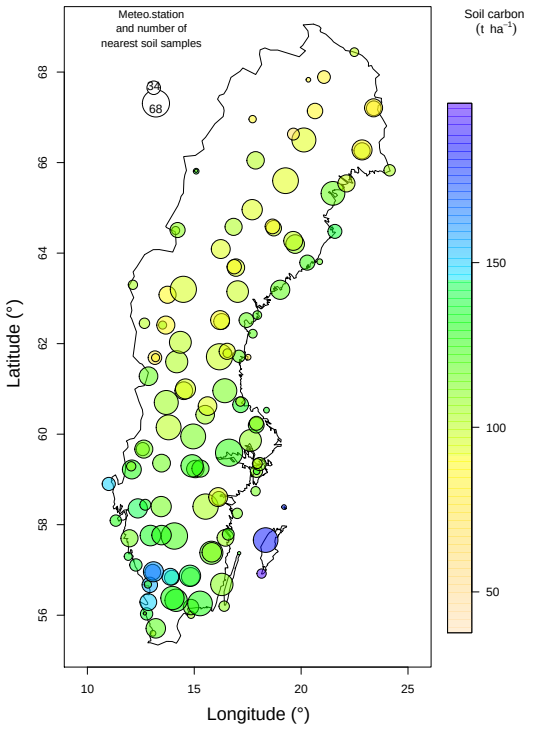

Figure 1. Geographical locations of meteorological stations with corresponding number of nearest soil samples (n, size of the circle) and their mean measured soil organic carbon stock (tC ha^{-1}, color of the circle) across Sweden.

rium forest stand structure for the species, latitude, and productivity (f_{APAR70}, Table A1 in Appendix A) and secondly by using f_{APAR70} with f_{APAR} biomass models (Table B1 in Appendix B) to estimate the biomass components.

We modeled the equilibrium biomass by applying the fitted exponential functions between the observed state forest biomass components (stem, branch, foliage, stump, coarse roots, fine roots, estimated by tree stand measurements and the allometric biomass functions) and the observed fraction of absorbed radiation (f_{APAR}; Appendix B) to the estimated f_{APAR70} of the equilibrium forest. The understory vegetation of the equilibrium forest was estimated by applying our ground vegetation models (Appendix C) to the modeled equilibrium forest characteristics, and plot-specific environmental conditions.

In order to derive the litter inputs, the annual turnover rate (TR), the fraction of living biomass that is shed onto the ground per year of biomass components, was applied to the modeled biomass components of the equilibrium forest. The needle litter TR was a linear function of latitude for pine and spruce and a constant for deciduous species (Ågren et al., 2007). The TR of branches and roots were from Mukkonen and Lehtonen (2004) and Lehtonen et al. (2004) and the TR of stump and stem were from Viro (1955), Mälkönen (1974, 1977) and Liski et al. (2006). For tree fine roots, we assumed there was a difference between tree species and between southern and northern Sweden. For pine, spruce, and birch the TR fine roots were 0.811, 0.868, and 1.0, respectively, as reported by Maidi (2001), Kurz et al. (1996), and Liski et al. (2006). Kleja et al. (2008) and Leppälampi-Kujansuu et al. (2014) reported different fine-root TR for southern (1 and 0.83) and northern Finland (0.5). We interpolated TR according to the mean annual temperature gradient between TR of fine roots in the south and the north. The fine-roots TR of 0.811, 0.868, and 1.0 in the warmest southernmost soil plots were thus reduced down to 0.5 in the coldest northernmost soil plots. The understory TR was applied as in Lehtonen et al. (2016b).

The major part of the litter input originated from the tree stand biomass components, which were modeled by the nonlinear functions with R^2 values close to 0.9 (Fig. B1, Tables A1 in Appendix A, and B1 in Appendix B). The linear understory vegetation models had low R^2 values (Table C1 in Appendix C). However, when the understory models (Appendix C) were applied only to plots close to equilibrium forest, as in our application, the R^2 values of predicted and observed understory components were larger (Fig. S9). In comparison to major understory litterfall originating from reasonably well-predicted dwarf shrubs and mosses (Figs. S9 and S10), the influence of poorer understory models (for herbs, grass, and lichens) was small on predictions of the understory litter and marginal on predictions of the total forest litterfall (Fig. S10). The main improvement on the accuracy of total litter input was achieved by avoiding the confounding effect of management on observed forest state by modeling the biomass/litterfall estimates representing the mean long-term conditions (defined by estimated equilibrium f_{APAR70}) for small regions (defined by degree of latitude and productivity index for dominant species; Fig. A1 in Appendix A). Thus the estimates accurately reflected the long-term spatial variability in dominant species, nutrient status and climate (Fig. S11) and lacked higher spatial and temporal precision; as attempts for high precision of the estimates applied for the period of the last few thousand years would be uncertain due to high variation of factors affecting plot history.

2.1.2 Correlation analysis

Overall our data consist of 3230 soil samples and their carbon stocks linked to soil physicochemical variables, stand and ground vegetation biomass and litterfall components, and nearest weather station environmental variables. We performed the Spearman's rank correlation analysis between the total soil carbon stock and the other soil variables, site, climate, and vegetation characteristics. As expected the total soil carbon stock most strongly correlated with the measured

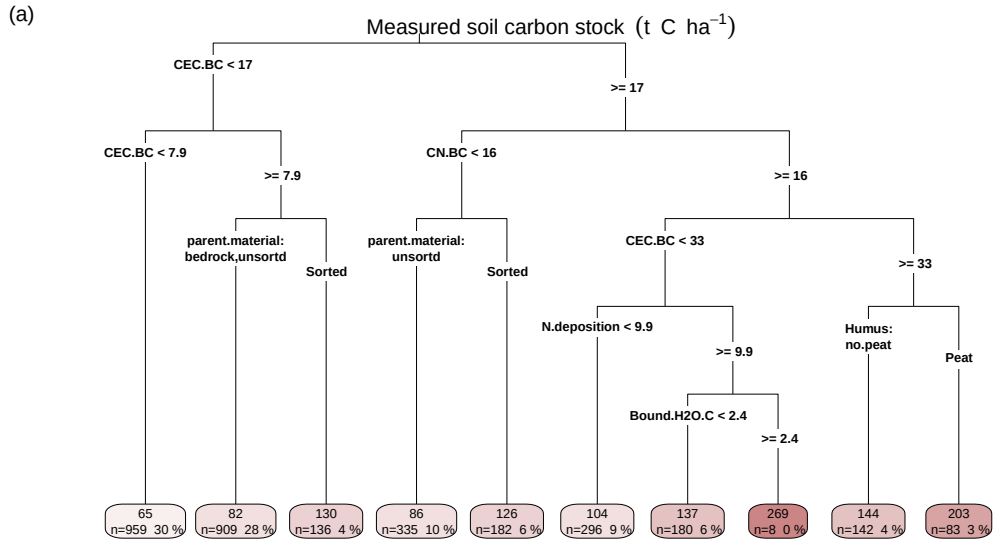

(b)

	n=959	n=909	n=136	n=335	n=182	n=296	n=180	n=8	n=142	n=83
Carbon	low	medium	high	medium	high	medium	high	extra	high	extra
Moisture	dry−fresh	fresh	moist−fresh	fresh	moist−fresh	fresh	fresh	fresh	fresh	moist−fresh
Fertility	low	medium	medium	medium	high	low	high	high	medium	medium
Soil group	1	2	3	4	5	6	7	8	9	10

Figure 2. (a) Classification/regression tree for the measured soil carbon stock (tC ha^{-1}), soil physicochemical properties, and site environmental characteristics; the cation exchange capacity of BC horizon (CEC.BC, (mmol$_c$ kg^{-1})), the C / N ratio (CN.BC), the nitrogen deposition (N.deposition kgN ha^{-1} y^{-1}), the highly bound soil water of C horizon (bound.H2O.C, %), and soil class variables as type of sorted or unsorted soil parent material and humus type. Note that variables used to calculate the soil carbon stock (bulk density, carbon content, depth, and stoniness) were excluded from the regression tree analysis. The values in the leaves of the tree show for the distinct environmental conditions mean soil carbon stock (tC ha^{-1}), number and percentage of samples. **(b)** The interpretation of 10 physicochemical soil groups of the regression tree model into the levels of carbon, soil moisture, and fertility roughly increasing from left to right.

variables used for its calculation, e.g., bulk density, depth of humus and mineral soil, carbon content, and stoniness. These variables were excluded from further regression tree analysis, which aimed to group data according to the processes of soil carbon stock development.

2.1.3 Regression trees

In order to organize SOC data into groups according to the physicochemical soil variables and to better understand the nature of measured data, we generated regression trees of SOC stocks by using recursive partitioning (RPART; Therneau and Atkinson, 1997). RPART is based on developing decision rules for predicting and cross-validation of continuous output of soil carbon stocks (regression tree). The classification tree was built by finding a single variable, which best splits the data into two groups. Each sub-group was recursively separated until no improvement could be made to the soil carbon stock estimated by using the split-based regression model. The complex resultant regression tree model was cross-validated for a nested set of sub-trees by computing the estimate of soil carbon stock to trim back the full tree.

When building the regression tree models, we excluded variables such as bulk density, carbon contents of soil layers, soil depth, and stoniness, since these measured variables were used for determining the total soil carbon stock. The selected variables for the RPART data mining were based on the correlations analysis (see Sect. 2.1.2), the processes of soil organic matter formation (e.g., Husson et al., 2013) and decomposition, and represented the soil categorical variables (sorting of parent material, soil texture, long-term soil moisture, and humus form), soil physicochemical variables

(sand, clay, and silt content, long-term soil moisture, highly bound water, C / N ratio, pH, CEC of organic, B, BC, and C horizons), climatic variables (annual mean air temperature, annual precipitation sum), and stand and site characteristics (tree species coverage of pine, spruce and deciduous, total foliar litter input, productivity class and N deposition). Alternatively, we also ran regression and classification analysis by excluding all measured soil variables because soil variables are often unavailable for landscape level modeling.

The regression tree model separated the measured total SOC stocks ($tC\,ha^{-1}$) into 10 groups. The cation exchange capacity of the BC horizon (CEC, $mmol_c\,kg^{-1}$) divided all the samples into two-thirds of lower SOC stock groups (means between 65 and 130 $tC\,ha^{-1}$) and one-third of larger groups (means between 86 and 269 $tC\,ha^{-1}$; Fig. 2a). The group of the smallest SOC stock consisted of 959 samples compared to eight samples of the group with the largest SOC stocks. We acknowledge that this is a small distinct group based only on eight observations. However, we did not have any reasons to exclude these data points as outliers. These observations indicated highly fertile conditions (high N deposition, the largest H100 among groups (31 m), second largest litter input, the highest temperature and precipitation on well-drained soil) (Fig. 2, Table S1 in the Supplement). Two-thirds of samples with smaller SOC stocks were subdivided by CEC and the type sorting of soil parent material (sorted or unsorted). One-third of samples with larger SOC stocks was subdivided by the C / N ratio, CEC, N deposition among others. Roughly generalized, groups from left to right or from 1 to 10 formed a gradient in levels of SOC stock, moisture, nutrient status, and production (Fig. 2, Table S1).

The alternative regression tree model was built with variables other than soil properties. The regression tree with the annual mean air temperature, the annual precipitation sum and the percentage of pine trees in the stand, and the nitrogen deposition separated measured SOC stocks ($tC\,ha^{-1}$) into five groups (Fig. S3). Colder groups with smaller SOC stocks (with means 67 and 85) had less litter input (below 3 $tC\,ha^{-1}$) and a low site productivity index (H100 < 20 m; Table S2).

2.2 Soil carbon stock modeling

The Q model (Rolff and Ågren, 1999) is a continuous mechanistic litter decomposition model describing change of soil organic matter over time. The decomposition rate for the branch, stem, needle, fine root, and woody litter fractions is controlled by the temperature, litter quality, microbial growth, and litter invasion rate. The model has been calibrated for seven climatic regions of Sweden in order to account for Swedish temperature and precipitation gradients (Ortiz et al., 2011; Table 3). The Q model was applied in several studies of SOC stock and change estimation in Sweden (e.g., Stendahl et al., 2010; Ortiz et al., 2013; Ågren et al., 2007). The Q model was run for seven Swedish climatic regions (Ortiz et al., 2011). The mean regional parameterization from the calibration of the 2011 Q model was used for the plot simulations. Thus, the simulations in each region represent variations in climate and litter input and not parameter variations. The equilibrium soil carbon stocks are estimated in the model using the equation for equilibrium soil carbon stock, which is derived from the decomposition functions with constant amounts and quality of litter input.

The Yasso07 model (Tuomi et al., 2009, 2011) is one of the most widely applied SOC models. The model was calibrated based on almost 10 000 measurements of litter decomposition from Europe, North and South America (Table 3). The required annual inputs of litterfall, its size and chemical composition, temperature, and precipitation determine the decomposition and sequestration rates of soil organic matter. Yasso07 estimates SOC stock to a depth of 1 m (organic and mineral layers), change of SOC stock, and heterotrophic soil respiration. Species-specific chemical composition of different litter compartments of Yasso07 were used according to Liski et al. (2009). The initial soil organic matter of Yasso07 was zero. The simulated soil carbon stock corresponding to equilibrium between the litter input and decomposition was achieved by a Yasso07 spin-up run of 10 000 years. Yasso07 runs used litter inputs of the equilibrium forest biomasses (see Sect. 2.1.1) and climate variables (annual air temperature, monthly temperature amplitude, and annual precipitation). The global parameter values of decomposition rates, flow rates, and other dependencies of the Yasso07 soil carbon model were adopted from Tuomi et al. (2011) and the estimates of Yasso07 SOC stocks were used in comparison with measurements and other models. We did not use the SOC stocks simulated with the more recent Yasso07 parameters based on the litter decomposition data from the Nordic countries (Rantakari et al., 2012), because the SOC stocks simulated with the global parameter values produced a better fit with SFSI measurements.

The CENTURY mathematical model originally developed for grassland systems (Parton et al., 1987, 1992) has been since modified for various ecosystems including boreal forests (Nalder and Wein, 2006). The CENTURY is also one of the most widely applied models. The soil organic matter in the model consists of active, slow, and passive pools, which have different TR (Table 3). The decomposition rates are modified by temperature and moisture, and in addition the decomposition rates of the slow and passive pools rely on lignin to N and C to N ratios, while the active pool decomposition rate relies on soil texture. The model simulates soil organic matter to a depth of 20 cm. The model simulates plant production and pools of living biomass, while TR for biomass pools determine the litterfall inputs to soil. To compare the performance of the soil sub-model with other soil carbon dynamics models, Q and Yasso07, we only used the CENTURY soil sub-model. We used the same litterfall inputs as used by the Q and Yasso07 simulations, which were estimated by our litterfall modeling (see Sect. 2.1.1).

Table 3. Description of models and data inputs relevant for this study.

Model	Yasso07	Q	CENTURY v4.0 soil submodel
Time step	Year	Year	Month
Parameterization	Global	Scandinavian	Combined global with site specific
Carbon pools	Labile (acid -, water -, and ethanol- soluble and non-soluble), recalcitrant (humus)	Cohorts (foliage, stems, branches, coarse roots, fine roots, "grass"), soil organic	Litter (surface structural and metabolic, belowground str. and met.), surface microbial, soil organic matter (active, slow and passive)
Biomass	Biomass components estimated by allometric biomass functions and provided stand data for litter input estimation		
Litter amount	Annual or monthly fractions of biomass components (species specific, same total litter inputs for all models)		
Litter quality	Literature-based solubilities	Estimated cohorts qualities	C / N ratios and lignin / N ratios
Temperature air	Annual mean, monthly amplitude	Annual mean	Max and min monthly mean
Precipitation	Annual total	–	Monthly total
Soil properties	–	–	Bulk density, sand, silt, and clay content
Soil depth (m)	1	–	0.2

The litter inputs reflected N deposition and site productivity (Fig. S11). For CENTURY we adopted general parameters from the parameter file "tree.100", parameters of site "AND H_J_ANDREWS" for conifers, and site "CWT Coweeta" for deciduous trees. The N dynamics in CENTURY sub-model included tuning site-specific parameters of topsoil mineral N relative to N deposition (Throop et al., 2004) and reduction of C / N ratio of the litterfall up to 15 % for most productive sites (Merilä et al., 2014). We also accounted for site-specific soil drainage by varying its parameter between 1 and 0.6 relative to long-term soil water content ranging between 10 and 50 % (Raich et al., 2000). The CENTURY SOC stocks simulation were run with equilibrium forest litter inputs, site-specific C / N ratios of litterfall, site-specific soil parameters (specific bulk density, sand, silt, and clay content, mineral N in topsoil, and drainage) and climate variables (monthly air temperature, and monthly precipitation). In order to account for the deep soil carbon (Jobbágy and Jackson, 2000), we scaled CENTURY estimates representing the topsoil horizon by adding 40 % of estimated site-specific SOC stock. The simulated equilibrium SOC stocks were estimated by a spin-up run of 5000 years. The number of years to reach equilibrium (equilibrium between the litter input and decomposition) was sought empirically on 100 random sites, and differs from Yasso07 and Q models.

3 Results

The distributions of Yasso07, Q, and CENTURY model estimates of total SOC stocks ($tC\,ha^{-1}$) were in agreement for two-thirds of the measured data with lower SOC stock (Fig. 3, distributions of groups 1, 2, and 4). The remaining one-third of SOC data were underestimated by models. This one-third of data were separated into seven physicochemical soil groups (means of groups ranging from 104 to exceptionally large 269 $tC\,ha^{-1}$, see Fig. 3, distributions of groups 3, and 5–10). The linear regression of mean levels of all 10 physicochemical soil groups (weighted by the number of samples in each group) between the modeled and measured SOC stocks showed smaller underestimation of CENTURY compared to Yasso07 and Q models (Fig. 4). The weighted root mean square error (RMSE) was 27.5 ($tC\,ha^{-1}$) for CENTURY and 31.6 and 38.8 for Yasso07 and Q, respectively. The proportion of explained variance was larger for Q ($r^2 = 0.58$) than for Yasso07 and CENTURY ($r^2 = 0.42$ and 0.32; Fig. 4). The deviation of the distributions of CENTURY SOC stocks, simulated using soil bulk density, sand, silt, and clay content, were lower than those of Yasso07 and Q estimates for 10 physicochemical soil groups (Fig. 3). Accounting for site-specific soil texture (clay, silt, and sand content) and structure (bulk density) by the CENTURY model improved SOC stock estimates for fertile sites with high clay content, but not for sites with high N deposition. Varying CENTURY parameters of site-specific topsoil mineral nitrogen and C / N ratio of the litterfall showed that this impact on SOC stocks estimates was small in comparison to sensitivity of SOC stock estimates to litterfall (Fig. S12). The application of site-specific drainage on our mostly well-drained soils showed minor impact on estimated CENTURY SOC stocks.

As expected, the models clearly showed less variation than the measurements. The shift of the mean values from the center of distribution, the width of confidence intervals of means, and the width of the tails of distributions were clearly larger for the measurements than for the modeled estimates (Fig. 3). The modeled distributions agreed for the poor–medium fertility soils with low and medium measured SOC stocks, low and medium CEC, unsorted parent material, low temperatures, and low production (groups 1, 2, and 4; Figs. 2, 3, Table S1). Disagreement between modeled and measured SOC stock distributions were formed on fertile soils with sorted parent material (groups 3 and 5), soils with higher water content (groups 3, 5, and 10), where nitrogen deposition was large (groups 7 and 8), and where CEC was median or large (Figs. 2, 3). The largest deviation between the

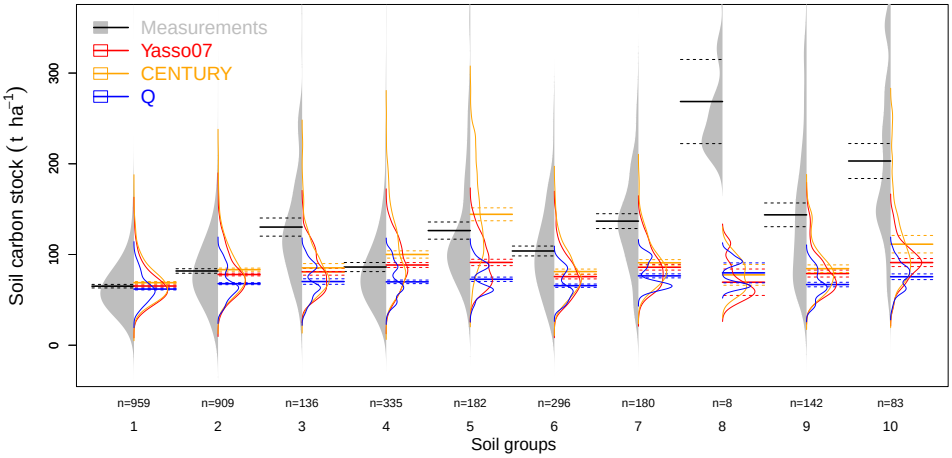

Figure 3. Bean plot of distributions of the soil carbon (tC ha^{-1}) measurements (gray fill) and estimates for 10 physicochemical groups. The full and dashed horizontal lines represent the group means and their confidence intervals. The n is the number of samples. For description of group levels of SOC stocks, moisture, and fertility see Fig. 2 and Table S1.

measured and modeled distributions was found for the relatively small physicochemical groups of soils (3 %) typical for highly bound water and peat humus types (groups 8 and 10; Figs. 2, 3). The distributions of measured total SOC stocks (tC ha^{-1}) generally increased for the groups with higher nutrient status (Figs. 3, S4). The distributions of SOC stocks in mineral soil were larger than those in humus horizon, and distributions of mineral SOC stocks increased with fertility slightly more than distributions of SOC stocks in humus horizon (Fig. S4).

After excluding all the soil physicochemical characteristics from the recursive partitioning, the SOC stock distributions of five group regression tree models (Fig. S3, Table S2) were in agreement between the measurements and model estimates for three groups (77 % of samples) and deviated for two groups (23 %; Fig. S5). The modeled SOC stock distributions agreed with measurements for all models on sites with low annual temperatures < 3 °C in northern sites (low-C.cold.pine, low-C.cold.other) and for warmer conditions in middle Sweden on sites with low nitrogen deposition and median SOC stocks (Fig. S5). However, the models underestimated SOC stocks on sites with high (> 10 kgN ha^{-1} y^{-1}) N deposition (21 % of samples) and on sites with warm and dry climate (2 % of samples; Fig. S5).

The variation of density functions of modeled SOC stocks for 10 physicochemical groups (Fig. 3) was similar to the variation of the total annual plant litter input (tC ha^{-1}; Fig. S6) indicating that litterfall was the main driver of SOC accumulation in the models . The mean levels of annual plant litter input and mean SOC stocks for 10 soil groups were more strongly correlated for Yasso07 and Q models (with r^2 values 0.86 and 0.96, respectively) than for CENTURY ($r^2 = 0.52$). Although, models performed reasonably well for the largest soil groups of nutrient and production levels (Figs. 3 and 4), none of the models was able to predict variation of individual samples (Fig. S7). The model estimates were well correlated between Yasso07 and CENTURY with r^2 ranging from 45 to 73 % for individual samples of 10 soil groups, whereas the correlations of estimates between Q and the other two models were lower (Fig. S8).

4 Discussion

4.1 SOC stock distributions linked to mechanisms of SOM stabilization

It has been suggested that process-based soil carbon models with the current formulation lacking major soil environmental and biological controls of decomposition would fail for conditions where these controls predominate (Schmidt et al., 2011; Averill et al., 2014). Even so, the effect of the soil properties on SOC stocks, e.g., soil nutrient status in the widely used models such as Yasso07, Q, and CENTURY, have not previously been quantitatively evaluated. We found that in comparison with Swedish forest soil inventory data, the models based on the amount and quality of inherent structural properties of plant litter (Q, Yasso07, and CENTURY) produced accurate SOC stock estimates for two-thirds of northern boreal forest soils in Sweden. Two-thirds of the distributions of SOC stocks measurements of SFSI agreed with distributions of SOC stock estimates of the Q, Yasso07, and CENTURY soil carbon models (Fig. 3, distributions of groups 1, 2, and 4). However, the SOC stocks underestimation by these models for one-third of the data (Fig. 3, distri-

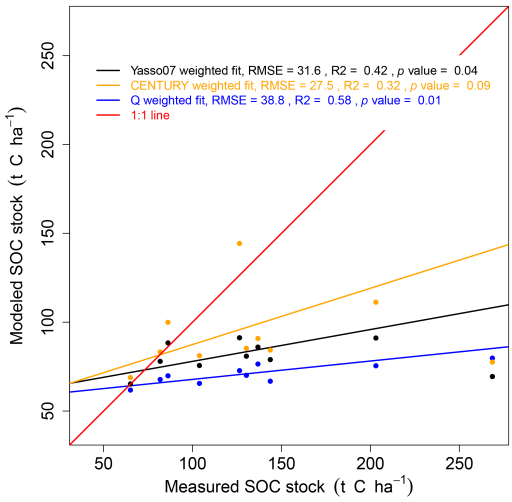

Figure 4. Scatter plot between mean measured and mean modeled soil organic carbon stocks ($tC\,ha^{-1}$) for 10 physicochemical groups for Yasso07, CENTURY and Q models. Data were fitted with weighted linear regression (lines). The number of samples in each group was used as weights for fitting and also as weights for the weighted mean of squared differences between the modeled and measured values (MSE, $tC\,ha^{-1}$). The RMSE is the square root of MSE. The r^2 is the proportion of explained variance. The p value is the calculated probability that the fit is significant.

butions of groups 3, and 5–10) indicated that some drivers other than molecular structure, especially site nutrient status, play an important role in higher SOC stocks sequestration.

Some level of deviation from measurements and poorly explained spatial variation (Fig. S7) was expected from the uncertainties of the SOC measurements, annual plant litter inputs and climate variability for the model SOC stock change estimates (Ortiz et al., 2013; Lehtonen and Heikkinen, 2015). For the long-term SOC stock development the model uncertainties are less known than for the short-term litter decomposition. Previously reported fine-scale comparison also showed poor agreement between Earth system models and the Northern Circumpolar Soil Carbon Database (Todd-Brown et al., 2013), although drivers of the deviation still remained open. Our results showed that if models strongly depend on the litter inputs (Fig. S6) then the spatial differences between measured and modeled SOC stock distributions could be linked to sites with rich nutrient status through cation exchange capacity, C / N ratio, N deposition, drainage (sorting of parent material) among other factors (Figs. 2 and 3). Additionally, when the soil properties were excluded from the regression, the estimates of SOC stocks also deviated for the fertile groups (Fig. S5). However, the rich nutrient status for these groups was linked to differences in species composition, N deposition, and climate (temperature, precipitation) instead of soil properties (Fig. S3).

Larger net soil carbon accumulation in nutrient-rich sites could be attributed to the relative differences in litterfall components (relatively more leaves and branches with higher N content than fine roots) and, to higher N availability and carbon use efficiency of decomposers, reduction of respiration per unit of C uptake (Ågren et al., 2001; Manzoni et al., 2012; Fernández-Martínez et al., 2014). The largest deviation between measured and modeled data in our study was found for fertile presumably N rich and fresh to fresh-moist sites. The soils with large N deposition were also highly productive and showed high to exceptionally high SOC stocks (Figs. 2, 3, soil groups 7 and 8). This was in agreement with fertilization and modeling study of Franklin et al. (2003) showing an increase in soil C accumulation with N addition. Our forest biomass and litterfall estimates were based on forest inventory and modeling, but the site nutrient status and N deposition was only partially reflected in the amount of biomass/litterfall (Fig. S11) and its quality. The quality was only reflected through the biochemical differences between species and plant litter components. The relative differences between the biomass/litterfall components or between C / N ratios of litterfall in relation to site fertility are not accounted for by the current biomass models, but soil fertility could be considered in an attempt of SOC stock modeling (included in CENTURY but missing in Yasso07 and Q models). For example the proportion of acid-, water-, and ethanol-soluble and non-soluble litter inputs for Yasso07 could be re-evaluated by allowing it to vary depending on site fertility, in addition to currently used variation specific for species and the litter components. Although CENTURY SOC stocks were sensitive to the amount of clay, the variation of topsoil mineral N and C / N ratio of litterfall did not improved SOC stock predictions for sites with high N deposition (Fig. 3 and Table S1).

The litter decomposition and SOC stabilization rates in Yasso07, Q, and CENTURY based on the litter quality "recalcitrance" originating from the litter bag mass loss measurements have major drawbacks. The mass loss from the litter bags is assumed to be fully mineralized, although the litterbags are subjected to non-negligible leaching (Rantakari et al., 2012; Kammer and Hagedorn, 2011). The SOC stabilization represented in models by the remaining litter mass is thus underestimated due to the fraction of particulate organic matter and dissolved organic carbon that is lost from the litterbags but later immobilized, e.g., through organo-mineral stabilization. The use of stable isotopes seems to determine the field carbon mineralization and accumulation rates from the labile (high C quality and N concentration) or recalcitrant (low C quality and N concentration) litter more accurately than litter bags (Kammer and Hagedorn, 2011).

A higher amount of more recalcitrant fine roots compared to more labile leaves (Xia et al., 2015) heavily increased the soil carbon sequestration in CENTURY model simulations,

which was in line with McCormack et al. (2015). Though, the contribution of fine roots to SOC stabilization is still not settled due to the significant role of mycorrhizal fungi in SOC accumulation (Averill et al., 2014; Orwin et al., 2011). Xia et al. (2015) claimed that more recalcitrant fine roots contribute to stable SOC more than leaf litter, because fine roots degrade slower. This would be supported by the fact that the derivatives of fine roots from degradation by fungi are more stable than the derivatives of leaves from degradation by microbes. However, more recalcitrant plant litter has been also suggested to stabilize fewer SOC stocks (Kammer and Hagedorn, 2011). This is a result of recalcitrant litter satisfying less of the microbial N demands promoting respiration and reducing the long-term production of microbial products, precursors for the organo-mineral stabilization (Cotrufo et al., 2013, Castellano et al., 2015). According to the microbial efficiency-matrix (MEM) stabilization mechanism (Cotrufo et al., 2013) fertile sites with relatively more labile plant litter, but with larger absolute production and larger microbial activity than poor sites, would in long-term stabilize more carbon through organo-mineral stabilization. Our results supported MEM stabilization theory by showing larger carbon stocks in mineral soil than in humus horizon, and by relatively more SOC stocks in mineral soil in fertile groups than in poor conditions (Fig. S4).

Expanding on the CENTURY model structure, the MySCaN model incorporating the organic nutrient uptake by mycorrhizal fungi estimated a positive effect on SOC accumulation, relatively larger in poor than in fertile sites (Orwin et al., 2011). Therefore, not accounting for the organic nutrient uptake by mycorrhizal fungi by the Yasso07, Q, and CENTURY models probably led to the underestimation of SOC stocks in sites with higher nutrient status. This hypothesis needs to be tested in further studies. We did not have all input data and the source code to include MySCaN into our model intercomparison. The spatial trends of N and P data of litter in Sweden that would be needed to make such a study were not available. However, adjusting biomass turnover rates, used for the litter input estimation, in dependence to site fertility would lead into larger inputs for fertile sites and increased SOC stock accumulation as a result of increasing plant productivity and inputs. It is well established that SOM increases soil fertility by improving the soil water and nutrient holding capacity; recycling of SOM increases CEC, humic substances and nutrient availability for plant resulting in larger biomass/litter production (Zandonadi et al., 2013). As an alternative to adjusting turnover rates with site fertility, we suggest that a feedback link in models between increasing fertility due to SOC stock accumulation (e.g., due to increased CEC relative to humus, increased nitrogen availability), increasing litter inputs, and reduced rates of SOC decomposition per unit of litter input (e.g., through satisfying more microbial N demand with less respiration, limited oxygen in increased moisture conditions) would also increase SOC stock accumulation.

Increased moisture and more frequent water saturation due to SOC accumulation limits soil oxygen availability and slows rates of microbial decomposition, which increases the rate of SOC stabilization. Our results, which were derived from mostly well-drained soils, suggest that measured high SOC stocks may be partly caused by reduction of decomposition at increased water content (Fig. 2). The CENTURY model has an optional function that represents the reduction of decomposition caused by anaerobic conditions. The function becomes active when a controlling parameter, "drain", is changed, and the value of the parameter has to be arbitrarily determined through parameter fitting against SOC data (e.g., Raich et al., 2000). However, this function was meant for anaerobic conditions in poorly drained soils; therefore, it was not applicable to the prevailing conditions of our sites. Accounting for drainage only on some sites slightly affected decomposition, when precipitation increased and potential evapotranspiration decreased in late spring or early autumn. Water availability affecting soil fertility and SOC formation is beside climate also affected by topography (Clarholm and Skyllberg, 2013), which was not accounted for by CENTURY. Detailed modeling of soil water conditions requires specific functions and many parameters, which are not included in simpler SOC models like Q and Yasso07. However, appropriate modeling of soil water conditions and reduction of decomposition in wet conditions (not necessarily at saturation) would potentially improve the performance of SOC models in particular for soils with high SOC stocks.

4.2 Intercomparison of models

The similarities between the variations of modeled SOC stocks and litterfall inputs for the soil groups with different fertilities (Figs. 3, S6) could be expected for the Yasso07 and Q models, which ignore the soil properties. These models run organic matter decomposition and humus stabilization with litterfall, temperature, and/or precipitations input data. Litter quality as input in Yasso07 and Q implicitly includes some information on soil properties, but as we saw litter quality hardly mapped any of soil fertility. Although, the impact of soil properties on the estimates was seen in the more complex CENTURY model for sites with high clay content, the SOC stock of sites with high N deposition were underestimated. The CENTURY model depended less on the amount of litter input. In testing multiple soil carbon models with the same litter inputs, Palosuo et al. (2012) observed larger variation in modeled SOC stocks at the early stage of the litter decomposition (10 years) but later on at 100 years the variation decreased. Although the variations of SOC stocks were similar between the models, the estimated CENTURY SOC stocks distributions were lower than the Yasso07 estimates when we did not accounted for deep soil carbon. CENTURY in its original configuration simulated SOC stock up to 20 cm soil depth (Metherell, 1993), whereas the Yasso07, Q, and measured SOC stock data represented up to 100 cm of the soil

(Tuomi et al., 2009; Stendahl et al., 2010). In Yasso07 model parameters were calibrated based on soil age chronosequence data of SOC stocks for soil depths up to 30 cm, which was assumed to represent 60 % of the total SOC stocks up to 100 cm soil depth (Liski et al., 1998, 2005 as cited by Tuomi et al., 2009). Therefore, when 40 % of the missing deep carbon (Jobbágy and Jackson, 2000) were added on top of the original CENTURY estimates as was done when calibrating Yasso07, the SOC stock levels for CENTURY were larger than those for the Yasso07 and Q models.

Although estimated SOC stocks of CENTURY were generally larger than those of Yasso07, the correlation between CENTURY and Yasso07 estimates was stronger than for Q model compared to two other models (Fig. S8). The reason was probably similar global parameterizations of Yasso07 and CENTURY whereas Q was specifically parameterized and applied for the regions in Sweden (Ågren and Hyvönen, 2003; Ortiz et al., 2013). Furthermore the Q model SOC stock estimates were more sensitive to differences in species coverage e.g., to pine and spruce (Ågren and Hyvönen, 2003) and formed two distinct point cloud distributions (one for pine and broadleaves, the other for spruce) when compared with the CENTURY or Yasso07 estimates (Fig. S8). In spite of similarities in Yasso07 and CENTURY SOC stocks estimates, Yasso07 was more sensitive to species coverage through species-specific litterfall solubility (Liski et al., 2009) than CENTURY, which treated conifers in a single group (Metherell et al., 1993). Pine and other species (spruce) coverage was shown to affect measured low and median SOC stocks of colder climate if the soil properties were not considered (Fig. S5). Therefore, the pattern of increased accumulation of SOC stock on sites with larger spruce coverage partially observed in distribution of Yasso07 estimates, and missing in the CENTURY estimates, could be related to the slightly lower solubility/decomposability of spruce compared to pine litterfall. However, the CENTURY model SOC stocks were also highly sensitive to accurate estimation of fine-root litterfall (McCormack et al., 2015) typically increasing with colder climate and increasing the C / N ratio of the organic layer (Lehtonen et al., 2016a), which is driven by the dominant tree species (Cools et al., 2014).

Large SOC stock measurements on sites with high long-term nitrogen deposition over $10\,\mathrm{kgN\,ha^{-1}\,y^{-1}}$ (Figs. 3 and S4) were underestimated by the Q, Yasso07, and CENTURY models. A positive correlation between nitrogen deposition and SOC stocks measurements in Sweden had been previously reported by Olsson et al. (2009), and the modeling study by Svensson et al. (2008) indicated that Swedish soil carbon was decreasing in the north and increasing in the south mainly as a result of different nitrogen inputs. The Q and Yasso07 models do not have nitrogen processes. As for CENTURY, it is reported that large N input could enhance plant productivity and then increase SOC (Raich et al., 2000). The purpose of our study was to evaluate the performance of soil carbon models against the SOC data using the same litter input, and the feedback of nitrogen input to plant productivity was primarily included in this study indirectly, through estimated equilibrium litter input based on site productivity index, which strongly correlated with N deposition (Figs. A1 in Appendix A and S11). In spite of a slight increase of SOC stock estimates when CENTURY accounted for the site-specific topsoil mineral N, the C / N ratio of litterfall (Fig. S12), in sites with large N deposition CENTURY still underestimated. However, as in the case of drainage discussed earlier, the CENTURY incorporates more detailed processes than the relatively simpler soil carbon models do, Q and Yasso07, and hence the CENTURY could potentially reproduce a wider range of SOC stocks if it was parameterized with more detailed data.

5 Conclusions

In this study we presented the reasons to re-evaluate the connection between the soil nutrient status and performance of widely applied soil carbon models (Yasso07, Q, and CENTURY). As previously described in detail, our simulation was based on the widely used process-based SOC models, accurate driving data including litter inputs, and massive SOC data points (Swedish inventory data, $N = 3230$). The models differed in the main controls and functions and their performance was expected to depend on model complexity (CENTURY outperforming Q and Yasso07). The intercomparison of SOC stocks between Yasso07, Q, and CENTURY models and Swedish soil carbon inventory data revealed that these process-based mathematical models developed for predicting short-term SOC stock changes can all in their current state predict accurate long-term SOC stocks for most soils. However, in medium–highly productive sites of southern Sweden for conditions where the high nutrient status predominates soil carbon accumulation, the models with their current formulation (lacking nutrient status-related controls of decomposition and SOC accumulation) underestimated SOC stocks. The estimates of CENTURY fitted generally better to measurements than those of Yasso07 and the Q model. Although the Yasso07 model, which requires fewer parameters and less input data, showed similar performance than CENTURY, except for sites with high clay content.

Through the intercomparison of three different widely used SOC models with massive data points, we identified that re-evaluation of the impact of nutrient status would improve the model development towards their accuracy. Particularly, the relationship between the soil nutrient status and the mechanism of soil organo-mineral carbon stabilization needs to be re-evaluated, because larger SOC stocks were found more in the mineral than in the humus soil horizon. We suggest evaluating enhanced microbial transformation of soil organic matter and the mycorrhizal organic nutrient uptake in relation to larger plant biomass/litter production in nutrient-rich sites resulting in higher SOC stock accumula-

tion in deeper soil layers. In addition to the organo-mineral carbon stabilization, we also suggest further model development accounting for the soil nutrient status through evaluating the effect of topography on sorting of the parent material, and its silt and clay complexes.

Our study is very useful for developing accurate soil carbon and Earth system models. Furthermore, developing accurate models that would account for the soil nutrient status as one of the key controls affecting the soil organic matter production and SOC stabilization improves estimation of feedback of global warming on SOC stock temperature sensitivity and soil CO_2 efflux, national reporting of soil carbon stock changes for UNFCCC, and implications of decisions mitigating the climate change effects on soil carbon stocks.

6 Data availability

The source codes of the Yasso07, Q, and CENTURY models used in this paper are available through the Supplement. Data used in this study can be available directly by contacting the authors.

Appendix A: Models of fraction of absorbed radiation for observed and equilibrium forest

The fraction of photosynthetically active absorbed radiation (f_{APAR}) for the observed state forest was calculated based on measurements of Swedish forest inventory as in Härkönen et al. (2010). For the main tree species f_{APAR} was also well correlated with the stand basal area (r^2 was 0.85, 0.86, and 0.88 for pine, spruce, and deciduous stands, respectively, coefficients of regressions in Table A1 in Appendix A). The observed state forest f_{APAR} varied between 0 and a maximum close to 1 (Fig. A1 in Appendix A).

The equilibrium forest f_{APAR} values were assumed to be ranging between the median and the maximum fraction of observed state forest f_{APAR} for given species, latitudinal degree, and site productivity index (indicated by the height of largest tress at 100 years of stands age). The equilibrium forest f_{APAR} values were set to 70th percentile of maximum (f_{APAR70}) for given species, latitudinal degree, and site productivity index. We selected 70th percentile from the range between 50th and 95th, because the modeled soil carbon distributions with the litter input from biomass of f_{APAR70} best agreed with measured soil carbon distributions (Fig. S2).

The f_{APAR70} values specific for pine, spruce, and deciduous stands were modeled with latitude and site productivity index (H100) in two steps. First, the $f_{APAR70LAT}$ and the $f_{APAR70H100}$ values were modeled separately by regression models with latitude and with site productivity index (Table A1 in Appendix A). Second, the $f_{APAR70LAT}$ was reduced by the difference between the $f_{APAR70H100}$ and the maximum $f_{APAR70H100}$ ($f_{APAR70} = f_{APAR70LAT} + f_{APAR70H100} -$ maximum $f_{APAR70H100}$). The f_{APAR70} equaled the $f_{APAR70LAT}$ only for the maximum site productivity index, otherwise it was reduced.

Table A1. Parameter estimates and their standard errors of the f_{APAR} regressions with the stand basal area (BA, $m^2\,ha^{-1}$), and the $f_{APAR70LAT}$ and $f_{APAR70H100}$ regressions with the latitude (LAT, °) and with the site productivity index (H100, m) for Scots pine, Norway spruce, and deciduous stands.

$f_{APAR} = a \times BA/(b + BA)$	$a \pm SE$	$b \pm SE$	$c \pm SE$	adj.R^2
Pine	1.00 ± 0.03	11.75 ± 0.81		0.85
Spruce	1.17 ± 0.03	10.67 ± 0.87		0.86
Deciduous	1.13 ± 0.06	7.41 ± 1.15		0.88
$f_{APAR70LAT} = LAT/(a + b \times LAT) + c$				
Pine	-9976 ± 3691[a]	143 ± 54[b]	0.72 ± 0.02	0.92
Spruce	-2689 ± 3507[c]	35 ± 50[d]	0.97 ± 0.09	0.74
$f_{APAR70LAT} = a + b \times LAT$				
Deciduous	1.36 ± 0.28	-0.01 ± 0.01[e]		0.26
$f_{APAR70H100} = a \times e^{(b/H100)}$				
Pine	0.86 ± 0.02	-5.22 ± 0.41		0.89
Spruce	0.97 ± 0.01	-2.85 ± 0.22		0.86
Deciduous	0.94 ± 0.02	-2.63 ± 0.50		0.51

$p < 0.001$ for all parameters except for [a] 0.023, [b] 0.024, [c] 0.461, [d] 0.498, and [e] 0.076.

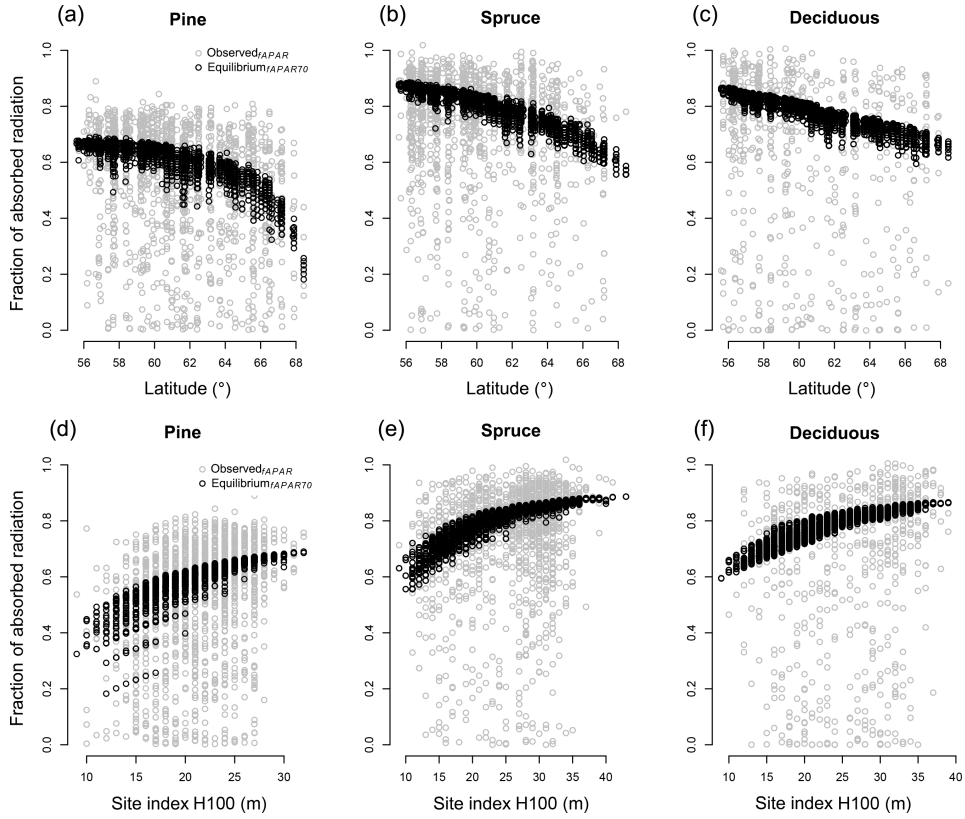

Figure A1. The fraction of photosynthetically active absorbed radiation (f_{APAR}; estimated as in Härkönen et al., 2010) observed f_{APAR} and equilibrium f_{APAR} (f_{APAR70}, set to 70th percentile of maximum f_{APAR} for given species, latitudinal degree, and site productivity index). Panels **(a)**, **(b)**, and **(c)** show relation between f_{APAR} and latitude (°) for forest stands dominated by Scots pine, Norway spruce, and deciduous species, whereas panels **(d)**, **(e)**, and **(f)** show relation between f_{APAR} and site index H100 (height of dominant trees at 100 years in meters).

Appendix B: Models of forest dry weight biomass with f_{APAR}

We fitted species-specific exponential regression models between the biomass components (stem, branch, foliage, stump, coarse roots, fine roots, all in kg ha^{-1}) of observed state forest and the observed fraction of absorbed radiation (f_{APAR}) (statistics of the regression models in Table B1 in Appendix B). The biomass components derived with allometric models (measured) and those derived with f_{APAR} models (modeled) showed strong correlations (Fig. B1 in Appendix B). In order to model the long-term mean forest biomass "equilibrium forest biomass" we applied the f_{APAR} biomass models to the modeled f_{APAR70} values.

Table B1. Parameter estimates and their standard errors for the coefficients of the dry weight biomass (kg ha^{-1}) models with the fraction of absorbed radiation ($y = ab^{f_{APAR}}$) for Scots pine, Norway spruce, and deciduous stands.

$y = ab^{f_{APAR}}$	Species	$a \pm$ SE	$b \pm$ SE	adj.R^2
Branch	pine	610 ± 21	122 ± 6	0.92
	spruce	877 ± 35	54 ± 2	0.92
	deciduous	290 ± 26	156 ± 16	0.89
Fine root	pine	422 ± 13	21 ± 1	0.84
	spruce	317 ± 14	15 ± 1	0.80
	deciduous	453 ± 28	14 ± 1	0.82
Foliage	pine	361 ± 24	86 ± 8	0.71
	spruce	766 ± 40	33 ± 2	0.83
	deciduous	141 ± 28	71 ± 16	0.56
Root	pine	703 ± 26	183 ± 10	0.92
	spruce	629 ± 32	113 ± 7	0.90
	deciduous	359 ± 33	150 ± 16	0.89
Stem and bark	pine	1793 ± 84	254 ± 17	0.89
	spruce	974 ± 72	229 ± 19	0.86
	deciduous	972 ± 98	161 ± 18	0.88
Stump	pine	232 ± 10	214 ± 13	0.89
	spruce	171 ± 10	129 ± 9	0.88
	deciduous	80 ± 8	216 ± 25	0.87

$p < 0.001$ for all parameters.

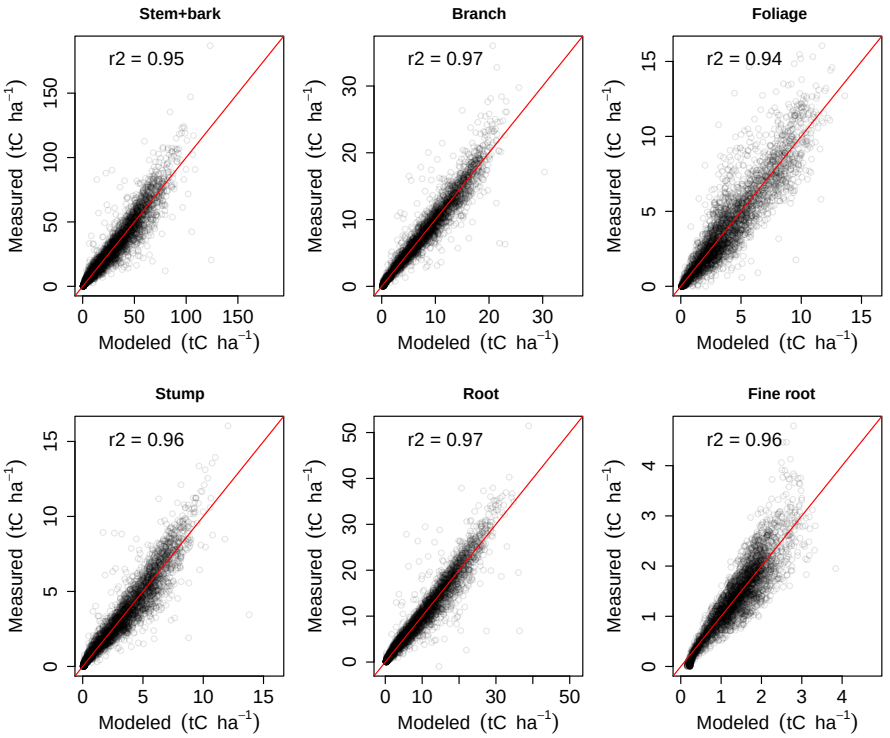

Figure B1. Scatter plots ($n = 3698$ in each panel) for the dry weight tree biomass components (tC ha^{-1}) between "modeled" (estimated based on fraction of absorbed radiation, f_{APAR}, and our f_{APAR} models) and "measured" (estimated based on basic tree dimensions and allometric biomass models). The r^2 values represent the coefficient of determination indicating how close the modeled values fit the measured values.

Appendix C: Models of understory vegetation

We used Swedish forest inventory ground vegetation coverage (%) data visually monitored between 1993 and 2002 on 2440 plots around Sweden with altogether 4472 observations separately for species of forest floor vegetation or their classes (Table S3). In order to derive the ground vegetation biomass and to apply the coverage/biomass conversion functions (Lehtonen et al., 2016), we grouped the species coverage observations into five functional types (dwarf shrubs, herbs, grasses, moss, and lichen; Table S3). The applied coverage/biomass conversion functions estimated separately the above- and below-ground biomass components for dwarf shrubs, herbs, and grasses, and total biomass for moss, and lichen.

Except the understory coverage, the forest inventory data also contained basic tree dimensions (diameter and height of trees) and stand variables (species dominance, age, basal area, site productivity class indicated by the height of largest tress at 100 years of stands age), and also we linked the plots by their closest proximity to SMHI weather stations with weather data (air temperature, precipitation) and location attributes of the weather stations (latitude, longitude, altitude). We built linear models for dry weight biomass of understory vegetation ($kg\,ha^{-1}$) in a two level selection of the predictors from stand, weather and location variables. First, we selected the predictors into linear models by using R package "Mass" and its stepwise model selection by exact Akaike's information criterion (AIC; Venables and Ripley, 2002). Second, we refined the model by using "relaimpo" R package estimating usefulness (Grömping, 2006), or relative importance for each of the predictors in the model, and by selecting only predictors with relative importance ≥ 0.1. The general form of the models was

$$y_i = a + b_1 x_1 + \ldots + b_n x_n + \varepsilon, \quad \text{(C1)}$$

where y_i is the understory dry weight biomass ($kg\,ha^{-1}$), $x_1 \ldots x_n$ are the predictors, a, $b_1 \ldots b_n$ are parameters of the ith understory functional type (Table C1 in Appendix C), and ε is the residual error. Statistics of the models are shown in Table C1 in Appendix C. Scatter plots between the measured coverage derived biomass and modeled dry weight biomass ($kg\,ha^{-1}$) of the functional types of ground vegetation for the forests in their observed state close to the estimated equilibrium are shown on Fig. S9.

Table C1. Parameter estimates and their standard errors for the coefficients of the forest understory vegetation dry weight biomass ($kg\,ha^{-1}$) models (Eq. C1) for functional types (1 – dwarf shrubs, 2 – herbs, 3 – grasses, 4 – mosses, and 5 – lichens) with intercept (a) and n – number of predictors ($b1$ – age (years), $b2$ – basal area ($m^2\,ha^{-1}$), $b3$ – annual air temperature (°C), $b4$ – latitude (°), $b5$ – H100 (height of trees at 100 years of age, m), $b6$ – H100 of spruce trees (m), $b7$ – H100 of pine trees (m), $b8$ – pine dominance (0/1), and $b9$ – spruce dominance (0/1)). For the latin names of species included into understory functional types see Table S3.

W		$a \pm$E	$b1 \pm$SE	$b2 \pm$SE	$b3 \pm$SE	$b4 \pm$SE	$b5 \pm$SE	$b6 \pm$SE	$b7 \pm$SE	$b8 \pm$SE	$b9 \pm$SE	adj.R^2
Above	1	24.28 ± 0.32	0.13 ± 0.01	-0.43 ± 0.02						7.13 ± 0.33		0.29
ground	2	-82.13 ± 6.8			-0.1 ± 0.1^a	1.23 ± 0.1		0.77 ± 0.03				0.12
	3	4.07 ± 0.30		-0.16 ± 0.01				0.27 ± 0.01		-1.36 ± 0.15		0.21
	4	32.9 ± 0.62					-0.78 ± 0.04		0.48 ± 0.06	3.66 ± 0.3	5.76 ± 0.29	0.22
	5	19.91 ± 0.57		-0.13 ± 0.01				-0.45 ± 0.02		6.31 ± 0.29		0.25
	total	43.68 ± 0.29	0.12 ± 0.01	-0.41 ± 0.01						6.34 ± 0.3		0.30
Below	1	-256.3 ± 3.5	0.1 ± 0.01	-0.35 ± 0.02		5.05 ± 0.06				8.56 ± 0.35		0.75
ground	2	-89.34 ± 7.85			-0.03 ± 0.1^b	1.4 ± 0.12		0.78 ± 0.04		-4.97 ± 0.27		0.19
	3	5.97 ± 0.37		-0.19 ± 0.01				0.32 ± 0.01		-1.78 ± 0.19		0.21
	total	-251.9 ± 3.3		-0.2 ± 0.01		5.15 ± 0.05						0.7
Total		-222.7 ± 4.0	0.12 ± 0.01	-0.44 ± 0.02		4.9 ± 0.07						0.67

$p < 0.001$ for all parameters except for [a] $p = 0.44$, and [b] $p = 0.84$.

The Supplement related to this article is available online at doi:10.5194/bg-13-4439-2016-supplement.

Acknowledgements. We thank the Finnish Ministry of Environment and the Finnish Ministry of Agriculture and Forestry for funding this work through the Metla project 7509 "Improving soil carbon estimation of greenhouse gas inventory", and Academy of Finland for funding the mobility projects 276300 and 276602. We would like to thank the editor and the reviewers for their valuable comments improving the manuscript.

Edited by: A. V. Eliseev
Reviewed by: three anonymous referees

References

Adair, E. C., Parton, W. J., Del Grosso, S. J., Silver, W. L., Harmon, M. E., Hall, S. A., Burke, I. C., and Hart, S. C.: Simple three-pool model accurately describes patterns of long-term litter decomposition in diverse climates, Global Change Biol., 14, 2636–2660, 2008.

Ågren, G. I., Bosatta, E., and Magill, A. H.: Combining theory and experiment to understand effects of inorganic nitrogen on litter decomposition, Oecologia, 128, 94–98, 2001.

Ågren, G. I. and Hyvönen, R.: Changes in carbon stores in Swedish forest soils due to increased biomass harvest and increased temperatures analysed with a semi-empirical model, Forest Ecol. Manage., 174, 25–37, 2003.

Ågren, G., Hyvönen, R., and Nilsson, T.: Are Swedish forest soils sinks or sources for CO2—model analyses based on forest inventory data, Biogeochemistry, 82, 217–227, 2007.

Amundson, R.: The carbon budget in soils, Annu. Rev. Earth Planet. Sci., 29, 535–562, 2001.

Averill, C., Turner, B. L., and Finzi, A. C.: Mycorrhiza-mediated competition between plants and decomposers drives soil carbon storage, Nature, 505, 543–545, 2014.

Berthrong, S. T., Jobbágy, E. G., and Jackson, R. B.: A global meta-analysis of soil exchangeable cations, pH, carbon, and nitrogen with afforestation, Ecol. Appl., 19, 2228–2241, 2009.

Boden, T. A., Marland, G., and Andres, R. J.: Global, regional, and national fossil-fuel CO_2 emissions, Carbon Dioxide Information Analysis Center, Oak Ridge National Laboratory, US Department of Energy, Oak Ridge, Tenn., USA, doi:10.3334/CDIAC/00001_V2010, 2010.

Castellano, M. J., Mueller, K. E., Olk, D. C., Sawyer, J. E., and Six, J.: Integrating Plant Litter Quality, Soil Organic Matter Stabilization and the Carbon Saturation Concept, Glob. Change Biol., 21, 3200–3209, doi:10.1111/gcb.12982, 2015.

Clarholm, M. and Skyllberg, U.: Translocation of metals by trees and fungi regulates pH, soil organic matter turnover and nitrogen availability in acidic forest soils, Soil Biol. Biochem., 63, 142–153, 2013.

Clemente, J. S., Simpson, A. J., and Simpson, M. J.: Association of specific organic matter compounds in size fractions of soils under different environmental controls, Org. Geochem., 42, 1169–1180, 2011.

Cools, N., Vesterdal, L., De Vos, B., Vanguelova, E., and Hansen, K.: Tree species is the major factor explaining C : N ratios in European forest soils, Forest Ecol. Manage., 311, 3–16, 2014.

Cotrufo, M. F., Wallenstein, M. D., Boot, C. M., Denef, K., and Paul, E.: The Microbial Efficiency-Matrix Stabilization (MEMS) framework integrates plant litter decomposition with soil organic matter stabilization: do labile plant inputs form stable soil organic matter?, Glob. Change Biol., 19, 988–995, 2013.

Deluca, T. H. and Boisvenue, C.: Boreal forest soil carbon: distribution, function and modelling, Forestry, 85, 161–184, 2012.

Dungait, J. A. J., Hopkins, D. W., Gregory, A. S., and Whitmore, A. P.: Soil organic matter turnover is governed by accessibility not recalcitrance, Glob. Change Biol., 18, 1781–1796, 2012.

Falloon, P., Jones, C. D., Ades, M., and Paul, K.: Direct soil moisture controls of future global soil carbon changes: An important source of uncertainty, Global Biogeochem. Cy., 25, GB3010, doi:10.1029/2010GB003938, 2011.

Fan, Z., Neff, J. C., Harden, J. W., and Wickland, K. P.: Boreal soil carbon dynamics under a changing climate: A model inversion approach, J. Geophys. Res.-Biogeo., 113, G04016, doi:10.1029/2008JG000723, 2008.

Fernández-Martínez, M., Vicca, S., Janssens, I. A., Sardans, J., Luyssaert, S., Campioli, M., Chapin III, F. S., Ciais, P., Malhi, Y., Obersteiner, M., Papale, D., Piao, S. L., Reichstein, M., Roda, F., and Penuelas, J.: Nutrient availability as the key regulator of global forest carbon balance, Nature Climate Change, 4, 471–476, 2014.

Franklin, O., Högberg, P., Ekblad, A., and Ågren, G. I.: Pine forest floor carbon accumulation in response to N and PK additions: bomb 14C modelling and respiration studies, Ecosystems, 6, 644–658, 2003.

Grömping, U.: Relative importance for linear regression in R: the package relaimpo, J. Stat. Softw., 17, 1–27, 2006.

Hagglund, B. and Lundmark, J.: Site index estimation by means of site properties, Scots pine and Norway spruce in Sweden, Stud. For. Suec., 138, 38, 1977.

Härkönen, S., Pulkkinen, M., Duursma, R., and Mäkelä, A.: Estimating annual GPP, NPP and stem growth in Finland using summary models, For. Ecol. Manage., 259, 524–533, 2010.

Husson, O.: Redox potential (Eh) and pH as drivers of soil/plant/microorganism systems: a transdisciplinary overview pointing to integrative opportunities for agronomy, Plant Soil, 362, 389–417, 2013.

Jobbágy, E. G. and Jackson, R. B.: The vertical distribution of soil organic carbon and its relation to climate and vegetation, Ecol. Appl., 10, 423–436, 2000.

Kammer, A. and Hagedorn, F.: Mineralisation, leaching and stabilisation of ^{13}C-labelled leaf and twig litter in a beech forest soil, Biogeosciences, 8, 2195–2208, doi:10.5194/bg-8-2195-2011, 2011.

Kirschbaum, M. U. F.: Will Changes in Soil Organic Carbon Act as a Positive or Negative Feedback on Global Warming?, Biogeochemistry, 48, 21–51, 2000.

Kleja, D. B., Svensson, M., Majdi, H., Jansson, P., Langvall, O., Bergkvist, B., Johansson, M., Weslien, P., Truusb, L., and Lindroth, A.: Pools and fluxes of carbon in three Norway spruce ecosystems along a climatic gradient in Sweden, Biogeochemistry, 89, 7–25, 2008.

Kurz, W. A., Beukema, S. J., and Apps, M. J.: Estimation of root biomass and dynamics for the carbon budget model of the C anadian forest sector, Can. J. Forest Res., 26, 1973–1979, 1996.

Lehtonen, A. and Heikkinen, J.: Uncertainty of upland soil carbon sink estimate for Finland, Can. J. Forest Res., 45, 1–13, 2015.

Lehtonen, A., Sievänen, R., Mäkelä, A., Mäkipää, R., Korhonen, K. T. and Hokkanen, T.: Potential litterfall of Scots pine branches in southern Finland, Ecol. Modell., 180, 305–315, 2004.

Lehtonen, A., Linkosalo, T., Peltoniemi, M., Sievänen, R., Mäkipää, R., Tamminen, P., Salemaa, M., Nieminen, T., Tupek, B., Heikkinen, J., and Komarov, A.: Soil carbon stock estimates in a nationwide inventory: evaluating performance of the ROMUL and Yasso07 models, Geosci. Model Dev. Discuss., in review, 2016a.

Lehtonen, A., Palviainen, M., Ojanen, P., Kalliokoski, T., Nöjd, P., Kukkola, M., Penttilä, T., Mäkipää, R., Leppälammi-Kujansuu, J. and Helmisaari, H.: Modelling fine root biomass of boreal tree stands using site and stand variables, Forest Ecol. Manag., 359, 361–369, doi:10.1016/j.foreco.2015.06.023, 2016b.

Leppälammi-Kujansuu, J., Aro, L., Salemaa, M., Hansson, K., Kleja, D. B., and Helmisaari, H.: Fine root longevity and carbon input into soil from below-and aboveground litter in climatically contrasting forests, Forest Ecol. Manage., 326, 79–90, 2014.

Lindén, A., G.: Swedish Geological Survey report, pp. 10, available at: http://resource.sgu.se/produkter/ae/ae118-beskrivning.pdf (last access: 3 August 2016), 2002.

Liski, J., Tuomi, M., and Rasinmäki, J.: Yasso07 user-interface manual, Finnish Environment Institute, Helsinki, 2009.

Liski, J., Lehtonen, A., Palosuo, T., Peltoniemi, M., Eggers, T., Muukkonen, P., and Mäkipää, R.: Carbon accumulation in Finland's forests 1922–2004–an estimate obtained by combination of forest inventory data with modelling of biomass, litter and soil, Ann. Forest Sci., 63, 687–697, 2006.

Majdi, H.: Changes in fine root production and longevity in relation to water and nutrient availability in a Norway spruce stand in northern Sweden, Tree Physiol., 21, 1057–1061, 2001.

Malkonen, E.: Annual primary production and nutrient cycle in a birch stand, Commun. Inst. For. Fenn., 91, 1–35, 1977.

Manzoni, S., Taylor, P., Richter, A., Porporato, A., and Ågren, G. I.: Environmental and stoichiometric controls on microbial carbon use efficiency in soils, New Phytol., 196, 79–91, 2012.

Marklund, L.: , Biomassafunktioner för tall, gran och björk i Sverige, Biomass functions for pine, spruce and birch in Sweden, Swedish University of Agricultural Sciences, Department of Forest Survey, Report 45, ISSN 0348–0496, 1988.

McCormack, M. L., Crisfield, E., Raczka, B., Schnekenburger, F., Eissenstat, D. M., and Smithwick, E. A.: Sensitivity of four ecological models to adjustments in fine root turnover rate, Ecol. Model., 297, 107–117, 2015.

Metherell, A. K.: Century: Soil Organic Matter Model Environment: Technical Documentation: Agroecosystem Version 4.0, Colorado State University, 1993.

Merilä, P., Mustajärvi, K., Helmisaari, H., Hilli, S., Lindroos, A., Nieminen, T. M., Nöjd, P., Rautio, P., Salemaa, M., and Ukonmaanaho, L.: Above-and below-ground N stocks in coniferous boreal forests in Finland: Implications for sustainability of more intensive biomass utilization, For. Ecol. Manage., 311, 17–28, 2014.

Muukkonen, P. and Lehtonen, A.: Needle and branch biomass turnover rates of Norway spruce (Picea abies), Can. J. Forest Res., 34, 2517–2527, 2004.

Nalder, I. A. and Wein, R. W.: A model for the investigation of long-term carbon dynamics in boreal forests of western Canada: I. Model development and validation, Ecol. Model., 192, 37–66, 2006.

Olsson, M. T., Erlandsson, M., Lundin, L., Nilsson, T., Nilsson, Å., and Stendahl, J.: Organic carbon stocks in Swedish Podzol soils in relation to soil hydrology and other site characteristics, Silva Fennica, 43, 209–222, 2009.

Ortiz, C., Karltun, E., Stendahl, J., Gärdenäs, A. I., and Ågren, G. I.: Modelling soil carbon development in Swedish coniferous forest soils—An uncertainty analysis of parameters and model estimates using the GLUE method, Ecol. Model., 222, 3020–3032, 2011.

Ortiz, C. A., Liski, J., Gärdenäs, A. I., Lehtonen, A., Lundblad, M., Stendahl, J., Ågren, G. I., and Karltun, E.: Soil organic carbon stock changes in Swedish forest soils – A comparison of uncertainties and their sources through a national inventory and two simulation models, Ecol. Model., 251, 221–231, 2013.

Orwin, K. H., Kirschbaum, M. U., St John, M. G., and Dickie, I. A.: Organic nutrient uptake by mycorrhizal fungi enhances ecosystem carbon storage: a model-based assessment, Ecol. Lett., 14, 493–502, 2011.

Palosuo, T., Foereid, B., Svensson, M., Shurpali, N., Lehtonen, A., Herbst, M., Linkosalo, T., Ortiz, C., Rampazzo Todorovic, G., Marcinkonis, S., Li, C., and Jandl, R.: A multi-model comparison of soil carbon assessment of a coniferous forest stand, Environ. Modell. Softw., 35, 38–49, 2012.

Parton, W. J., Schimel, D. S., Cole, C. V., and Ojima, D. S.: Analysis of Factors Controlling Soil Organic Matter Levels in Great Plains Grasslands, 51, 1173–1179, 1987.

Parton, W., Ojima, D., and Schimel, D.: Environmental change in grasslands: Assessment using models, Climate Change, 28, 111–141, 1994.

Parton, W.J., McKeown, R., Kirchner, V., and Ojima,D.: CENTURY Users' Manual, Natural Resource Ecology Laboratory, Colorado State University, Ft. Collins., 1992.

Peltoniemi, M., Pulkkinen, M., Aurela, M., Pumpanen, J., Kolari, P. and Mäkelä, A.: A semi-empirical model of boreal-forest gross primary production, evapotranspiration, and soil water–calibration and sensitivity analysis, Boreal Environ. Res., 20, 2015.

Petersson, H. and Ståhl, G.: Functions for below-ground biomass of Pinus sylvestris, Picea abies, Betula pendula and Betula pubescens in Sweden, Scand., J. For. Res., 21, 84–93, 2006.

Raich, J. W., Parton, W. J., Russell, A. E., Sanford Jr, R. L., and Vitousek, P. M.: Analysis of factors regulating ecosystemdevelopment on Mauna Loa using the Century model, Biogeochemistry, 51, 161–191, 2000.

Rantakari, M., Lehtonen, A., Linkosalo, T., Tuomi, M., Tamminen, P., Heikkinen, J., Liski, J., Mäkipää, R., Ilvesniemi, H., and Sievänen, R.: The Yasso07 soil carbon model–Testing against repeated soil carbon inventory, Forest Ecol. Manage., 286, 137–147, 2012.

Rapalee, G., Trumbore, S. E., Davidson, E. A., Harden, J. W., and Veldhuis, H.: Soil Carbon stocks and their rates of accumulation

and loss in a boreal forest landscape, Global Biogeochem. Cy., 12, 687–701, 1998.

Repola, J.: Biomass equations for birch in Finland, Silva Fenn., 42, 605–624, 2008.

Rawls, W. J., Pachepsky, Y. A., Ritchie, J. C., Sobecki, T. M., and Bloodworth, H.: Effect of soil organic carbon on soil water retention, Geoderma, 116, 61–76, 2003.

Rolff, C. and Ågren, G. I.: Predicting effects of different harvesting intensities with a model of nitrogen limited forest growth, Ecol. Model., 118, 193–211, 1999.

R Core Team R: A language and environment for statistical computing. R Foundation for Statistical Computing, Vienna, Austria, available at: http://www.R-project.org/ (last access: 3 August 2016), 2014.

Scharlemann, J. P., Tanner, E. V., Hiederer, R., and Kapos, V.: Global soil carbon: understanding and managing the largest terrestrial carbon pool, Carbon Management, 5, 81–91, 2014.

Schlesinger, W. H.: Carbon Sequestration in Soils, Science, 284, 2095–2095, 1999.

Schmidt, M. W. I., Torn, M. S., Abiven, S., Dittmar, T., Guggenberger, G., Janssens, I. A., Kleber, M., Kogel-Knabner, I., Lehmann, J., Manning, D. A. C., Nannipieri, P., Rasse, D. P., Weiner, S., and Trumbore, S. E.: Persistence of soil organic matter as an ecosystem property, Nature, 478, 49–56, 2011.

Six, J., Conant, R. T., Paul, E. A., and Paustian, K.: Stabilization mechanisms of soil organic matter: Implications for C-saturation of soils, Plant Soil, 241, 155–176, 2002.

SLU: Markinfo, available at: http://www-markinfo.slu.se/eng/index.html (last access: 3 August 2016), 2011.

Smith, P.: An overview of the permanence of soil organic carbon stocks: influence of direct human-induced, indirect and natural effects, Eur. J. Soil Sci., 56, 673–680, 2005.

Sollins, P., Homann, P., and Caldwell, B. A.: Stabilization and destabilization of soil organic matter: mechanisms and controls, Geoderma, 74, 65–105, 1996.

Statistics Finland: Greenhouse gas emissions in Finland 1990–2011, in: National Inventory Report to the UNFCCC Secretariat, Ministry of the Environment, Helsinki, Finland, 285–286, 2013.

Stendahl, J., Johansson, M., Eriksson, E., Nilsson, Å., and Langvall, O.: Soil organic carbon in Swedish spruce and pine forests—differences in stock levels and regional patterns, Silva Fenn., 44, 5–21, 2010.

Swedish Statistical Yearbook of Forestry: Official Statistics of Sweden, 370 pp., Skogsstyrelsen, 2014.

Svensson, M., Jansson, P., and Kleja, D. B.: Modelling soil C sequestration in spruce forest ecosystems along a Swedish transect based on current conditions, Biogeochemistry, 89, 95–119, 2008.

Therneau, T. M. and Atkinson, E. J.: An introduction to recursive partitioning using the RPART routines, 1997.

Throop, H. L., Holland, E. A., Parton, W. J., Ojima, D. S., and Keough, C. A.: Effects of nitrogen deposition and insect herbivory on patterns of ecosystem level carbon and nitrogen dynamics: results from the CENTURY model, Glob. Change Biol., 10, 1092–1105, 2004.

Todd-Brown, K. E. O., Randerson, J. T., Hopkins, F., Arora, V., Hajima, T., Jones, C., Shevliakova, E., Tjiputra, J., Volodin, E., Wu, T., Zhang, Q., and Allison, S. D.: Changes in soil organic carbon storage predicted by Earth system models during the 21st century, Biogeosciences, 11, 2341–2356, doi:10.5194/bg-11-2341-2014, 2014.

Todd-Brown, K. E. O., Randerson, J. T., Post, W. M., Hoffman, F. M., Tarnocai, C., Schuur, E. A. G., and Allison, S. D.: Causes of variation in soil carbon simulations from CMIP5 Earth system models and comparison with observations, Biogeosciences, 10, 1717–1736, doi:10.5194/bg-10-1717-2013, 2013.

Torn, M. S., Trumbore, S. E., Chadwick, O. A., Vitousek, P. M., and Hendricks, D. M.: Mineral control of soil organic carbon storage and turnover, Nature, 389, 170–173, 1997.

Tuomi, M., Rasinmäki, J., Repo, A., Vanhala, P., and Liski, J.: Soil carbon model Yasso07 graphical user interface, Environ. Modell. Softw., 26, 1358–1362, 2011.

Tuomi, M., Thum, T., Järvinen, H., Fronzek, S., Berg, B., Harmon, M., Trofymow, J. A., Sevanto, S., and Liski, J.: Leaf litter decomposition – Estimates of global variability based on Yasso07 model, Ecol. Model., 220, 3362–3371, 2009.

Viro, P.: Investigations on forest litter, Valtioneuvoston Kirjap, 1955.

Wiesmeier, M., Hübner, R., Spörlein, P., Geuß, U., Hangen, E., Reischl, A., Schilling, B., von Lützow, M., and Kögel-Knabner, I.: Carbon sequestration potential of soils in southeast Germany derived from stable soil organic carbon saturation, Glob. Change Biol., 20, 653–665, 2014.

Xia, M., Talhelm, A. F. and Pregitzer, K. S.: Fine roots are the dominant source of recalcitrant plant litter in sugar maple-dominated northern hardwood forests, New Phytol., 208, 715–726, doi:10.1111/nph.13494, 2015.

Yurova, A. Y., Volodin, E. M., Agren, G. I., Chertov, O. G., and Komarov, A. S.: Effects of variations in simulated changes in soil carbon contents and dynamics on future climate projections, Glob. Change Biol., 16, 823–835, 2010.

Venables, W. N. and Ripley, B. D.: Modern applied statistics with S-PLUS, Springer Science & Business Media, 2013.

Zandonadi, D. B., Santos, M. P., Busato, J. G., Peres, L. E. P. ,and Façanha, A. R.: Plant physiology as affected by humified organic matter, Theoretical and Experimental Plant Physiology, 25, 13–25, 2013.